Nagra
Nationale
Genossenschaft
für die Lagerung
radioaktiver Abfälle

Cédra
Société coopérative
nationale
pour l'entreposage
de déchets radioactifs

Cisra
Società cooperativa
nazionale
per l'immagazzinamento
di scorie radioattive

TECHNICAL REPORT 85-58

FINAL REPORT OF THE BUFFER MASS TEST
Volume I: Scope, preparative field work, and test arrangement

R. Pusch (Swedish Geological Co)
J. Nilsson (Swedish Geological Co)
G. Ramqvist (El-tekno AB)

July 1985

Parkstrasse 23 5401 Baden/Schweiz Telephon 056/20 55 11

Nagra
Nationale
Genossenschaft
für die Lagerung
radioaktiver Abfälle

Cédra
Société coopérative
nationale
pour l'entreposage
de déchets radioactifs

Cisra
Società cooperativa
nazionale
per l'immagazzinamento
di scorie radioattive

TECHNICAL REPORT 85-58

FINAL REPORT OF THE BUFFER MASS TEST
Volume I: Scope, preparative field work, and test arrangement

R. Pusch (Swedish Geological Co)
J. Nilsson (Swedish Geological Co)
G. Ramqvist (El-tekno AB)

July 1985

Parkstrasse 23 5401 Baden/Schweiz Telephon 056/20 55 11

Der vorliegende Bericht betrifft eine Studie, die für das Stripa-Projekt ausgeführt wurde. Die Autoren haben ihre eigenen Ansichten und Schlussfolgerungen dargestellt. Diese müssen nicht unbedingt mit denjenigen des Auftraggebers übereinstimmen.

Le présent rapport a été préparé pour le projet de Stripa. Les opinions et conclusions présentées sont celles des auteurs et ne correspondent pas nécessairement à ceux du client.

This report concerns a study which was conducted for the Stripa Project. The conclusions and viewpoints presented in the report are those of the authors and do not necessarily coincide with those of the client.

Das Stripa-Projekt ist ein Projekt der Nuklearagentur der OECD. Unter internationaler Beteiligung werden von 1980-86 Forschungsarbeiten in einem unterirdischen Felslabor in Schweden durchgeführt. Diese sollen die Kenntnisse auf folgenden Gebieten erweitern:
- hydrogeologische und geochemische Messungen in Bohrlöchern
- Ausbreitung des Grundwassers und Transport von Radionukliden durch Klüfte im Gestein
- Verhalten von Materialien, welche zur Verfüllung und Versiegelung von Endlagern eingesetzt werden sollen
- Methoden zur zerstörungsfreien Ortung von Störzonen im Fels

Seitens der Schweiz beteiligt sich die Nagra an diesen Untersuchungen. Die technischen Berichte aus dem Stripa-Projekt erscheinen gleichzeitig in der NTB-Serie der Nagra.

The Stripa Project is organised as an autonomous project of the Nuclear Energy Agency of the OECD. In the period from 1980-86, an international cooperative programme of investigations is being carried out in an underground rock laboratory in Sweden. The aim of the work is to improve our knowledge in the following areas:
- hydrogeological and geochemical measurement methods in boreholes
- flow of groundwater and transport of radionuclides in fissured rock
- behaviour of backfilling and sealing materials in a real geological environment
- non-destructive methods for location of disturbed zones in the rock

Switzerland is represented in the Stripa Project by Nagra and the Stripa Project technical reports appear in the Nagra NTB series.

Le projet Stripa est un projet autonome de l'Agence de l'OCDE pour l'Energie Nucléaire. Il s'agit d'un programme de recherche avec participation internationale, qui sera réalisé entre 1980 et 1986 dans un laboratoire souterrain, en Suède. Le but de ces travaux est d'améliorer et d'étendre les connaissances dans les domaines suivants:
- mesures hydrogéologiques et géochimiques dans les puits de forage
- chimie des eaux souterraines à grande profondeur
- écoulement des eaux souterraines et transport des radionucléides dans les roches fracturées
- comportement des matériaux de colmatage et de scellement des dépôt finals
- méthodes de localisation non destructive des zones de perturbation de la roche

La Suisse est représentée dans le projet Stripa par la Cédra. Les rapports techniques du projet Stripa sont publiés dans la série des rapports techniques de la Cédra (NTB).

ABSTRACT

The Buffer Mass Test was conducted in a 30 m long drift at 340 m depth in the Stripa mine, the main objective being to check the predicted functions of certain bentonite-based buffer materials in rock environment. These materials were blocks of highly compacted sodium bentonite placed in large boreholes simulating deposition holes for canisters, and on-site compacted sand/bentonite mixtures used as tunnel backfill. The blocks of bentonite embedded electrical heaters which served to produce heat so as to create conditions similar to those in a repository. The temperature in the initially non-saturated buffer materials was expected to be a function of the water uptake from the rock, which was also assumed to lead to rather high swelling pressures. The recording of these processes and of the moistening of the buffer materials, as well as of the associated build-up of piezometric heads at rock/buffer interfaces, was the major item of the field test. For this purpose the buffer materials and the rock were equipped with a large number of thermal elements, pressure and piezometric cells as well as moisture sensors. The choice of positions and properties of these gauges, which were connected to an effective data acquisition system, was based on predictions that required a careful site documentation with respect to the fracture characteristics and hydrological properties of the surrounding rock.

RESUME

L'essai sur la masse-tampon a été réalisé dans la mine de Stripa, dans une galerie de 30 m de long, à 340 m de profondeur. Il avait pour objectif principal de contrôler, dans la roche, le comportement prévu de certains matériaux-tampon à base de bentonite. Ces matériaux étaient des blocs de bentonite-sodium hautement compactée, que l'on avait placés dans de grand puits de forage semblables à ceux creusés en vue de l'emmagasinage de conteneurs de stockages final, ainsi que des mélanges sable compacté-bentonite réalisés sur le terrain, tels qu'on les utilise comme matériaux de remplissage des galeries. Des corps de chauffe électriques ont été encastrés dans les blocs de bentonite, afin de simuler la production de chaleur observée dans un dépôt final. On s'attendait à ce que la température des matériaux-tampon, à l'origine non saturés, soit fonction de l'absorption d'eau par la roche, ce qui devait aboutir aussi à des pressions de gonflement assez élevées. Les enregistrement de ces processus, de la pénétration d'humidité des matériaux-tampons et des tensions piézométriques mesurées aux interfaces roche/colmatage ont constitué l'objet prinicpal de l'essai sur le terrain. Dans ce but, les matériaux-tampon et la roche ont été pourvus de nombreuses sondes de températures, capteurs piézometriques de pression et de tension, ainsi que de senseurs d'humidité. Le choix du positionnement et des propriétés de ces sondes de mesure, qui ont été connectées à un système de saisie des données, s'est basé sur des prévisions nécessitant une soigneuse documentation sur le site, concernant les caractéristiques des diaclases et les propriétés hydrologiques de la roche environnante.

ZUSAMMENFASSUNG

Der Puffer-mass-test wurde in einem 30 m-langen Stollen in einer Tiefe von 340 m in der Stripa Mine ausgeführt; das Hauptziel war die Ueberprüfung des prognostizierten Verhaltens bestimmter auf Bentonit basierenden Verfüllmaterialien im Fels. Diese Materialien waren hochverdichtete Natrium-Bentonitblöcke, die in grosse Bohrlöcher, ähnlich jenen für die Einlagerung von Endlagerbehältern, gebracht wurden, und in-situ-verdichtete Sand/Bentonit-Gemische wie sie als Stollenverfüllmaterial zum Einsatz kommen. Elektrische Heizkörper wurden in den Bentonitblöcken eingebettet, um die Wärmeproduktion in einem Endlager zu simulieren. Es wurde erwartet, dass die Temperatur der ursprünglich ungesättigten Verfüllmaterialien eine Funktion der Wasseraufnahme aus dem Gestein sein würde, was auch zu ziemlich hohen Quelldrücken führen sollte. Die Registrierung dieser Prozesse und der Durchfeuchtung der Verfüllmaterialien sowie der piezometrisch gemessenen Spannungen an Gestein/Verfüllungs-Uebergängen waren die Hauptkomponenten des Feldtests. Zu diesem Zweck, wurden die Verfüllmaterialien und das Gestein mit einer Vielzahl an Temperaturfühlern, piezometrischen Druck- und Spannungs-Messzellen sowie Feuchtigkeitssensoren ausgerüstet. Die Auswahl der Standorte und Eigenschaften dieser Messsonden, die an ein Datenerfassungssystem angeschlossen wurden, basierte auf Voraussagen, die eine sorgfältige Standort-Bestandesaufnahme bezüglich der Kluftcharakteristik und der hydrologischen Eigenschaften des umgebenden Gesteins notwendig machen.

CONTENTS

SUMMARY

The general objective of the Buffer Mass Test was to check the suitability and predicted functions of certain bentonite-based buffer materials under real conditions on site. It also served to illustrate various practical means of preparing, handling and applying soil type backfills. The test site was located in a 30 m long drift at 340 m depth in the Stripa mine.

The test arrangement consisted of six large boreholes, 0.76 m in diameter and about 3 m in depth, for hosting 600 W electrical heaters surrounded by tightly fitting blocks of highly compacted sodium bentonite. The power, which was increased up to 1800 W in certain tests, simulated the heat production of waste canisters. The holes were covered by sand/bentonite backfill that was compacted on site in the tunnel. In the inner 12 m long part of the drift, which was separated from the outer part by a rigid bulwark, the entire tunnel section was backfilled. Two of the heater holes were located here, while the other four were situated below a 1.6 m thick concrete slab with boxing-outs that were backfilled with sand/bentonite.

The development of temperature fields in the heater overpacks as well as in the backfill and the rock was of major interest. Also, the build-up of swelling pressures and water pressures was of profound interest. They were all expected to be functions of the rate and uniformity of the uptake of water from the rock by the initially non-saturated buffer materials. The prediction of these processes and the interpretation of the recordings required detailed site documentation with respect to the rock fracture pattern and to the hydrological and rock mechanical conditions in the rock.

This work was focused on determining the frequency and distribution of joints and fractures and of estimating the amount and distribution of the inflowing water. Much information was gained from the preceding "Macropermeability Test" in the drift, which was conducted by the Lawrence Berkeley Laboratory. Their recordings concerned water heads in the rock and the inflow into the drift. Additional measurements were made with respect to the latter process before the buffer materials were applied.

The rock and buffer components were instrumented for recording temperatures, swelling and water pressures, as well as the moistening of the buffer materials. In addition, internal displacements in these materials and changes in rock joint aperture were recorded.

The temperatures were measured by more than 1200 copper-constantan thermal elements. Swelling, or rather total pressures, were measured by use of about 130 Gloetzl pressure cells, and this system was also applied for recording water pressures in heater holes and in the confining rock (28 gauges). 25 BAT piezometers were used as a back-up of the Gloetzl system and for the recording of low water pressures.

The moistening of the clay materials was evaluated by use of specially developed sensors which yielded signals that reflected the capacitance of these materials. 560 gauges were applied for this purpose.

The water uptake and swelling of the highly compacted bentonite in the heater holes was expected to produce displacements of the interface between this bentonite and the overlying bentonite/sand backfill. These displacements were determined by accurate measure ment of the changes in position of copper "coins" and plastic tape stripes applied in connection with the backfilling operations.

The expansion of the highly compacted bentonite was expected to affect the aperture of rock joints intersecting the heater holes. One of them was therefore equipped with Kovari instrumentation so that possible aperture changes could be identified.

The huge number of recordings required effective data logging and storing facilities. A data acquisition system in Stripa, consisting of a computer part on ground and an instrumentation part down in the mine, produced raw-data log tapes and copies of these tapes were mailed to the computer center at the University of Luleå for storing and processing. The latter activity was later largely transferred to Stripa.

1 SCOPE OF TEST

1.1 General

The ability of bentonites to serve as effective barriers or buffers in the migration of water and solutes through waste repositories in rock has been conclusively demonstrated by numerous experiments on a laboratory scale (1). It is due to the very low hydraulic conductivity and relatively low ion diffusivity even at fairly low bulk densities. These properties partly result from the very pronounced hydrophilic properties and microstructural homogeneity of smectite-rich clays, which also give them the swelling and self-healing potential that is required to establish and maintain a tight contact with the confining rock and embedded waste canisters. This potential implies that a swelling pressure is exerted by bentonite, the magnitude of this pressure being of great significance. In particular, its rate of development and uniformity, which depend on the water absorption process, are practically important since they determine whether unwanted stresses in embedded canisters will be generated.

Short-term laboratory experiments show that temperature elevation from room conditions to about 100°C does not yield unacceptable changes in swelling pressure, hydraulic conductivity, and ion diffusivity, while higher temperatures may lead to smectite alteration and a loss in isolating efficiency of the bentonite in the long run. This means that the heat conductivity of clay buffers is of fundamental importance, especially close to hot canisters which are expected to produce local drying of the contacting buffers.

The general objective of the Buffer Mass Test was to check the suitability and predicted functions of certain bentonite-based buffer materials under real conditions on site. The testing con-

cerned the rate and uniformity of water uptake and swelling of initially non-saturated materials, and the development of temperature fields produced by buffer-embedded electrical heaters. Also, the test served to illustrate various practical means of preparing, handling and applying soil type backfills. In addition, the interaction between buffer materials and confining rock was investigated with respect to hydrology and rock mechanics. An attempt was also made to identify possible heat-induced crystal lattice alterations of montmorillonite.

1.2 Main features of the BMT

1.2.1 Location

The Buffer Mass Test was located in the approximately 30 m long drift at about 340 m depth in the Stripa mine that was previously used by the Lawrence Berkeley Laboratory (LBL) for the so-called "Macropermeability Test" (Fig 1.1). This test gave very valuable information of the groundwater pressure situation and natural flow characteristics of the surrounding rock, by which the hydraulic interaction between the rock and the buffer materials could be predicted at an early stage and evaluated at the end of the experiment.

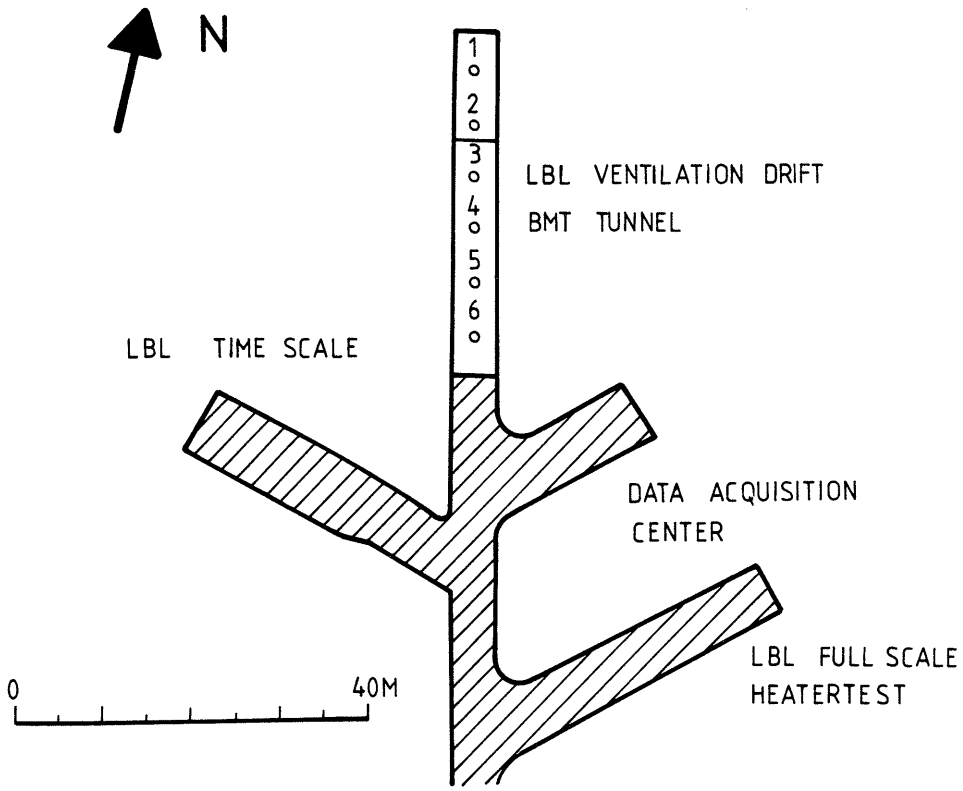

Fig 1.1. Location of the Buffer Mass Test

1.2.2 Geometry

The main idea in designing the Buffer Mass Test was to apply a geometrical shape that largely eliminates scale effects, and to arrange the test so that the influence of different rock conditions on the behavior of the buffer materials could be observed. This was achieved by using six large, suitably located and vertically oriented holes for the testing of dense bentonite embedding elektrical heaters (Fig 1.2). The degree of fracturing of the rock varied from fracture-poor, very dry rock to richly fractured and strongly water-bearing rock. Two of the holes, which were richly equipped with gauges for measuring temperatures, water uptake, swelling and water pressures, were located in the inner part of

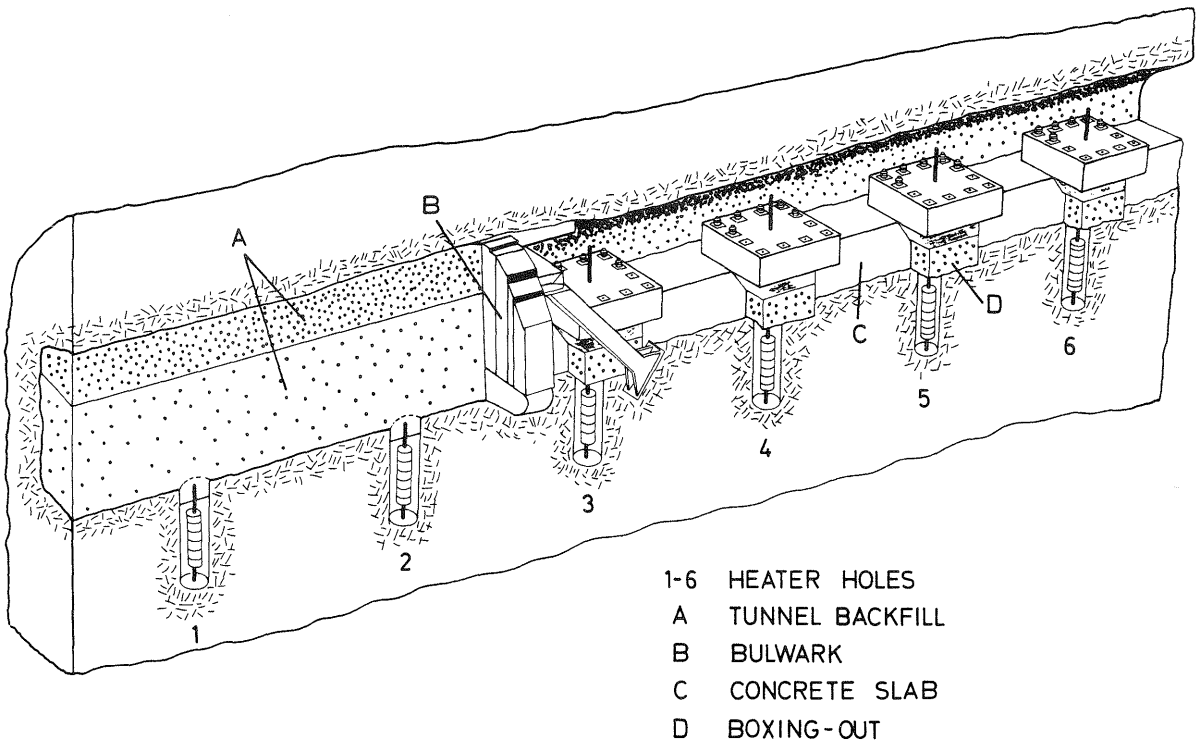

Fig 1.2 View of the BMT test site

the drift which was separated from the rest of the drift by a steel/concrete bulwark. This part of the drift was backfilled with buffer materials consisting of mixtures of sand and bentonite, the intention being to test, on a full scale, various techniques of applying and compacting such materials. The backfill in the closed part of the drift was instrumented so that the heat flow from the heater holes and the wetting and piezometric build-up by inflowing groundwater from the rock could be recorded. The four other heater holes were also covered by sand/bentonite backfills but they were confined in boxing-outs in a 1.6 m thick concrete slab simulating a rock tunnel with dimensions that are related to the heater holes in approximately the same way as in several national concepts suggested for storing highly radioactive wastes in crystalline rock. The boxing-outs were covered by concrete lids that could be removed for excavation and sampling. This arrangement made it possible to stop each individual test in the outer four holes at any desired time for excavation and determination of the actual physical state of the bentonite.

The detailed design of the test arrangement had to be based on preliminary calculations of the physical behavior of the buffer materials, the major question being whether a sufficient amount of groundwater would be available for the wetting in a test period of a few years. This matter was intensively discussed in the Technical Subgroup no 2, the decision being to install infiltration wells in the concrete slab to accelerate the wetting of the buffer materials if necessary. The estimated access to water for the wetting actually governed most of the geometrical features of the entire field test, several compromises being necessary in order to minimize the negative effect of various scale factors. The major points are as follows.

The distance between the heater holes was taken as 6 m, which was suitable with respect to the available length of the drift and to the aim of running the heater tests with only minor overlapping of the individual generated temperature fields. The dimensions of the heater holes, which had a diameter of 0.76 m and a depth about 3 m, correspond to about 1/2 to 1/5 of those of the deposition holes or tunnels of the various national concepts that are based on the use of dense bentonite as canister overpack. As to the dimensions and power of the heaters it was decided to apply a design that would give a maximum heater surface temperature of about 80°C and a maximum temperature gradient of 1.5 - 2.5°C/cm in the dense bentonite. Taking the power as 600 W, which was considered to be representative of waste canisters at that time, and applying ordinary heat conductivity data of the bentonite and rock, the diameter of the heaters should be approximately 50 % of the heater hole diameter. Since a relatively uniform temperature distribution along the heater would require a heater length of at least four times the diameter, the dimensions of the 600 W heaters were taken as 1.5 m in length and 0.38 m in diameter. Thus, the annulus of dense bentonite in the heater holes had a radial thickness of 0.19 m, which is rather small but acceptable with respect to the requirement of arriving at a high degree of water saturation in the available testing time.

1.2.3 Specification of tested buffer material functions

In summary, the following main buffer material functions were investigated:

Dense bentonite in heater holes

I **Practical**

* Preparation of dense bentonite material
* Application of blocks of dense bentonite

II **Physical**

* Heat conductivity, development of temperature fields in the bentonite/rock system
* Rate and distribution of water uptake
* Swelling and self healing
* Development of swelling pressures
* Stress/strain interaction of dense bentonite and overlying sand/bentonite backfill
* Stress/strain interaction of dense bentonite and confining rock
* Sealing of joints and fractures by expanding bentonite
* Development of water pressures at the bentonite/rock interface

III **Chemical**

* Smectite alteration

Sand/bentonite tunnel backfill

I **Practical**

* Large scale preparation of sand/bentonite mixtures
* Application and compaction of sand/bentonite backfill
* Check of practical means of quality control (composition, density)

II Physical

* Development of temperature fields
* Rate and distribution of water uptake
* Swelling
* Development of swelling pressures
* Erodibility (effect of inflowing water from confining rock)
* Development of water pressures at the bentonite/rock interface

1.2.4 Time schedule

The planning of the Buffer Mass Test started in late 1979 and most of the detailed design, which was based on a preliminary prediction of the rate of wetting of the buffer materials, was finished one year later. The construction work started in November 1980 and the first heater was in operation in June 1981, which was therefore the actual start of the field test.

The total time of the field tests was originally set at about 3 years but in the course of the experiment it turned out that much could probably be gained by extending this time by slightly more than half a year. The field operations thus terminated in mid February 1985, while the evaluation of certain mineralogical tests, which were added to the test program at a late stage, will continue until summer 1985.

2 PREPARATIVE FIELD WORK

2.1 Civil engineering and rock drilling

2.1.1 Introduction

The Buffer Mass Test (BMT) was conducted in the former "ventilation drift" in which a number of rock investigations were previously made and a number of pressure gauges were still in operation when the BMT was prepared. A light wooden wall, anchored to the rock in a shallow slot, formed an outer boundary of the preceding LBL test and the removal of this wall was the first step in the preparation of the BMT test. Next, a number of vertical pilot holes were drilled from the tunnel floor to get information of the water inflow in possible heater hole positions. The final decision of the location of the heater holes was then made, the main principle being that much water should be available in at least three holes. Thereafter, the large Ø 0.76 m heater holes were drilled to a depth of 3-3.3 m. Additional holes were then drilled for rock anchoring of the lids of the four outer heater holes, for the rock mechanical investigation, as well as for a number of water pressure gauges.

The inner, about 12 m long part of the tunnel, was separated from the outer by a bulwark which had to be designed so as to withstand the swelling pressure as well as the water pressure that was expected to be built up in the course of the test.

Outside the bulwark an approximately 1.5-1.7 m thick concrete slab was cast on the tunnel floor to a distance of almost 25 m from the bulwark. Boxing-outs extending down to the tunnel floor and with the horizontal dimensions 1.8 x 1.8 m, were made and rock-anchored concrete lids were cast on top of them after backfilling. This

arrangement and the general features of the Buffer Mass Test are shown in Fig 2.1.

Much attention was paid to the establishment of a very accurate geodetical reference system. For this purpose, a number of "polygon points" were mounted which made it possible to relate to the general coordinate system of the mine. Stereophotography, teodolite and laser techniques were applied extensively since a very high accuracy was required for many measurement, construction and drilling purposes, especially for the location and orientation of the drill rigs when performing the heater holes.

The major preparative operations in the drift were:
1) drilling of the heater holes, which was preceded by a pilot hole study, 2) construction of the concrete slab, and 3) construction of the bulwark. They will be shortly described in this chapter. The comprehensive preparation of the field test in the form of drilling of holes for installation of thermocouples, piezometers and rock displacement gauges, as well as the construction of various supporting arrangements will be omitted here.

Since the Buffer Mass Test concerns backfilling of repository tunnels in general, the term tunnel will be used in this report instead of drift.

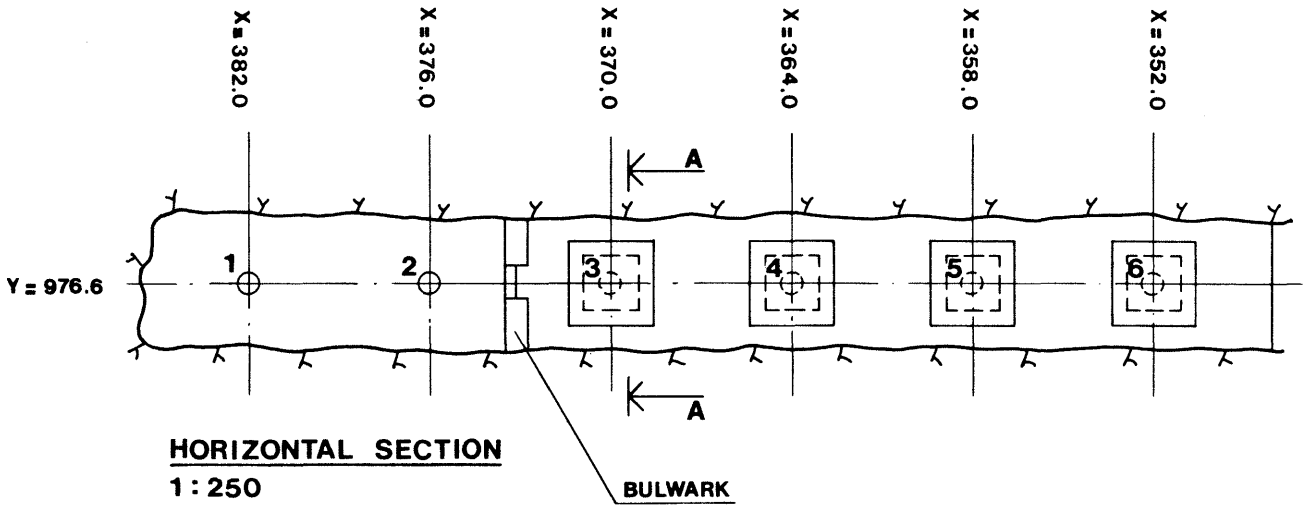

HORIZONTAL SECTION
1 : 250

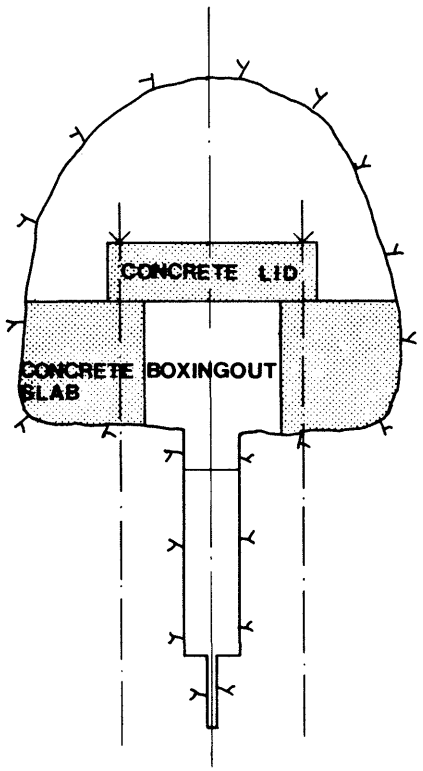

A, CROSS SECTION
1:100

Fig 2.1 Schematic sections through the BMT drift.

2.1.2 Heater holes

2.1.2.1 **Pilot drillings**

The final choice of location of the six heater holes was preceded by drilling pilot holes. Eleven Ø 56 mm holes (1a-6a, 1b-6b) were drilled vertically to about 4 m depth and with 3 m spacing by Hagby Bruk AB using core drilling technique (Fig 2.2). The cores were examined to characterize the rock while the boreholes were used for simple hydrological testing purposes. This procedure, i.e. to produce twice as many pilot holes as heater holes, was applied in order to simulate the situation in a true repository where rapid and fairly simple tests in pilot holes have to be run as a basis of the selection of suitable deposition holes sites.

The rock represented by holes 1a, 1b and 2a was found to be very fractured and richly percolated by groundwater. Hole 2b was rather dry while 3a, 3b, 4a, and 5a were fairly wet. 6a and 6b, finally, were very dry. No hole was drilled in the 4b position since it almost coincided with a previously drilled deep borehole. The criterion to have access to much water in some of the holes and the implication to have a constant spacing of the heater holes to get the same overlap of the temperature fields, gave the final location of deposition holes: 1a, 2a, 3a, 4a, 5a, and 6a. They are referred to as holes no 1-6 in the subsequent text, i.e. without the index "a".

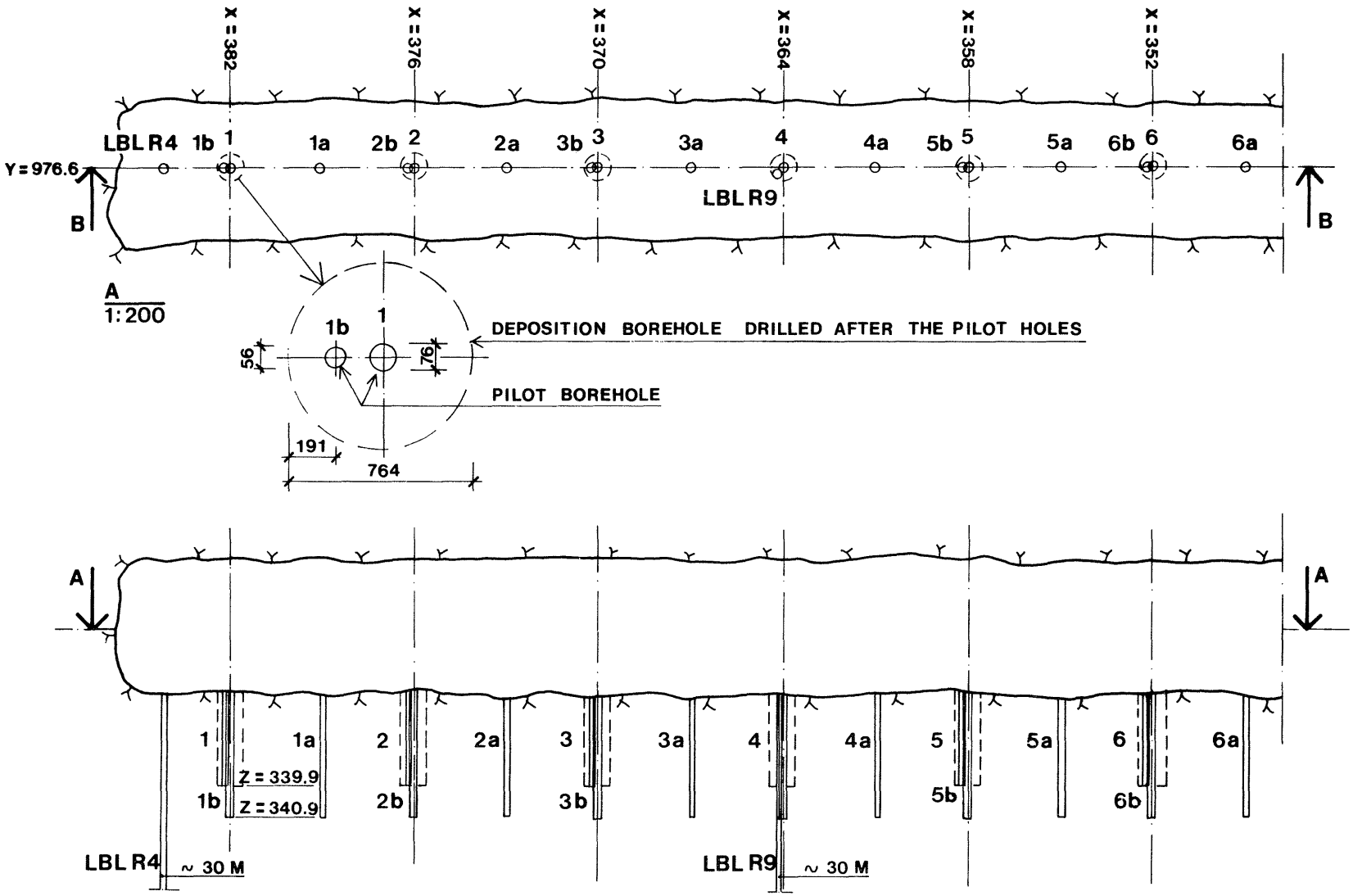

Fig 2.2. Location of pilot boreholes.

2.1.2.2 Drilling and preparation of heater holes

Six large test holes, i.e. the holes for the bentonite/heater units, were made by use of a recently developed technique which is similar to conventional core drilling (Hagby Bruk AB). A Ø 0.76 m steel tube equipped with bits welded to the edge of the tube, was rotated and manoevered by means of hydraulic machineries. The drilling speed was improved considerably in the course of the project and it turned out to be possible to drill about 3 m a day in fracture-poor rock with the final version of the drilling equipment (Fig 2.3). The pilot holes were essential for the drilling operation since they were used for guiding the large tube and expanding bolts were anchored in them so that the heavy cores could be lifted out of their holes (Fig 2.4). Extensive fracture mapping and rock classification was made after visual inspection of the holes and cores.

The cores were separated from the underlying rock by expanding a wedge that was lowered in the narrow slot around the core. In all the holes, except for hole no 5, the base of the core and thus the bottom of the hole, were fairly plane and perpendicular to the hole axis. In hole no 5 percussion drilling had to be used for trimming the bottom to form a reasonably flat and even surface.

Some of the cores were fairly coherent while others, such as the fractured cores from holes 1 and 2, disintegrated in the course of the lifting operation (Fig 2.5).

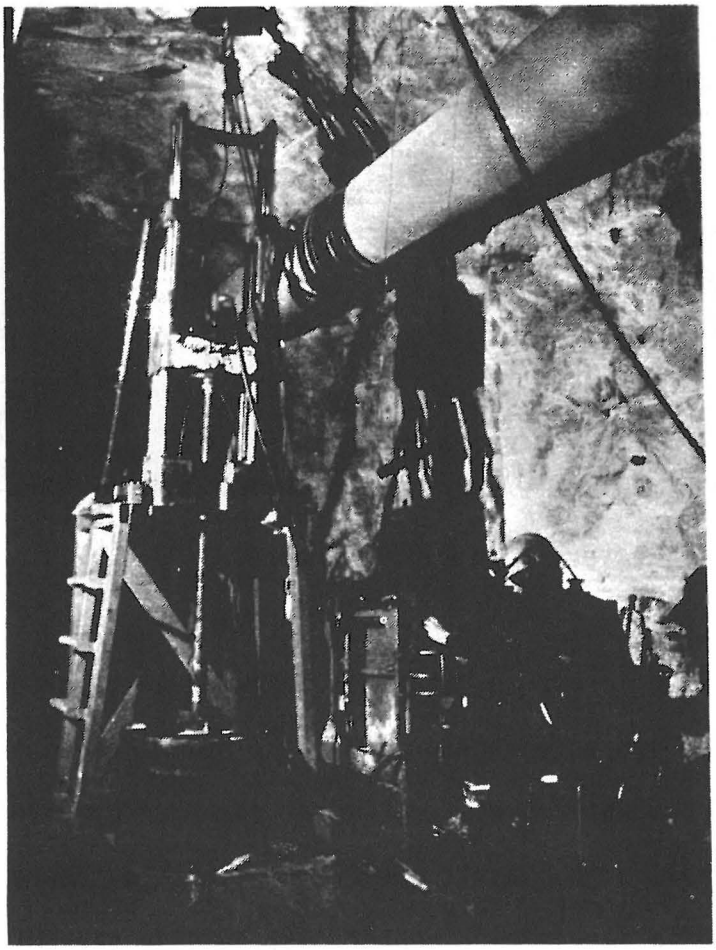

Fig 2.3. Hagby Bruk AB equipment for Ø 0.76 m core drilling. The large tube has penetrated the tunnel floor to about 0.5 m depth.

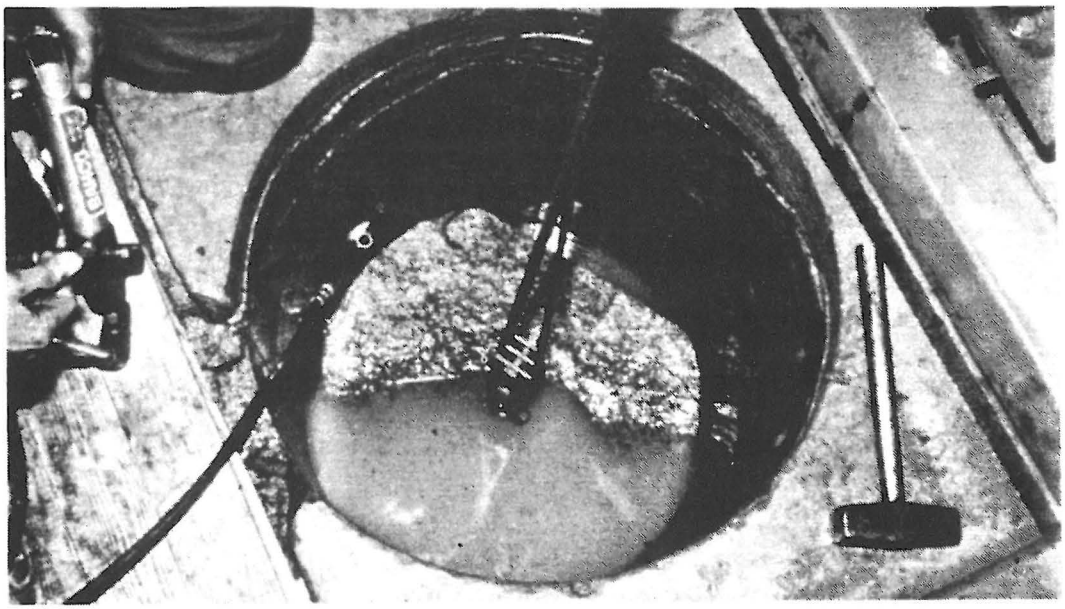

Fig 2.4. A Ø 0.76 m core being lifted from its hole.

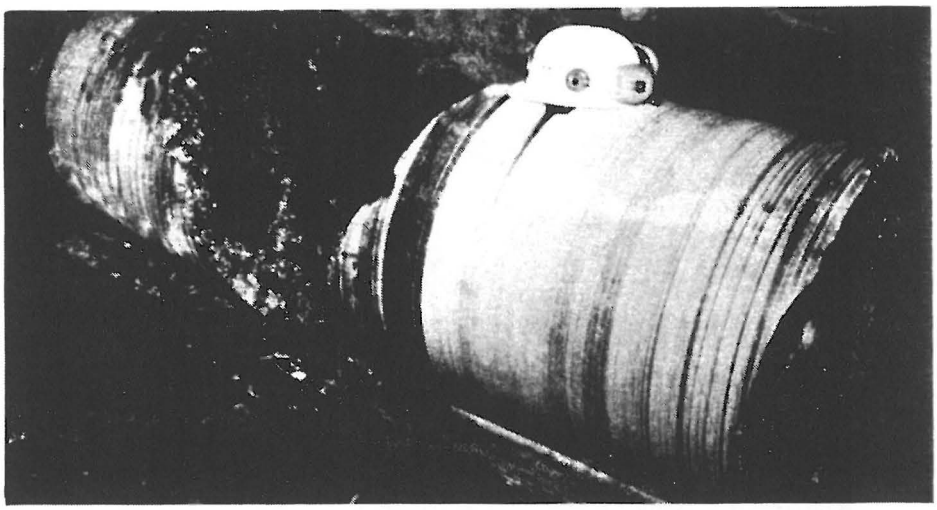

Fig 2.5. Fracture-poor Ø 0.76 m core.

The swelling pressure that was expected to be produced by the expanding, compacted bentonite in the heater holes and the superimposed groundwater pressure, were recorded by using disc-shaped Gloetzl cells with plastic tube connections to the recording unit in the data acquisition center just outside the BMT drift. The dimensions of the cells (250x150x60 mm including the valve component) required location in rock recesses in order not to occupy space in the heater holes. Since the tubings also needed to be placed in the rock, vertical slots had to be cut in each hole (Fig 2.6). They were produced by making two parallel cuts by use of a rotating diamond-coated saw-blade and by removing the rock between the cuts by means of a percussion hammer. Thereby, an average slot width of 70x40 mm was obtained for the tubings, while the corresponding dimensions were 70x170 mm for the cells. These were fixed with rock bolts and rigidly mounted in expanding cement mortar so that the smooth, regularly curved rock surface in the heater holes was preserved (Fig 2.7).

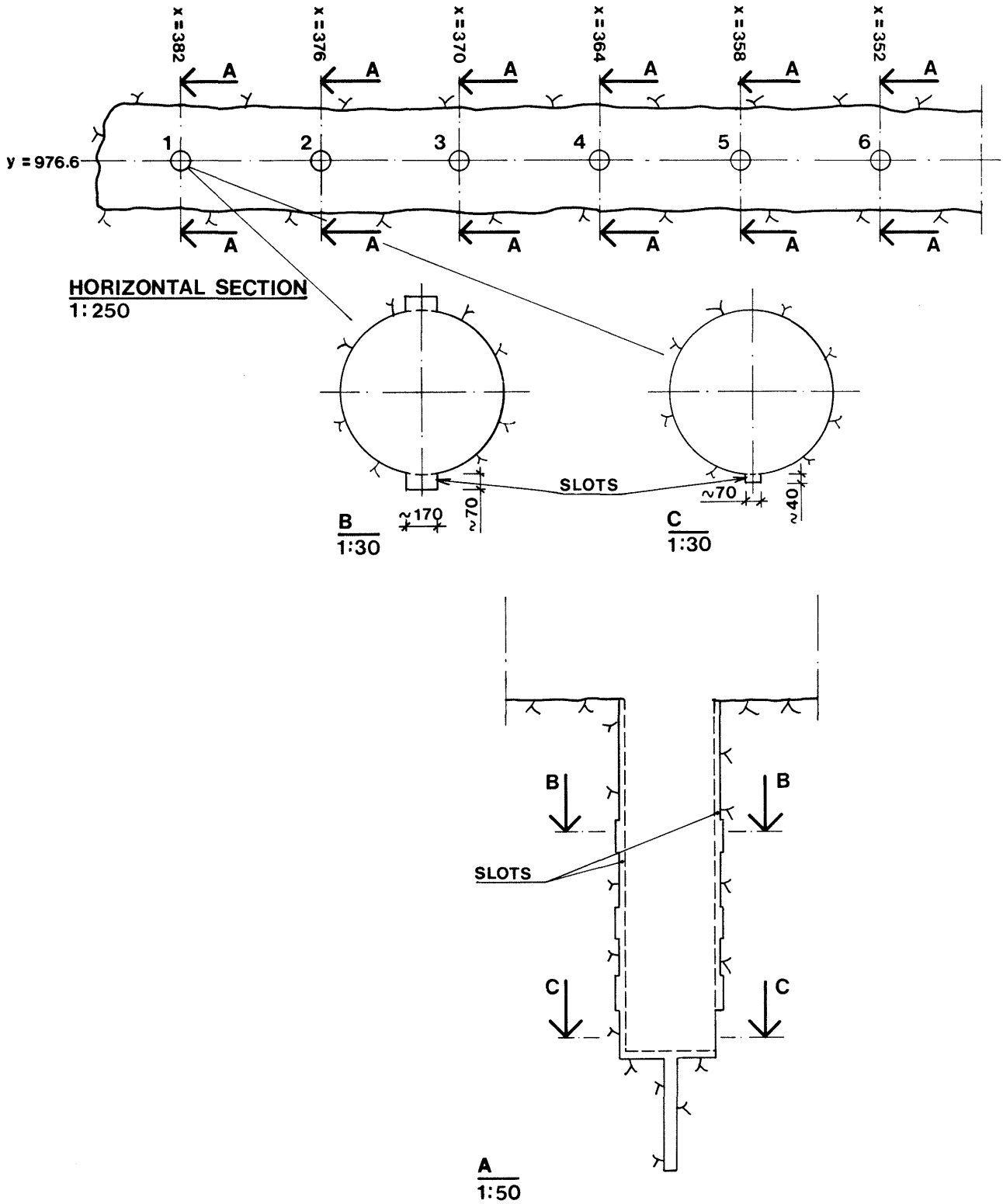

Fig 2.6. Slot arrangements for Gloetzl cells in the heater holes.

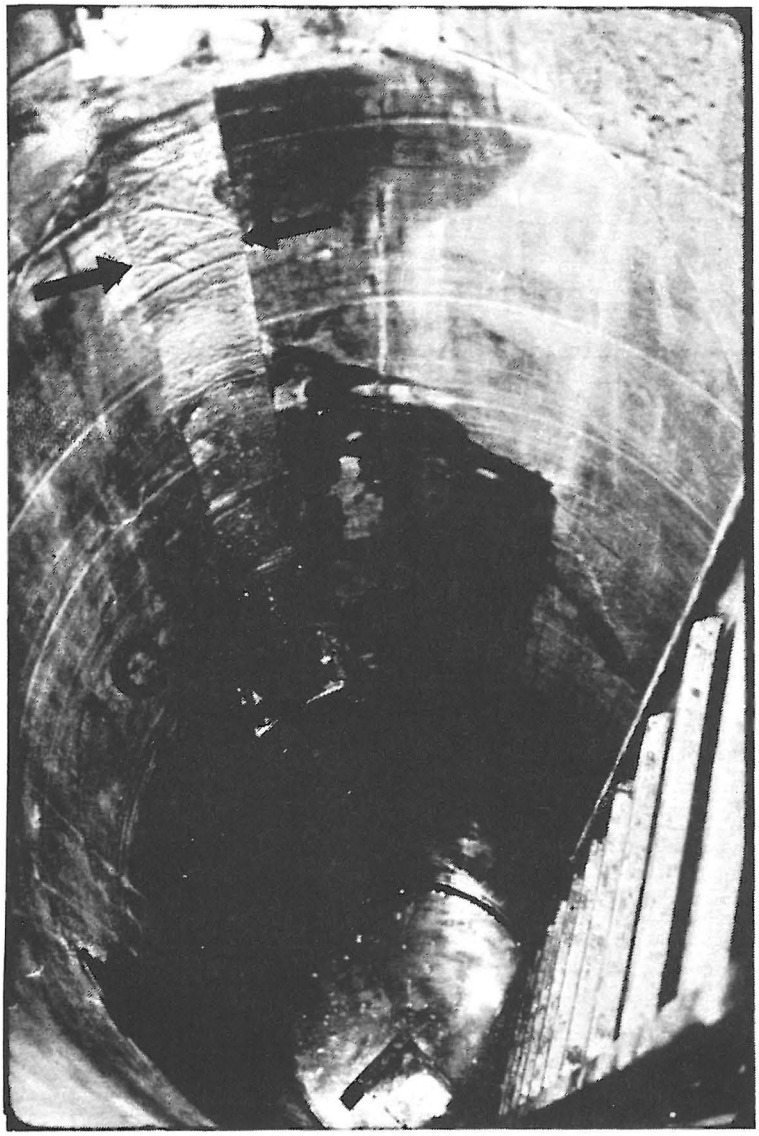

Fig 2.7. Example of sealed slot (within arrows). Notice the smooth surface of the sealing where the cell is situated (C). Notice also the groundwater that flows from a series of subhorizontal fractures in the rock.

2.1.3 Bulwark

2.1.3.1 Design criteria

The bulwark (bulkhead) was required for confining the tunnel backfill and for establishing an effective sealing so that groundwater would not flow directly from the backfill into the open tunnel. The forces acting upon the bulwark were the earth pressure at rest, the swelling pressure, and the groundwater pressure. The

first one is negligible compared to the other two, the water pressure being the main source. Since certain LBL gauges have indicated water heads of more than 100 m close to the tunnel, it was decided to take 250 m water head, or 2.5 MPa, as a safe limit. The maximum swelling pressure was assumed to be 0.5 MPa when the design criteria had to be decided, since up to 30 % bentonite contents were still being discussed at that time. Later, it was concluded that the present, rather bentonite-poor backfills would not yield higher swelling pressures than 0.1-0.3 MPa. Minimum displacement of the bulwark was desirable and this suggested the choice of a very rigid and well supported structure.

The 60 MN horizontal force which was expected to affect the bulwark had to be transferred to the rock without noticeable displacements. This problem was solved by applying steel supports and by excavating recesses in the rock surrounding the entire bulwark. The rock excavation involved in this activity was made with great care in order not to disturb the rock and increase its hydraulic conductivity.

These requirements suggested the use of a very rigid steel structure and this was also accepted as a design criterion. The 25.5 ton steel components were prefabricated and welded together on site. The suc-cessive steps in the establishment of the bulwark are listed as follows (cf. Fig 2.8).

1 Casting of footing.

2 Mounting of lateral structure components.

3 Sealing with concrete of the space between these structures and the adjacent rock.

4 Lifting of the steel structure to establish close contact with the rock. The procedure required the use of a system of flat-jacks, each producing 1.5 MN.

5 Embedding the flat-jacks with expanding cement mortar.

6 Injection of expanding cement mortar into the oil-filled flat-jacks.

7 Closing of the opening by welding steel beams in the opening.

8 Sealing with concrete of the space between the steel structure above the previous opening and the overlying rock.

9 Welding of yoke unit and steel supports. The appearance of the finished bulwark is illustrated by Fig 2.9.

10 Ultrasonic testing of weldings.

2.1.4 Concrete slab

The purpose of the concrete slab was to simulate rock so that boxing-outs in the slab could be used to represent the tunnel in a true-scale version of a deposition hole in a repository tunnel. The length of the slab was 24.7 m and its thickness 1.5-1.7 m. The horizontal dimensions of the boxing-outs were 1.8 x 1.8 m.

For various production-based as well as functional reasons that have to do with temperature etc, the slab had to be cast step-wise (I, II, III, IV, V and VI in Fig 2.10). Rubber water bars were applied in the joints between the various concrete units to prevent water leakage and steel casings were cast-in for rock anchors and piezometers.

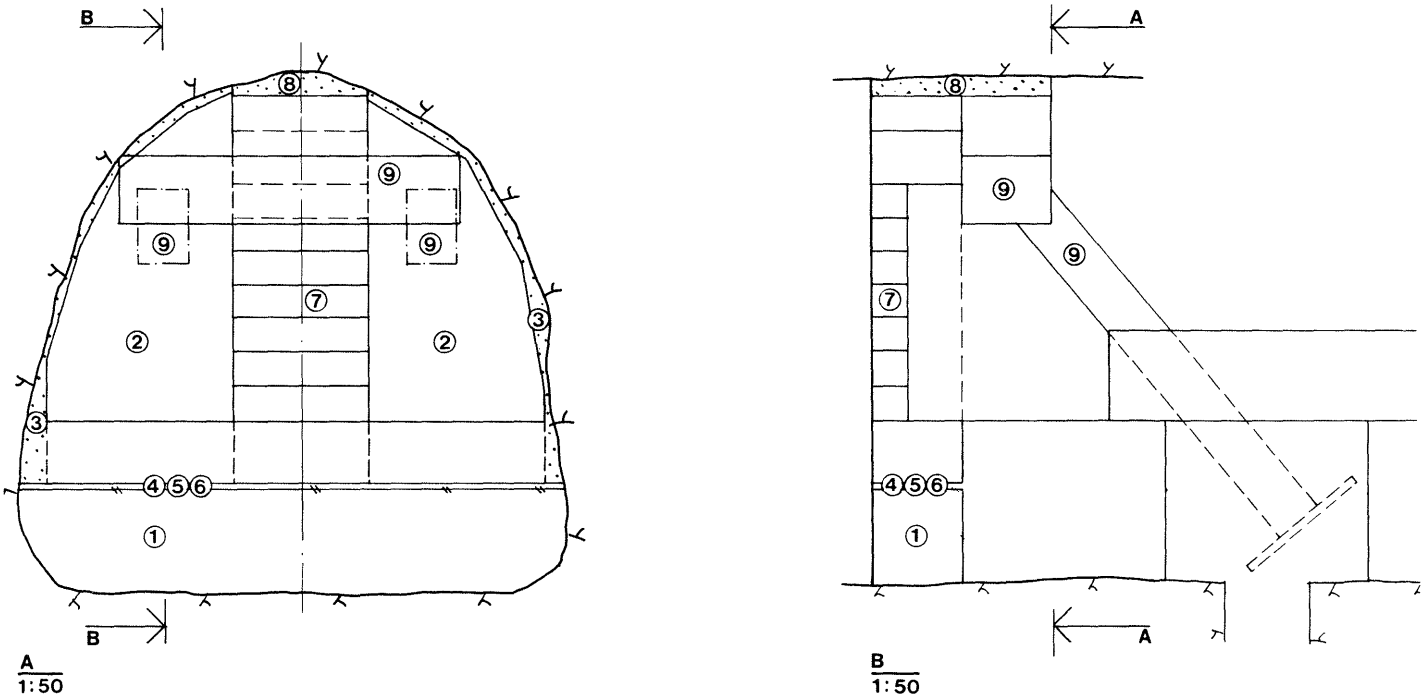

Fig 2.8. Bulwark

1 Concrete footing (part 1)
2 Steel structure
3 Expansive cement mortar
4 12 flat jacks for prestressing
5 Expansive mortar around jacks
6 Grouting of jacks with expansive mortar
7 "Door" of steel beams
8 Expansive cement mortar above door
9 Yoke and supports of steel

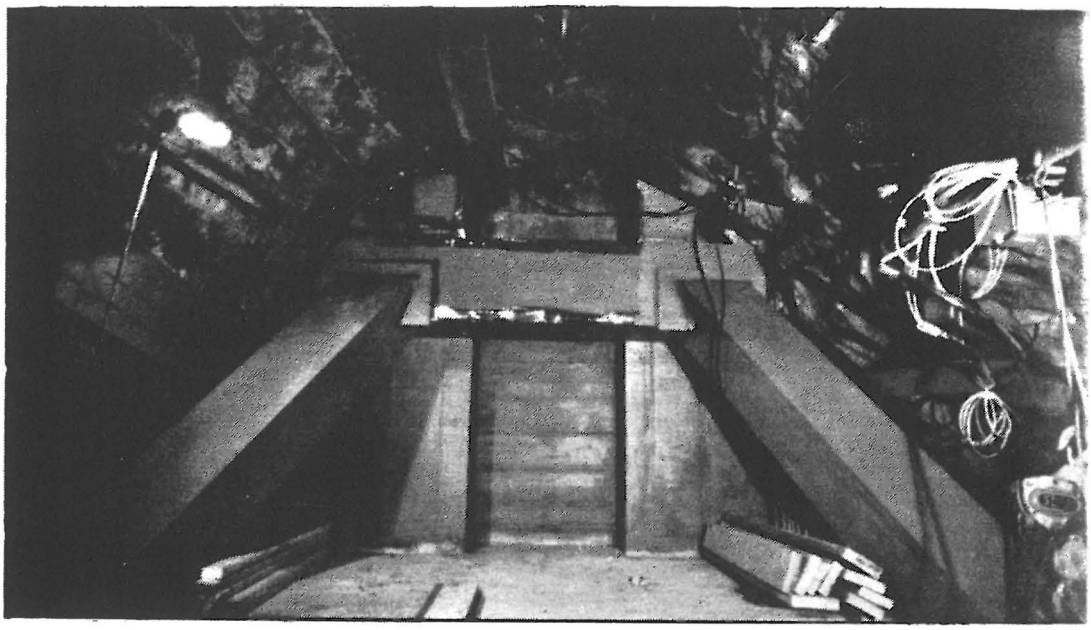

Fig 2.9. Photograph of the finished bulwark.

Fig 2.11 shows the rather heavy reinforcement and the form of one boxing-out. The strength of the concrete was checked continuously according to the standards prescribed by Swedish building authorities. This involved the preparation of test cubes, the compressive strength of which was found to exceed 40 MPa for all the tested specimens.

The backfilled boxing-outs were covered by casting concrete lids on top of the compacted sand/bentonite fill, the design criteria being the following ones:

1 Excess water from the concrete casting must not enter the backfill.

2 The lids must be easily moved to the side when excavation of the backfill is to be started.

3 A sealing between each lid and the underlying slab must be applied to prevent water to pass through these joints.

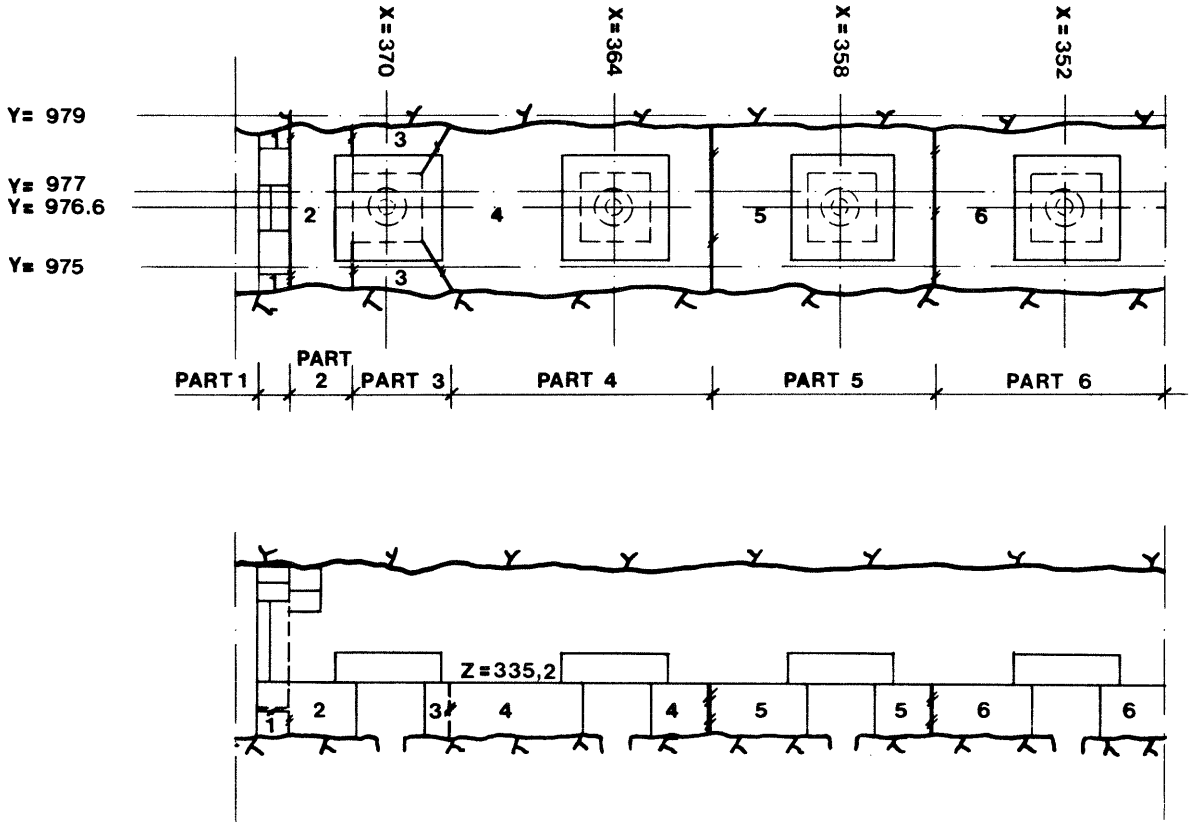

Part	Concrete volume	Date for casting
1	4,0 m3	81-04-09
2	13,5 m3	81-06-24
3	12,0 m3	82-01-11
4	55,0 m3	81-08-17-81-08-19
5	39,0 m3	82-02-10-82-02-11
6	49,0 m3	82-02-24-82-02-25
	Total;172,5 m3	

Fig 2.10. Layout of concrete slab.

The first requirement was met with by using 5 mm steel forms (2.5 x 2.5 x 0.85 m), the base plates of which were penetrated by tightly connected casings for the power cables of the heaters and for the rock mechanical instrumentation in hole no 5. The huge bunches of tubes and cables from all the other gauges were placed in slots in the concrete slab below the lids, the space being filled with expanding cement mortar at a late stage (summer 1982). The removal of the heavily reinforced lids was made by using the two traversing steel profiles through which steel beams could be inserted for lifting purposes (Fig 2.12).

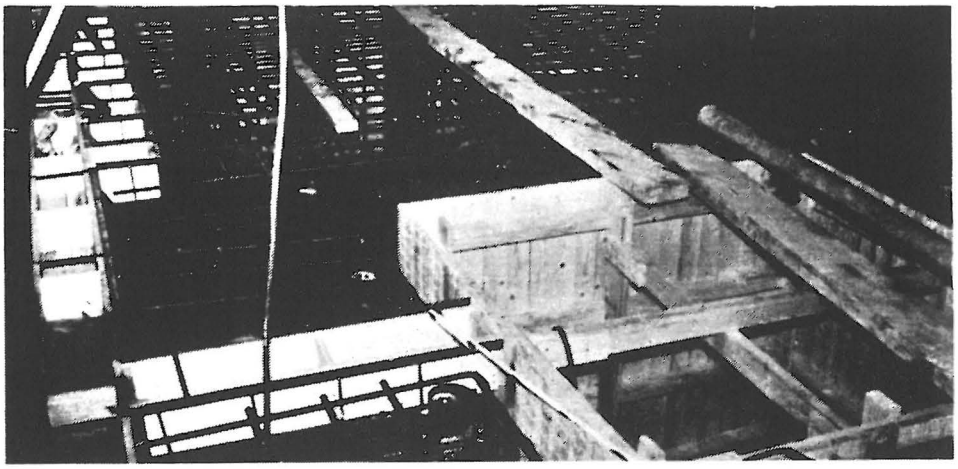

Fig 2.11. Slab reinforcement and wooden form for boxing-out.

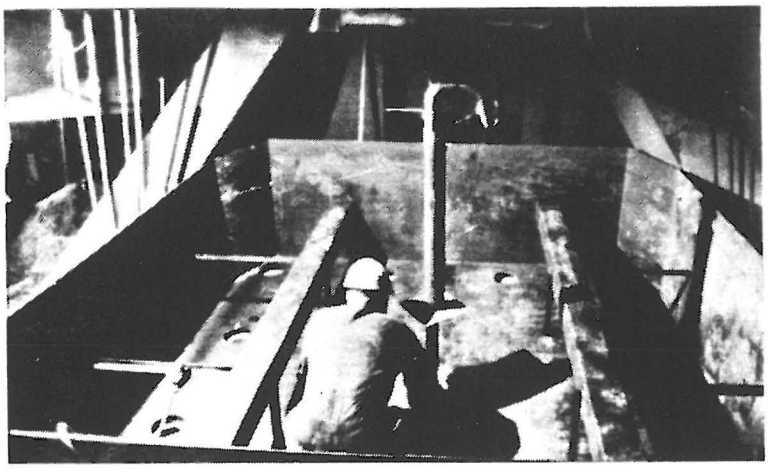

Fig 2.12 Steel form for lid. Notice the two traversing steel profiles.

6 m^3 of concrete were used for each lid, the time for casting each of them being about 8 hours. The sealing between the lids and the concrete slab was arranged by use of asphalt-impregnated polyurethane plastic strips. These sealings were somewhat compressed but it was assumed that swelling of the buffers at a late stage would tend to lift the lids by which the sealings would expand. The theoretical maximum increase of the joint width was calculated to be about 20 mm and this could well be compensated by the corresponding swelling of the sealing. In practice, the expansion became much less than that.

The rock anchors of the lids had to be designed so as to withstand the swelling pressure exerted by the compacted bentonite in the deposition holes, the swelling pressure of the backfill in the boxing-outs, and the groundwater pressure. The dominant stress component was assumed to be that produced by the compacted bentonite. Assuming it to be 10 MPa ultimately and applying the conventional 2:1 pressure distribution in the overlying backfill, we find the vertical force to be about 6 MN. The design of the anchors was based on a somewhat smaller force since none of the outer 4 holes was expected to experience 10 MPa swelling pressure during the test period. 500 kN was the estimated maximum vertical force and this yielded 12 Ø 36 mm GWS rods per lid. The technical data are the following:

* Cross section of each rod 1018 mm^2
* Weight 8.3 kg/m
* Yield stress: 0.83 kN/mm^2; maximum tension 1.03 kN/mm^2

The rods were applied in 5 sections, the entire free length being protected against corrosion by a closely fitting plastic tube (Raychem). The total anchor length was 13.5 m, the lower 4 m being

50 kN except for the anchors of deposition hole no 5 where the applied load was only 10 kN to allow for some vertical rock displacement caused by the vertical expansion of the heater overpack in this wet hole. This is essential since the rock mechanical investigations in hole no 5 imply that such displacements can actually take place. The tension force in all the anchors in this hole were also recorded.

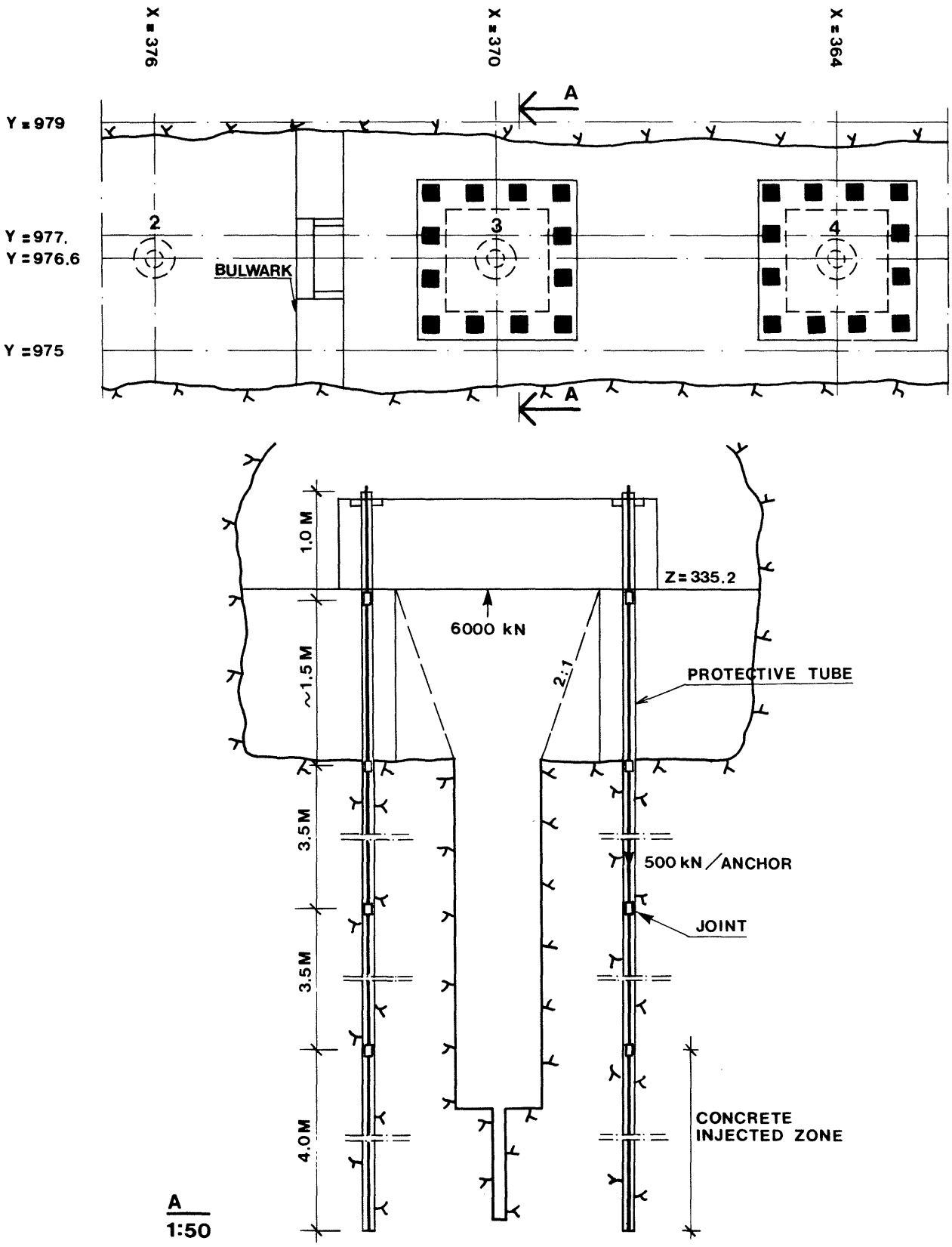

Fig 2.13. Rock anchor arrangement.

3 SITE DOCUMENTATION

3.1 Introduction

A huge material is available for site documentation from various sources, particularly from a number of careful and comprehensive field tests ran by the Lawrence Berkeley Laboratories, California, USA, in conjunction with earlier Swedish-American joint ventures in the Stripa mine. For the sake of clarity only really essential data for this test have been compiled here, however. Thus, mineralogic and petrologic reporting as well as information of geochemical properties will be very sparse, while fracture mappings and hydrologic surveys are given considerable space.

3.2 Temperature conditions

The average rock temperature in the mine has been found to be in the range of 10-13°C at the depth where the BMT tunnel is located. The "Macropermeability Test", which preceded BMT in the same place, involved heating of the tunnel to 20, 30, and 45°C in different tests lasting for somewhat less than one year. After a fourth test at 20°C, the ordinary ambient air temperature 15°C prevailed for a few months before the installation phase of the BMT started. The rock temperature had then dropped to 12.5-13.0°C, which can therefore be taken as the initial temperature of the buffer mass test.

The test area has been ventilated throughout the test by which the air temperature was maintained at approximately 15°C and the relative humidity at about 65-75 %.

3.3 Gas conditions

Gas was noticed in a number of boreholes, particularly in some of the Ø 76 mm LBL holes that extend from the BMT tunnel. These holes, which will be further discussed in Chapter 3.5.2.1, were equipped with gas-operated packers that had probably been leaking nitrogen gas into rock joints extending tens of meters from the holes for quite a long time. It is anticipated, however, that the deflating and replacement of the original packers led to a high degree of water saturation of joints and fractures before the BMT backfilling operations started.

It should be mentioned that radon emanates from the rock to an extent that requires continuous ventilation in all test areas at depth in the mine.

3.4 Rock constitution

3.4.1 General mineralogy

The BMT tunnel is dominated by a medium-grained, massive grey/reddish granite. The grain size, which is typically about 3 mm, varies between 1 and 5 mm (2). The LBL chemical analyses of reddish and grey granite in the area show the following representative compositions expressed in volume %:

Reddish granite		Grey granite	
Quartz	44	Quartz	35
Partly sericitised plagioclase	39	Partly sericitised plagioclase	35
Microcline	12	Microcline	24
Chlorite	3		
Muscovite	2	Subordinate: biotite, muscovite, chlorite, epidote	
Accessory: zircon, opaques		Accessory: zircon, opaques	

Table 3:1 shows the result of a number of chemical analyses of the Stripa granite (2).

Table 3:1. Chemical characteristics of the Stripa granite, (percent)

Sample	S 3	S 2	S 6	S 4	S 12
SiO_2	75.3	74.8	74.0	74.3	74.9
TiO_2	0.06	0.05	0.06	0.06	0.05
Al_2O_3	12.09	13.1	13.5	13.3	13.3
Fe_2O_3	1.8	1.7	1.6	1.0	1.7
MnO	0.03	0.02	0.02	0.06	0.03
CaO	0.6	0.4	0.5	0.7	0.7
MgO	0.22	0.22	0.18	0.20	0.18
K_2O	4.5	4.6	4.8	4.6	4.5
BaO	0.02	0.03	0.03	0.03	0.02

3.4.2 Joints and Fractures

3.4.2.1 General

The Stripa granite has been extensively investigated by LBL and the stochastic character of the joints and fractures of crystalline rock in general is thereby well demonstrated. The average spacing of four major sets of discontinuities that were identified by LBL is illustrated in Table 3:2.

Table 3:2. Fracture spacing parameters of Stripa granite (2)

Set no	Mean vertical spacing m	Mean dip angle (°)	Normal spacing, m
1	0.73	41	0.55
2	0.50	59	0.25
3	0.32	39	0.25
4	0.42	0	0.42

The persistence of joints, or the trace length, was also determined by LBL for the Stripa granite and it can be concluded from this study that the persistence of the large majority of joints is remarkably small. Actually, only 15 % of the total number of discontinuities, closed or open, persist more than 4 meters, and only about 2 % have an extension of 7 m. This is a determinant of the gross hydraulic conductivity and porosity of the rock as well as of its stress/strain properties and this points, in turn, to the importance of the degree of cross-linking of the joints.

3.4.2.2 Tunnel

The orientation of joints and fractures in the BMT tunnel has been determinded by LBL in an early survey, their projected site being illustrated by the histogram in Fig 3:1. Detailed mapping of the more prominent discontinuities was later made by LBL as well as by the Division of Soil Mechanics, University of Luleå.

LBL:s detailed study was aimed at providing data for the interpretation of the macropermeability test which was run by that organization in the period 1979-1980 (2) (cf. Fig 3.2). The main observed feature was a zone of closely spaced (2-5 cm), subparallel

joints which trends approximately N 15°E and dips about 70° to the west. This study also showed that two directions of the joints dominated: 1) a W-NW direction with joints dipping steeply to the north or to the sourth, and 2) a N-NE direction with joints that generally dip 50-60° to the west. Most joints and fractures were found to show evidence of groundwater seepage in the form of either drops or moist planes. The first-mentioned set of joints (the W-NW-trending set that dips to the south) consisted of discontinuities that were either planar or slightly curved and with an extension of at least 2 m.

The set of W-NW-trending joints that dip to the north were seen to be continuous over at least 4 m, and they show evidence of movement according to the LBL study. Joints with the N-NE trend are generally curved and continuous over 3-4 m, and they show evidence of shear displacements.

A general conclusion from these studies is that the rock is rich in fractures in the inner part of the BMT tunnel and that heater holes no 1 and 2 were located in particularly water-bearing zones.

The usual practical means of determining or estimating the aperture of joints and fractures is by steady-state injection testing. It yields equivalent "hydraulic" apertures assuming ideally smooth, parallel plate flow. They are somewhat smaller than the actual aperture, which can hardly be measured in a direct way. Typical data derived by LBL are presented in Table 3:3.*

---

* Pers comm with Dr Charles R Wilson, formerly at LBL.

Table 3:3. Single open rock joint apertures (mm) in Stripa granite as interpreted from 320 m packer-sealed borehole tests (LBL). Total number = 169.

Interval d, mm	Fraction %
≤ 0.01	78.7
$0.01 < d < 0.05$	13.6
$0.05 \leq d < 0.10$	6.5
$0.10 \leq d < 0.20$	1.2
≥ 0.20	0

It is obvious from Table 3:3 that this particular granite, although fairly rich in discontinuities, contains very few large passages. Even if it is assumed that the theoretical derivation underestimates the aperture by 100 % it would still mean that less than 10 % of all joints have an aperture larger than 0.1 mm and only slightly more than 1 % of all joints are as wide as 0.2 - 0.4 mm.

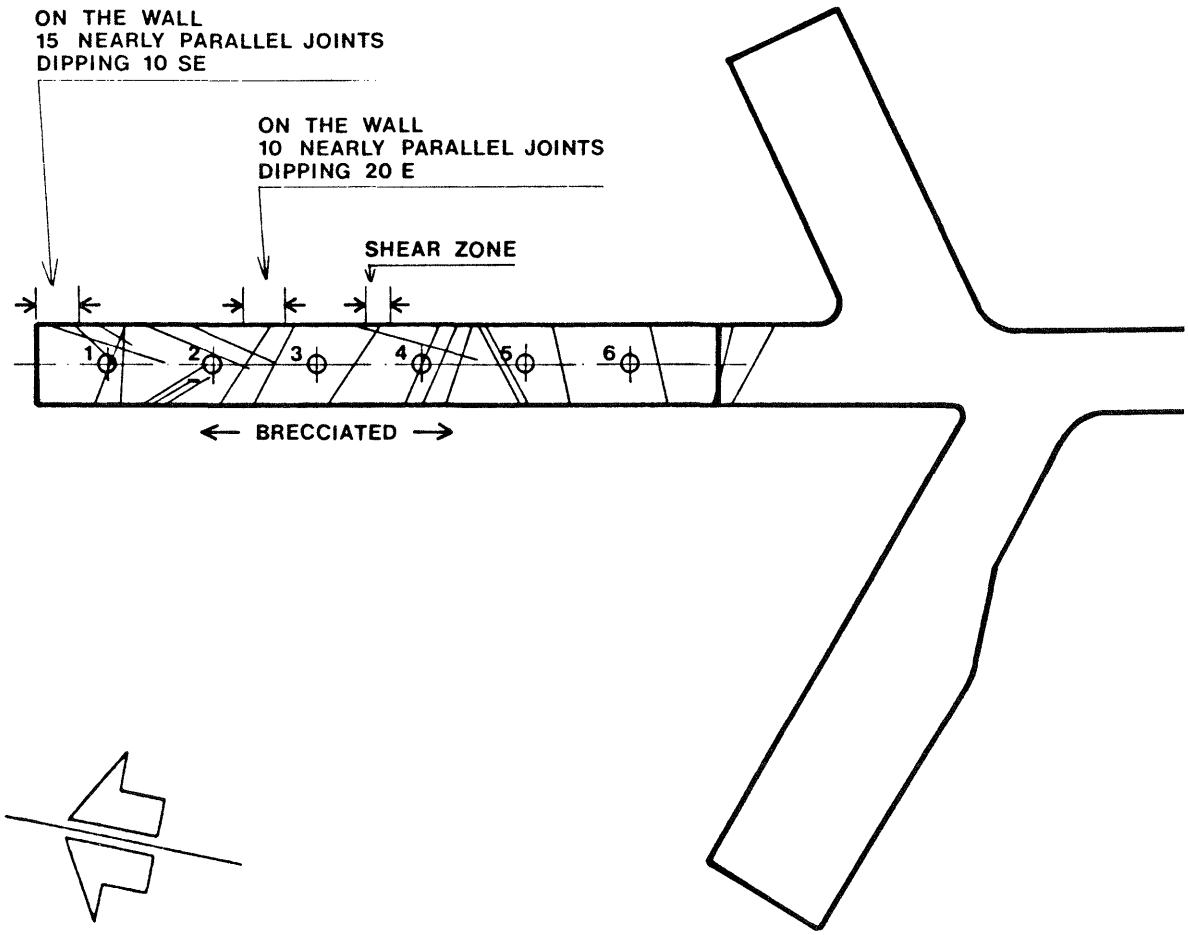

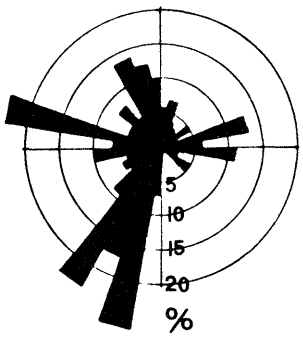

Fig. 3.1. Major rock structure features in the BMT area according to LBL surveys.

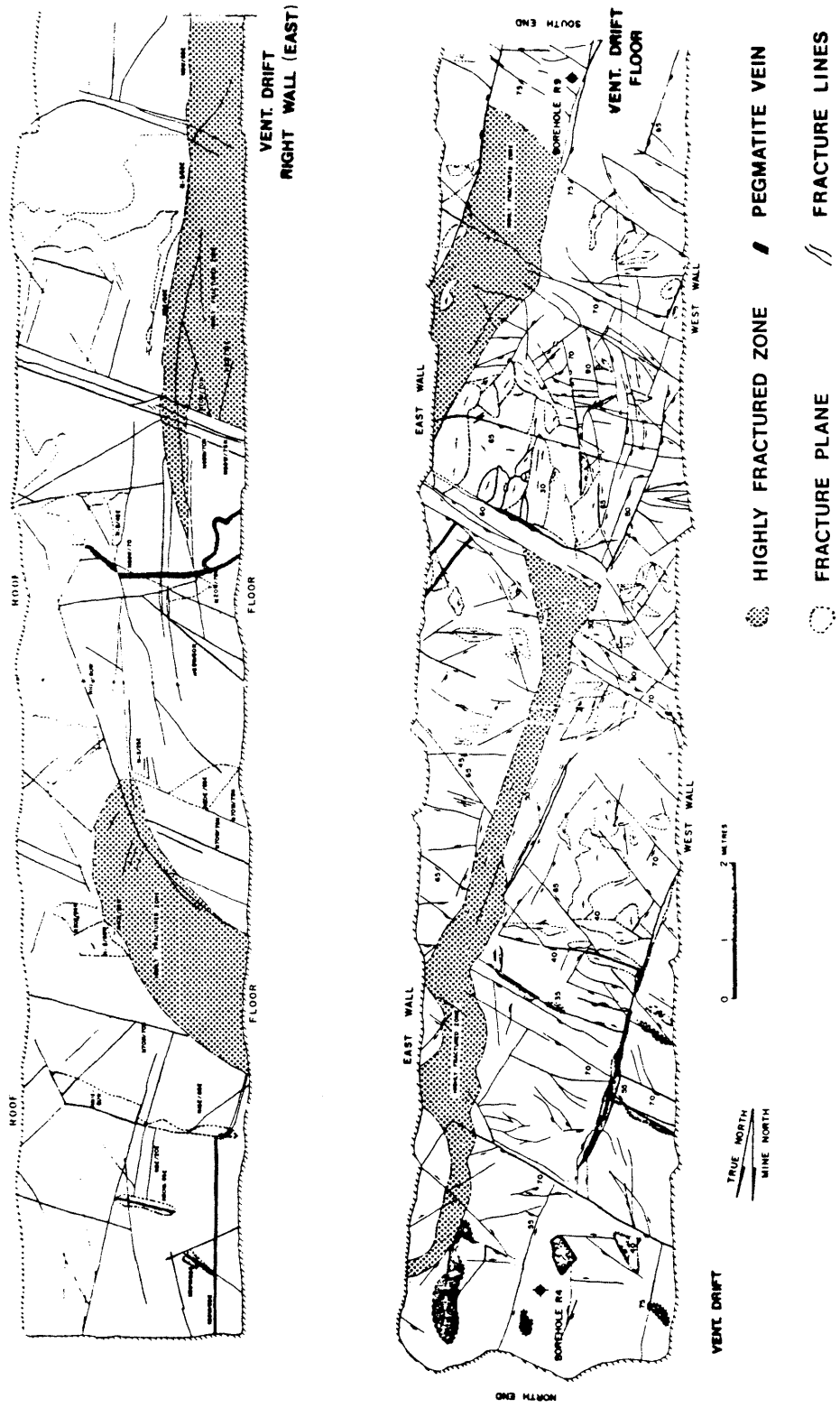

Fig 3.2. Detailed fracture map of the east wall and floor of the BMT tunnel (LBL).

The BMT study has involved modelling of the apertures of the joint and fracture sets in the tunnel by LBL. Fig 3.3 shows a generalized element model based on LBL:s mapping and evaluation of the inflow of water into the tunnel. Their computer-based derivation of the aperture of the major discontinuities suggests that it ranges from about 0.003 to 0.013 mm with a distribution similar to that of Table 3:3. It should be noticed that there is hardly any water inflow from the western side of the cylindrical tunnel according to this model, which will be discussed later in the report.

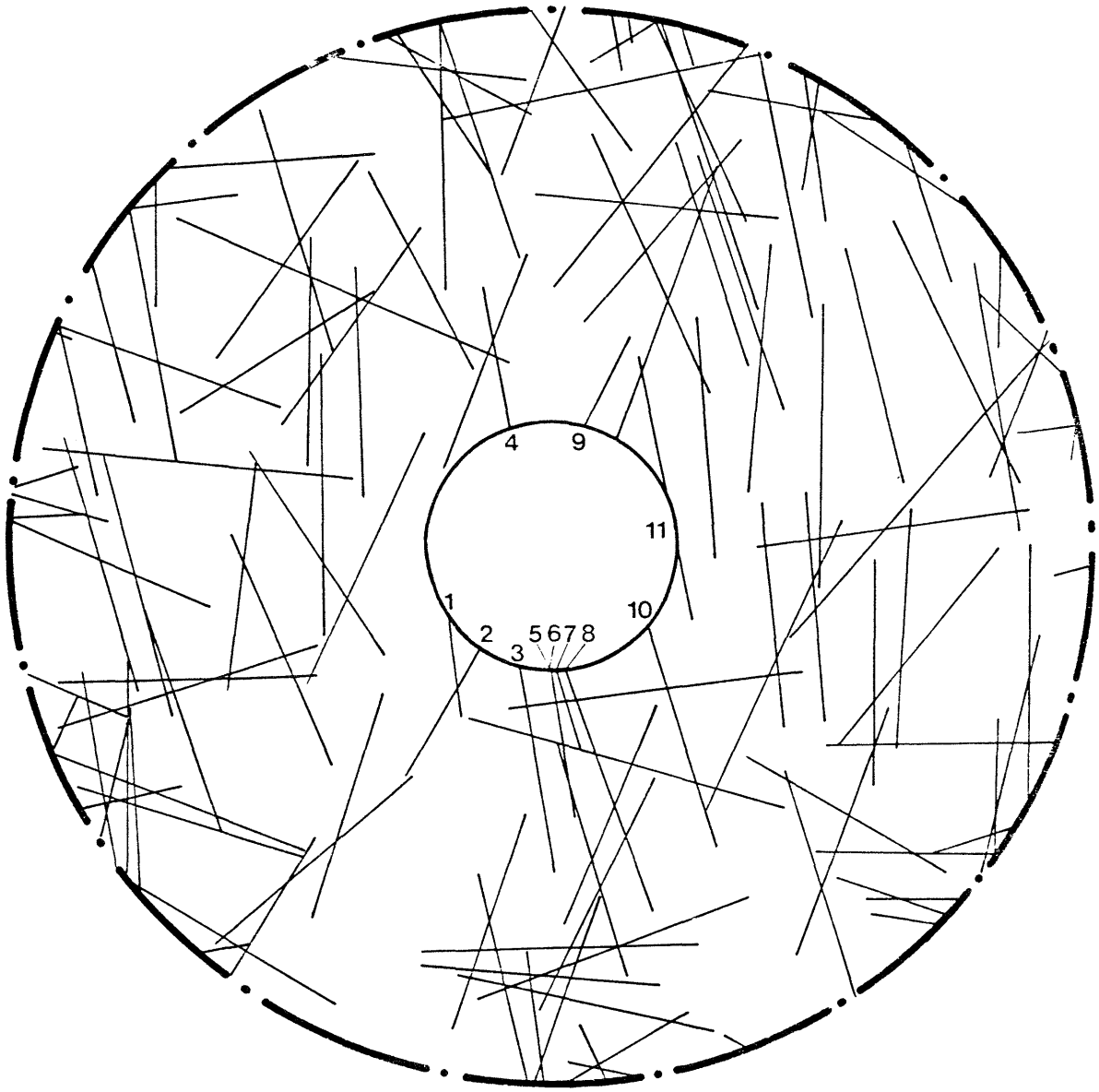

Fig 3.3. Generalized fracture mesh for computer treatment showing numbered fractures intersecting the tunnel, which is approximated to have a circular cross section (LBL). The left side is the western wall, the right one is the eastern wall

3.4.2.3 Heater holes

The selection of suitable sites for the heater holes was based on simple hydrologic tests in a number of Ø 56 mm pilot boreholes. These tests also involved core mapping which indicated that large differences in rock constitution could be expected in the finally

produced heater holes. This was confirmed when these holes were mapped with special reference to the presence of water-bearing joints and fractures (Fig 3.4-3.9). Holes no 1 and 2 were found to be located in rather fractured rock, while very few water-bearing discontinuities were observed in holes no 4 and 6. Holes no 3 and 5 were intermediate in this respect.

The fracture frequency is highest in the upper part of all the holes as can also be expected since the tunnel had been blasted with no particular caution. A few steeply oriented, intersecting joints or fractures were identified in all the holes. The correlation between the mapping of joints and fractures on one hand and the inflow of water on the other will be discussed in Chapter 3.5.3.

The mineralogical examination showed that most fractures were sealed by or coated with epidote, chlorite or calcite. Initially, little attention was paid to such features in the present study since they were not assumed to contribute to the inflow into the holes but, as will be discussed later, they are not unimportant water sources.

KEY TO FRACTURE LOGS

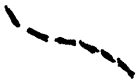

Open fracture without infilling material. The fracture caused by blasting (no infilling material, irregular fracture surfaces)

Distinct water-bearing open fracture. Natural fracture with infilling material or fracture induced by blasting (—·—·—·—)

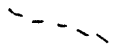

Open, not water-bearing fracture. Natural fracture with infilling material

Closed, dry natural fracture with infilling material

High concentration of infilling material

Pegmatite

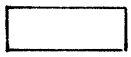

Concrete plate necessary for drilling of deposition hole

INFILLING MATERIAL IN FRACTURES

List of abbreviations

C	Calcite
K	Chlorite
E	Epidote
Pc	Pegmatite

REMARK

The mapping was executed by the Geological Survey of Sweden

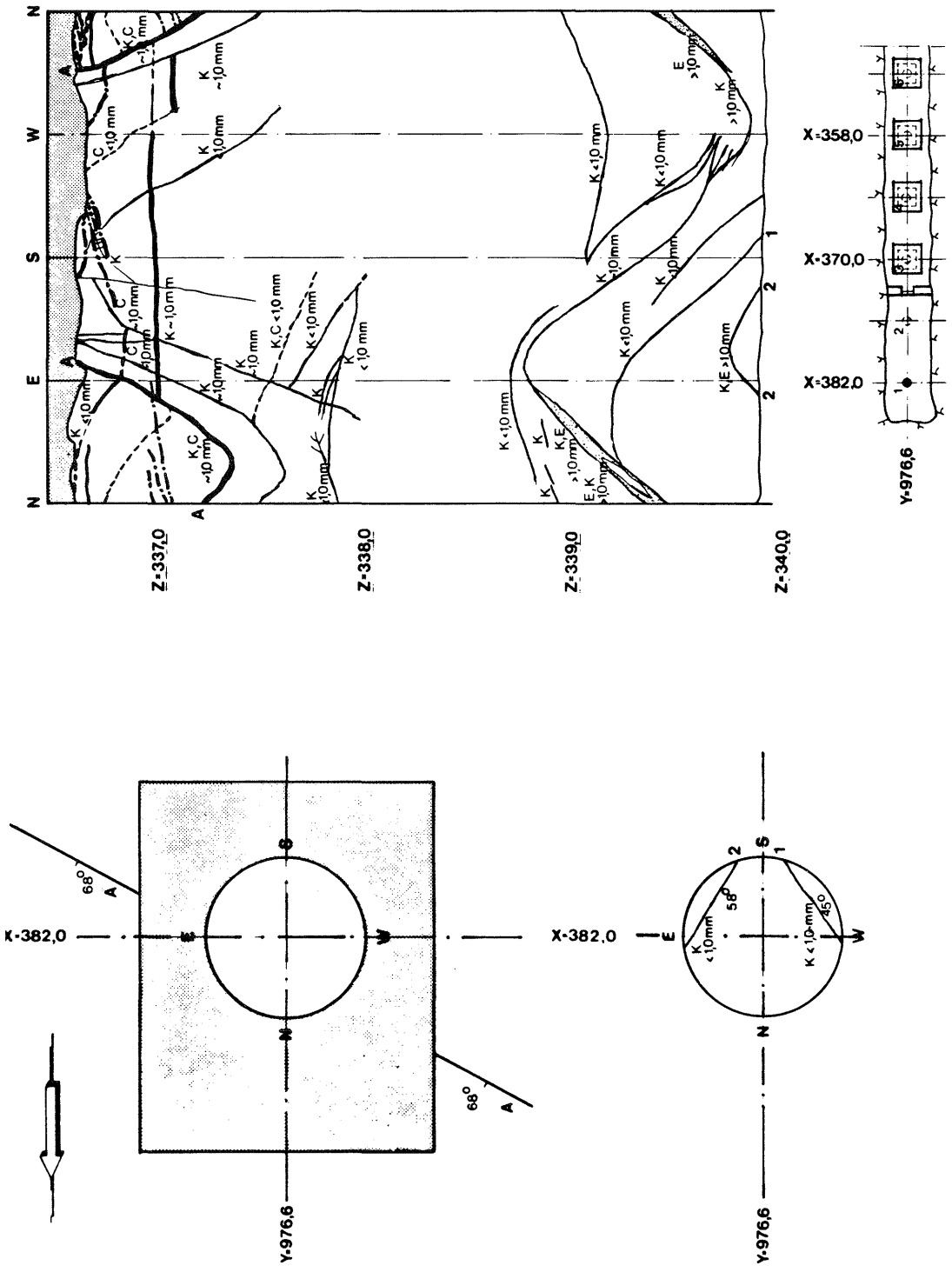

Fig 3.4. Major discontinuities in hole no 1

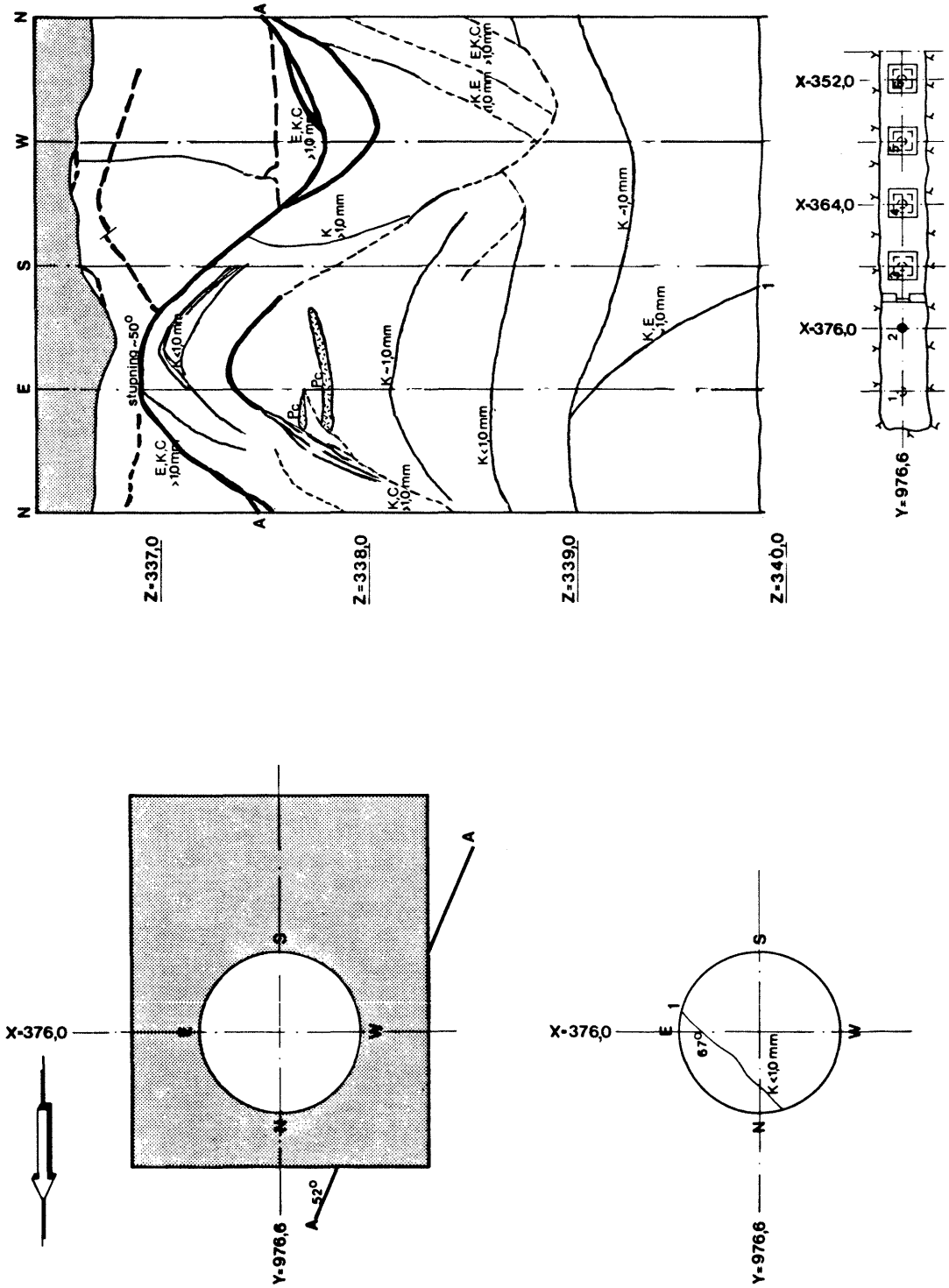

Fig 3.5. Major discontinuities in hole no 2

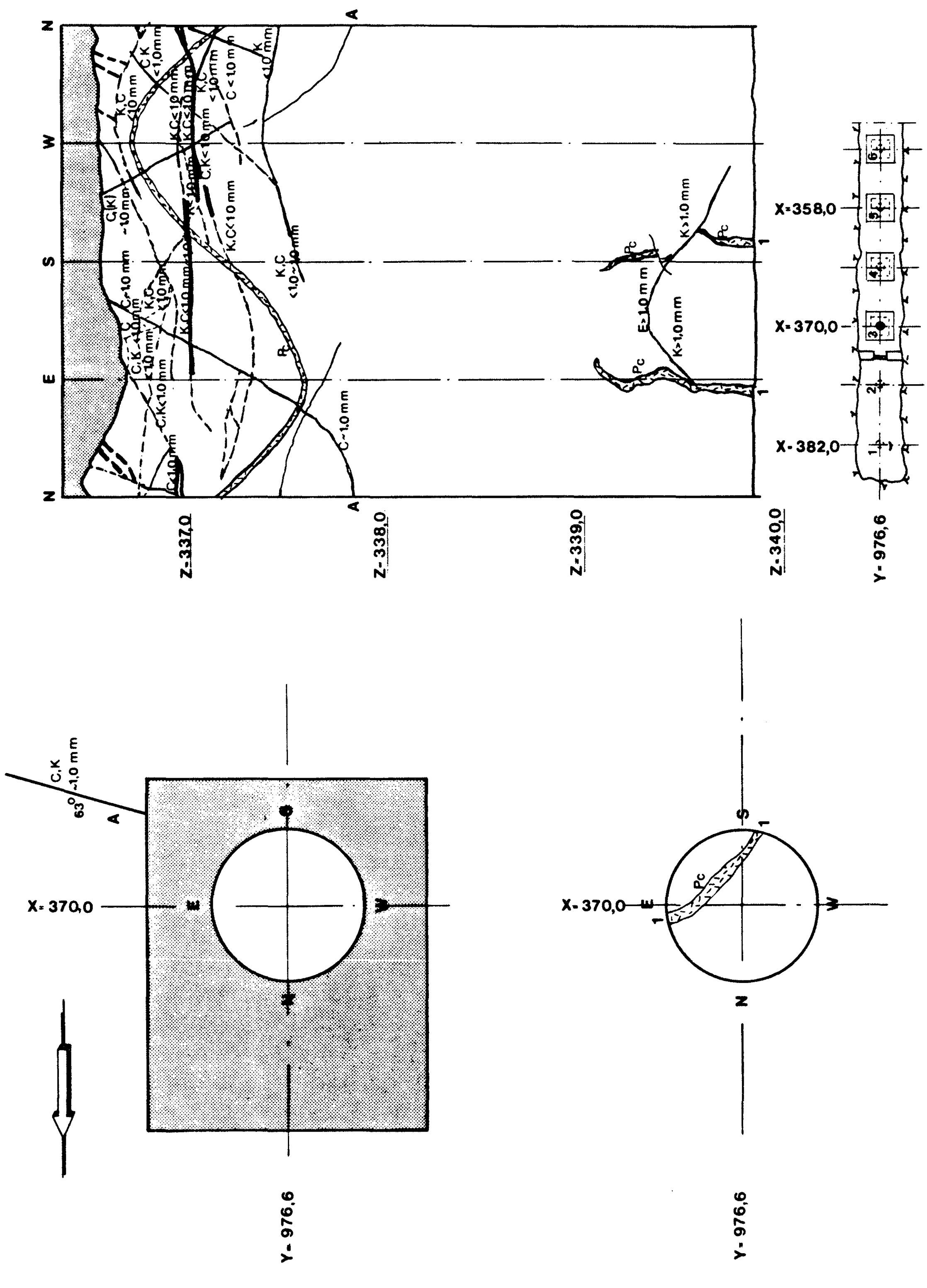

Fig 3.6. Major discontinuities in hole no 3

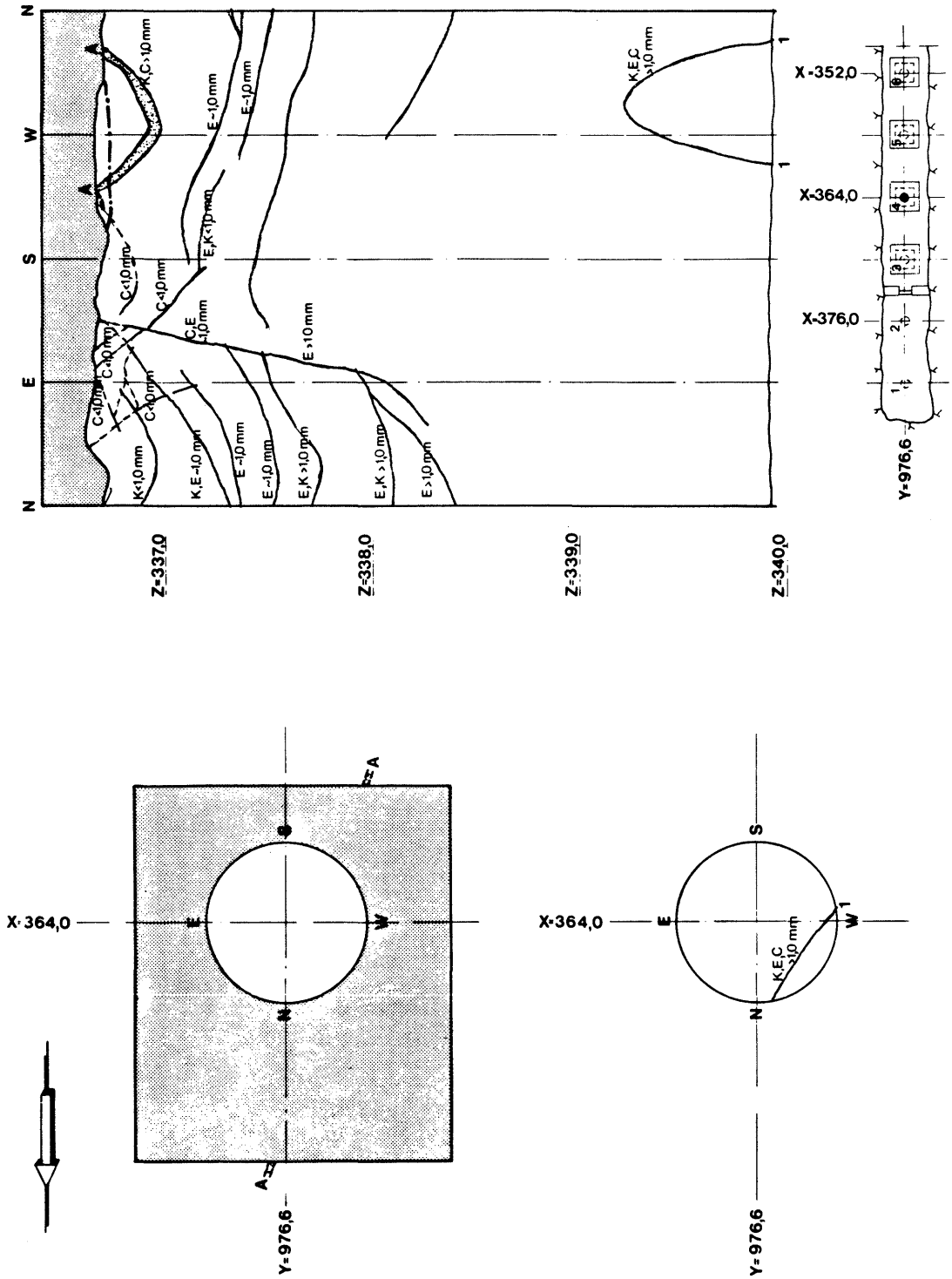

Fig 3.7. Major discontinuities in hole no 4

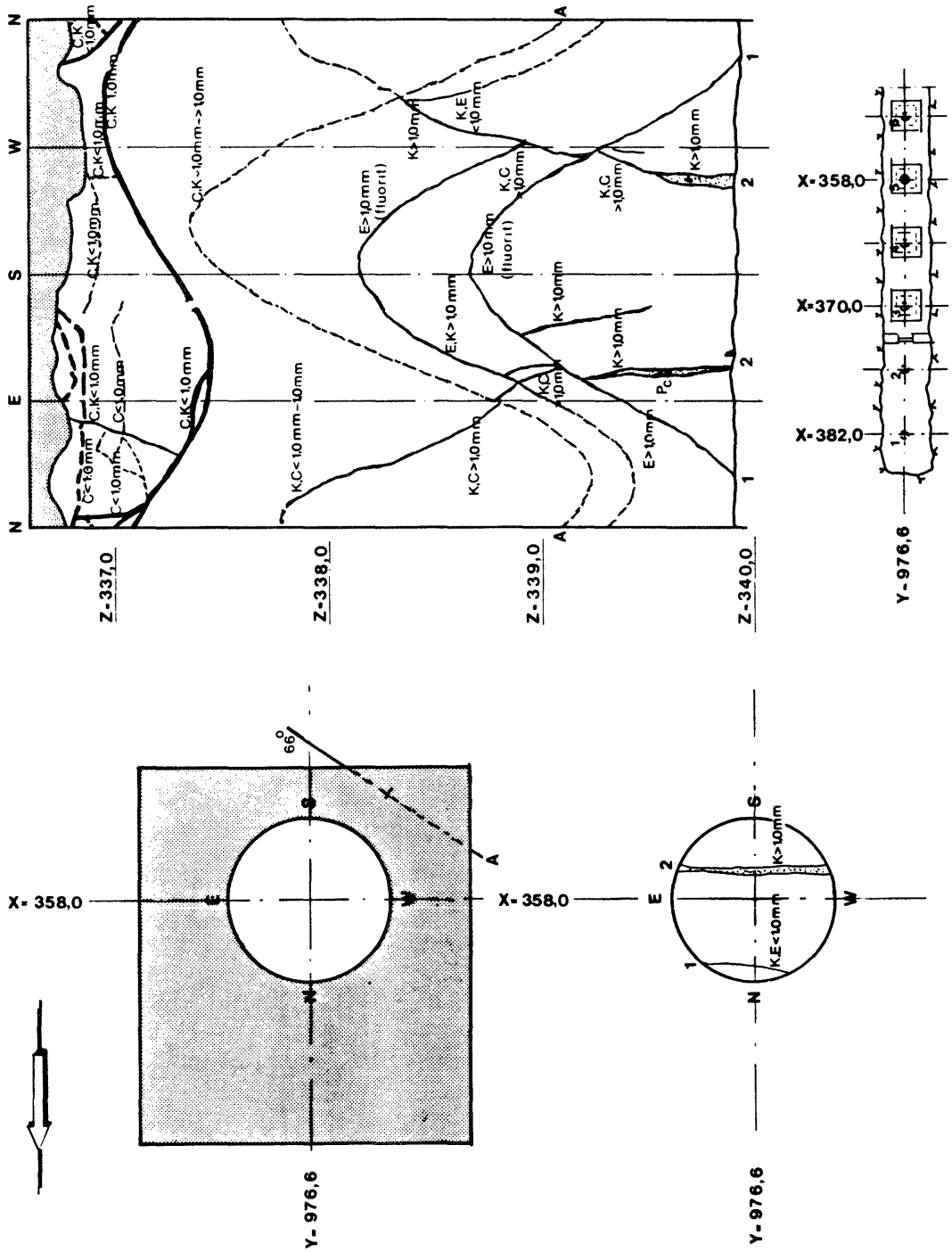

Fig 3.8. Major discontinuities in hole no 5

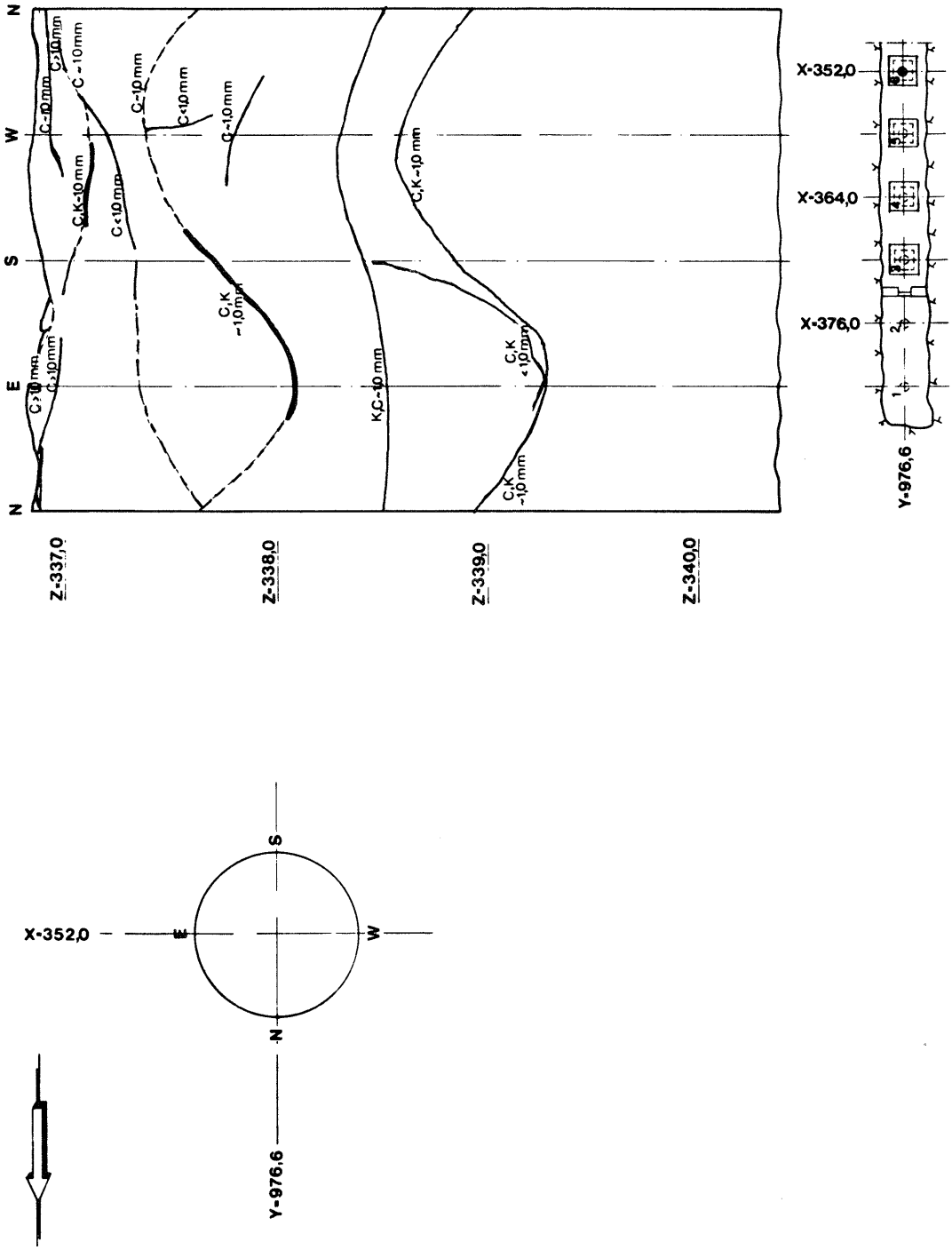

Fig 3.9. Major discontinuities in hole no 6

3.4.3 Rock Stress State

The in-situ stresses have not been measured in the BMT area but the general stress field is expected to be about the same as in the relatively closely located "Pilot Heater Test" and "Full-scale Heater Test" areas (Fig 3.10). Here, the Division of Rock Mechanics, University of Luleå, has determined the rock stresses by applying Leeman 3D overcoring technique (3). It is concluded from these investigations* that:

1 The major principle stress is about 20 MPa. It is horizontal and almost perpendicular to the BMT tunnel

2 The intermediate principle stress is about 10 Mpa. It is horizontal and almost parallel to the BMT tunnel

3 The minor principle stress is about 4 MPa. It is practically vertical

The vertical principal stress is significantly lower than the theoretical gravitational stress which may be caused by large-scale stress distribution effects generated by the excavations.*

The tangential stresses are probably low at the tunnel periphery in cross sections through the tunnel due to stress redistribution generated by the blasting, except for local contacts between neighboring blocks. The horizontal rock stress is probably up to 30 MPa one or two meters above the crown and below the floor of the tunnel, respectively. Superposition of induced stresses on the general stress field yields a tangential stress at the periphery of the heater holes of 5 to 55 MPa.

---

* Bengt Leijon, Division of Rock Mechanics, University of Luleå, pers. comm.

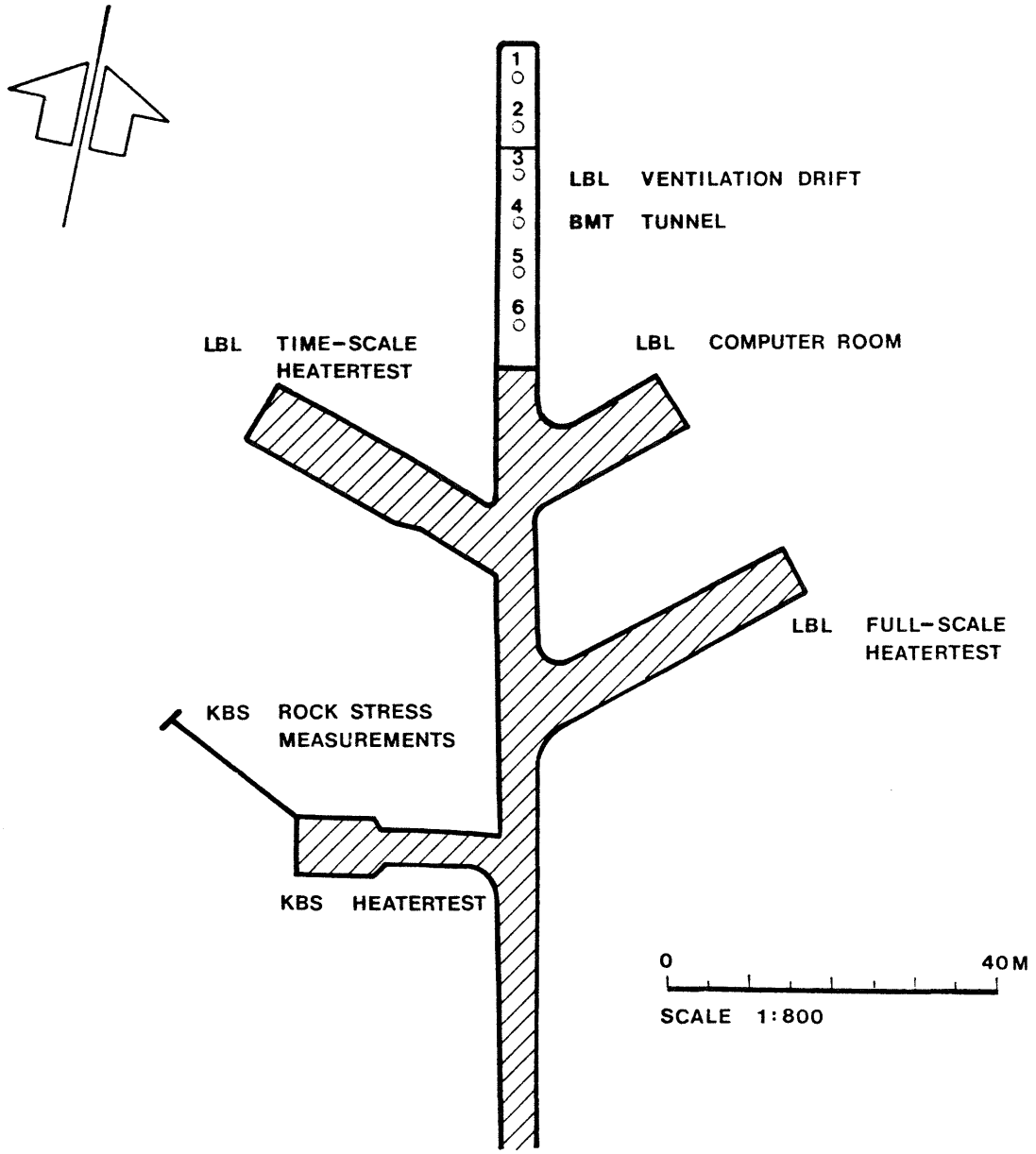

Fig 3.10. Location of sites for rock stress measurements

3.5 Hydrology

3.5.1 General

The average hydraulic conductivity of the Stripa rock mass is known to be low, as can be inferred from the very moderate pumping that is required to drain the mine. Evaluation of various tests has yielded a range of the hydraulic conductivity of 10^{-12} to about 10^{-10} m/s for most of the granite rock. Attempts have also been made to determine the hydraulic conductivity in the local BMT area. Thus, the LBL Macropermeability Test offers very valuable information on the water inflow characteristics, and additional tests of similar type that were performed later have also contributed to the understanding of the rather complex hydrologic conditions in the test area.

Careful petrologic studies by LBL (4) have shown that the granite, termed quartz monzonite by the investigators, is medium grained with very obvious microfracturing in the natural state of the rock. Although many of the very narrow discontinuities are closed, a fraction of them stay open and contribute to the hydraulic conductivity and to the migration of dissolved species. The rock matrix can therefore be regarded as a porous medium with a very low, but still practically important permeability. Laboratory experiments on block samples free from visible fractures, have yielded an average hydraulic conductivity of the crystal matrix of $5 \cdot 10^{-13}$ m/s (5).

For certain purposes, such as the choice of sufficiently corrosion-resistive steel qualities for various gauges, and for the prediction of possible mineral transformations, certain groundwater chemical data had to be known. In this respect, the conditions in the BMT area are assumed to be similar to those in the

rest of the mine, which are summarized in Table 3:4. The data are based on various tests by LBL and by the Geological Survey of Sweden (6).

Table 3:4 Chemical analyses of Stripa groundwater. Sample no 6 represents water from the DbH2 hole, which is very close to the BMT tunnel

Analysis	Water sample						
	1	2	3	4	5	6	7
pH field	6.7	6.5	7.3	7.0	8.7	9.1	8.9
Ca ppm			21	24	14	19	17
Mg ppm			5.7	4.7	0.3	0.5	0.3
Na ppm			4.0	4.5	51	37	61
K ppm			2.0	1.0	0.2	0.4	0.2
Cl ppm			1.5	4.0	49	44	85
SO_4 ppm			2.0	10.0	1.4	2.4	2.4
HCO_3 ppm	1	5	93	82	73	79	52
SiO_2 ppm			13.6	9.9	12.0	12.0	12.1
Fe ppm					0.06		
NO_2 ppm					0.01		
NO_3 ppm					0.12		
PO_4 ppm					0.01		
NH_4 ppm					0.14		

3.5.2 Tunnel

3.5.2.1 The Macropermeability Test

The Macropermeability Test was an attempt by LBL to determine the hydraulic conductivity of a large volume, i.e. about 200 000 m^3, of rock (7). It was evaluated on the basis of measured water inflow into the sealed, 33 m long inner part of the tunnel, and

recorded water pressures at various distances from the tunnel periphery. Since the flow rate into the tunnel was so low and the surface area so large that a significant fraction of the inflow would be lost to evaporation and the remainder impossible to collect, the LBL group decided to evaporate all inflowing water and determine the seepage rates by measuring the net moisture pickup in the heated air of a closed ventilation system. Tests were run at air temperatures of about 20, 30, and 45°C followed by a cool-down test back to 20°C.

The average "radial" hydraulic gradient, which had to be known for the evaluation of the gross hydraulic conductivity, was determined by measuring the water pressure in 90 isolated intervals in Ø 76 mm boreholes (Fig 3.11-3.13). Each packer-confined interval was about 5 m long, i.e. a length intended to include 15 to 20 water-bearing fractures.

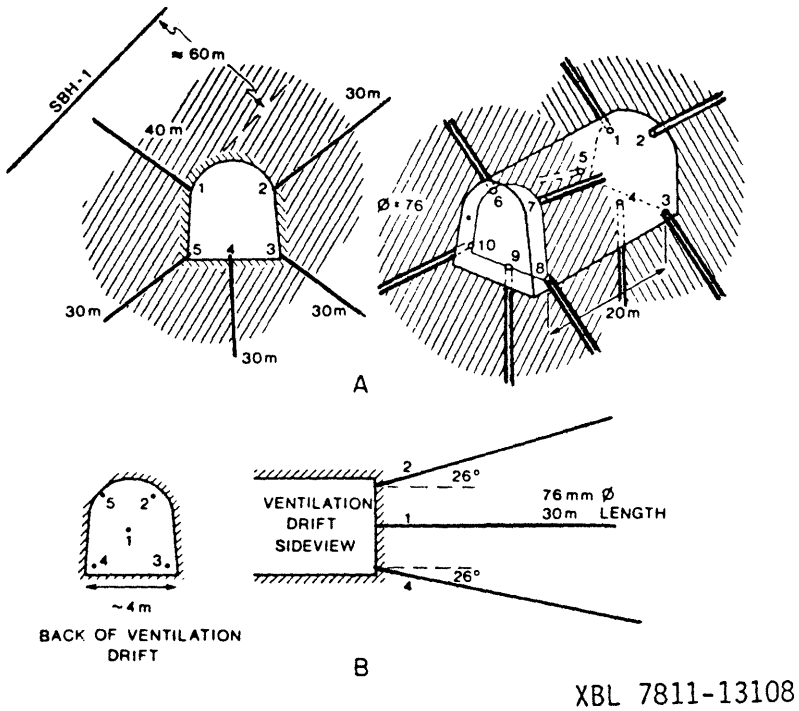

Fig 3.11. LBL boreholes used for the Macropermability Test

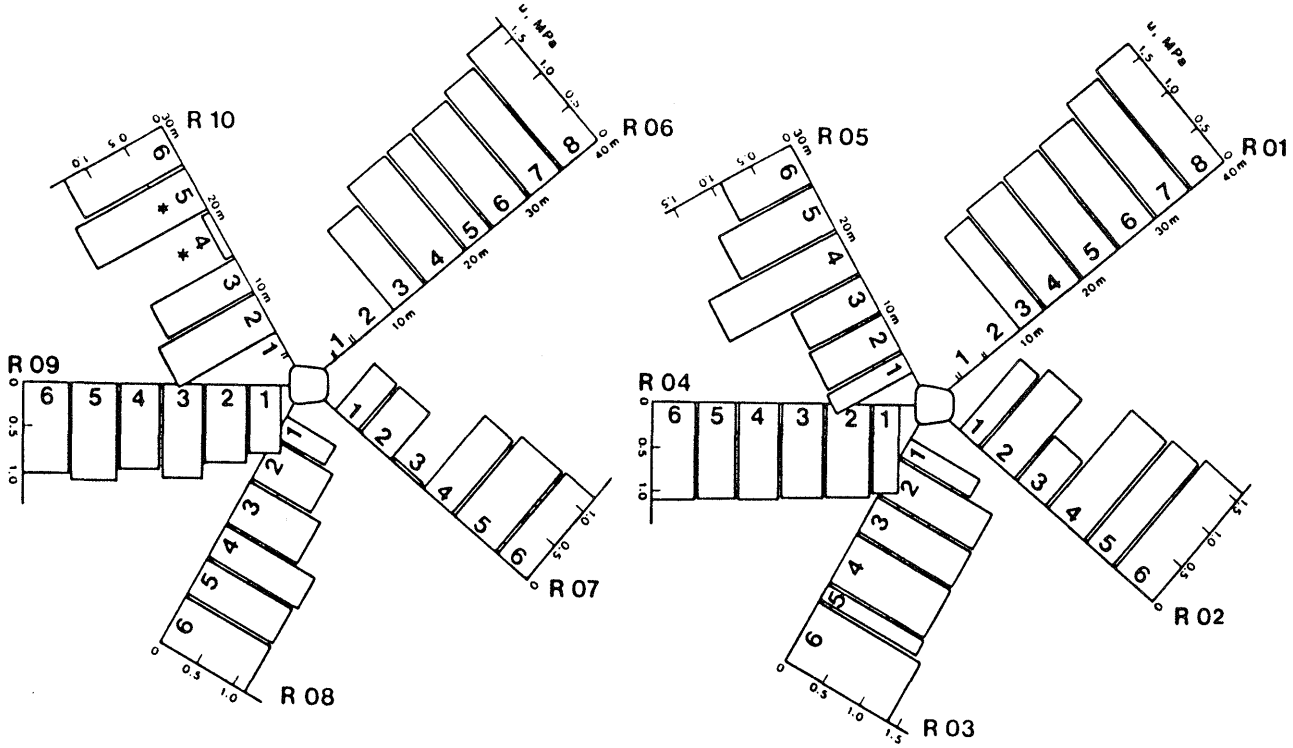

Fig 3.12. Pressure diagrams representing the water pressure distribution in the final phase of the LBL test. R 01 is equivalent to the radially oriented no 1 in Fig 3.11, R 02 to radial no 2 etc

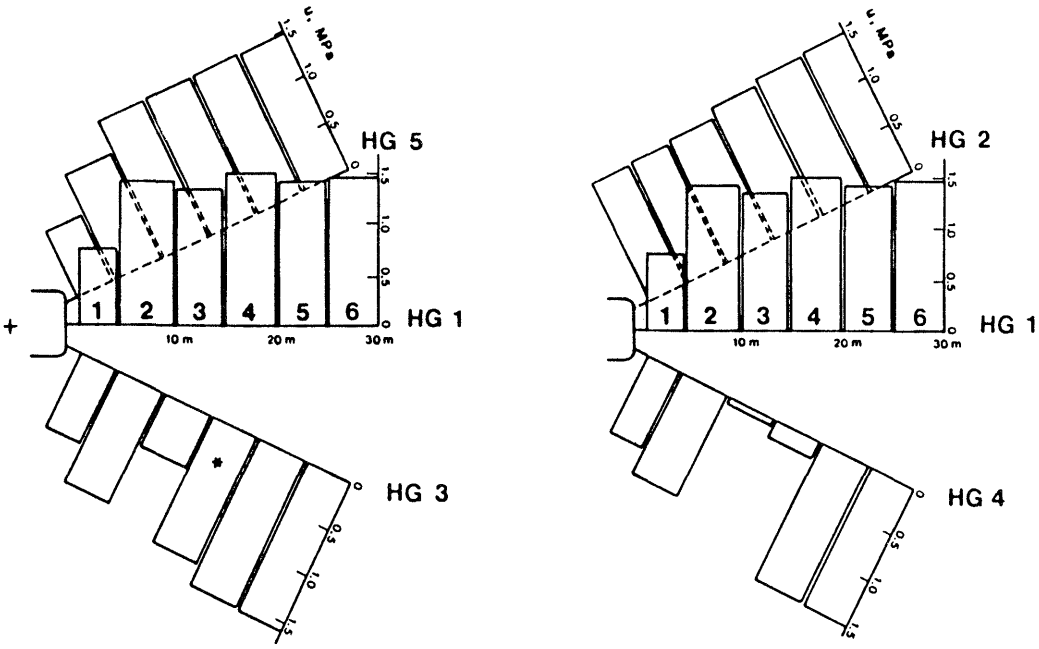

Fig 3.13. Pressure diagrams representing the water pressure distribution in the final phase of the LBL test. HG 1 is equivalent to the front face hole no 1 in Fig 3.11, HG 2 to hole no 2 in the same figure, etc

The outer end of the sealed tunnel in LBL:s experiment was situated approximately where heater hole no 6 is located in the Buffer Mass Test, so the inflow characteristics determined by LBL are of profound interest to the latter test. The average inflow under reasonably steady flow conditions in LBL:s tests with different temperatures are summarized in Table 3:5.

Table 3:5. Results of the Macropermeability Test (8)

Test no	Nominal temp °C	Average flow ml/min	Gross hydraulic conductivity, m/s
1	20	50	$1.0 \cdot 10^{-10}$
2	30	42	$9.4 \cdot 10^{-11}$
3	45	43	$1.0 \cdot 10^{-10}$
4	20	47	$9.8 \cdot 10^{-11}$

The evaluated gross hydraulic conductivity was derived by application of the Thiem equation for steady radial flow to a long cylindrical opening in a homogeneous isotropic porous medium. As will be shown later the water inflow data may underestimate the real inflow at normal rock temperature.

When the establishment of the BMT field work started in October 1980 practically all of the LBL equipment was still in operation and the installations were left in the holes except for those of hole R9, which coincides with heater hole no 4. Each of the HG- and R-holes was equipped with 5-8 packers expanded by use of nitrogen gas, the pressure being about 5 MPa, and already in the course of the LBL study, gas leakage was noticed and it became obvious at the onset of the Buffer Mass Test. Since the recorded pressures could be significantly affected by this, the installations were rearranged so that the gas could be omitted. In all the holes, except for R5 and R9, the packer situated closest to the tunnel wall was removed and replaced by a steel tube. The equipment was then inserted again to approximately the original position with the remaining packers deflated. After inflating the outer packer the space in the hole between this packer and the tunnel wall was injected with cement mortar which was left to solidify. The gas pressure was then released so that that the sealing was thereafter produced only by the outer cement plug. Thus, the rest of the hole formed one continuous chamber which was filled with water by using the tubings of the old LBL arrangement (Fig 3.14). They were reconnected to the manometer panel but while the LBL study allowed for individual determination of the piezometric head in several sections of the holes, the BMT readings represented average pressures over the entire length of each hole.

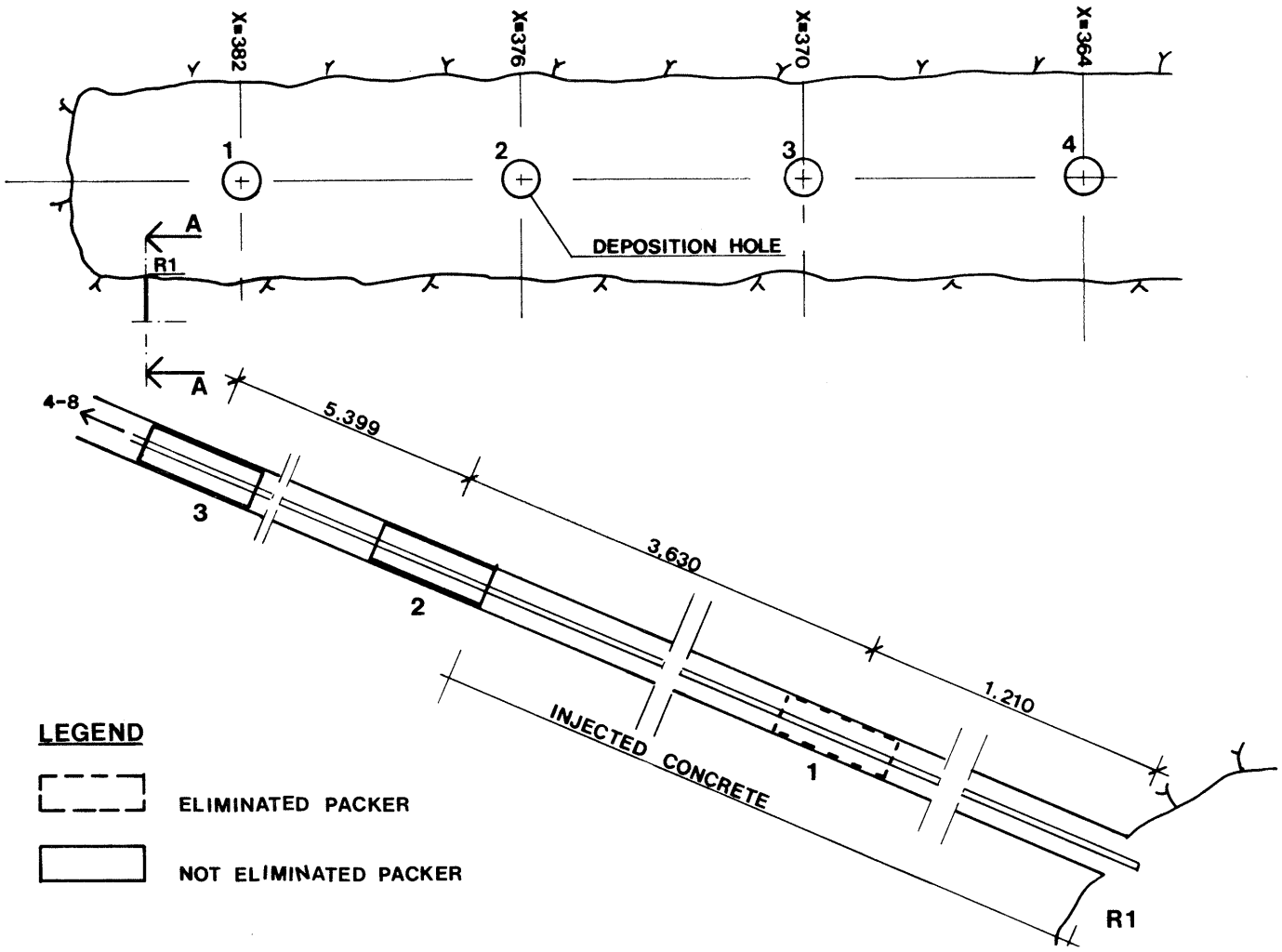

Bore-hole Nº	Injected zone in m	Distance between packer in m 2-3	3-4	4-5	5-6	6-7	7-8
HG 1	4.740	5.260	4.709	5.005	4.918		
HG 2	5.370	4.384	4.882	5.112	5.332		
HG 3	4.640	4.990	4.900	5.112	5.211		
HG 4	4.640	5.268	4.669	4.989	5.235		
HG 5	4.680	4.991	5.008	4.996	5.003		
R 1	4.640	5.399	3.501	5.443	5.410	5.148	4.720
R 2	4.060	5.154	4.761	5.514	4.135		
R 3	4.370	4.848	4.589	6.189	2.556		
R 4	4.450	5.387	5.001	4.999	4.535		
R 5	~1.000	--	--	--	--		
R 6	3.860	5.555	4.706	5.861	3.833	5.337	4.802
R 7	4.730	4.961	4.488	4.683	6.301		
R 8	3.990	5.370	5.549	4.252	4.799		
R 9		No packers					
R 10	3.590	5.002	4.478	5.363	5.341		

Fig 3.14. Equipment in LBL-holes after rearrangement.

3.5.2.2 The simplified "drying" procedure

In conjunction with the preparation of the bulwark for the Buffer Mass Test it was suggested* that a simple version of the macro-permeability test be run to estimate the inflow into the inner part of the BMT tunnel. The suggested technique was to use large standard air-drying units which are ordinarily installed for removing moisture from buildings. Two devices of this sort, which were set to keep the relative humidity constant at about 70 %, were in operation for a few weeks (Fig 3.15). This was sufficient to yield approximate equilibrium between water inflow and condensation, the evaluated inflow being estimated at about 13 ml/min into the inner 12 m long part of the tunnel. This quantity would thus correspond to 1/3 to 1/4 of the inflow in the entire 33 m long tunnel, which suggests that water enters it rather uniformly. Recently, it has been concluded that the heat generated in the drying process most probably had a significant effect on the water inflow. Thus, the air temperature, which ranged between 30 and 35°C, produced a heating of shallow rock through which the aperture of water-bearing fractures must have been reduced. This effect has been observed in the ongoing tunnel plug test (Stripa Phase II), where the tunnel dimensions are about the same as in the BMT case, and where the flow drop was approximately 50 % at heating from virgin rock temperature to 30-35°C. Applying this finding to the BMT, the real water inflow into the inner 12 m long part of the drift would probably be about 25 ml/min at a rock temperature of 13-15°C. This would correspond to 35-40 l per day.

---

* Anders Bergström, SKBF/KBS

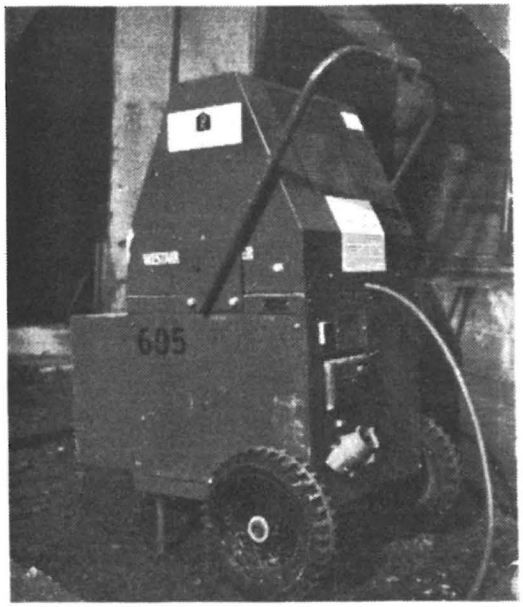

Fig 3.15. Air-drying unit with condensate collector

The distribution of the inflow of water into the BMT tunnel was also estimated by identifying the successive moistening of the roof and walls after stopping the ordinary ventilation during one weekend. The evaluation of these observations* was rather subjective and uncertain because of the difficulty of deciding whether the moisture which appeared orginated from areas with many narrow fractures or from water flowing from individual large discontinuities. Fig 3.16 - 3.19 show the interpretation of the study, which can only be taken as a rough illustration of where water preferably enters the roof and walls. The floor could not be mapped in this way.

It is obvious from the plottings that the eastern wall has the largest water-bearing zones, while the tunnel front is the driest part of the test site. The flow through the western wall is largely dominated by a few discontinuities which are strongly or moderately water-bearing. The roof shows an inflow pattern that is similar to that of the western wall. Most water seems to enter the central part of the roof, i.e. between heater holes no 1 and 2.

---

* Observations by Hans Carlsson, KBS, and Lennart Börgesson, SGAB

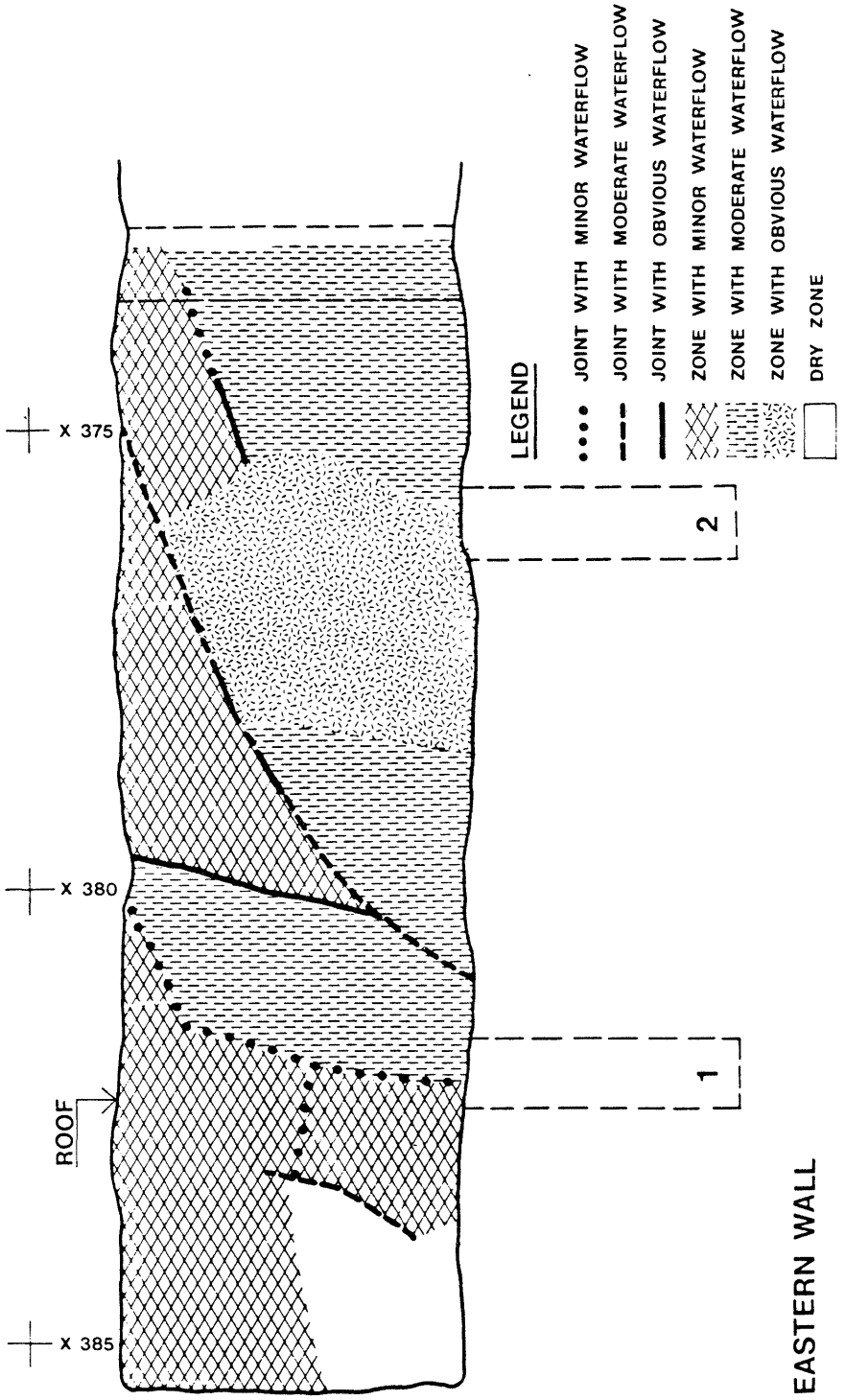

Fig 3.16. Generalized water inflow pattern in the BMT tunnel, eastern wall

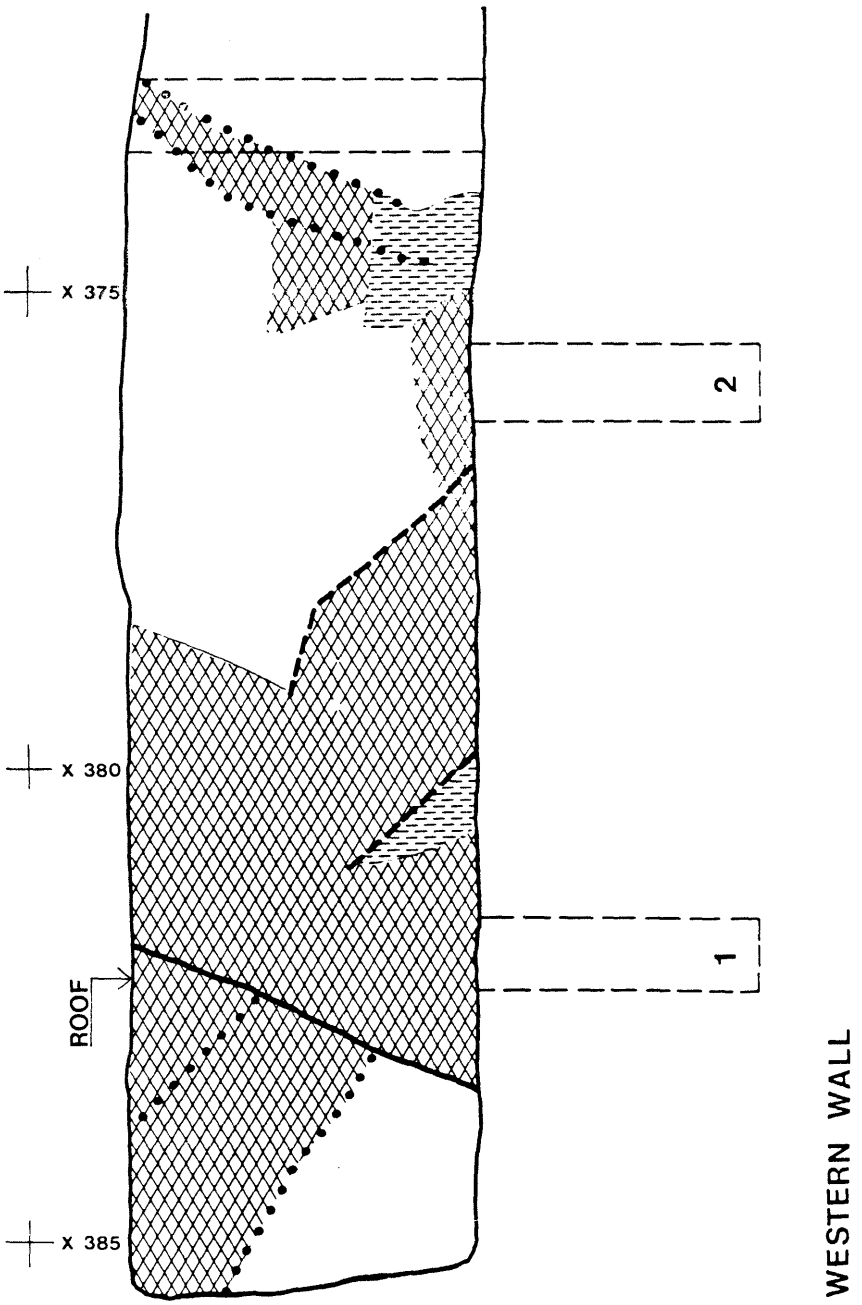

Fig 3.17. Generalized water inflow pattern in the BMT tunnel, western wall

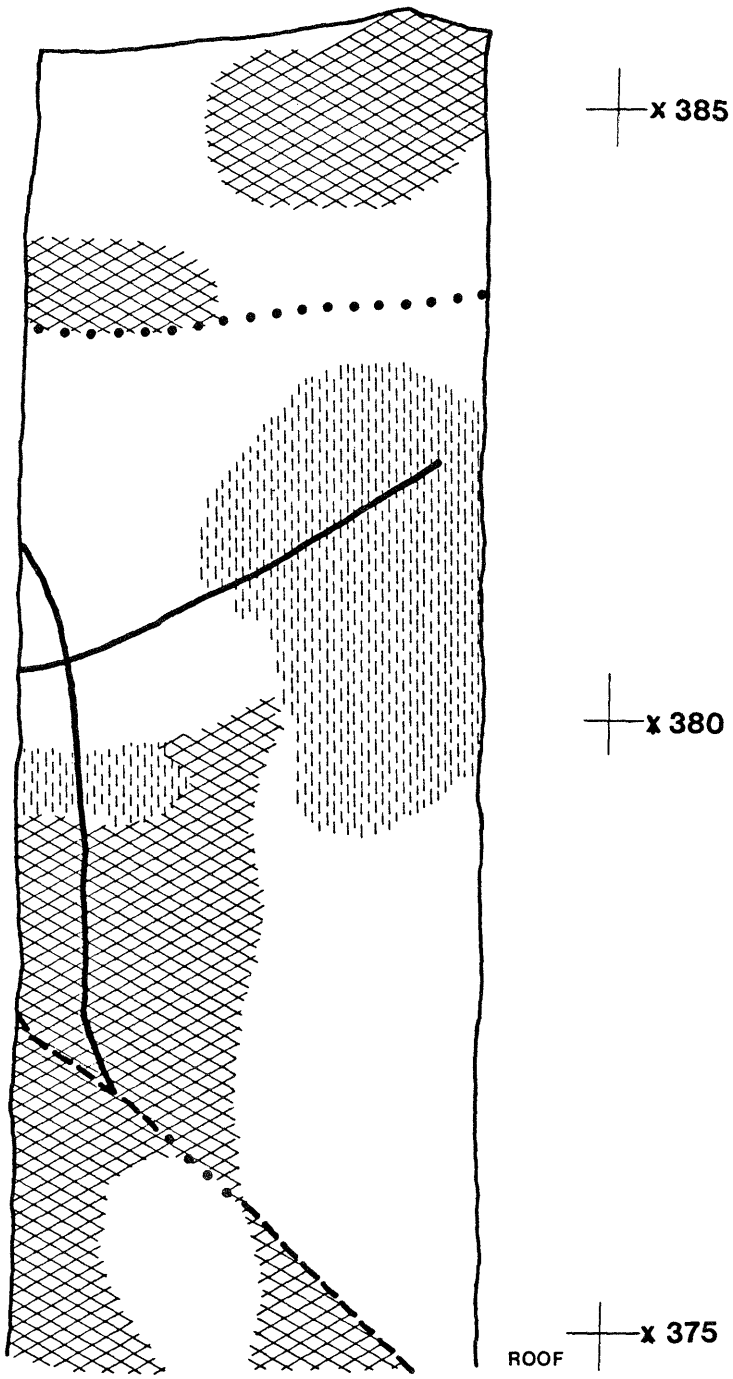

Fig 3.18. Generalized water inflow pattern in the BMT tunnel, roof

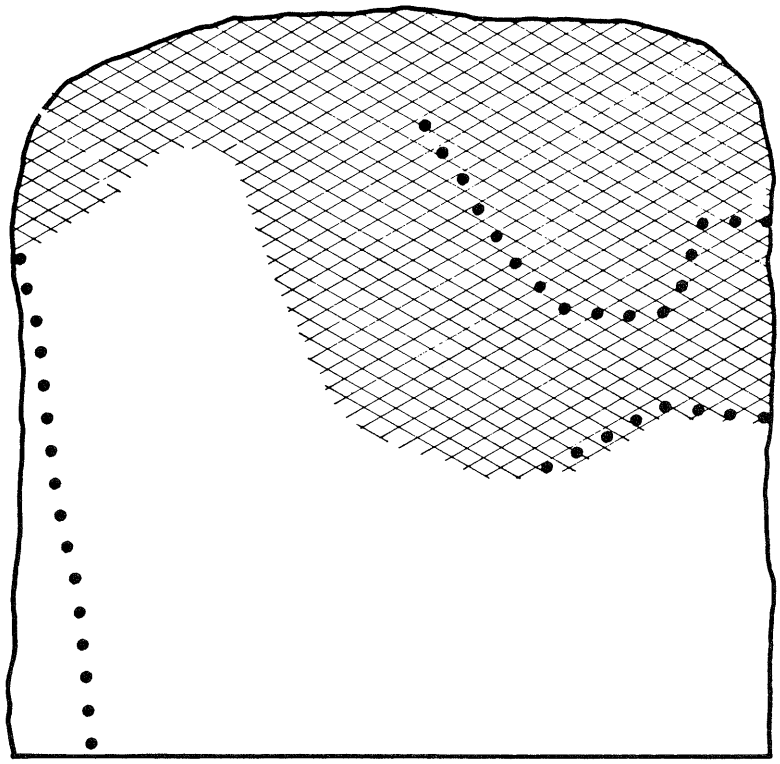

Fig 3.19. Generalized water inflow pattern in the BMT tunnel, front

3.5.3 Heater holes

3.5.3.1 Pilot holes

Twelve Ø 56 mm pilot holes were drilled in the tunnel floor to find proper positions of the six large heater holes (1). Six of the pilot holes (1A - 6A) indicated suitable conditions with respect to water inflow and degree of fracturing and these pilot holes were core-mapped and used for water inflow tests. The location of open, natural joints or fractures in the cores is summarized in Table 3:6.

Table 3:6. Fracture mapping of pilot holes. Figures denote the number of natural discontinuities in each core length interval (L Jacobsson & H Norlander)

Depth below tunnel floor m	Hole number					
	1A	2A	3A	4A	5A	6A
0 - 0.25	1	2	RF*	2	0	2
0.25 - 0.50	2	2	RF	1	0	1
0.50 - 0.75	1	0	3	2	2	0
0.75 - 1.00	2	1	4	1	RF	0
1.00 - 1.25	3	1	3	1	2	0
1.25 - 1.50	1	1	2	0	2	2
1.50 - 1.75	0	1	0	0	1	0
1.75 - 2.00	2	1	2	0	2	0
2.00 - 2.25	0	0	1	1	0	0
2.25 - 2.50	2	3	1	1	1	1
2.50 - 2.75	RF	3	1	0	0	1
2.75 - 3.00	1	1	2	4	1	0
3.00 - 3.25	3	0	1	1	3	0

---

* RF stands for richly fractured rock

The mapping shows that while holes no 1A, 3A and 5A are rich in joints and fractures, 4A and particularly 6A contain few discontinuities. Hole no 2 is intermediate in this respect. Holes no 4A and 6A are fracture-free over a considerable axial length, while the discontinuities are fairly uniformly distributed in the other holes.

Simple inflow tests were run in the holes to get a rough measure of the water-bearing capacity of the intersecting joints and fractures. For this purpose, the holes were first completely drained and then allowed to be filled by inflowing groundwater, which was pumped out after 1 day. The inflow capacity is given in Table 3:7.

Table 3:7. Inflow rate in pilot holes; average over 4 days

Hole no	Water inflow l/day
1A	6.2
2A	5.6
3A	3.0
4A	0.2
5A	1.9
6A	0.2

It is concluded that the water inflow is roughly in accordance with the fracture frequency. Thus, holes no 1A, 3A and 5A carry much water, while holes no 4A and 6A are fairly dry. It is reasonable to believe that the moderate inflow in the fracture-rich hole no 3A is due to rather small apertures.

3.5.3.2 Full-size heater holes

Ocular inspection was made to identify water-bearing parts of the holes in connection with the detailed fracture mapping which was described in Chapter 3.4.2.3. This operation was difficult because surface water flowing from the tunnel walls and floor drained into the holes and masked the inflow regions deeper down in the holes.

A qualitative determination was made by use of a simple movable packer for the collection of inflowing water on various levels (Fig 3.20). Unforeseen practical difficulties and time shortage appeared at the recording of hole no 3, while the other holes could be investigated reasonably well. However, the inflow data, which are given in Table 3:8, can only be taken as a rough relative measure of the water-bearing capacity since surface water emanating from ongoing drilling operations nearby in the tunnel probably affected the measurements.

Table 3:8. Inflow rate in heater holes

Hole no	Water inflow, l/day			
	Upper half	Lower half exc. lowest 20 cm	Lowest 20 cm	Total
1	3.7	1.1	0.7	5.5
2	8.0	1.2	1.6	10.8
3	-	-	-	-
4	2.7	3.2	-*	5.9
5	-	-	-	6.7
6	Upper and lower halves = 0.8		0.2	1.0

---

* Water flowed richly from a deep preexisting LBL hole (R9)

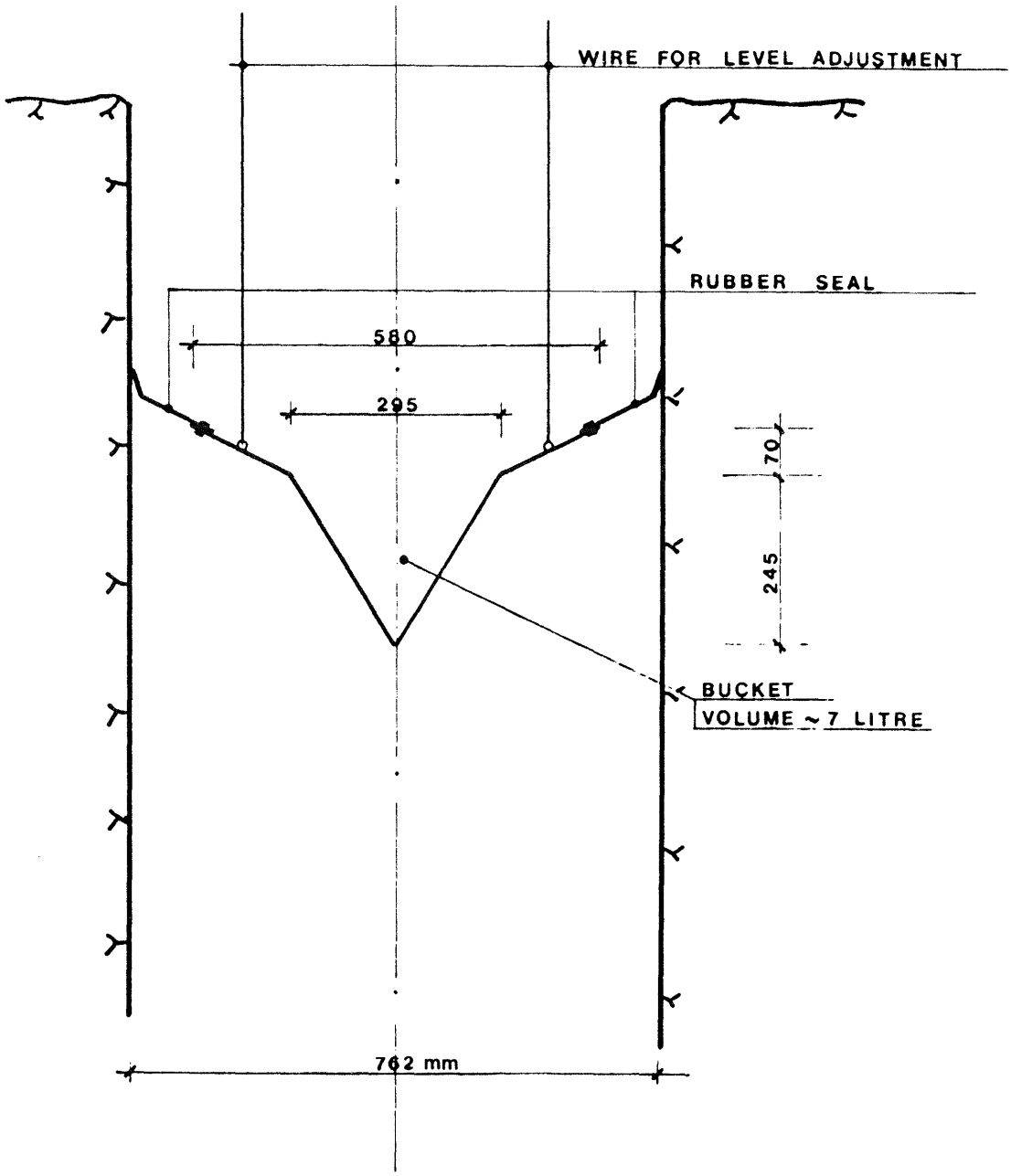

Fig 3.20. Device for collecting inflowing water in the heater holes

This investigation indicates that the general conclusions from the pilot hole study hold also for the large concentric heater holes, except for no 4 which has an inflow comparable to that of hole no 1. A critical analysis of all the inflow recordings for the heater holes shows that no direct comparison can be made between the pilot holes and the full-size heater holes because the hydrologic conditions were largely different when the respective tests were run. Thus, the inflow into all the holes was dominated by the fracture-rich tunnel floor which was exposed to quite different amounts of water at different occasions. The most reliable inflow characteristics are probably offered by the pilot holes.

After the termination of the BMT, i.e. after removal of all the buffer materials, a comprehensive inflow measurement was made in the heater holes. It yielded the total inflow data shown in Table 3:9 which demonstrates that hole no 3 behaved as a relatively "wet" hole, most of the water entering the hole at its base. The measuring technique was different from the previously applied one which does not allow for a direct comparison between Tables no 3:8 and 3:9.

Table 3:9. Repeated measurement of the inflow rate in heater holes 2 months after removal of the buffer materials

Hole no	Water inflow, l/day
1	6
2	85
3	11
4	-
5	11
6	1

4 TEST ARRANGEMENT

4.1 Buffer materials

4.1.1 Bentonite component

4.1.1.1 General

Commercial Na Bentonite (MX-80) produced by the American Colloid Co was chosen as clay component of the buffer material at an early stage of the BMT planning since much of the preceding systematic laboratory investigations concerned this particular bentonite, and since it is reasonably well defined from a soil classification point of view. Other smectite-rich clays may well be used in repositories for barrier purposes.

The bentonite, which was deposited in the form of volcanic ash in shallow sea where Wyoming and South Dakota are now situated, is of Ordovician age. It is rich in smectite minerals, mainly montmorillonite, and is largely saturated with sodium ions.

The shaly clay is mined and stockpiled for several months near the pit and is then ground and dried. The MX-80 material used for the BMT was bulk-transported to the Bentonit Int., GmbH, plant in Duisburg in West Germany where it was stockpiled and filled in paper bags for railway transportation to Stripa. The Swedish company Ahlsell IR, Stockholm, delivered the material.

4.1.1.2 Composition

Numerous determinations of the granular, mineralogical and chemical properties of the Wyoming bentonites have been reported in literature. The clay content (particles with a Stoke diameter less than 2 μm) is known to be 80-90 % as concluded from sedimentation analyses of ultrasonically dispersed material and this fraction

has a montmorillonite content of 80-90 %. Fig 4.1 shows a typical X-ray diffractogram with a (001) peak displacement from 12.9 Å to 17.4 Å upon ethylene glycol treatment, the displacement being diagnostic of sodium saturation of the montmorillonite. Silt is the dominant remaining fraction which mainly contains quartz and feldspars as well as some micas, sulphides and oxides. The chemical composition is typical of such mineral assemblies, an example being given in Table 4:1.

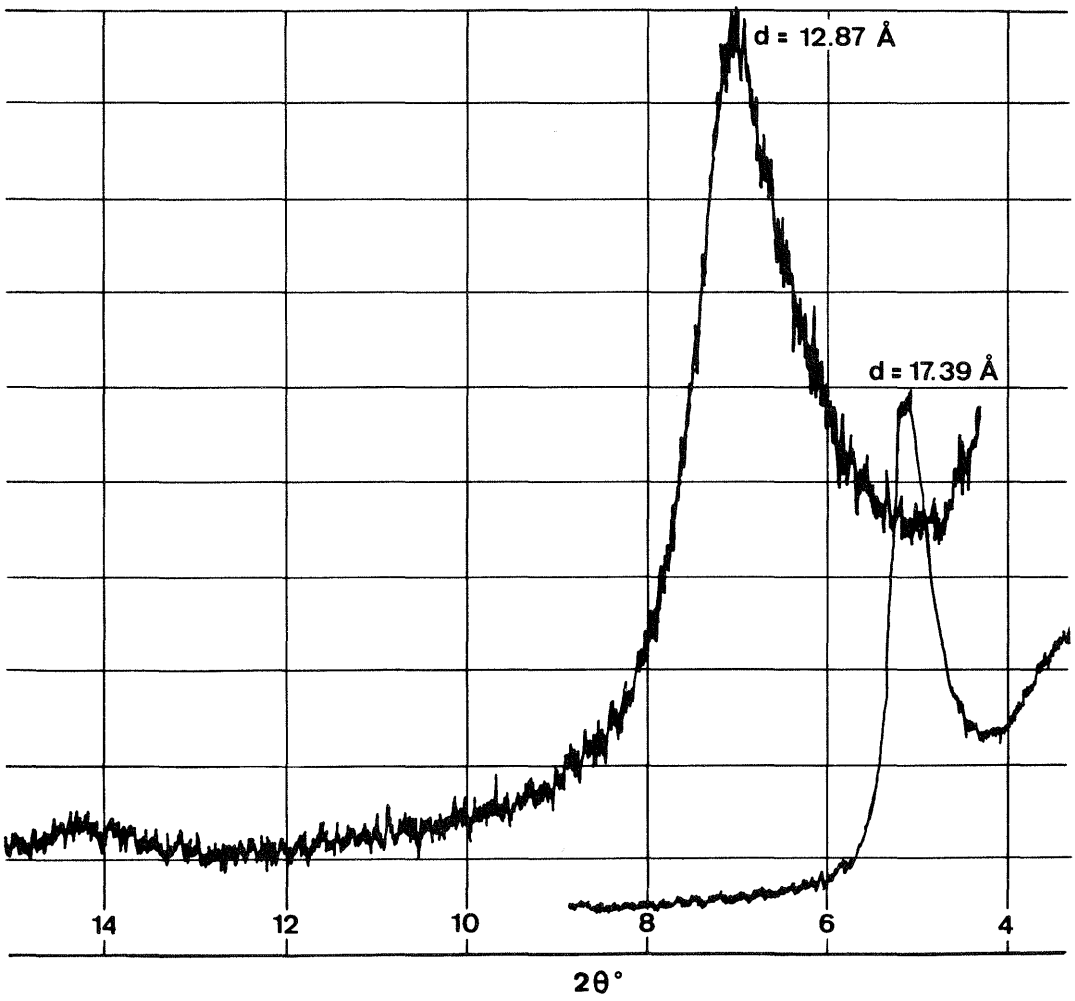

Fig 4.1. X-ray diffractogram of MX-80 powder. $2\theta^{o}$ is given by the horizontal scale. 12.87 Å is the 001 spacing of air-dry clay which is expanded to 17.39 Å by ethylene glycol treatment (lower curve)

The industrial processing yields an aggregated (granulated) state of the bentonite powder which is very suitable for effective compaction. The size distribution of the aggregates is illustrated by Fig 4.2, each aggregate consisting of a large number of flaky montmorillonite particles oriented in a more or less parallel fashion.

The processing and conditions of storage, which involve protection from rain but not from humid air, yield a "hygroscopic" water content (w) of 8-14 %.

As to the organic content ("humic compounds") of the MX-80 it is usually low ($\leq$5.000 ppm) considering its mode of formation in nature, but occasionally it has been found to be much higher due to contamination in the heating phase at the plant. A large part of the organics then consists of carbon which stems from sawdust.

Spectrometric cation analyses have shown that the pore water of MX-80 has a content of about 30 ppm Ca, 15 ppm Mg, and 70 ppm Na.

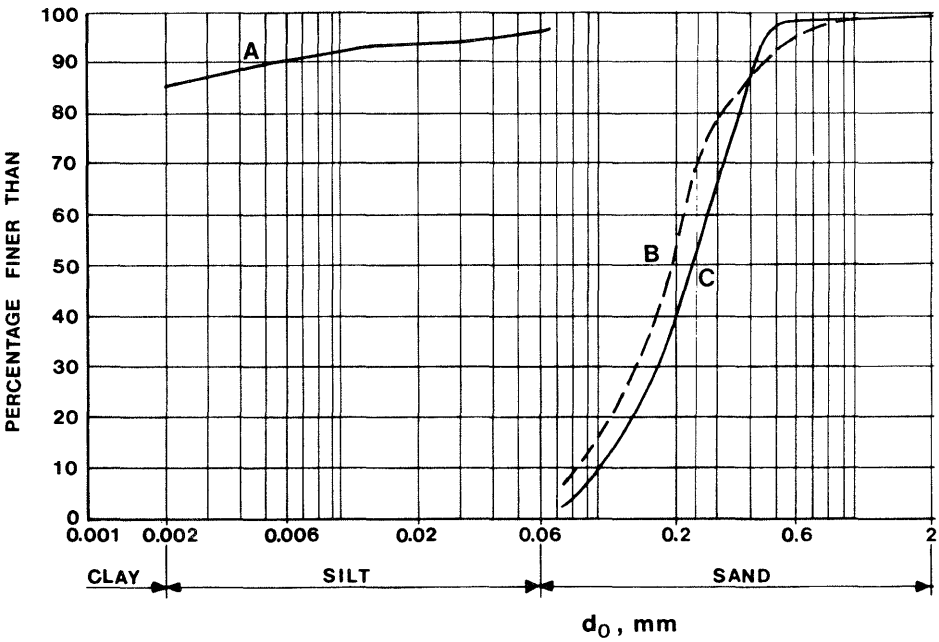

Fig 4.2. Grain size characteristics of the MX-80. A) represents the particle size distribution according to sedimentation analyses. B) and C) represent powder from different deliveries after sieving in air-dry condition

Table 4:1. Chemical analysis of MX-80 bentonite (Asea-Atom)

SiO_2	63.0 %
Al_2O_3	16.1 %
Fe_2O_3	3.0 %
CaO	1.1 %
MgO	1.6 %
Na_2O	2.2 %
K_2O	0.48 %
Li_2O	< 0.01 %
MnO	0.03 %
TiO_2	0.10 %
F	0.10 %
Cl	< 0.01 %
S	0.12-0.23 %
Cu	< 0.01 %
Zn	0.01 %
Cr	< 0.01 %
Ni	< 0.01 %
AsO_4	0.018 %
NO_3	none
PO_4	0.060 %
S in sulphides	~ 0.12 %

4.1.1.3 Characterization, quality checking

Characterization of the MX-80, mainly for quality checking before delivery, requires determination of a few easily recorded parameters which reflect the most important property of the bentonite, namely the high content of Na montmorillonite. Such parameters are, in combination, the clay content, the natural water content, and the liquid limit, all three having a bearing on the surface activity which is related to the clay mineral composition. The liquid limit has a wide use in soil mechanics and was chosen as a standard for the quality checking of the bentonite for the BMT. 1 kg per ton clay powder delivered from the Duisburg plant - the samples being distributed among the entire mass - have been checked with respect to the clay content (sedimentation analyses), the natural water content (w), and the liquid limit (w_L). The latter was found to be in the interval 350-450 %. The clay content was found to vary between 80 and 90 %, while the natural water content ranged between 9.5 and 13.5 %.

4.1.2 Ballast component

The choice of ballast composition was made so as to obtain a high bulk density of the field-compacted backfills with the bentonite added, and to find materials which are commercially available in large amounts for the BMT as well for future repositories.

The following fractions were used; 1) and 2) delivered by AB Linde Grus & Betong, Lindesberg, and 3) by Nordiska Mineralprodukter AB, Örebro:

1 0.5-2.0 mm, (forming 30 % of the total ballast)

2 0.1-1.0 mm, (forming 50 % of the total ballast)

3 $\leq$ 0.3 mm, "filler", (forming 20 % of the total ballast)

The mixture was characterized by the grain size distribution shown in Fig 4.3. The filler can be obtained with quartz or feldspar as dominating mineral. For the Stripa test, which was planned to run for a few years only, the possible, very slight trend of certain smectite components to pick up potassium from potassium feldspars and to become partially transformed to illite-type minerals, was assumed to be insignificant. Therefore, feldspar-rich filler was chosen since it represents a conservative case with respect to the heat conductivity. The coarser ballast fractions consisted of feldspars (sodium and potassium) and quartz and a very minor amount of heavy minerals.

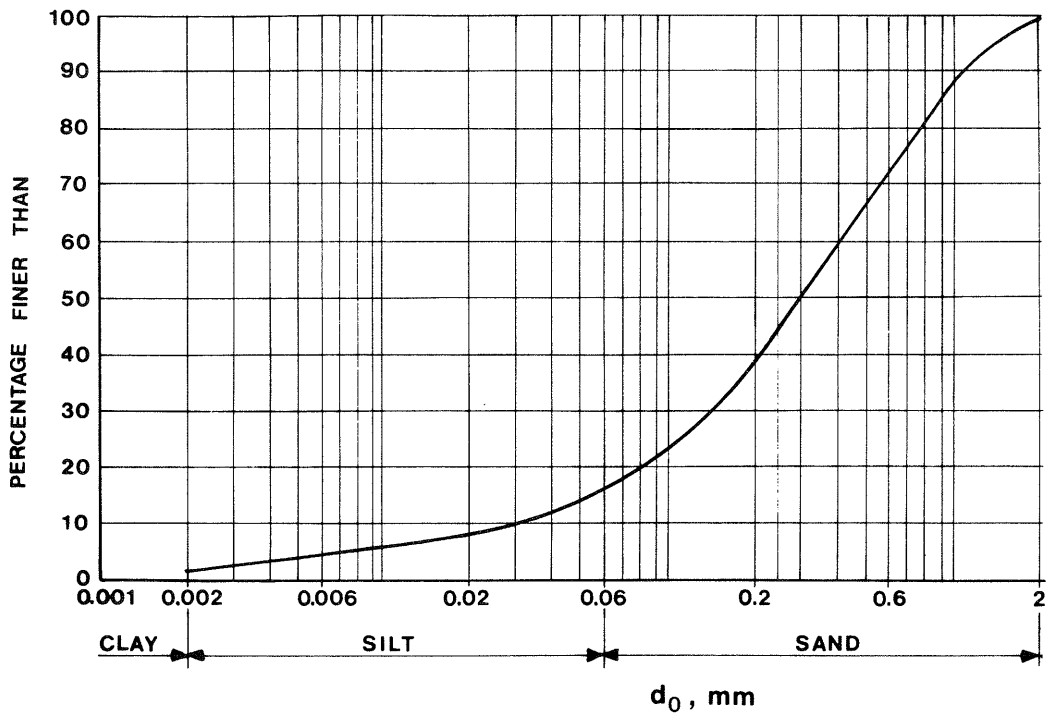

Fig 4.3. Grain size distribution of the ballast material

4.1.3 Highly compacted bentonite

4.1.3.1 Bulk density

The required high density of the bentonite overpack of waste canisters in actual repositories can be obtained by compacting air-dry granulated bentonite powder under high pressure to form blocks and this technique was also applied for the BMT. A suitable density of the highly compacted bentonite in the final, water saturated and swollen state in the deposition holes of repositories is ρ_m=2.0-2.1 t/m^3. This implies an initial bulk density of the only partly water saturated, compressed bentonite blocks of 2.1-2.2 t/m^3 to arrive at this condition after completion of the water uptake from the rock and after swelling to fill up the holes completely. Two block series were produced with a bulk density that turned out to be 2.09-2.14 t/m^3 for bentonite powder with an average water content of 13 %, and ρ=2.07-2.11 t/m^3 for bentonite powder with an average water content of 10 %.

In order to fit the heater holes as closely as possible and to form a tight contact with the heaters, the bentonite had to be prepared in the form of specially shaped blocks that could be arranged to form a tightly fitting brickwork.

4.1.3.2 Compaction and manufacturing

Bentonite cylinders with a diameter of about 0.4 m and a length of 1.5 m were prepared by the IFÖ company, Bromölla, Sweden, by applying cold "isostatic" compaction technique (Fig 4.4). This process involved filling of the powder in a cylindrically shaped rubber sleeve with rigid base plates and compressing it radially by applying an outer pressure of approximately 100 MPa to obtain

the desired densities. The pressure was held constant for a few minutes before releasing and extracting the bentonite core. The required compression pressure and time were found to depend on the water content and some preliminary tests had to be made before the operation ran properly.

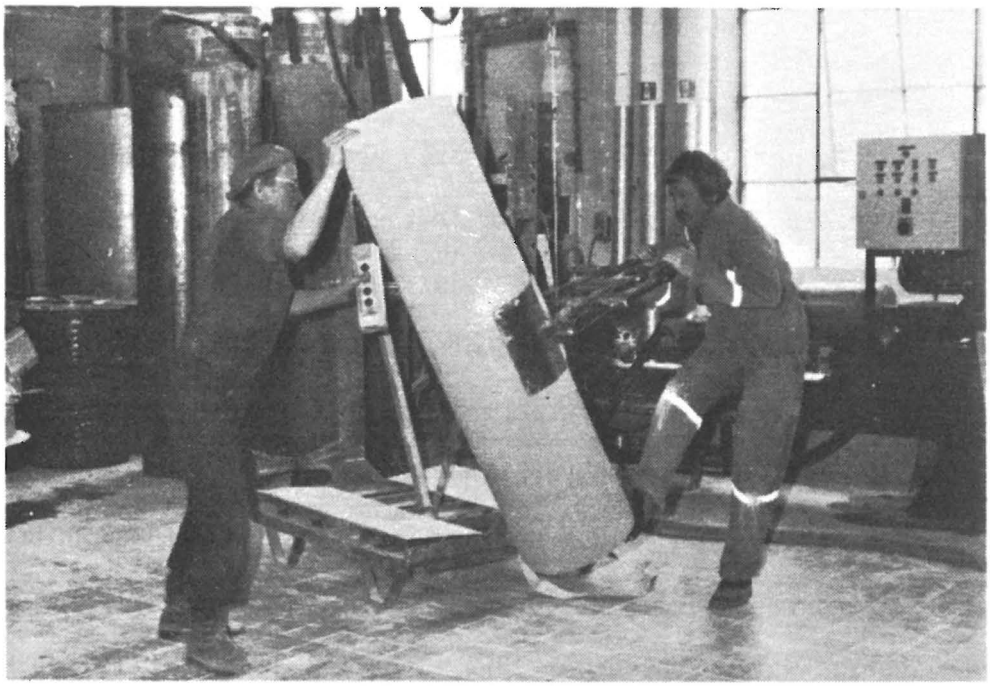

Fig 4.4. Highly compacted bentonite cylinder in the IFÖ factory. Notice the regular shape, the diameter being approximately 0.4 m.

The cylinders were cut into disc- and rod-shaped blocks by using a machine saw. This operation yielded blocks of various predetermined shapes for the build-up of instrumented columns of the bentonite-confined heaters which had to fit tightly in the heater holes (Fig 4.5-4.7). The blocks were wrapped in air-tight "welded" 0.15 mm plastic cover to preserve the original water content. They were then placed in strong plastic boxes for transportation to Stripa. Unwrapping and drilling of holes for application of temperature gauges and moisture sensors was made shortly before the insertion in the holes.

The different initial bulk density of the two block series would yield different final densities and physical properties if the geometrical conditions were the same in all the heater holes. It was therefore decided to use different starting conditions chosen so as to yield the same ultimate bulk density and water content in all the holes, namely ρ_m=2.10 t/m^3, and about 20 %, respectively. Considering radial swelling only, this was achieved by manufacturing the blocks so that a 30 mm slot between the rock and the bentonite annulus was formed for the low initial bock density ρ=2.07-2.11 t/m^3, the slot being filled with loose bentonite powder with an average bulk density of 1.2 t/m^3. For the high initial block density ρ=2.09-2.14 t/m^3, a 10 mm open slot was chosen to arrive at the same ultimate bulk density. The latter slot width was in fact considered to be a minimum for bringing the bentonite/heater unit down into its hole.

The rate of water inflow into the holes had to be considered in deciding in which holes the wide slots with the loose powder should be located, since rapid inflow would make the application of the powder difficult. Such conditions were expected in holes no 1, 2 and 5 so the following arrangement was chosen:

* Heater holes nos 1, 2 and 5 with open, 10 mm wide slots
* Heater holes nos 3, 4 and 6 with backfilled, 30 mm wide slots

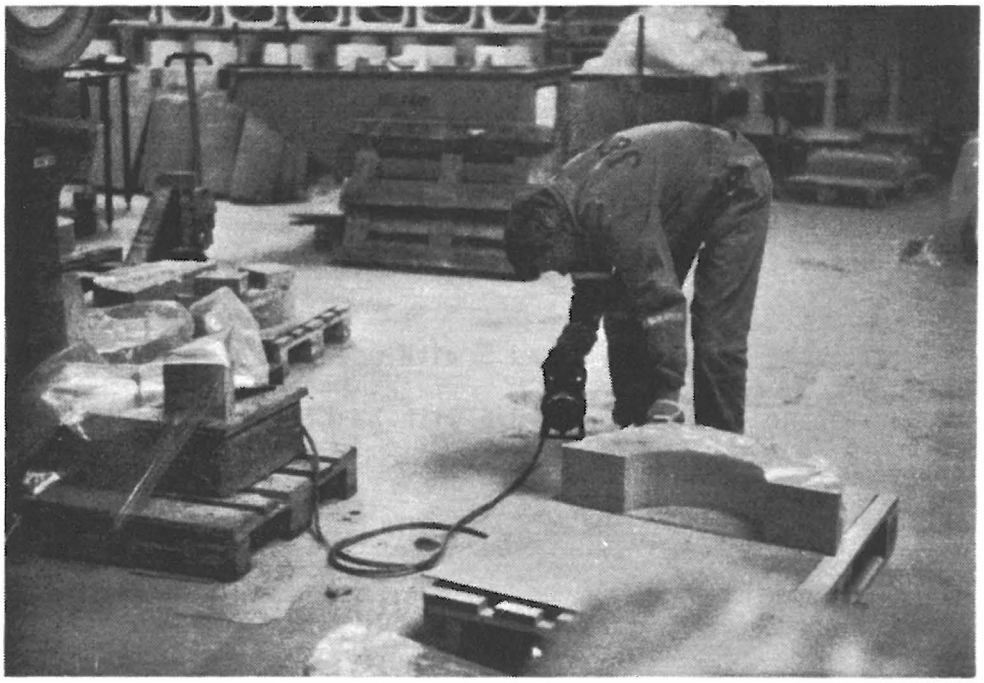

Fig 4.5. Block cutting operations

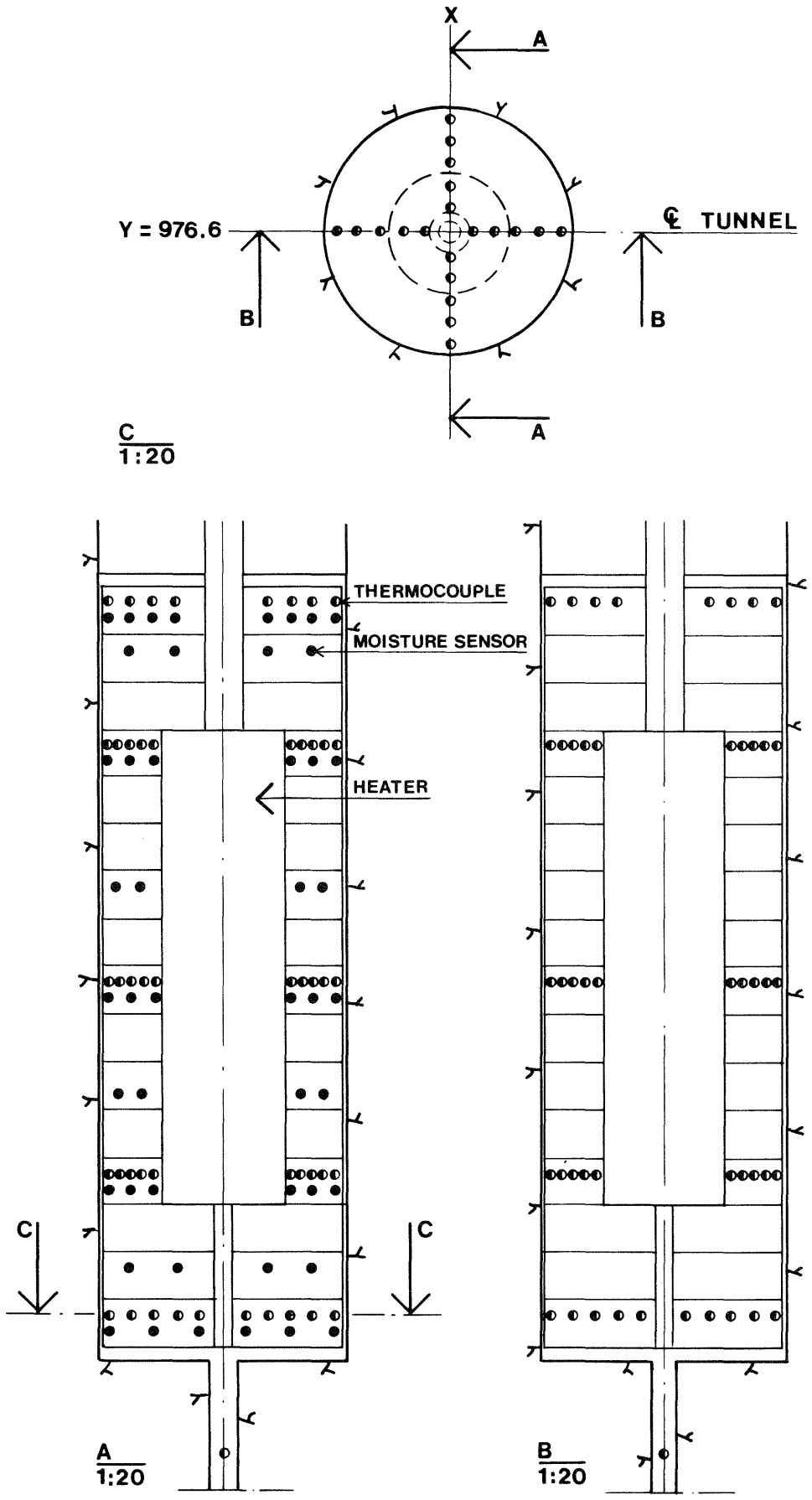

Fig 4.6. Schematic section through a deposition hole indicating the principle of block arrangement and instrumentation

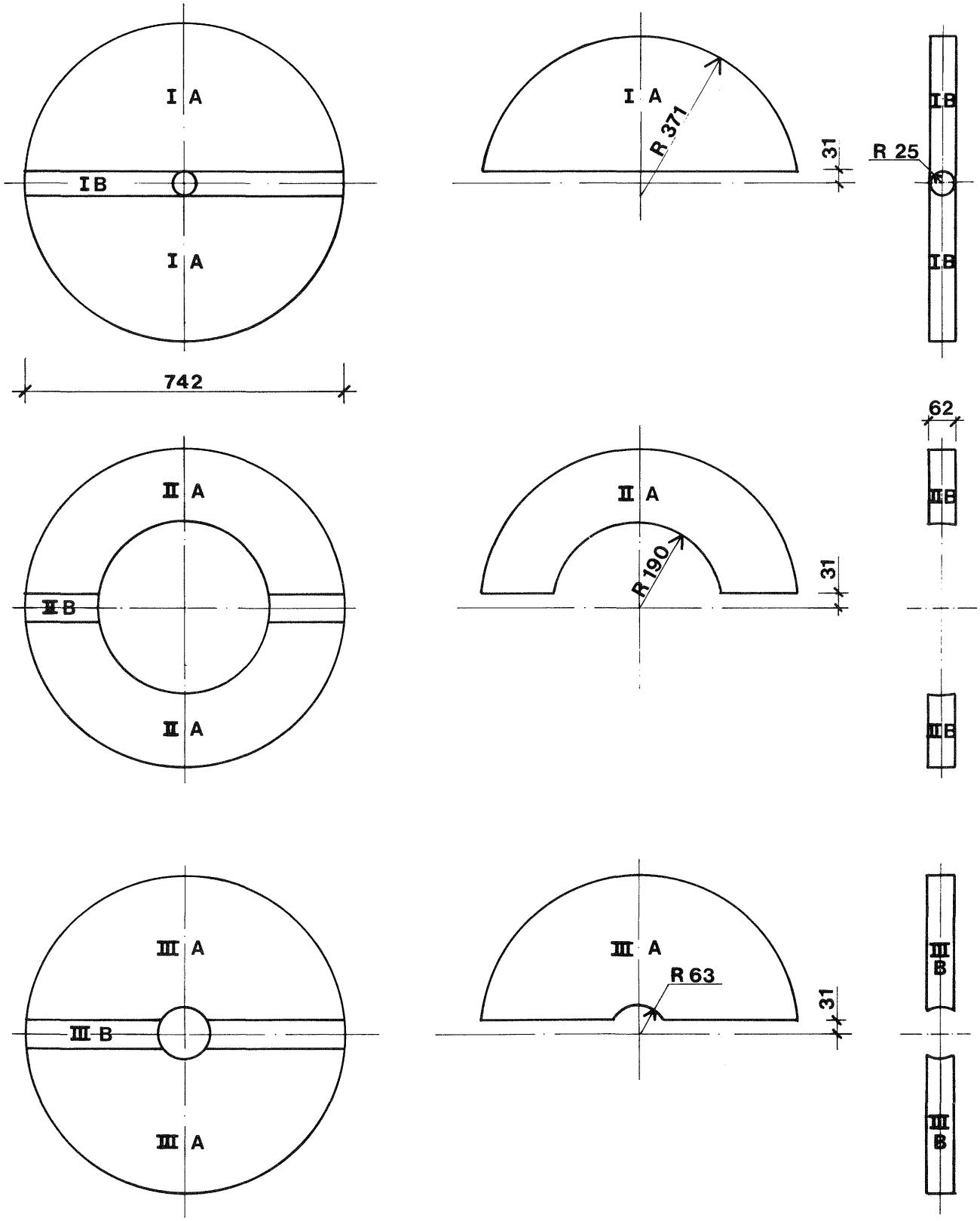

Fig 4.7. Example of layout of block shapes (dimensions in mm). The thickness of the blocks was 150 mm

4.1.3.3 Physical, laboratory-determined properties of highly compacted MX-80 powder

The physical properties of highly compacted MX-80 have been reported in a number of technical papers and they are currently being investigated at various laboratories. This chapter gives a number of characteristic data that may serve as preliminary reference values. They refer to the case of saturation with synthetic groundwater ("Allard water") with 65 ppm Na, 18 ppm Ca, 4 ppm Mg, 4 ppm K, 123 ppm HCO_3, 70 ppm Cl, 12 ppm H_2SiO_4 and SO_4, (pH 8), cf (9).

Porosity, water content

The water uptake and swelling processes in the heater holes were expected to change the bulk density as well as the porosity and water content. Ultimately, some of the bentonite blocks were assumed to become water saturated and in this state the relation between bulk density, porosity (expressed here as the void ratio) and water content should be that in Table 4:2. The values have been calculated by applying the density value 2.7 t/m^3 of the minerals.

Table 4:2 Relation between bulk density ρ_m, void ratio e, and water content w

ρ_m t/m^3	e	w %
2.15	0.49	18
2.10	0.54	20
2.05	0.62	23
2.00	0.70	26
1.95	0.78	29

Permeability

For water saturated MX-80 the relationship between permeability and bulk density is given by Table 4:3, cf (10).

Table 4:3 Permeability k in m/s versus bulk density of MX-80

ρ_m	k, m/s	
t/m^3	Room temp very low gradients	70°C, gradient 10^{-4} to 10^{-3}
2.1	$1.5 \cdot 10^{-14}$	$1.5 \cdot 10^{-13}$
2.0	$2 \cdot 10^{-14}$	$2 \cdot 10^{-13}$
1.9	$3 \cdot 10^{-14}$	$5 \cdot 10^{-13}$
1.8	$5 \cdot 10^{-14}$	$8 \cdot 10^{-13}$
1.7	$8 \cdot 10^{-14}$	10^{-12}

Swelling pressure

When the Buffer Mass Test was designed, the relationship between swelling pressure and bulk density in Table 4:4 was assumed to be valid (11). Ongoing investigations indicate that the pressures are overestimated by about 10-20 %. The water uptake of confined, highly compacted bentonite samples is a complex process in which capillary suction and superimposed diffusion-type molecular migration are major mechanisms. They are associated with redistribution of the smectite particles under constant dry density conditions in completely confined specimens, and with particle redistribution leading to a lower dry density when the bentonite is allowed to swell, which was the case in the BMT heater holes (12).

Table 4:4. Swelling pressure p_s in MPa versus bulk density of MX-80 at different temperatures

ρ_m	p_s, MPa		
t/m³	20°C	90°C	70°C (estimated)
2.15	45	35	40
2.10	30	17	20
2.05	15	8	10
2.00	7	4	5
1.95	4.5	2.5	3

Ion diffusion

Laboratory experiments have been conducted for determination of diffusion rates of Sr^{2+}, Cs^+, I^- and Cl^- in water saturated MX-80 samples with different bulk densities (13). The diffusion rate can be described mathematically by the simple diffusion equation with a correction term for the slow-down caused by ion adsorption (K_d-effect). The recorded concentration profiles in the experiments were used to evaluate equivalent diffusion coefficients which were found to be $D=10^{-12}$-$3\cdot10^{-11}$ m²/s for Sr^{2+}, $D=10^{-13}$-$7\cdot10^{-12}$ m²/s for Cs^+ and 10^{-13}-$4\cdot10^{-12}$ for I^- and Cl^-. Ongoing investigations point to significantly higher anion diffusivity, however. As a general rule it can be assumed that ion diffusion takes place a hundred times slower in highly compacted bentonite than in bulk water.

Thermal properties

The heat conductivity of the highly compacted bentonite is particularly important soon after the application of canisters in a repository because the bentonite will not be water saturated at

this stage and its ability to transfer heat to the rock will consequently not be very high. A number of experimental determinations of the heat conductivity λ and heat capacitivity c of MX-80 at different bulk densities and degrees of water saturation have yielded the results collected in Table 4:5 (14).

Table 4:5. Heat conductivity versus bulk density and water content (average temperature 20°C of MX-80)

ρ	w	λ	c
t/m^3	%	W/m,K	Ws/kg,K
2.2	11	1.01	1140
2.1	14	1.15	1220
2.1	5	0.96	960
2.0	5	0.83	960
1.2	10	0.33	1110

4.1.4 Backfill of Tunnel and Boxing-Outs

4.1.4.1 General

The main principle in the choice of a suitable composition of the backfill of tunnels and shafts in repositories is that these masses should have a low permeability. It is also required that they have a low compressibility in order to minimize the displacement caused by the swelling power of the highly compacted bentonite. A sufficiently small average pore size is required as well to prevent the minute montmorillonite particles to migrate from the deposition holes into the pore system of the backfill. Finally, backfills must have a certain swelling potential to fill up voids that might arise in the course of its application.

4.1.4.2 Composition

For practical reasons, the upper part of tunnels in repositories of the KBS type has to be filled by blowing the backfill in place, while the lower two thirds can be filled by ordinary, layer-wise application and compaction with vibrating tools. Since these two techniques yield different bulk densities, the bentonite content should be higher in the upper part to yield approximately the same permeability as the lower part. For this purpose the upper part of the backfill of the BMT had a 20 % bentonite content while the corresponding fraction of the lower part was 10 % (Fig 4.8), the remainder in both cases being the ballast material described previously. The two mixtures have the grain characteristics shown in Fig 4.9.

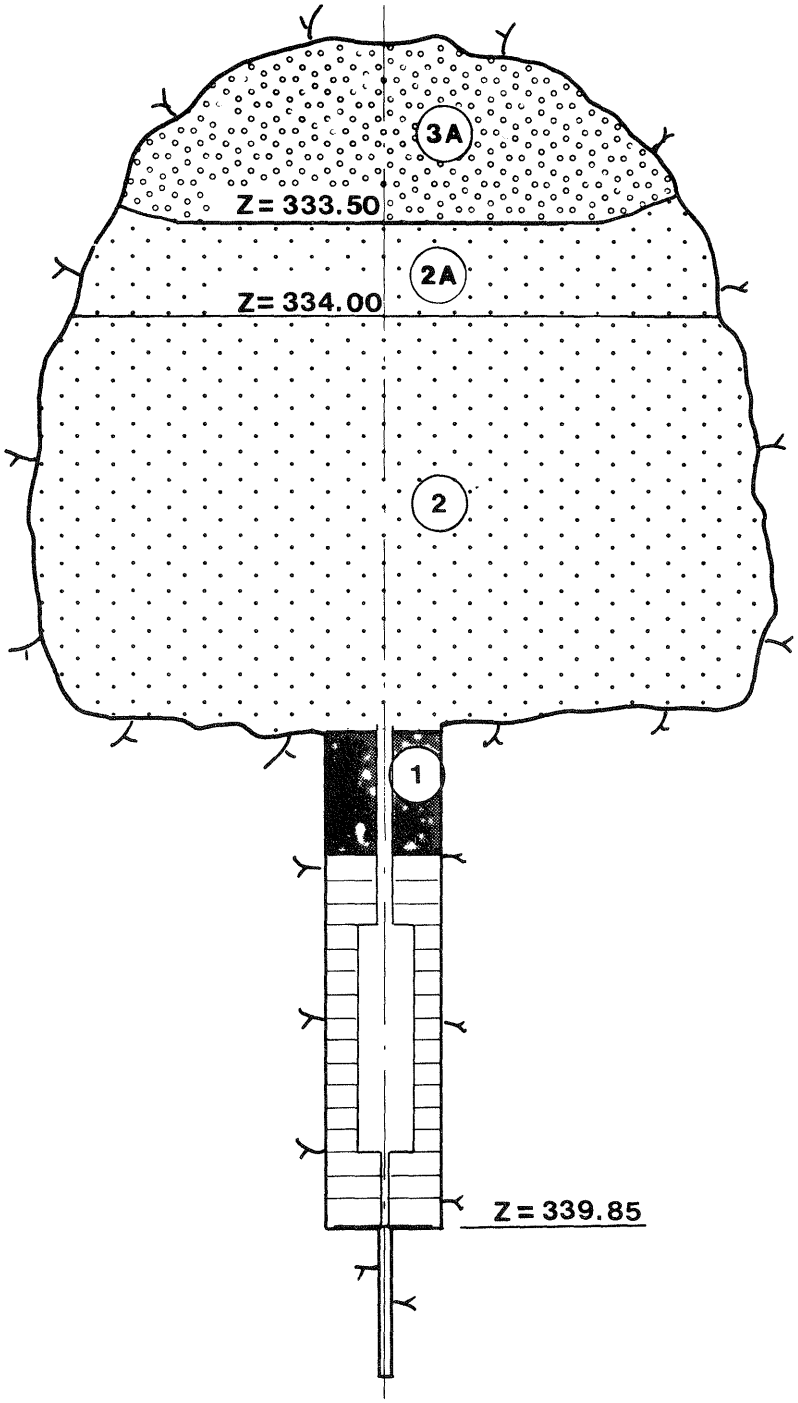

Fig 4.8. Tunnel backfill. 1) Manually applied and compacted 90 % sand/10 % bentonite. 2) Layer-wise compacted 90 % sand/ 10 % bentonite. 3) blown-in 80 % sand/20 % bentonite

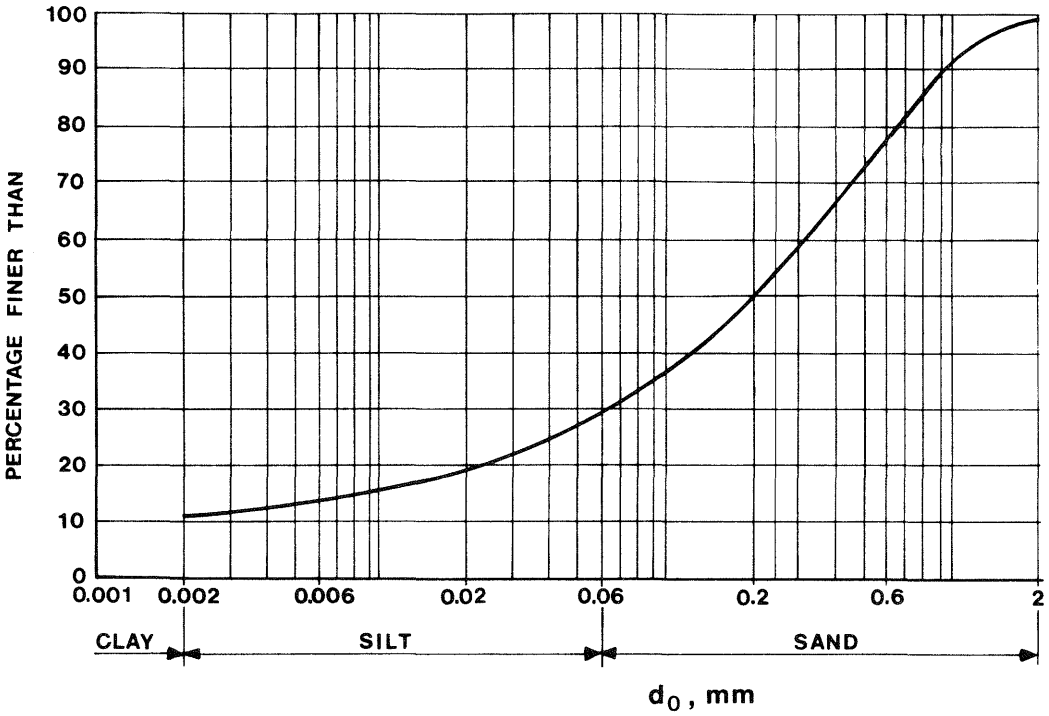

a) 10 % bentonite mixture

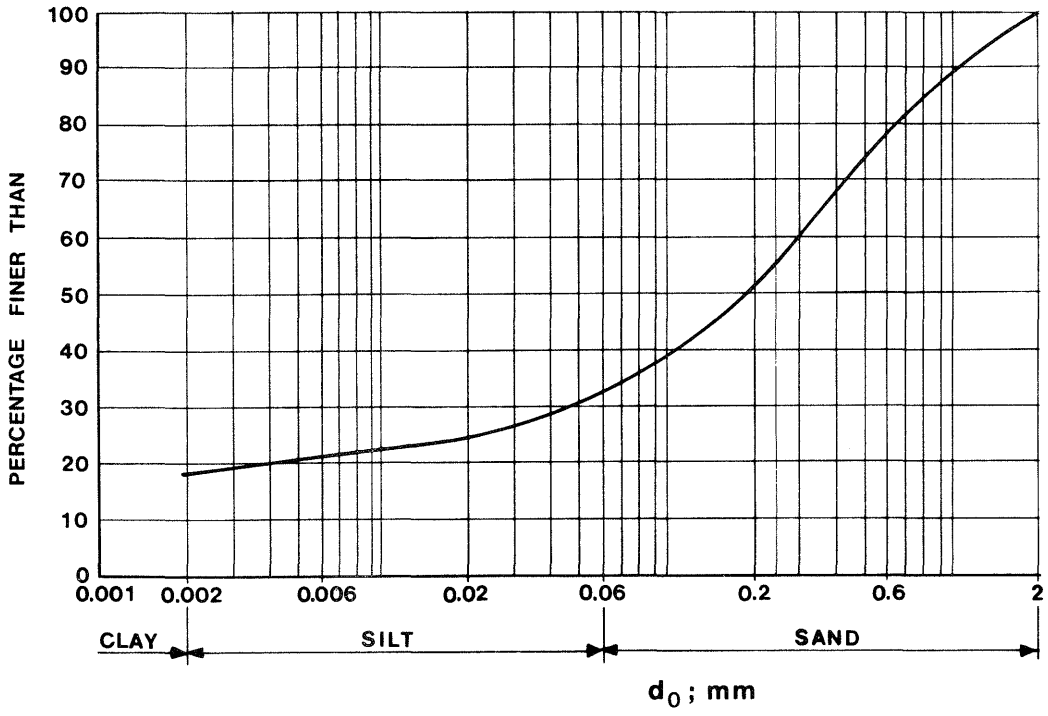

b) 20 % bentonite mixture

Fig 4.9. Grain characteristics of the backfill

4.1.4.3 Bulk Density

The 10 % bentonite mixture has an optimum water content of about 14 % as concluded from the diagram in Fig 4.10. This value corresponds to about 80 % degree of water saturation, so the water content in the field study was taken lower, i.e. 10 $\pm$1 %, to make it possible to detect the water uptake. The expected bulk density of the compacted mass was 2.0-2.05 t/m^3 which should increase to 2.15-2.2 t/m^3 when the water uptake was completed under constant volume conditions. As to the 20 % bentonite-mixture a large-scale test by Stabilator AB in Upplands Väsby showed that a water content of 15 % was suitable. A slight amount of angular gravel-sized (4-8 mm) quartzite had to be added to clean the nozzle. The Stabilator test gave for 4 samples the ρ-values 1.64, 1.71, 1.56 and 1.59 t/m^3, and the water contents 16, 15, 21, and 21 %, respectively, and a density of 1.5-1.6 t/m^3 was therefore expected for the shotcreted BMT backfills as well. After water saturation the bulk density should consequently be of the order of 1.8-1.9 t/m^3.

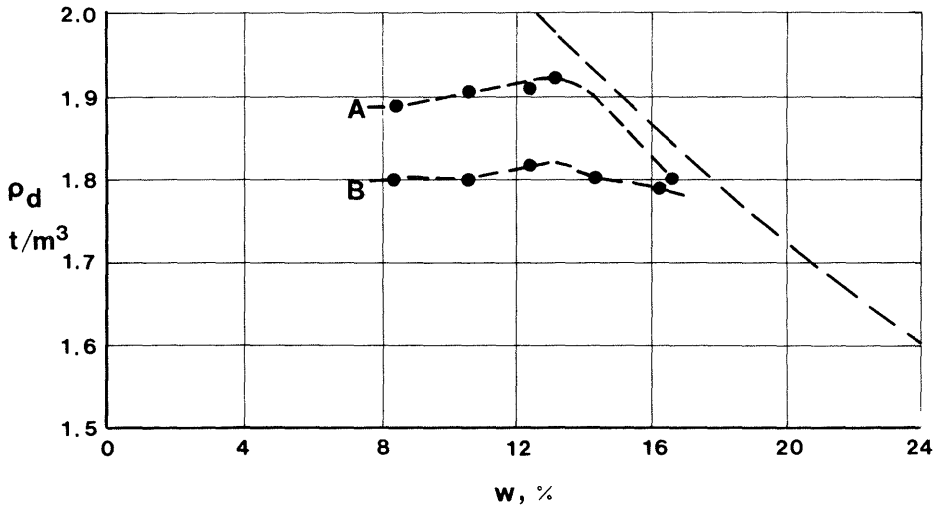

Fig 4.10. Compaction curves for the backfill. (Modified Proctor technique). A) 10 % bentonite mixture. B) 20 % bentonite mixture

4.1.4.4 Physical properties of the backfill

Porosity, water content

As in the case of the highly compacted bentonite in the deposition holes, the tunnel backfill will ultimately be water saturated. In this condition the relation between bulk density, void ratio (ratio of pore volume and volume of minerals) and water content will be as shown in Table 4:6. The values were calculated on the basis of the density values 2.7 t/m^3 for the montmorillonite particles and 2.65 t/m^3 for the ballast material.

Table 4:6. Relation between bulk density (saturated state), void ratio e, and water content

	ρ_m t/m^3	e	w %
10 % bentonite content	2.2	0.41	15
	2.1	0.54	20
	2.0	0.70	26
	1.9	0.89	33
20 % bentonite content	2.0	0.70	26
	1.9	0.89	33
	1.8	1.13	42
	1.7	1.43	53
	1.6	1.84	68
	1.5	2.40	89

Permeability

The permeability of water saturated backfill materials with the present compositions have been determined in the laboratory, the results being collected in Table 4:7.

Table 4:7. Permeability k in m/s versus bulk density of bentonite/sand mixtures

	ρ_m t/m³	k m/s
10 % bentonite content	2.1	$\leq 10^{-9}$
20 % bentonite content	2.1	$\leq 10^{-10}$
	2.0	$\leq 1.5 \cdot 10^{-10}$

Swelling pressure

Table 4:8 gives the swelling pressure of the backfills as a function of the bulk density. The values are rough estimates based on a limited amount of laboratory tests.

Table 4:8 Swelling pressure p_s in MPa versus bulk density of bentonite/sand mixtures

	ρ_m t/m³	p_s MPa
10 % bentonite content	2.1	0.15
	1.9	0.02
20 % bentonite content	1.9	0.10
	1.8	0.05

Ion diffusion

Very few ion diffusion tests have been run in the laboratory and at present there are only rough indications of the magnitude of the ion diffusion coefficents. A safe assumption is that only tortuosity retards the diffusion, irrespectively of the bentonite content, and this should yield diffusion rates of the order of 10 % of those of bulk water (15).

Thermal properties

As in the case of highly compacted bentonite, the heat conductivity and capacitivity are of primary interest in the first phase when the backfill is still not water saturated. A number of experimental determinations have yielded the results collected in Table 4:9 (14).

Table 4:9. Heat conductivity λ and capacitivity c versus bulk density and water content. S_r is the degree of water saturation

	ρ t/m³	w %	λ W/m,K	c Ws/kg,K	S_r %
10 % bentonite content	1.64	11	1.05	1130	37
	1.64	21	1.1	1390	58
	1.59	1	0.35	840	4
20 % bentonite content	1.56	2	0.35	870	7
	1.54	12	0.60	1160	34
	1.49	22	0.65	1420	50
	1.3	10	0.46	1110	21

Compressibility

The compressibility of the bentonite/sand backfills, primarily the 10 % bentonite mixture, is of importance with respect to the displacement of the interface between the highly compacted bentonite in the deposition holes and the overlying backfill. It has been determined in the laboratory by means of the Rowe oedometer (Fig 4.11). The curves are suitable for determination of the compression of the backfill exposed to compressive stresses.

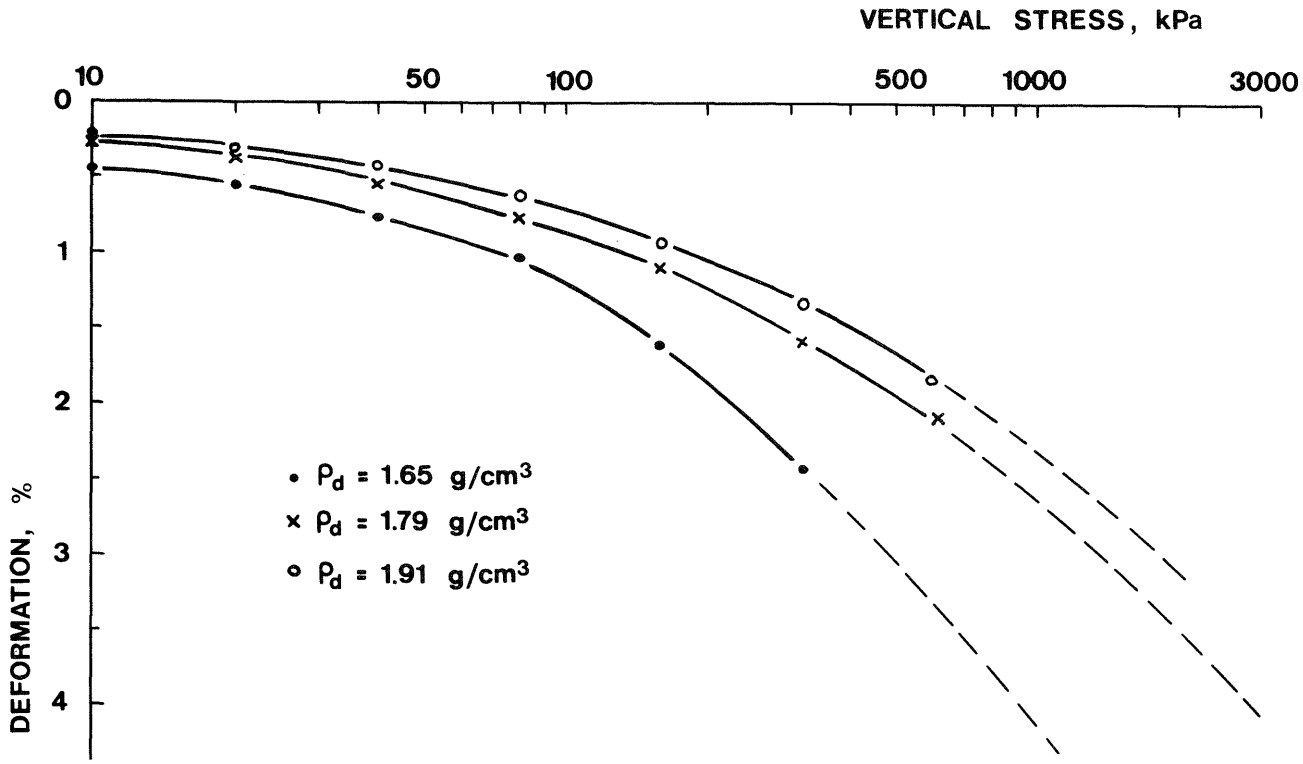

Fig 4.11. Compressibility of 10 % bentonite mixture at different dry densities

4.2 Field preparation and application of buffer materials

4.2.1 Highly compacted bentonite

The individually plastic-coated blocks of compacted bentonite were so effectively shielded that they could be stored down in the mine without being affected by the high humidity there. They were unwrapped and prepared for the instrumentation by drilling holes and carving grooves for the cable connections in the air-conditioned field laboratory located in the same shed as the data acquisition center on the 340 m level, and were then transferred to the respective heater hole for build-up of the heater/bentonite units. The joints between the blocks were very narrow and the expected net volume of the block assemblies was almost achieved. Thus, the slot width at the bentonite/rock interface, 10 and 30 mm respectively, was actually arrived at. The matter is further dealt with in the subsequent chapter on "Instrumentation" (Chapter 4.3).

4.2.2 Backfilling of tunnel and boxing-outs

4.2.2.1 General

The backfilling of the tunnel and boxing-outs was made by using mixtures of bentonite, filler and sand with addition of some water. Detailed data on the compositions and material components of the backfills were given in Chapter 4.1.4.2.

The backfilling involved solving of several practical problems which will appear also in future repositories, such as 1) current checking of the granulometry and mineralogy of large quantities of successively delivered bulk soil-type materials, 2) storing of soil type materials under winter conditions, 3) thorough mixing of several soil components and water to reach homogeneous conditions, 4) transportation of soil-type materials by use of elevators and trains in vertical shafts and long tunnels, 5) application and compaction of soil-type materials in tunnels, and 6) in-situ checking of the bulk density of the applied backfill. These points will be commented on in this chapter.

4.2.2.2 Storing

The bentonite bags arrived at Stripa in the fall 1981 and were stored in unheated sheds on the ground surface until the mixing started. Part of the bentonite was not used until March 1982 when the boxing-outs were filled and this material was exposed to temperatures lower than -20°C for several weeks. The clay character was not markedly changed by this, suggesting that the hygroscopic water, which may have dropped to less than 9 % during the winter, was not frozen. This assumption is strongly supported by several investigations of the physical character of smectite-adsorbed water (16).

The ballast fractions, except for the "filler", were stockpiled on the ground surface. The piles were covered by canvas for protection from rain and snow. The "filler", which was delivered in paper bags, was stored together with the bentonite.

4.2.2.3 Mixing operations

The mixing took place on the ground surface in a simple shed where a large concrete mixer was placed for the treatment, and where bentonite and "filler" bags as well as ballast components were stored, the latter ones in open boxes (Fig 4.12). Water was available from the local community. A local constructing company, Gustavsson & Eriksson Byggnads AB, was responsible for the organization and operation of the mixing plant as well as for backfill transportation.

The mixer operated well with as much as 500 kg of soil material and water at a time, and produced reasonably homogeneous mixtures. Certain trends of the bentonite to form coatings and large granules were occasionally noticed, especially when the components were successively added in the mixer. The standard procedure was therefore to fill the loading box of the mixer with bentonite, "filler" and sand, the mass then being dropped into the mixer after which water was successively added.

For the 20 % bentonite mixture the water content was not allowed to exceed 5 % to avoid blocking of the feeding system used for blowing this backfill in place. Water therefore had to be added at the nozzle of the robot aggregate to arrive at the required 15 % moisture content. The gravel specified in Table 2 contributed to keep the nozzle open.

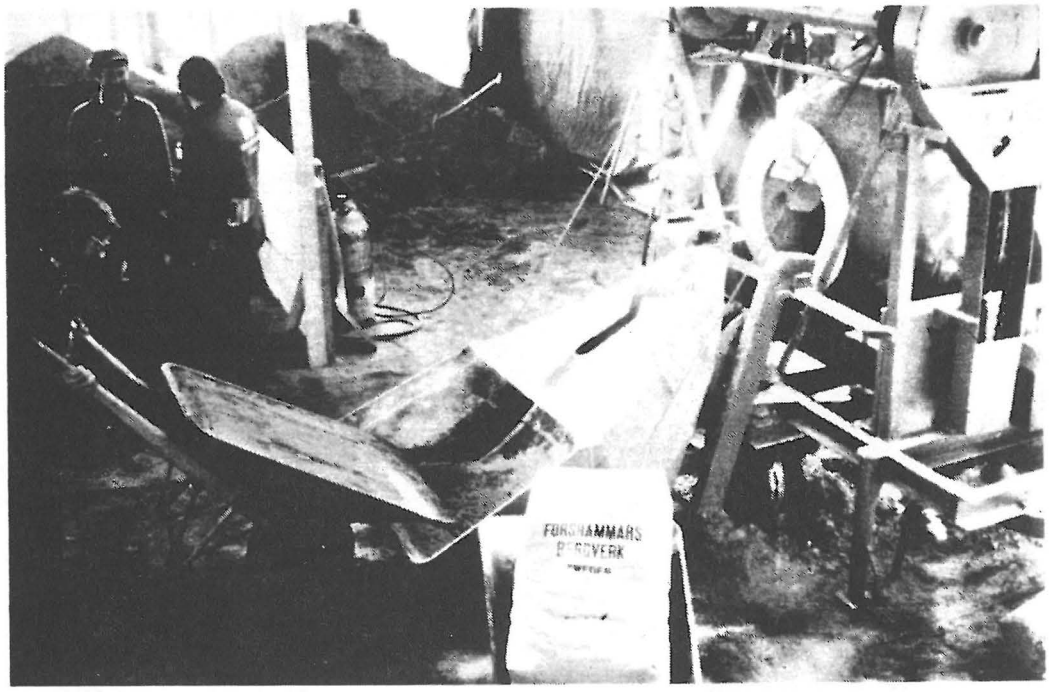

Fig 4.12. Mixing station. A wheelbarrow with a wheighed amount of one of the sand components is about to be filled in the loading box of the mixer. Sand boxes are seen in the background

4.2.2.4 Transports

The mixed material was filled in 0.5 m^3 containers ("självtippare") which were brought to the main elevator of the mine by an ordinary tractor, the transport distance being about 150 m. One container at a time was loaded on a decauville car and placed in the elevator for transport to the 360 m level. Here, a set of cars was arranged to form a train which ran about 700 m to a place where the containers were collected and then individually transported the final 250 m distance to the BMT site by use of a tractor (Fig 4.13). The total number of elevator transportations of full containers was 720 and the total number of trains about 145. These figures illustrate that the transportation was the key problem which largely determined the time schedule of the whole project.

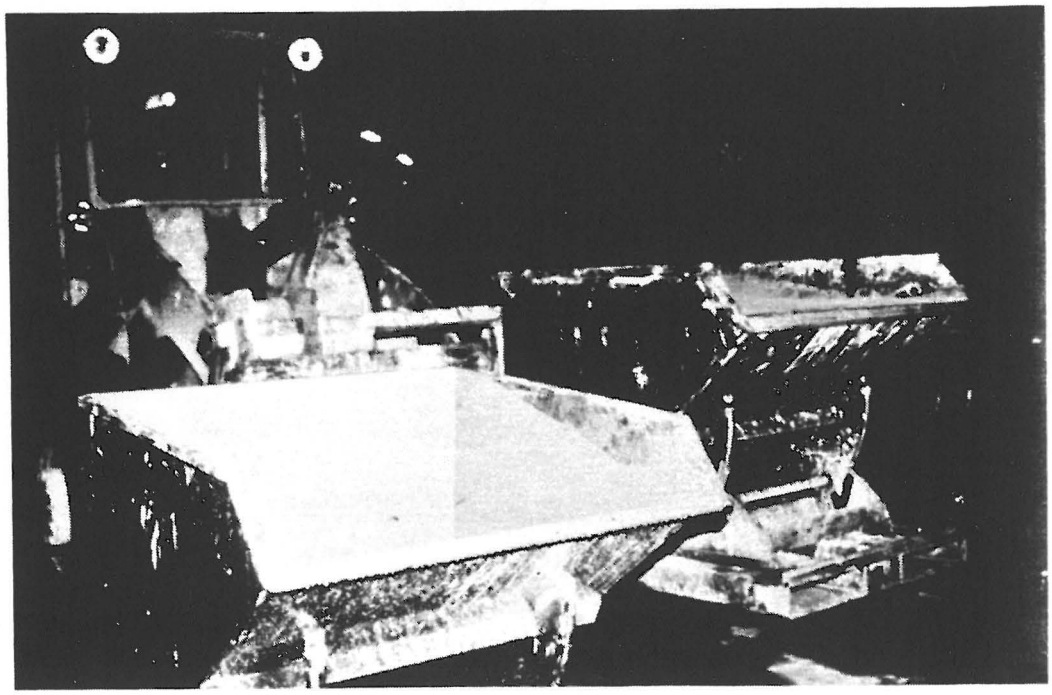

Fig 4.13. Containers for backfill transportation

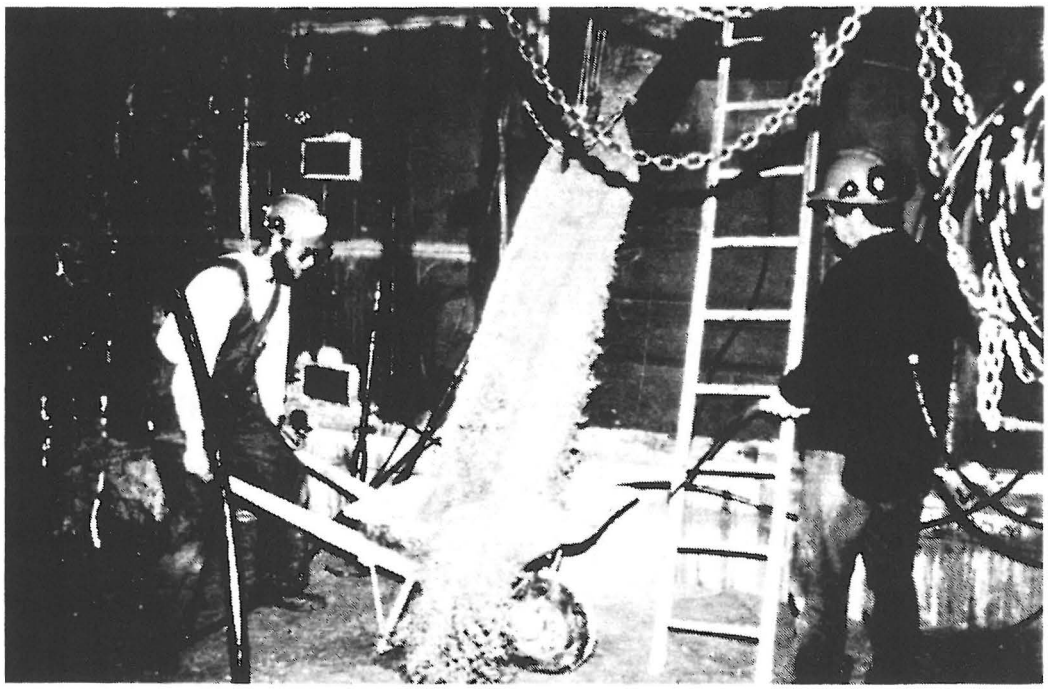

Fig 4.14. Backfill material flowing from the conveyor belt into a wheelbarrow for subsequent distribution and compaction

When the containers reached the BMT area they were emptied, the contents being transferred to a conveyor belt which brought the fill to the place where it was going to be applied, i.e. the space behind the bulwark and in the boxing-outs, respectively (Fig 4.14). The entire transportation system is schematically shown in Fig 4.15.

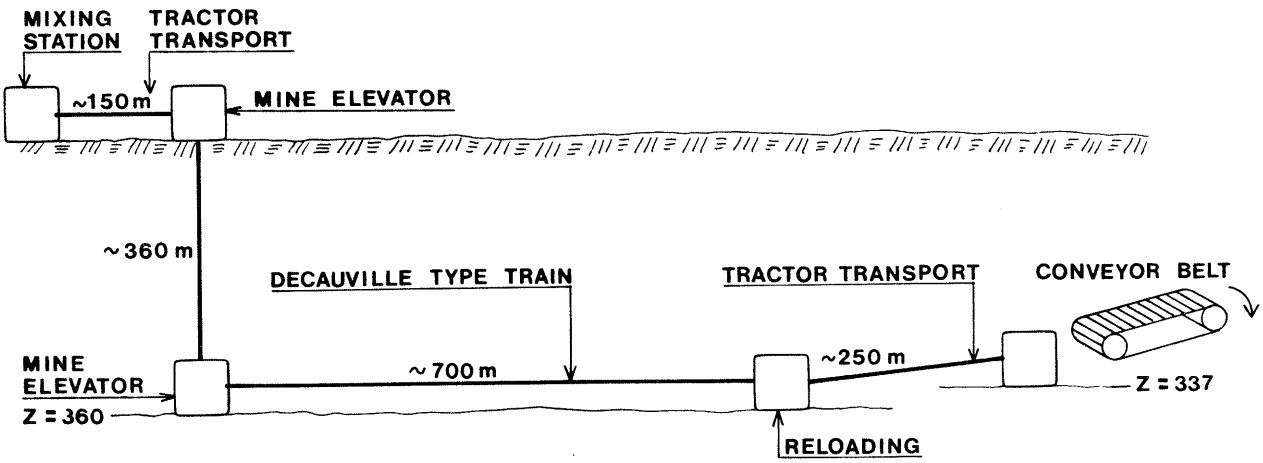

Fig 4.15. Schematic transport system

4.2.2.5 Application and compaction

The first step in the backfilling operation was to apply backfill into the upper, open part of the heater holes, i.e. on top of the compacted bentonite. In certain holes the slot between the bentonite blocks and the rock had been filled with loose bentonite powder while there was an open slot in the rest of the holes. In the latter case small pieces of compacted bentonite were used to cover the slot so that the backfill could be applied homogeneously. The restricted space available in the deposition holes required small tools for the compaction and this was also the case in other areas when compaction of the backfill had to be made close to the rock, cables etc. Hand-held plates mounted onto percussion drills were used for this purpose (Fig 4.16).

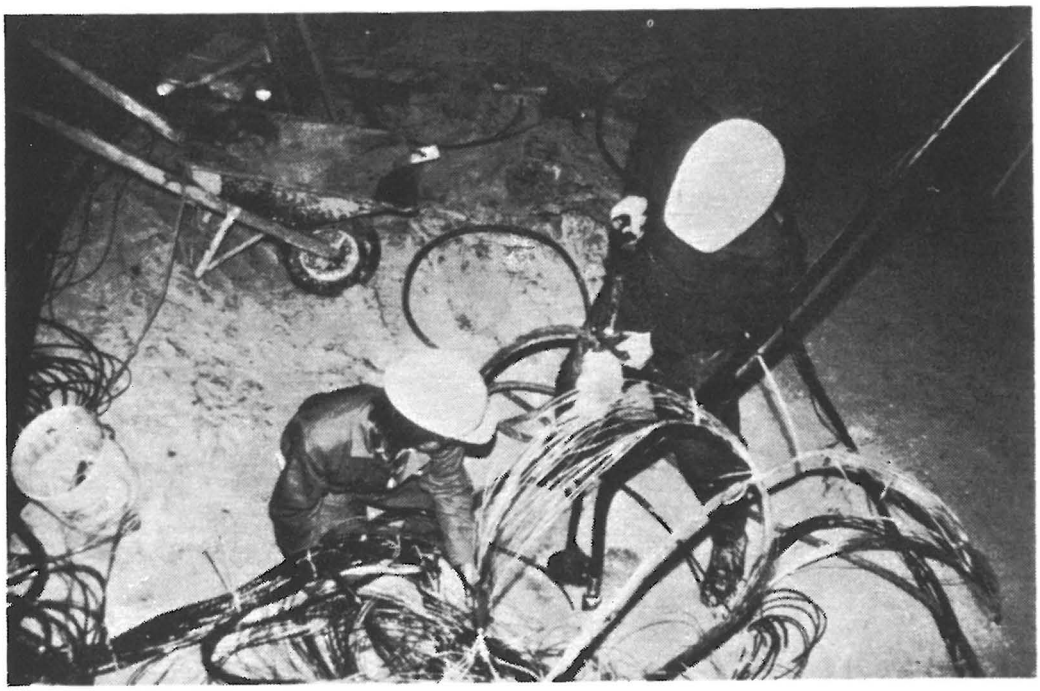

Fig 4.16. Small plates used for compacting backfill

The backfill consisting of 10 % bentonite mixture was applied in 0.15 to 0.30 m layers in the tunnel and boxing-outs and was then compacted by 10-15 runs with a 400 kg electrically operated Dynapac plate vibrator (Fig 4.17). The compaction reduced the thickness of each layer to about 65 % of its original height.

The experience from the compaction work is primarily that the bentonite, although it only forms 10 % of the total backfill, has a considerable damping effect so that only about 0.15 m thick layers can be effectively compacted with the equipment used here.

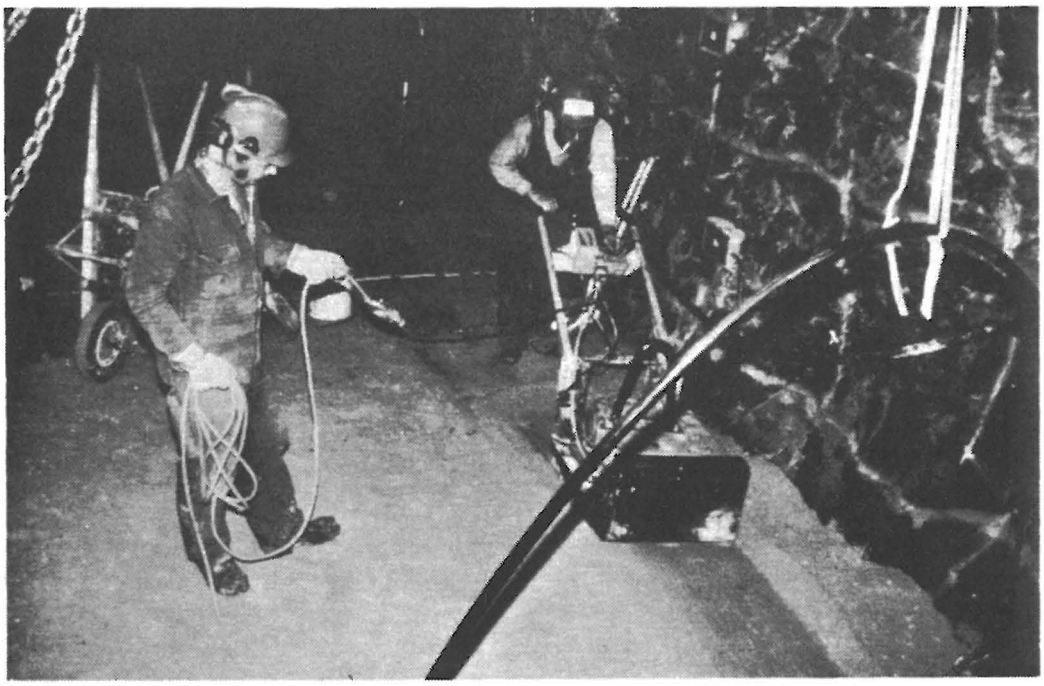

Fig 4.17. 400 kg Dynapac plate vibrator in operation. Notice the power cable of one of the buried heaters

The 20 % bentonite mixture was used for filling the upper part of the tunnel where layer-wise application and compaction could not be made. Previous tests by Stabilator AB had shown that blowing (shotcreting) of such a backfill can be made successfully with a high degree of homogeneity and with a reasonably high bulk density. The same type of robot aggregate (cf. Fig 4.18) as in the

previous tests was therefore used in Stripa. It was mounted on a chassi along which it could be moved and at the same time the front part, which carried the nozzle could be tilted and turned in practically all directions.

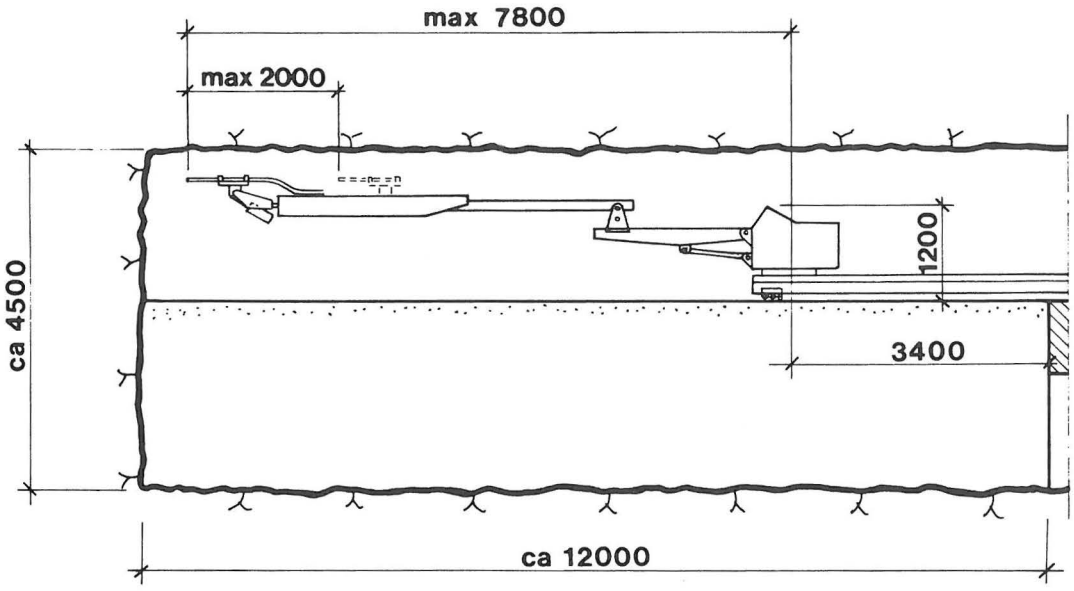

Fig 4.18. Schematic picture of robot for shotcreting the 20 % bentonite backfill. Dimensions in mm

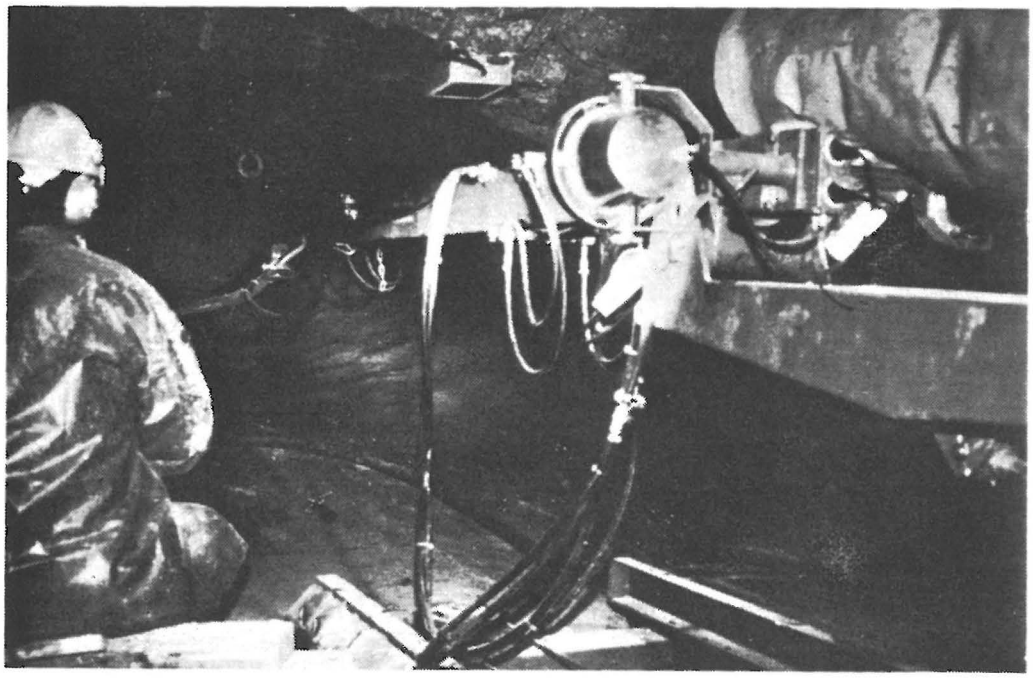

Fig 4.19. The Stabilator robot in action

Since the nozzle was also individually movable it was easy to apply the backfill in a fairly homogeneous condition also where the rock surface was irregular. Figs 4.19 and 4.20 show the robot and its nozzle.

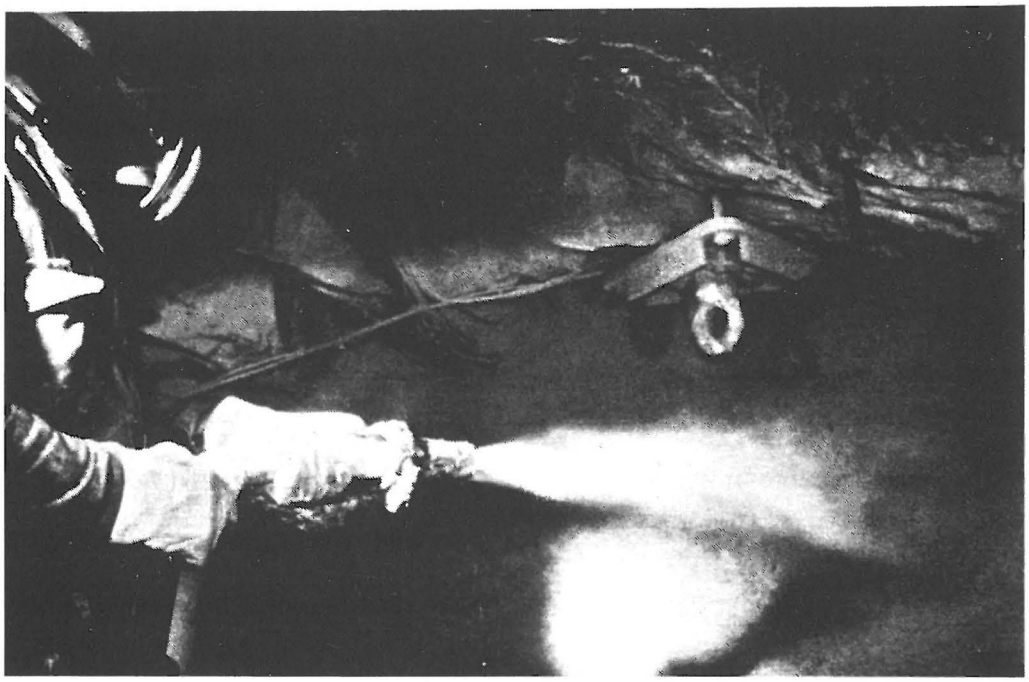

Fig 4.20. Shotcreting backfill

The feeding of backfill material through the flexible tube to the nozzle was achieved by use of pressurized air. The procedure is rather sensitive and the shotcreting requires continuous checking of the air pressure as well as the water flow. Rather extensive tests had to be run before the operation ran properly. Once started, it involved blowing of backfill to form a very steep wall that moved in the course of the filling and from which some material bounced back and formed a lower berm of loose material. Usually this effect was not very obvious but occasionally, i.e. when disturbances in the feed of material and water occurred, the berm had to be removed. Some shallow parts of the steep wall tended to slide down when the work stopped for adjustment, pauses or for the

or for the application of the numerous gauges which were inserted in the mass in certain sections. All these factors probably caused some variation in density, which may have been considerable, locally.

Figs 4.21 and 4.22 show the position of the various backfill materials. "H" in Fig 4.22 indicates the practical minimum free height for application and compaction of bentonite-poor backfill. It was found to be about 1.5 m with the equipment and staff available in Stripa.

4.2.2.6 Checking of bulk densities and water contents

The comprehensive weighing of all the backfill material that was prepared in the mixing station and the careful space determination, have given very accurate values of the average bulk densities and water contents. Thus, the backfill denoted "1" in Fig 4.21 was expected to have an average bulk density of ρ = 1.90 t/m^3 and a water content of 10 % immediately after the application and compaction. The density was checked by using densitometers (Fig 4.23) which gave ρ-values in the range of 1.83-2.12 t/m^3, with an average of 1.98 t/m^3. The water content was determined on excavated samples and found to be in the range of 9.0-9.4 %. The backfill denoted 2 and 2A in Fig 4.21 had a calculated average bulk density of ρ= 1.92 t/m^3 and an average water content of 10 %. For this zone the actually determined density was found to be in the range of 1.81-2.19 t/m^3, the average being 1.95 t/m^3. The numerous water content determinations gave the range of 8-13 %, the average being 10.1 %. The backfill denoted 3A, finally, was estimated to have an original average bulk density of ρ = 1.38 t/m^3 and an average water content of 15.5 %. The checking, at which cylindrical samples were punched into the mass for determi-

nation of the parameters required for the derivation of bulk density values, showed that the bulk density varied between 1.14 and 1.76 t/m^3, with the average 1.44 t/m^3, while the water content was in the range of 11-22 %, the average being 15.3%.

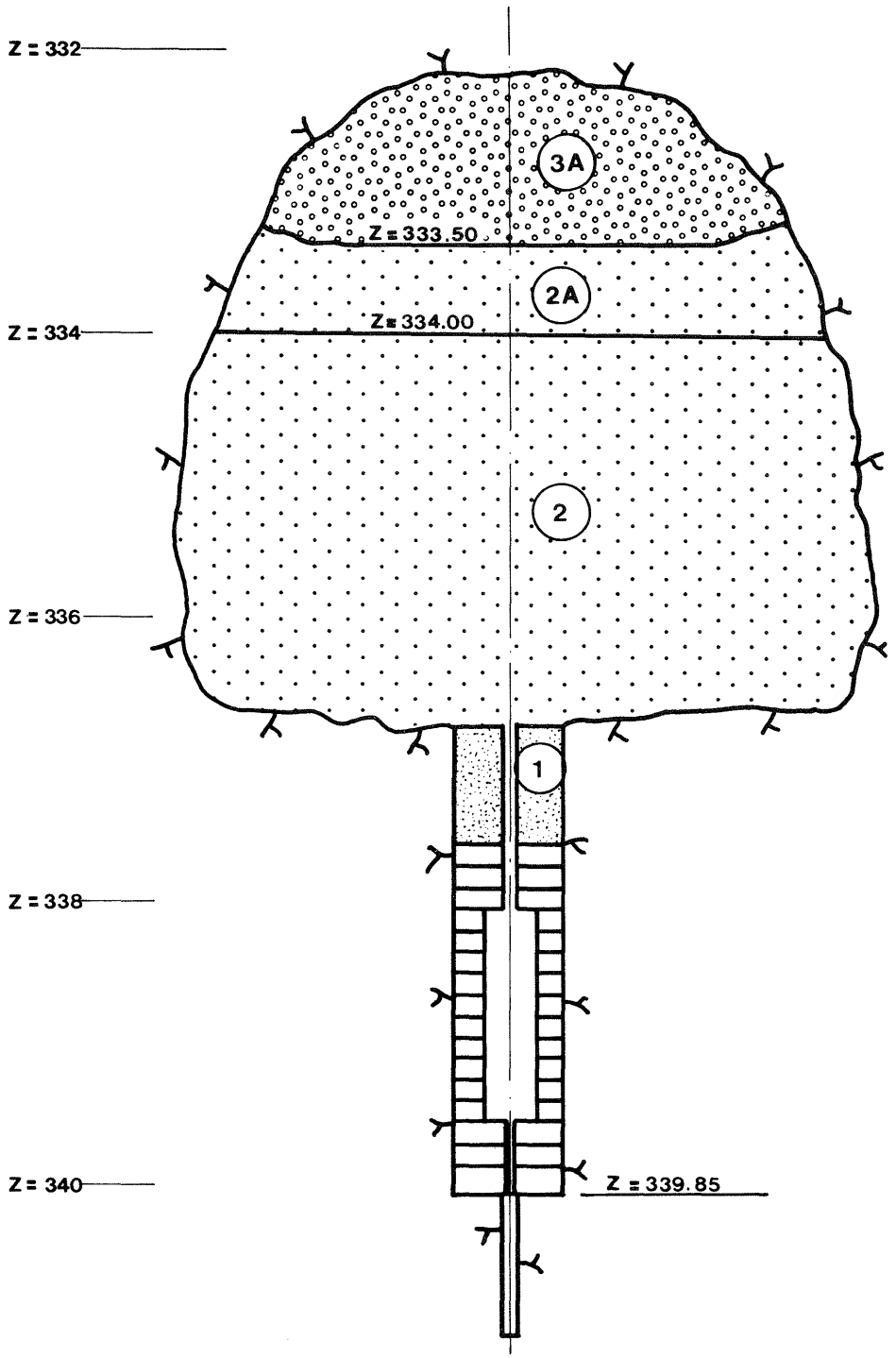

Fig 4.21. Cross section through backfilled tunnel and deposition hole

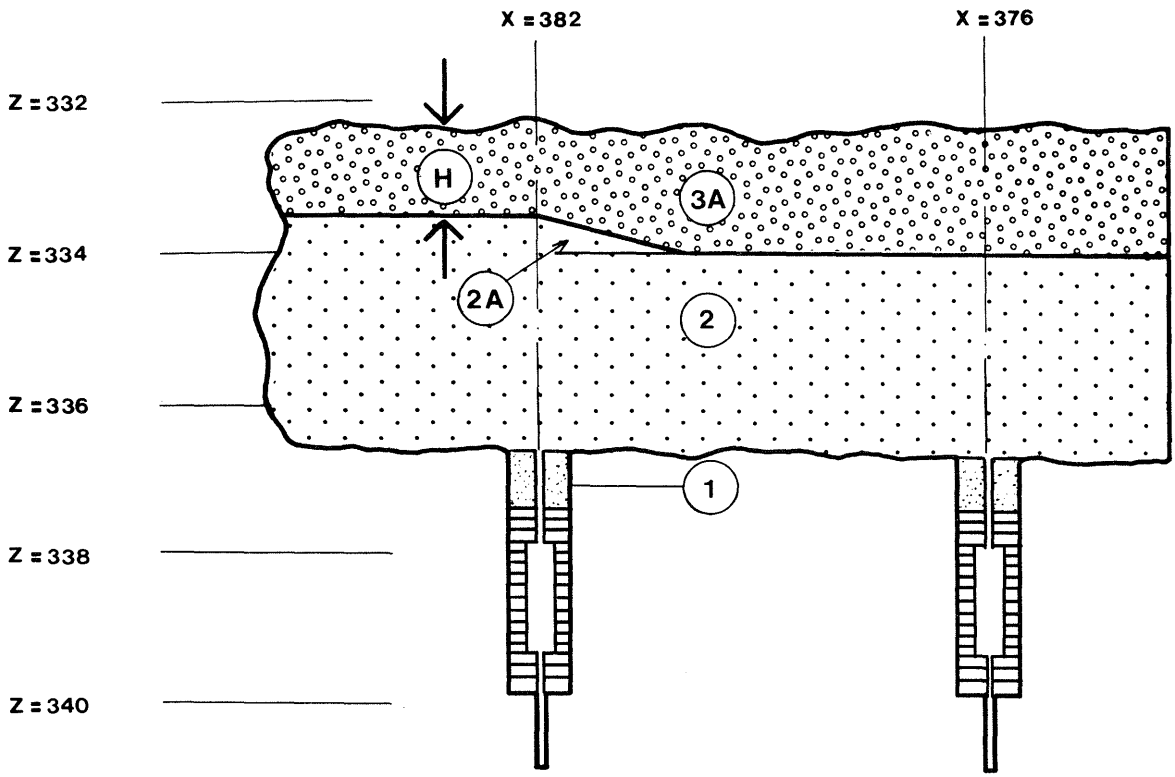

Fig 4.22. Section through tunnel axis

The field determination of the density and water content of the 10 % bentonite mixture showed that the application and compaction in the tunnel had been successful. The average bulk density was thus about 95 % of the laboratory-derived value using the modified Proctor compaction technique. It is clear however, that much better results had been obtained if vibrating rollers could have been used.

The 20 % bentonite mixture was slightly softer than expected, the predicted bulk density being 1.5-1.6 t/m^3. The deviation was due to the special conditions which were valid at the field test, such as the frequent interruptions for instrumentation. In short, the bulk densities arrived at were probably lower than the ones which can be obtained when continuous shotcreting is applied. However, development of more effective application and compaction techniques when the available space is limited is still being asked for.

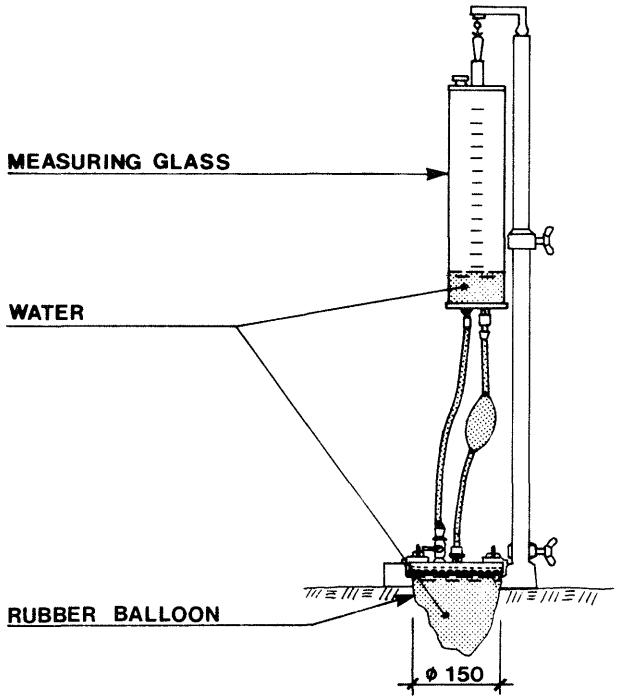

Scenario:
1 Make the ground surface even
2 Dig hole with the shape of half-sphere
3 Measure the volume required to fill the balloon
4 Determine weight of excavated soil

Fig 4.23. Determination of volume of excavated sample. After weighing the sample the bulk density is obtained by dividing the weight by the volume. The accuracy is within 3-5 %.

4.3 Instrumentation

4.3.1 General

The major objective of the Buffer Mass Test was to record the development of temperature fields, water uptake, and swelling and water pressures in the highly compacted bentonite in the heater holes, as well as in the tunnel backfill. In addition, internal displacements in the clay materials and change of rock joint apertures were to be observed in the heater holes. The instruments and recording devices for these determinations are described in this chapter.

While the measurement of temperature and pressure implied application of ordinary, wellknown technique, the other measurements had to be made by applying unconventional methods. Thus, the recording of rock strain was made by use of a recently accessible, rather sophisticated method (Kovari). No suitable commercial gauges for moisture measurement were available and new equipment therefore had to be developed for the recording of water uptake. Finally, the expected internal displacements in clay backfillings were measured by careful determination of the position of reference objects ("coins", plastic stripes) at the excavation of these materials since electronic gauges were not found to be reliable under the present test conditions.

4.3.2 Temperature gauges

4.3.2.1 Properties

The choice of a suitable instrumentation system for temperature measurement was based on the criteria that the gauges have to be mechanically and chemically stable, that the system must offer a

simple way of recording, and that the accuracy must be at least $\pm 0.5^{o}C$. A further requirement was that the gauges must yield stable signals for at least four years at temperatures up to $90^{o}C$. Pentronic's* steel-sheathed copper/constantan ISA type T thermal elements (thermocouples) with MgO insulation were found to be most suitable for the BMT (Fig 4.24). They sustain temperatures of at least $400^{o}C$, and their accuracy is about $\pm 0.1^{o}C$ in the temperature interval $0\text{-}160^{o}C$ as shown by calibration tests made by the National Testing Institute, Borås, Sweden. 25 elements were tested in two series, one extending from $0\text{-}90^{o}C$, the other from $100\text{-}160^{o}C$. The net accuracy of the temperature readings, which is a function of the accuracy of the integrated measuring and recording systems, is estimated at $\pm 0.5^{o}C$.

Experience from earlier heater tests in the Stripa mine indicates rapid corrosion of the steel coating of thermal elements when ordinary steel qualities are used. Although this seems to be related to the case of elements being submerged in freely flowing water, a less corrosive steel quality, SS 2343, was chosen for the BMT gauges. The Swedish company ASEA-ATOM specified, on request, that the elements can be expected to operate satisfactorily for at least 4 years in an environment characterized by a chloride content of less than 85 ppm, a pH in the range of 6.5-9, and a temperature not exceeding $80^{o}C$. This applies approximately to the conditions in the BMT.

---

*) Pentronic, Box 36, 59093 Gunnebo Bruk, Sweden.

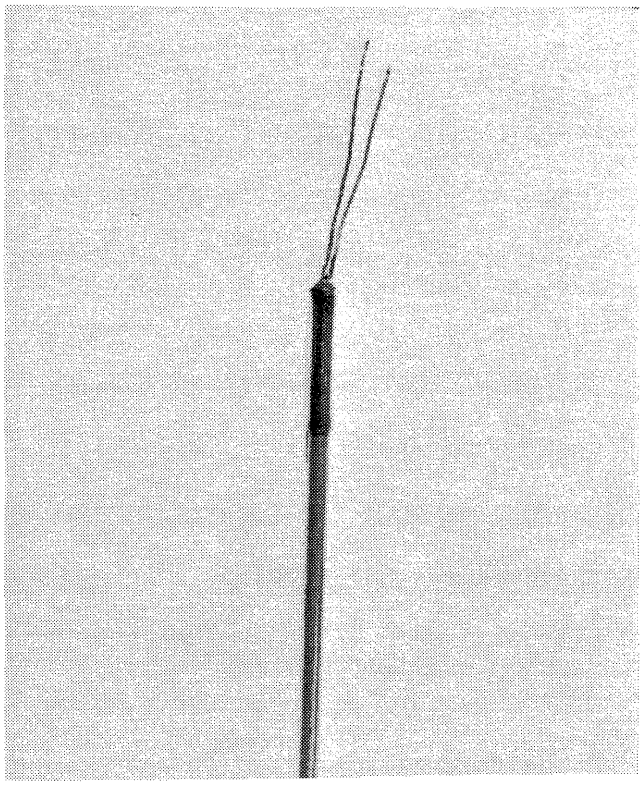

Fig 4.24. Pentronic ISA/T thermal element.
(Approximately full scale)

4.3.2.2 Preparation and installation

The large number of thermal elements, the total being 1242, called for systematic handling, installation and labelling. The large variation in distance between the individual positions of the elements and the switch boxes in the outer part of the BMT tunnel caused a corresponding variation in wire length, which required careful estimation of this length for ordering and manufacturing. For practical reasons, however, certain length intervals had to be chosen for fairly large groups of elements. Plastic tape labels were attached to the respective elements and at their connections in the switch boxes, the codes referring to the respective position of the gauges. The code consisted of 8 symbols, the first denoting heater number 1-6, backfill 7, or rock 8; the next two symbols representing the type of gauge (TS for temperature sensor). The subsequent two symbols referred to the level (z-coordi-

nate), while the last three represent the lateral position (y-coordinate). Thus, 1 TS 13014 characterized a thermal element in heater hole no 1 at mid-height of the heater, the element being located at the rock/clay interface.

The elements located in the blocks of highly compacted bentonite were inserted in drilled holes with a close fitting of the gauges (Fig 4.25). The manufacturer's specified minimum radius of curvature of the wires was 2 cm, which was achieved by using a special device for the bending operation and by carving correspondingly curved grooves in the bentonite blocks (Fig 4.26). In the sand/-bentonite backfills, the elements were simply pushed into the fill.

The same type of elements were also used to measure rock temperatures in the rock surrounding heater hole no 5. For this purpose the gauges were embedded in sand in 30 mm diameter percussion-drilled boreholes.

The wires from each heater hole and instrumented section in the rock and backfill were collected in bundles that extended to the switch boxes, which were in turn connected with the data acquisition system in the mine by insulated multicables. The bundles passed through the bulwark inside steel profiles which were sealed by use of epoxy resin to prevent water leakage along the cables.

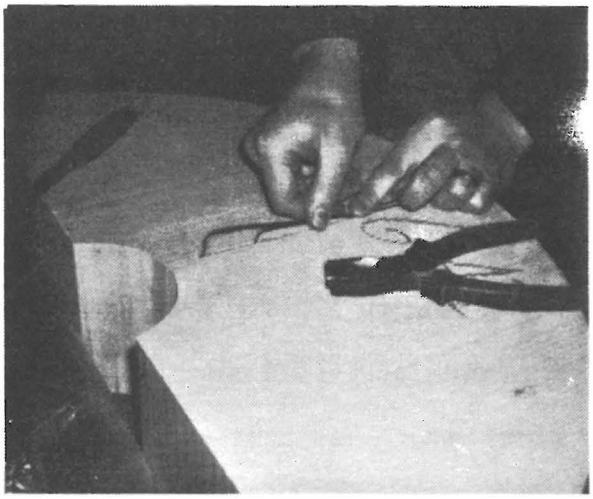

Fig 4.25. Insertion of thermal elements in blocks of highly compacted bentonite

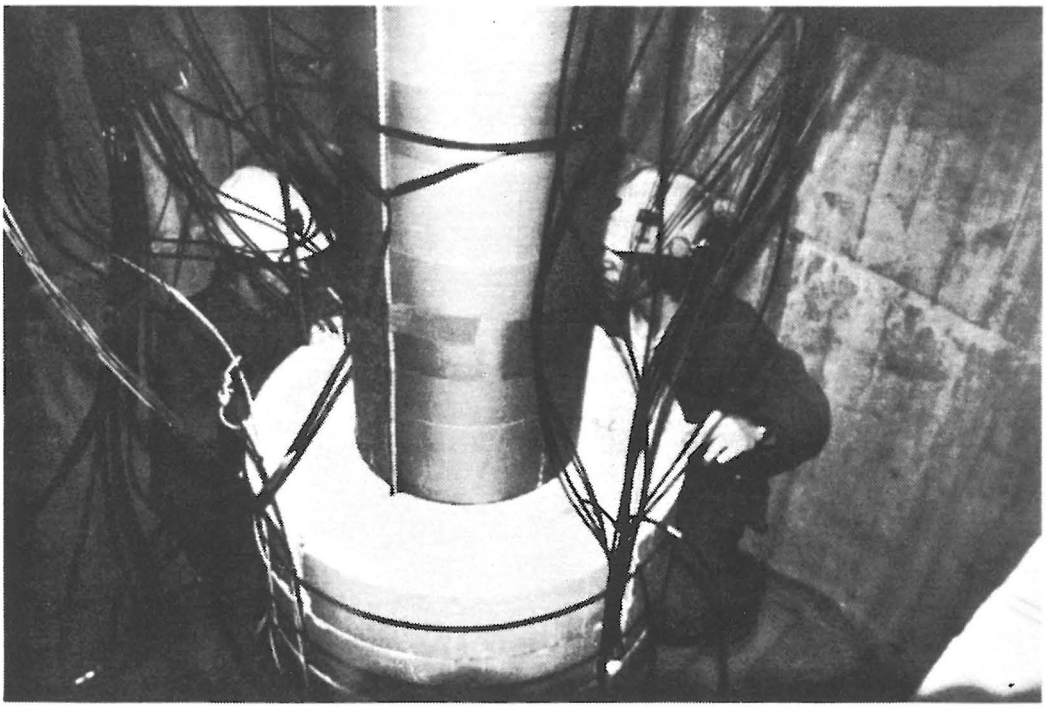

Fig 4.26. Application of bentonite blocks to form the bentonite heater unit. Notice the grooves for wires and cables

4.3.2.3 Positions

The array-type arrangement of the heater holes means that their temperature fields were superimposed, which produced asymmetric temperature distributions in the holes. A proper monitoring principle was therefore to locate the gauges in the longitudinal plane through all the centers of the holes, and in the perpendicular plane through each hole. In each of these planes the elements were located in radial arrays on five levels, so that the detailed temperature variation with the distance from the heater surface could be identified. The arrangement is illustrated in Figs 4.27 and 4.28 for sections through hole no 3, which is the first one outside the bulwark. In the longitudinal direction (Fig 4.27), the three central instrumented levels contained six elements on each side, the inner one contacting the heater and the outer one being in contact with the rock. The distance between the elements was slightly less than 4 cm. In the perpendicular plane only five elements were used on each side. These drawings also show the positions of the thermal elements in the overlying bentonite/sand backfill in the boxing-out, and below and above the heaters in their holes.

The tunnel backfill had three instrumented sections, two corresponding to the cross sections perpendicular to the tunnel axis through heater holes no 1 and 2, and one representing the cross section at half-distance between these holes. The positions of the elements are shown in Fig 4.29, which represents the section through hole no 1.

The rock around heater hole no 5 was monitored for measuring the rock temperatures in 25 boreholes. They were located as shown in Fig 4.30, the vertical distribution of elements being shown in Fig 4.31.

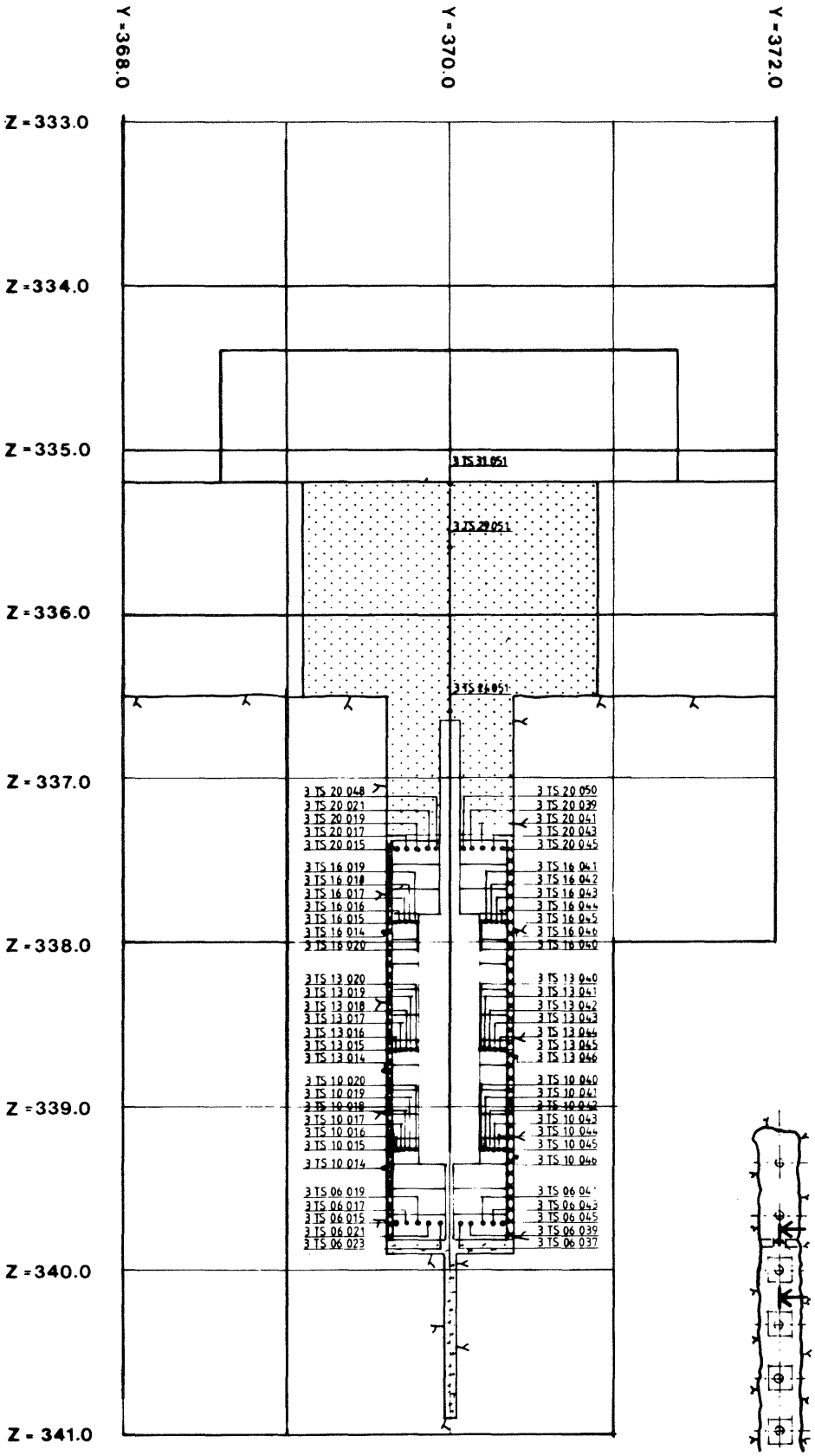

Fig 4.27. Longitudinal section through heater hole no 3, illustrating the positions of the thermal elements in this plane

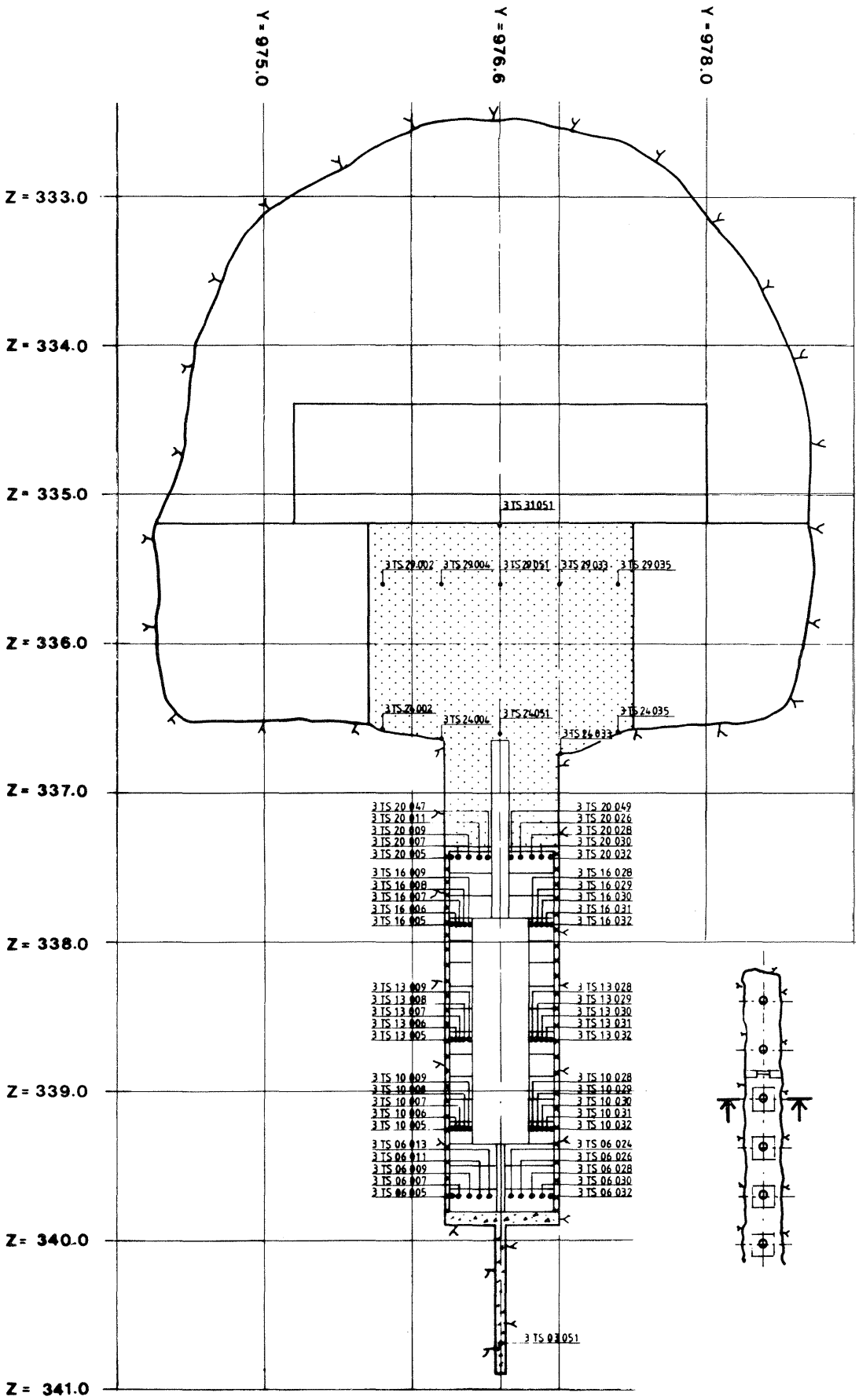

Fig 4.28. Cross section through heater hole no 3, illustrating the positions of the thermal elements in this plane

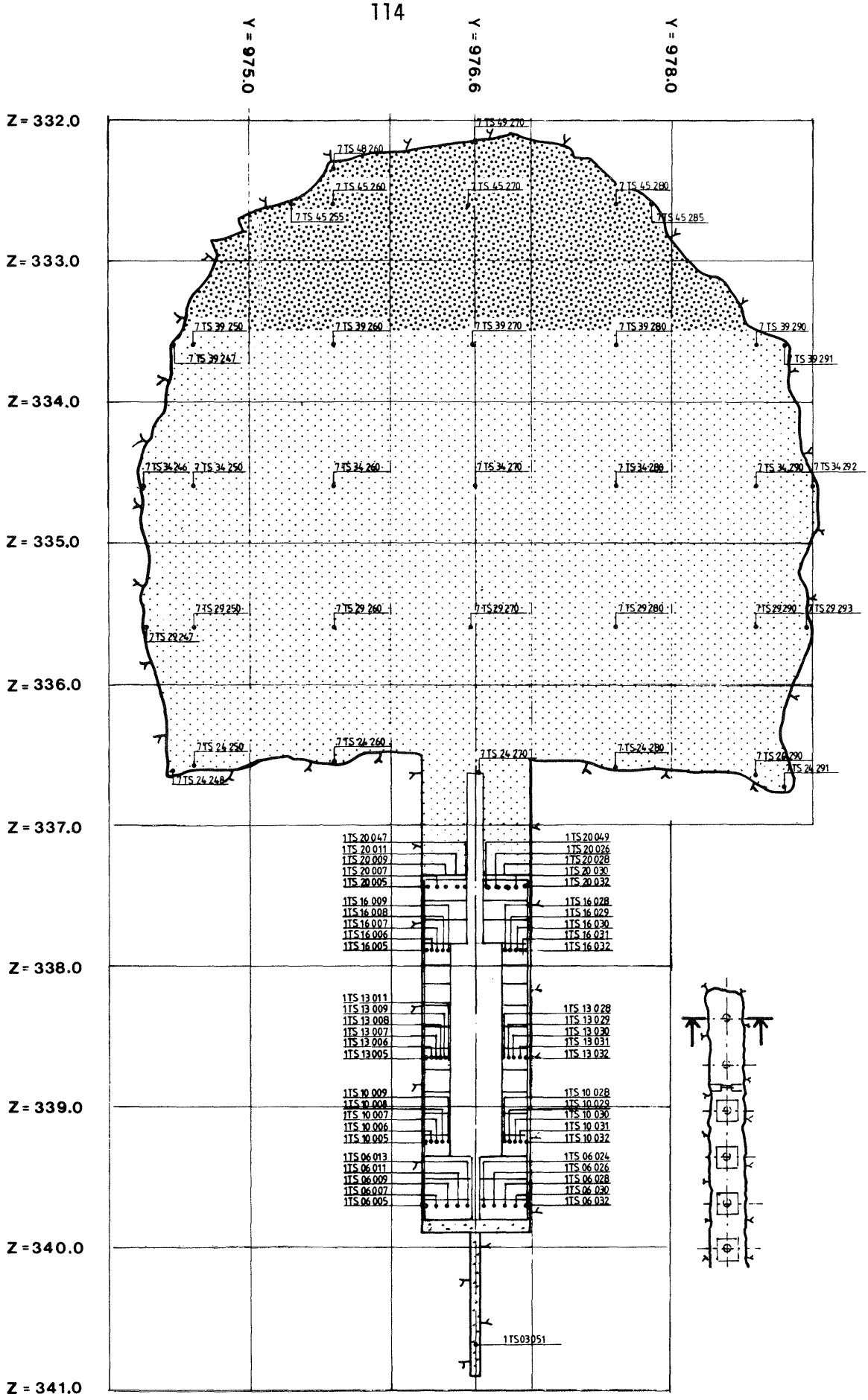

Fig 4.29. Cross section through heater hole no 1, illustrating the positions of the thermal elements in the highly compacted bentonite in the hole and in the tunnel backfill

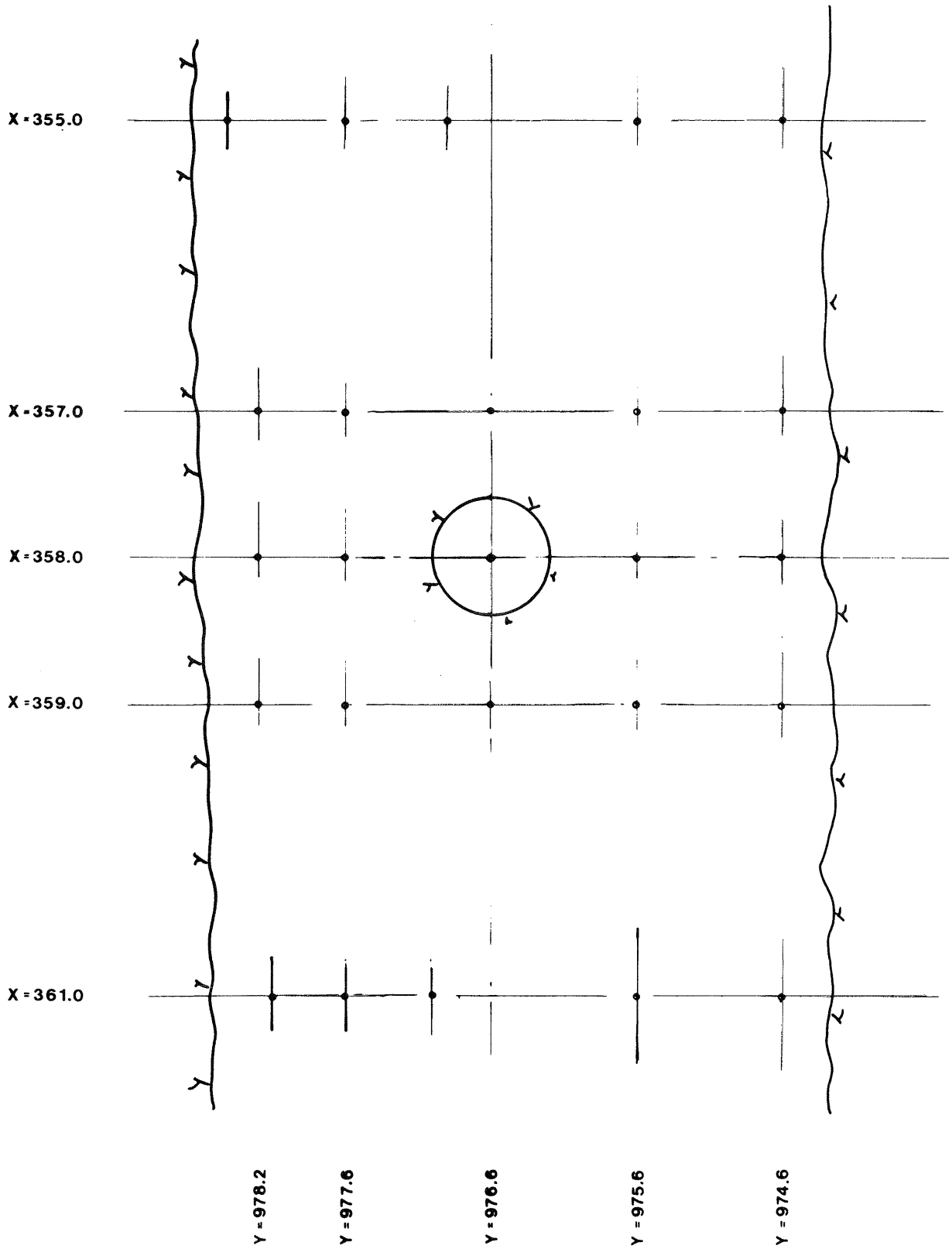

Fig 4.30. Location of 25 Ø 30 mm boreholes filled with water saturated sand in which thermal elements were embedded

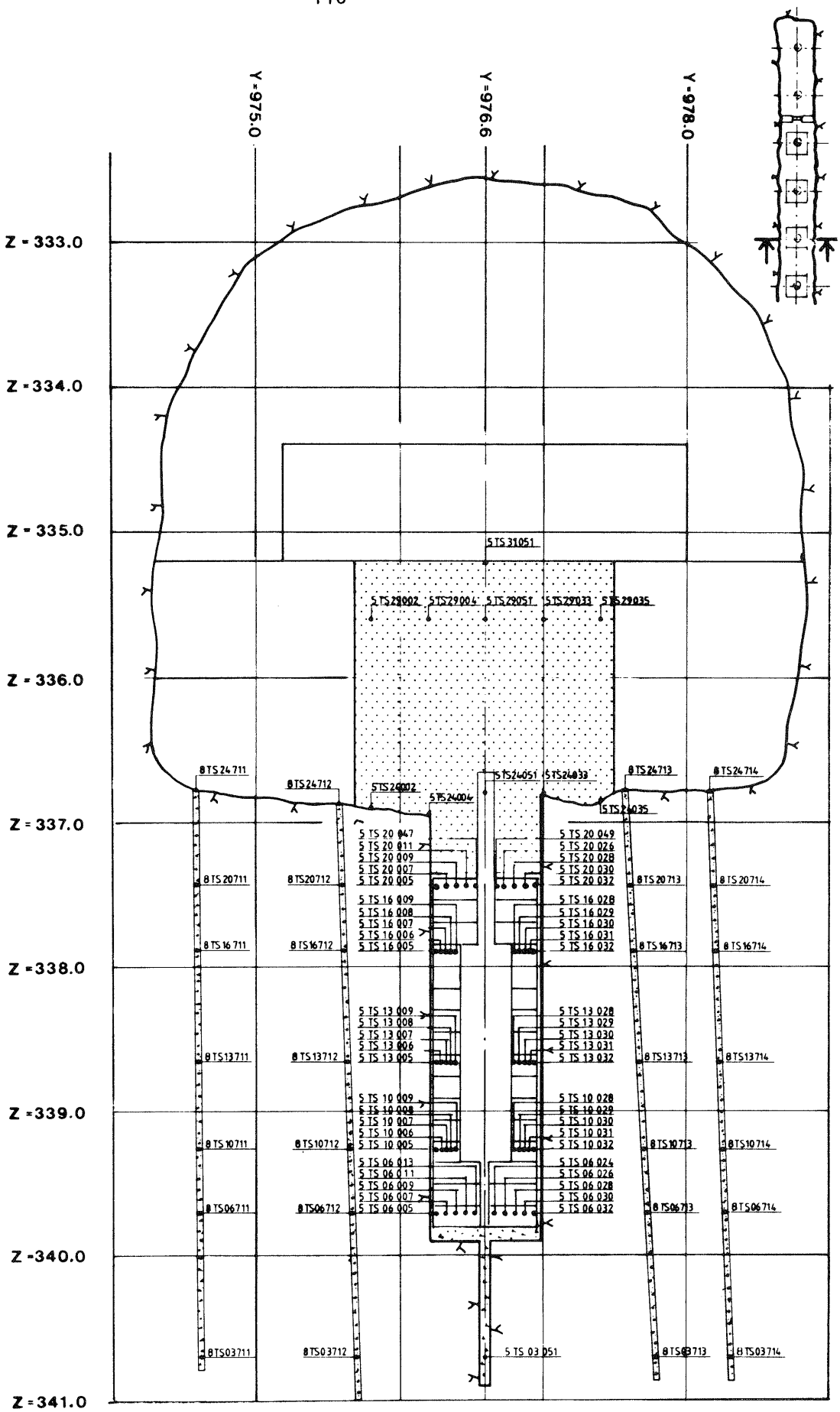

Fig 4.31. Cross section through heater hole no 5, illustrating the positions of the thermal elements in the heater hole and in the boxing-out

4.3.3 Pressure gauges

4.3.3.1 Properties

The expected swelling pressures in the highly compacted bentonite ranged from a few hundred kPa to about 10 MPa, while the corresponding pressures in the sand/bentonite backfills were assumed to be lower than 500 kPa, except were pressures were transferred from the heater holes in which case they were assumed to approach 5 MPa. This large span and the long duration of the BMT experiment called for pressure gauges with proven durability and mechanical strength, and with the property of yielding stable pressure values, the latter quality not being offered by electric transducers. The Gloetzl* pressure cell was found to be the most suitable device, although it has certain disadvantages, such as being temperature-sensitive and requiring tedious measuring and recording operations.

The cell consists of a pressure pad filled with mercury, a pressure valve against which the mercury exerts the same external pressure as that which affects the pad (if temperature effects are ignored), and a pressure measurement unit (Fig 4.32). At the recording, the pump starts at a given time by which oil is slowly pumped through the pressure pipe to the valve, in which the membrane deflects when the applied pressure exceeds the mercury counterpressure. The measured pressure, with a certain low treshold value subtracted from it, equals the actual external pressure on the pad.

---

* Gloetzl Baumesstechnik, D-7512 Rheinstetten 4-Fo, West Germany

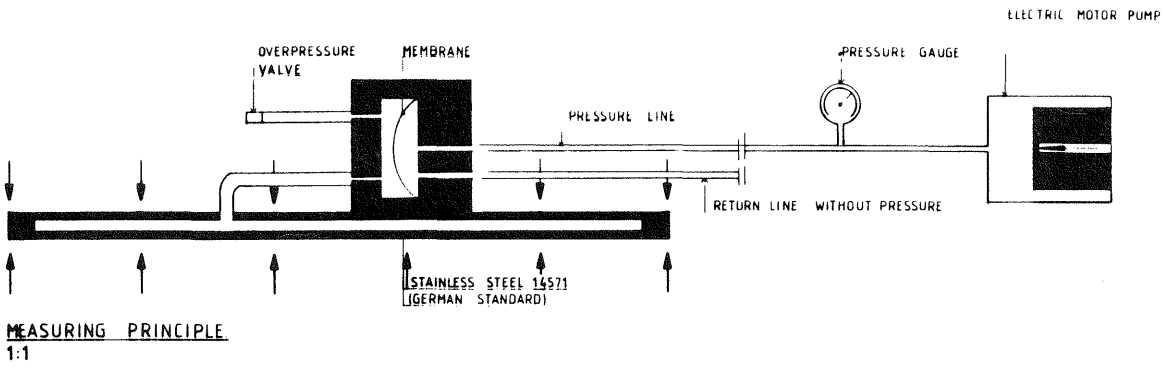

Fig 4.32. Schematic section through a Gloetzl pressure cell

Pressure cells of type B 15/25 QM 100 F with pads and pressure tubes of stainless steel and nylon, and return tubings of Polyamid 11 were chosen for the measuring of swelling pressures - or in practice - total pressures since water pressures were superimposed on swelling (effective) pressures. The read-out unit was equipped with two manometers and two transducers for different pressure intervals (0-4 MPa, 0-16 MPa), digital reading and printing facilities, as well as with an output for the interface to the data acquisition system (Fig 4.33). The time for measuring and recording of each individual circuit was 1-10 minutes with the automatic device. The total number of cells was 128 so a complete recording cycle took about five hours.

The accuracy of Gloetzl pressure readings mainly depends on the oil pumping rate and the temperature, provided that the cells have been properly installed so that no bending or twisting or incomplete embedding has taken place. Experience shows that the accuracy is within ±4% when the system is operated at room temperature (17). At increased temperatures the "prestress" of the valve increases and too high pressures are recorded but the influence is minimized by using mercury in the cells. The manufacturer claims that the readings change by 0.02-0.04 MPa per degree centrigrade, the higher value having been reported also in a careful study of

the Gloetzl stress gauge for use in concrete structures (18). It is obvious that, in practice, the temperature effect is a determinant of the accuracy and that it needs to be taken into consideration. Thus, with a predicted temperature increase in the heater holes of about 30°C at the rock interface, the readings would yield an overestimation by as much as 1.2 MPa if volume changes of the rock/clay system are not considered. A general conclusion, taking all major effects into consideration, is that the recorded values overestimated the actual swelling pressure by approximately 0.02 MPa per degree centigrade in the temperature interval 30-70°C.

4.3.3.2 Installation

The pressure pad of the cells had the dimensions 250x150x7 mm, the valve attached to one side of the pad extending to about 50 mm from the pad surface. The irregular shape of the pressure device was a complication because the whole cell needs to have a perfect and uniform support on the valve side in order to operate satisfactorily. For the measurement of internal pressures in the backfills, this was achieved by applying and compacting the backfill material carefully on top of the cell, which rested with the flat pad side on an even surface of previously applied backfill material. For the measurement of swelling pressures exerted by the clay materials on surrounding rock, the cells need to be cast in cement mortar. For this purpose a box-shaped wooden form was bolted to the rock and filled with cement mortar to form a support of the cell. This technique was applied in the backfilled tunnel, while vertical slots were cut in the rock to host the cells and their cable connections in the heater holes. The labelling was analoguous to that of the thermal elements, the letter code now being SS.

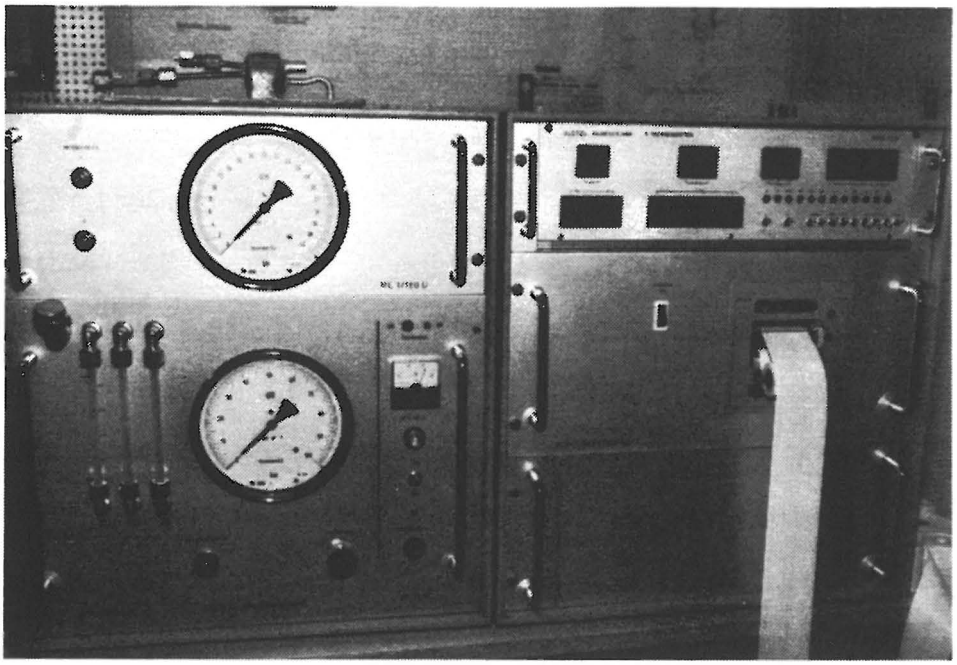

Fig 4.33. Complete automatic measurement and read-out unit for the Gloetzl pressure cells

4.3.3.3 Positions

The large dimensions of the pressure cells limited the number of cells that could be installed in each heater hole without interfering too much with the rock. Fig 4.34 shows the positions of the ten cells that were placed in the heater holes: three on each side of the heater hole, one on top of the heater and one immediately below it, one at the interface between the bentonite blocks and the overlying backfill, and finally one at the base of the heater hole. Fig 4.35 illustrates the arrangement in the heater holes outside the bulwark; here three cells were embedded in the backfill right over the respective heater.

As in the case of the thermal elements, three sections of the tunnel backfill were monitored, i.e. the two cross sections through heaters no 1 and 2, and the one at mid-distance between these two holes. In addition, eight pressure cells were also mounted on the bulwark, the positions being shown in Fig 4.36.

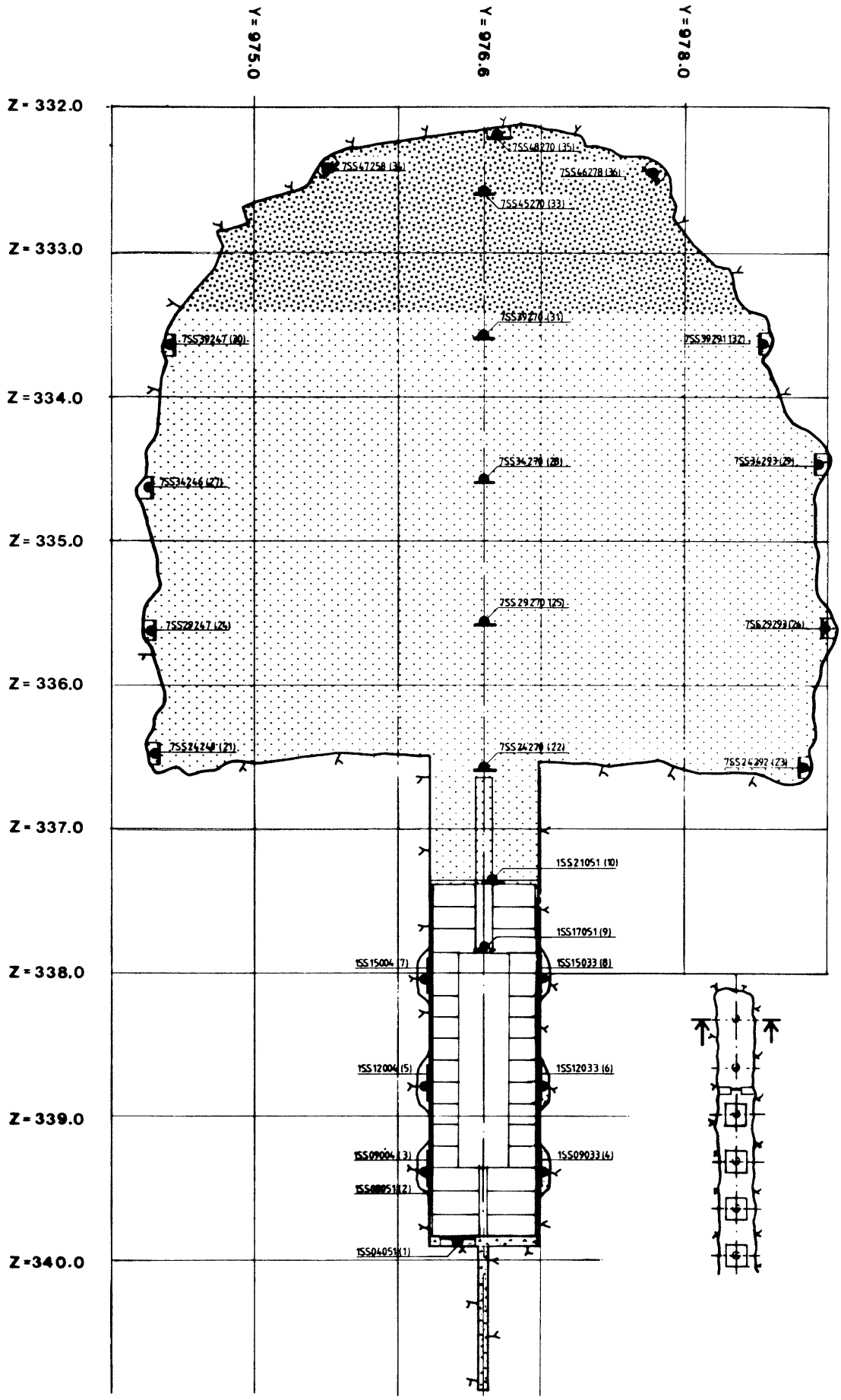

Fig 4.34. Location of pressure cells in heater holes no 1 and 2

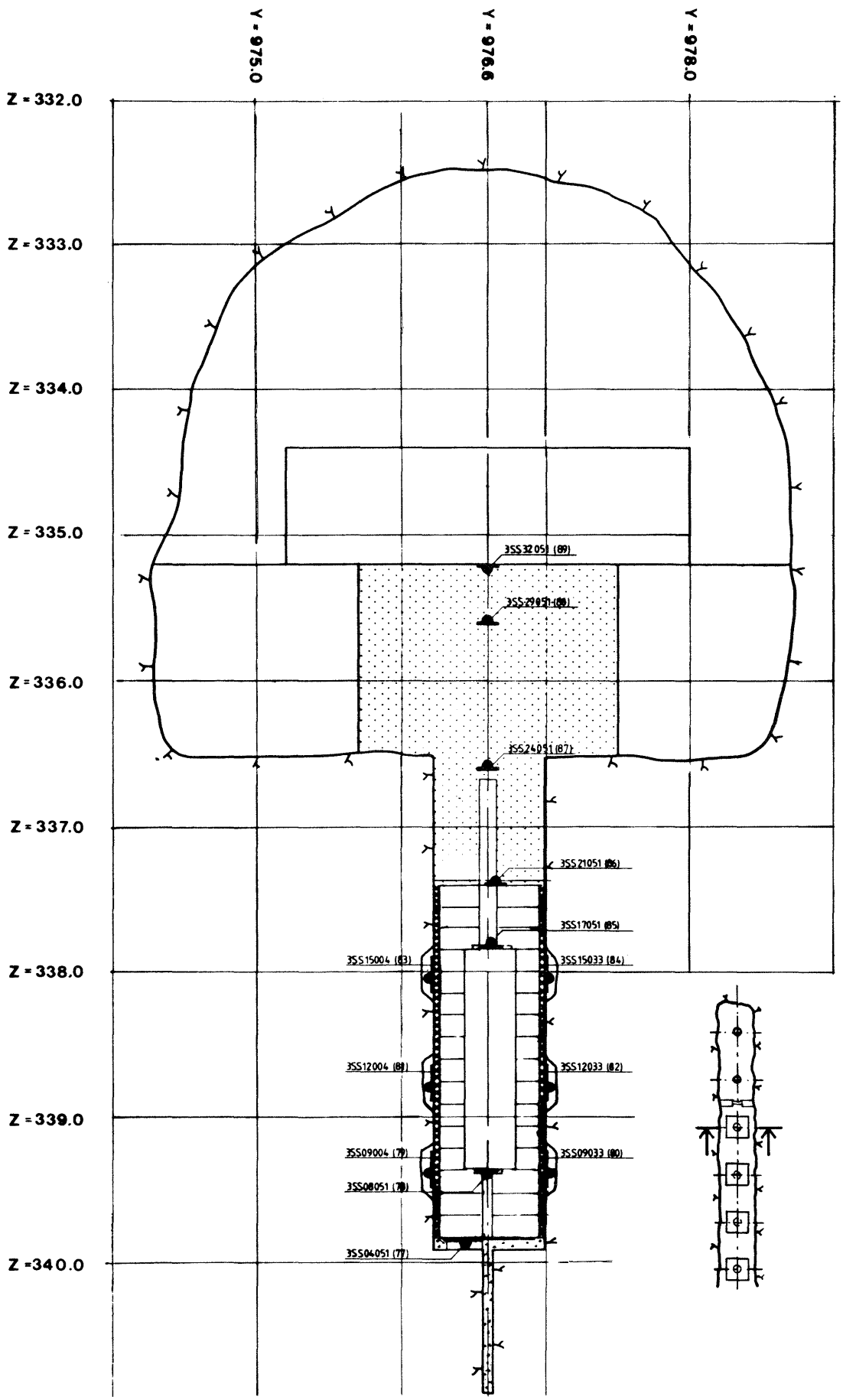

Fig 4.35. Location of pressure cells in heater holes and boxing outs (holes no 3-6)

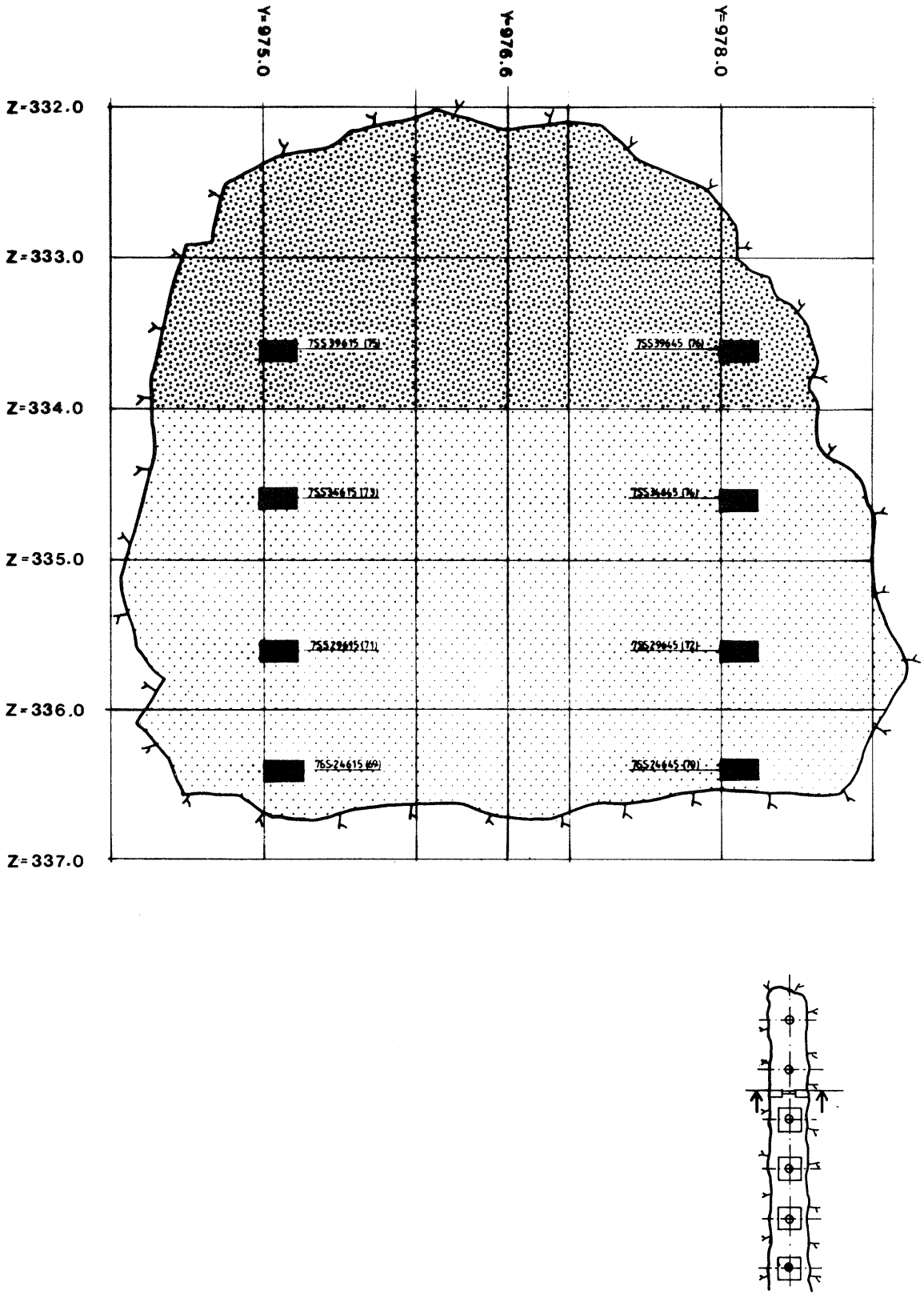

Fig 4.36. Location of pressure cells attached to the bulwark

4.3.4 Tie-rod Forces

4.3.4.1 Function

The concrete lids covering the boxing-outs were pressed against the slab by use of prestressed tie-rods, which were anchored in boreholes at about 10 m depth. This offered a possibility of determining the integrated swelling pressure exerted on the base of the lid by measuring the expected increase in anchoring forces. One of the lids was therefore equipped with AD/1000 load cells* applied between the lid and the nut of each of the twelve tiebacks (Fig 4.37). Hole no 5 was picked for this purpose since it is the wettest hole outside the bulwark with the best chance to exhibit increased tie-rod forces in the rather short test period.

The load cell consists of a steel tube equipped with strain gauges shielded by a rubber-type coating. Readings were taken by use of a compensated bridge circuit connected to the general data acquisition system. The maximum force is specified by the manufacturer to be 1 MN, the accuracy of the evaluated force value being ±2 %.

4.3.5 Piezometers

Three different systems for the measurement of water pressures were used: precision manometers, Gloetzl piezometers, and BAT piezometers.

---

* Geo-Beräkningar AB, Box 9002, 102 71 Stockholm 9, Sweden

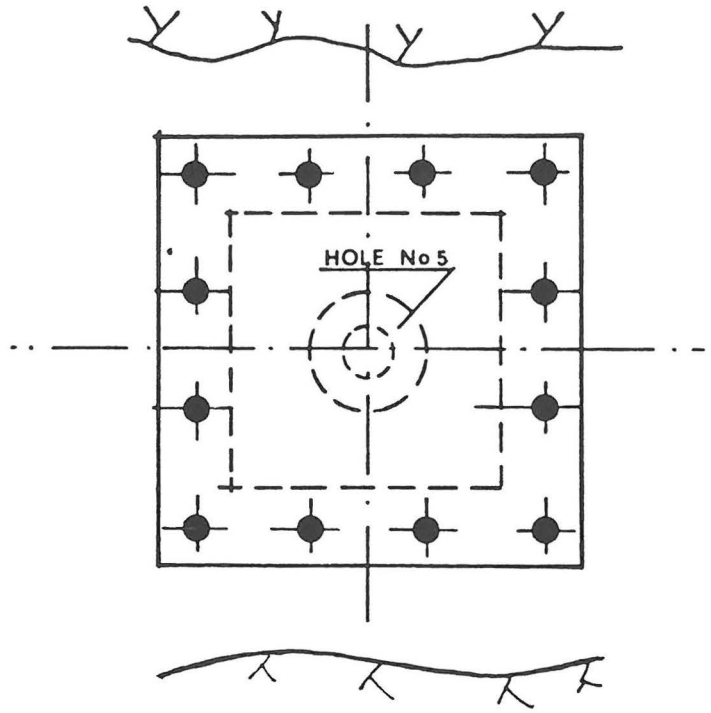

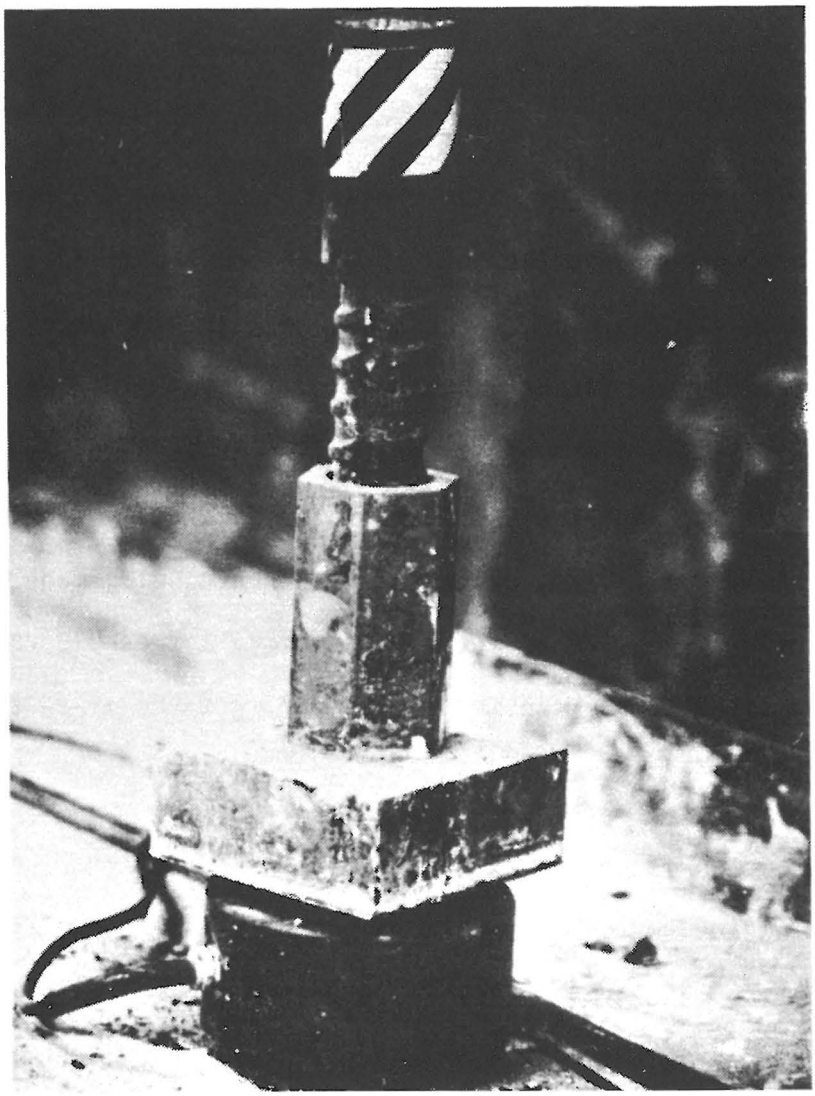

Fig 4.37. Load cells for measurement of tie-rod forces

4.3.5.1 Manometers

Manometers were used for measuring the water pressure in 15 Ø 76 mm boreholes, which extend radially from the tunnel periphery or from the tunnel front (cf. Chapter 3.5.2.1). The holes were orginally multipacker-sealed for measuring the water pressure at different distances from the tunnel, the sealed-off intervals being connected to manometers through nylon tubings. After the previously described rearrangement of the packers the tubings were connected with manometers at the outer end of the BMT drift. The accuracy of the readings was about ±5kPa, the expected pressure range being 1-1.5 MPa.

4.3.5.2 Gloetzl piezometers

Gloetzl piezometers for water pressure determination were chosen on the same grounds as the soil pressure cells: it is a reliable and simple system, and since the same measuring and recording units were used for both equipments, it was also an economic alternative. The piezometer operates in the same way as the soil pressure cells, but the pad is replaced by a cylindrical tip with a sintered metal filter, all metal components being made of stainless steel. According to the manufacturer, a treshold value of 80 kPa has to be overcome before oil overflow takes place and proper readings can be taken.

The piezometer is somewhat sensitive to heat but since none of the gauges was going to be exposed to higher temperatures than about 30°C in the test program for 600 W heater power, this influence should be negligible. Fig 4.38 shows a piezometer of the presently used type (P4 SF 30), which has a pressure range of 0-3 MPa. It was concluded that the accuracy of the recorded pressure values

was of the order of 10 kPa and that no reliable readings could be obtained for lower pressures than about 100 kPa.

The positions of the 28 Gloetzl piezometers were as follows:

* 1 gauge in each of the pilot holes which extend downwards from the centers of the heater holes

* 1 gauge in each of the two short vertical boreholes which had been drilled from the lower corners of the tunnel in the cross section through each heater hole

* 5 gauges in the tunnel backfill in the cross sections through heater holes no 1 and 2. Fig 4.39 illustrates the location of the piezometers in these two sections, while Fig 4.40 represents the piezometer positions in the sections through holes no 3-6

* The labelling was analoguous to that of the pressure cells, the letter code now being XS

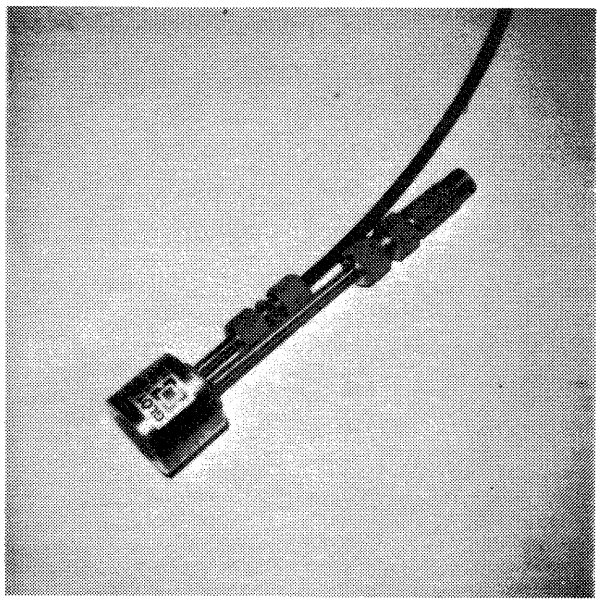

Fig 4.38. View of the Gloetzl piezometer

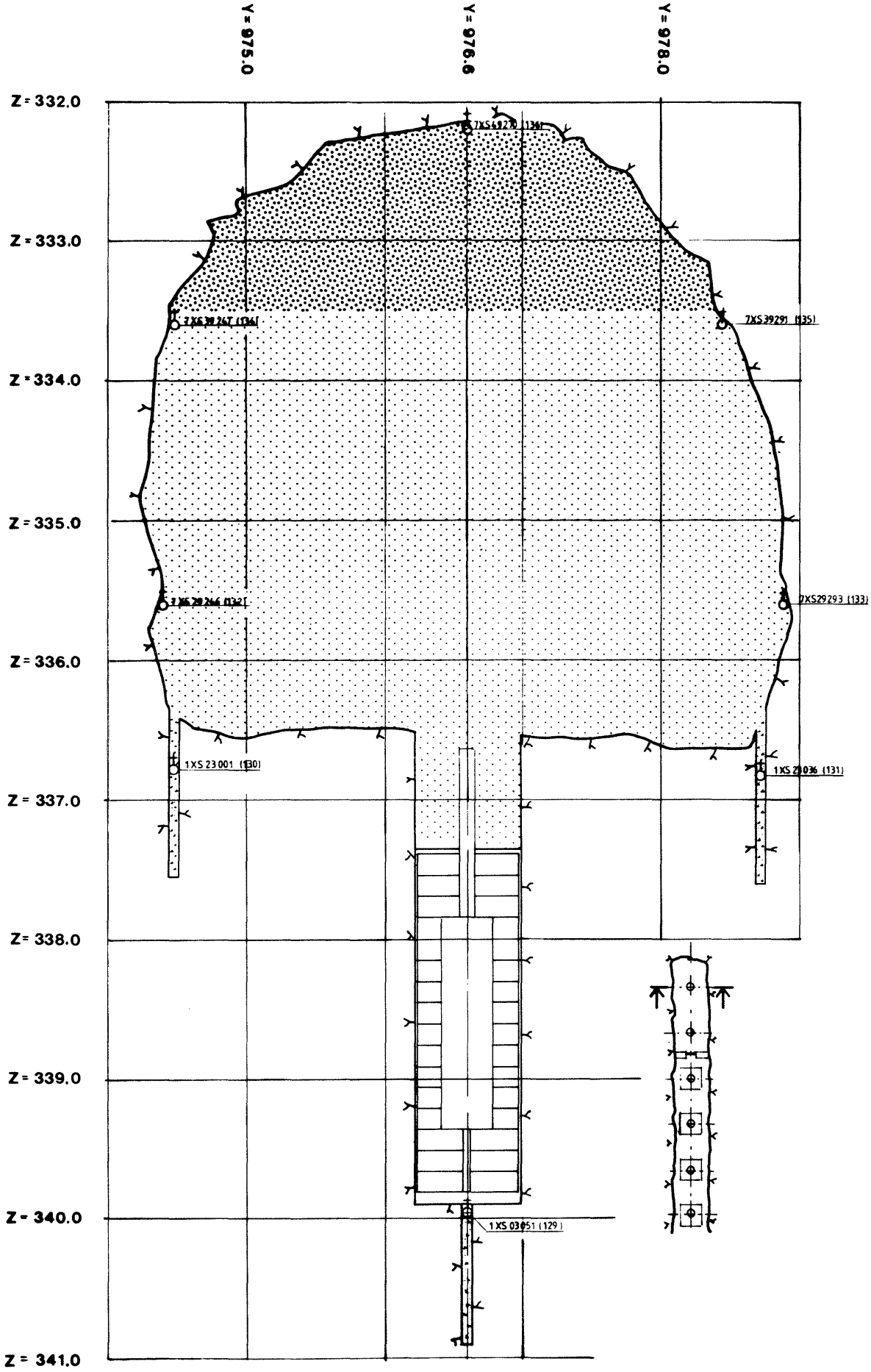

Fig 4.39. Location of Gloetzl piezometers in the cross sections through heater holes no 1 and 2

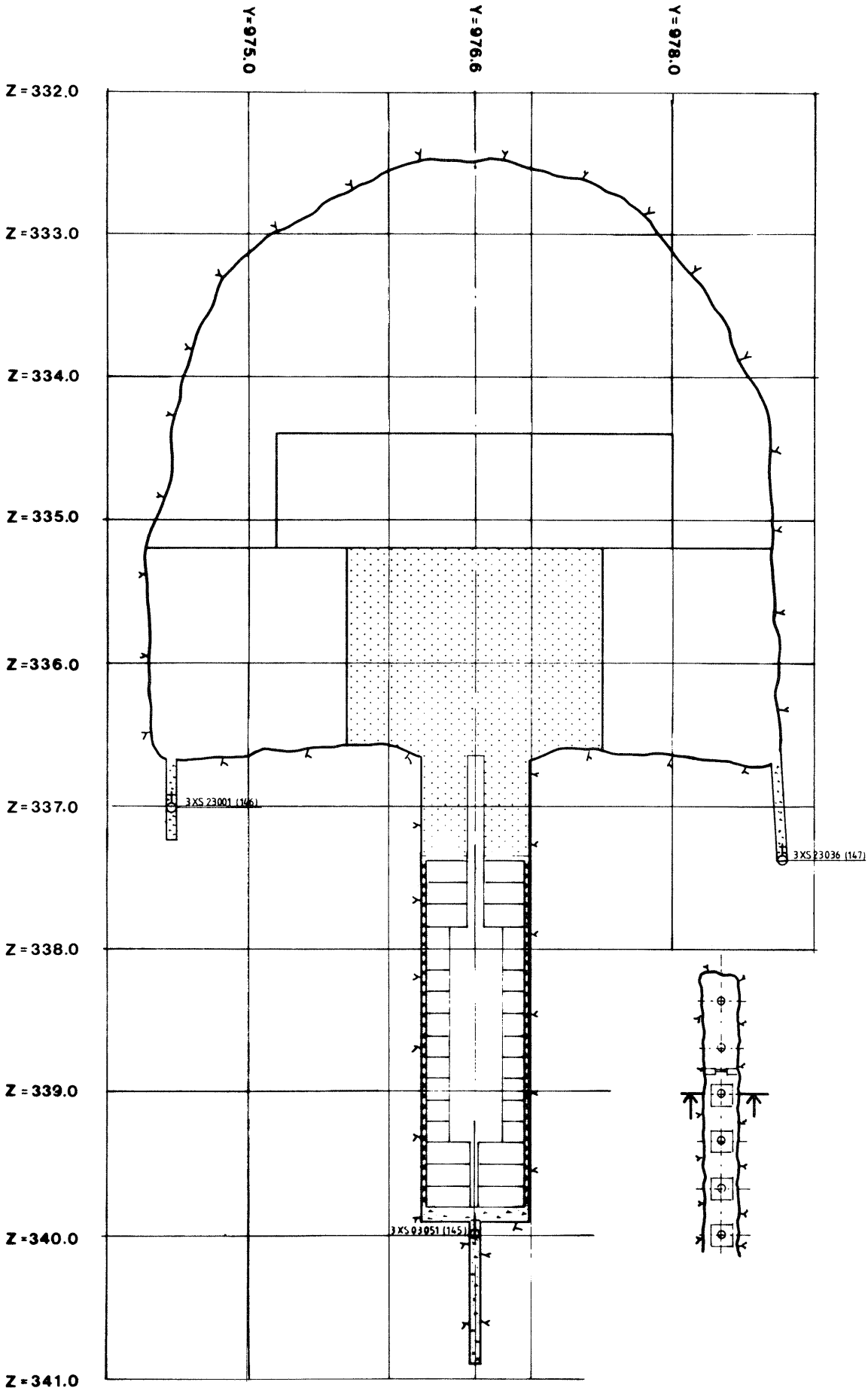

Fig 4.40. Location of Gloetzl piezometers in the cross sections through heater holes no 3-6

4.3.5.3 BAT Piezometers

The BAT* piezometer system was installed in order to have an independent, redundant instrumentation for measuring water pressures, and to have access to injection filters for possible flow and diffusion experiments in the backfill. The latter require two separate pipe connections to each filter tip which is offered by the BAT gauges (Fig 4.41). A second application was to use this equipment for measuring the water pressure in rock joints close to the rock/backfill interface. Here, much air was expected to be present, which would delay the build-up of water pressures in the filter and pipes if it could not be removed by saturating the filter tip through percolation. The last-mentioned application also required effective isolation of the piezometer from the air-rich backfill. This was achieved by insertion of the gauge in shallow boreholes intersecting the respective joint, and sealing the space between rock and piezometer with cement mortar and rubber rings (Fig 4.42).

The operation principle of the BAT piezometer is illustrated in the same figure. Two separate stainless steel pipes with shut-off valves lead from the ceramic filter tip to easily accessible "quick connects" to which a pressure transducer associated with a digital read-out unit was adapted when readings were taken.

The accuracy of the water pressure measurements is better than 1 kPa and there is no influence of temperature as long as the pick-up unit is located in room temperature.

---

* Bengt-Arne Torstensson AB, Box 27194, 102 52 Stockholm, Sweden

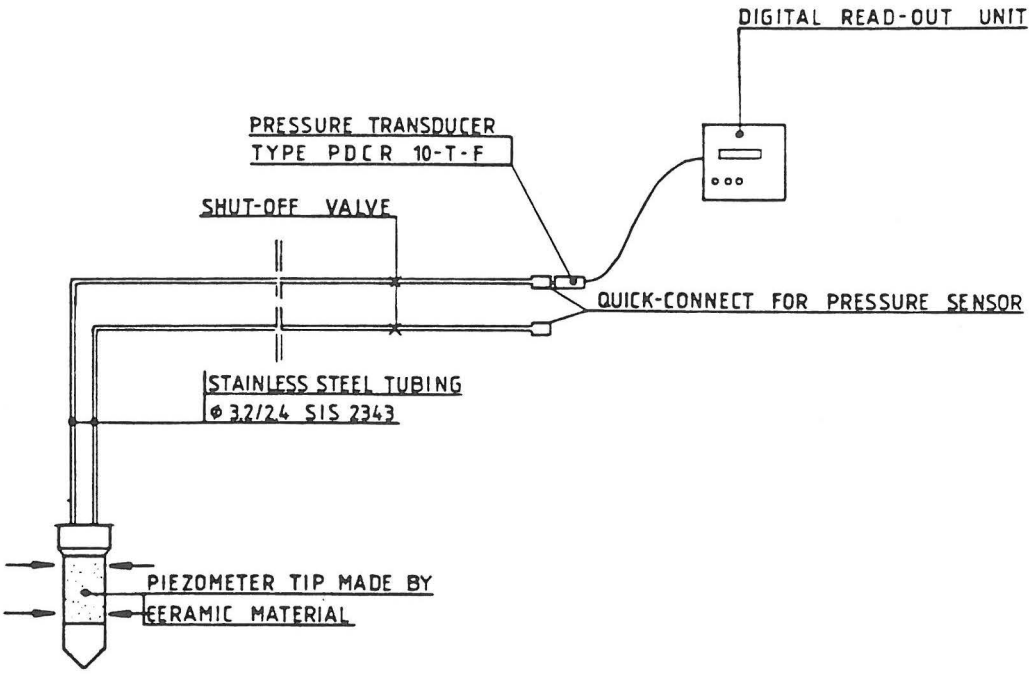

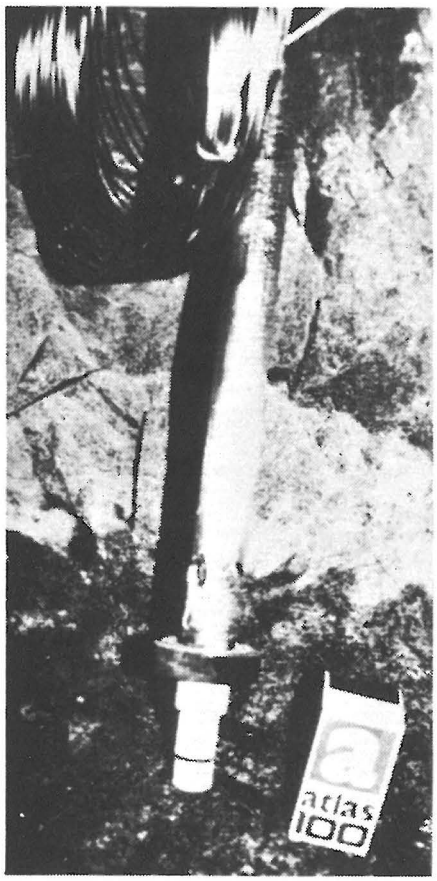

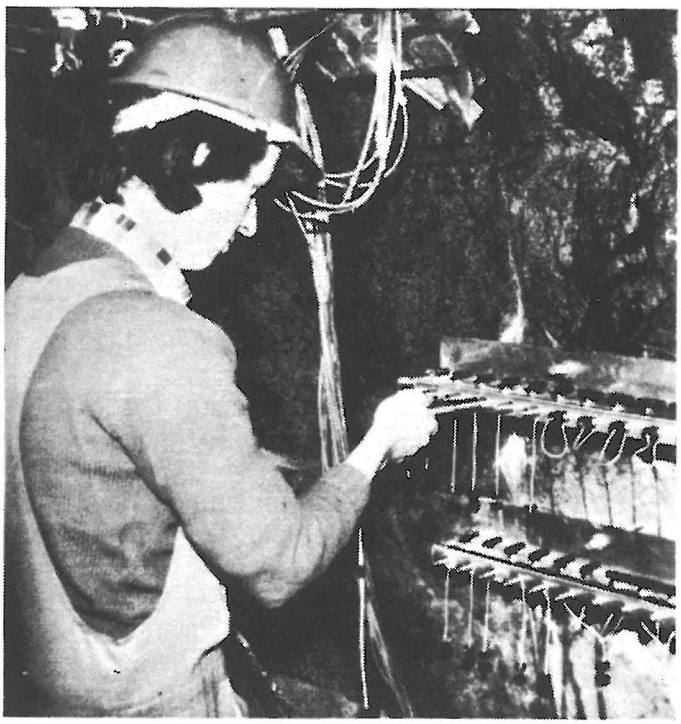

Fig 4.41. The BAT piezometer equipment. Upper picture shows the measuring principle while the lower illustrate the appearance of the filter tip and the recording unit

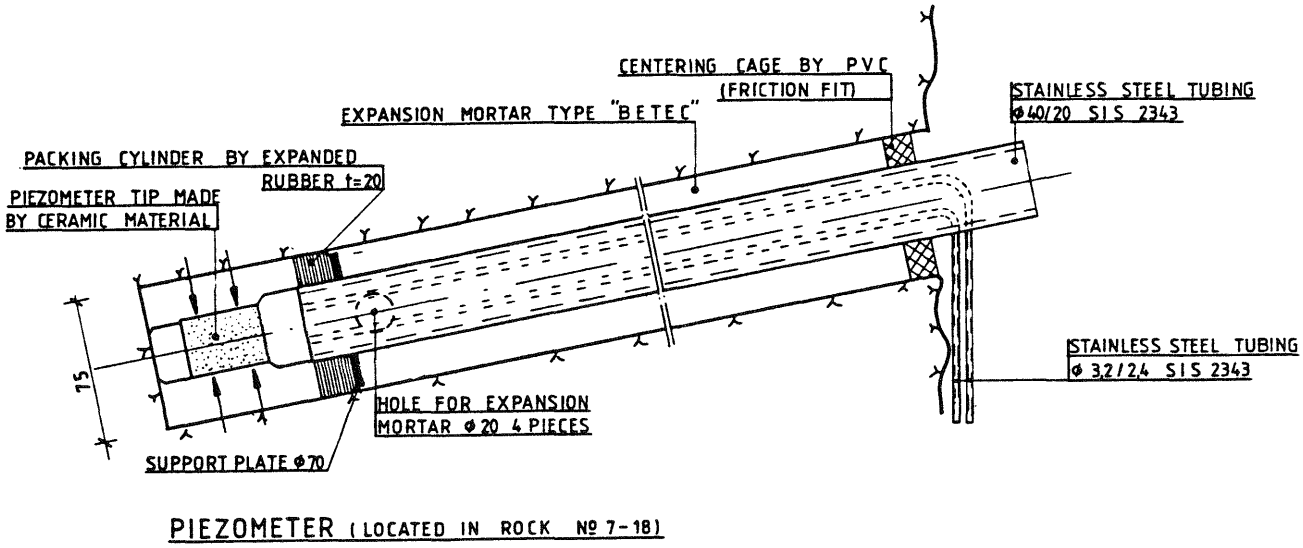

Fig 4.42. Application of BAT piezometer in shallow borehole

The positions of the BAT piezometers were as follows:

* 1 gauge in each of the pilot holes which extend downwards from the centers of heater holes no 1 and 2

* 1 gauge in each of the two short vertical boreholes which have been drilled from the lower corners of the tunnel in the cross sections through heater holes no 1 and 2

* 2 gauges in the tunnel backfill in the cross section through heater hole no 1 (Fig 4.43)

* 1 gauge in the tunnel backfill in the cross section between heater holes no 1 and 2 (Fig 4.44)

* 3 gauges in the tunnel backfill in the cross section through heater hole no 2 (Fig 4.45)

* 15 gauges in shallow boreholes in the rock, the positions being shown in Figs 4.46 and 4.47

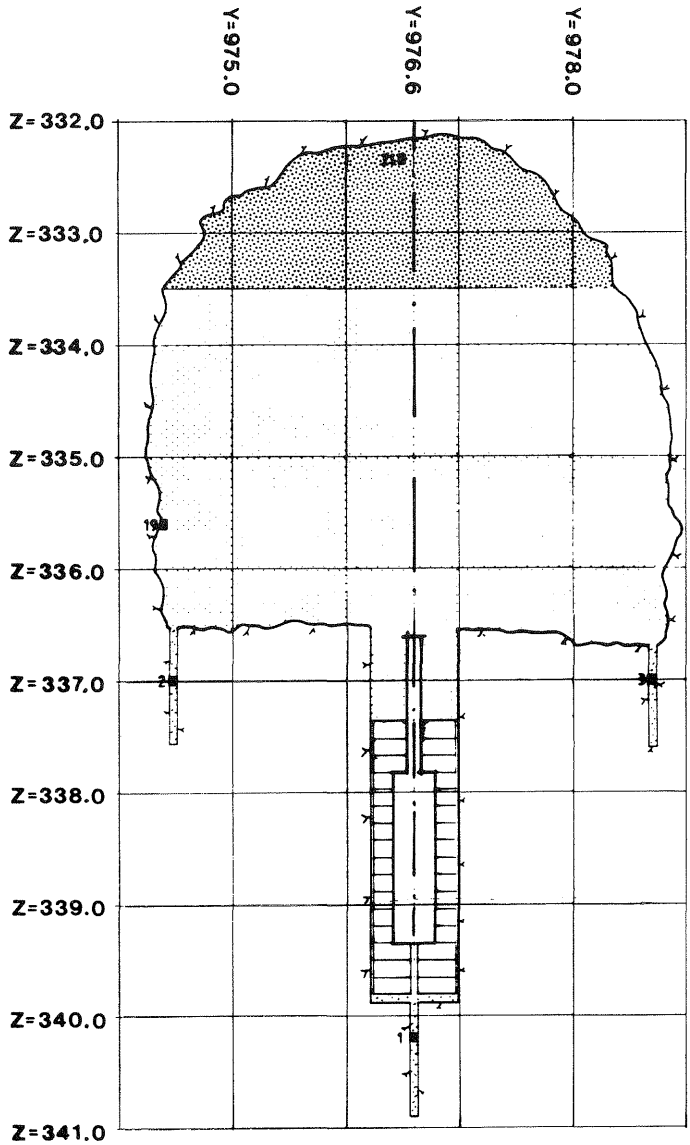

Fig 4.43. Location of BAT piezometers in the cross section through hole no 1

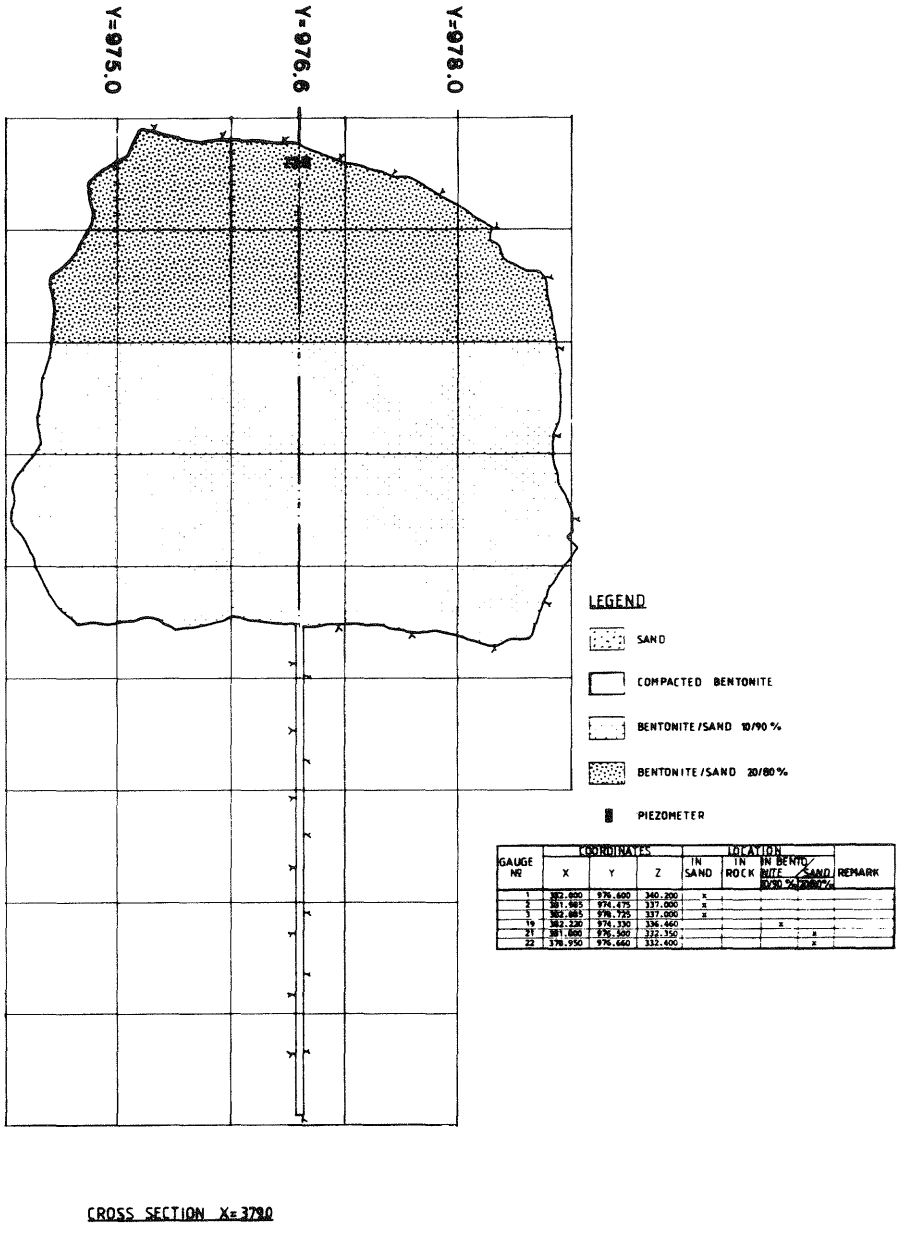

Fig 4.44. Location of BAT piezometers in the cross section between heater holes no 1 and 2

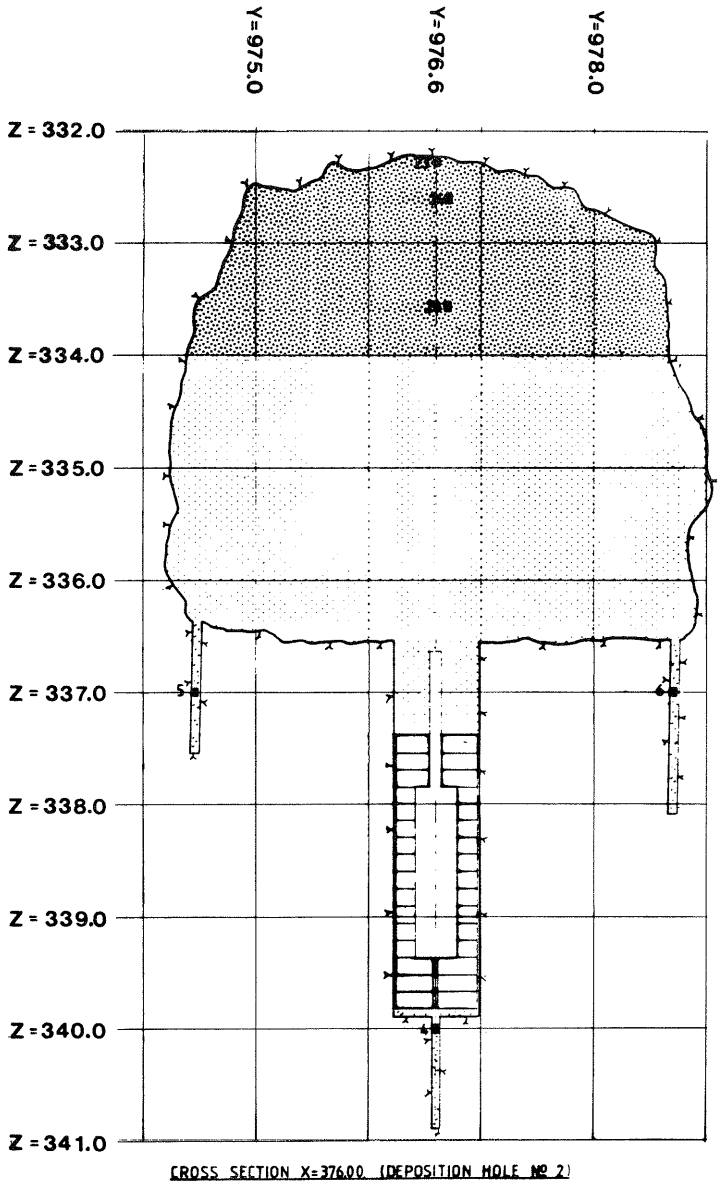

Fig 4.45. Location of BAT piezometers in the cross section through heater hole no 2

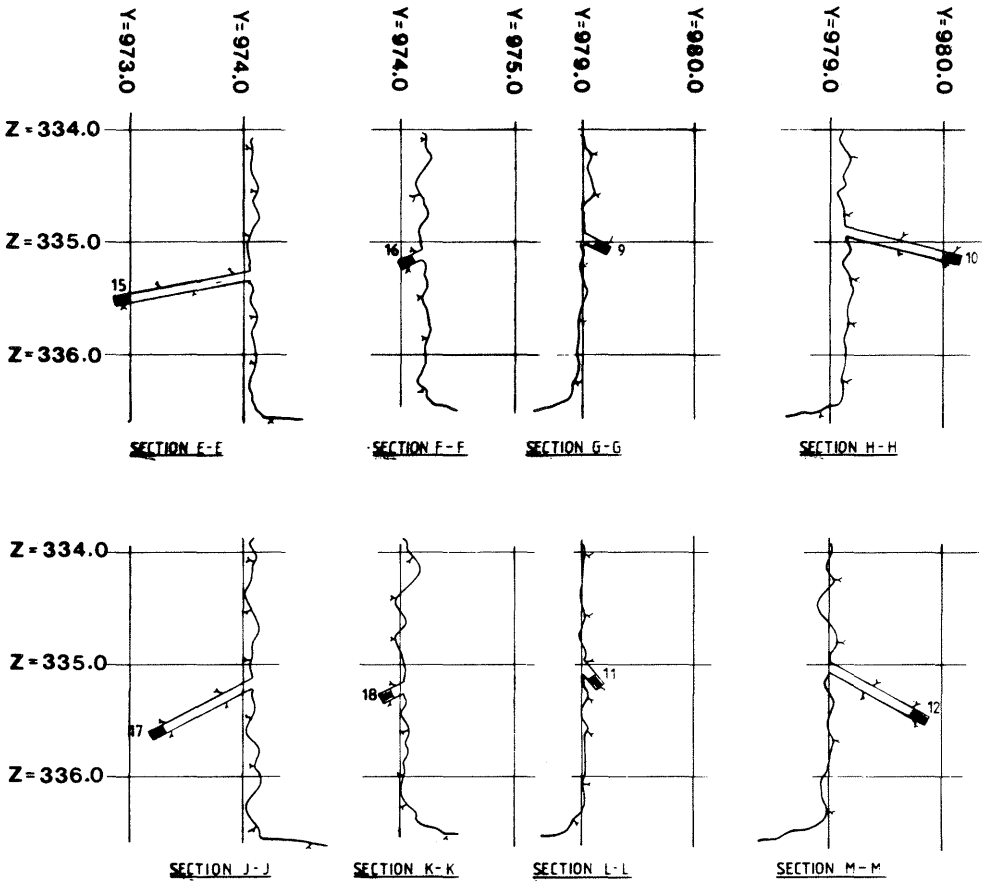

GAUGE Nº	COORDINATES X	Y	Z	LOCATION IN SAND	IN ROCK	IN BENTONITE/SAND 80/20 %	REMARK
4	376.800	976.600	340.20	x			
5	375.965	974.455	337.00	x			
6	376.015	978.650	337.00	x			
20	379.100	976.790	333.60			x	
23	376.300	976.600	332.30			x	
24	376.800	978.780	332.60			x	
15	379.050	972.890	335.520		x		
16	378.050	974.800	335.190		x		
9	379.400	979.240	335.08		x		
10	379.780	980.150	335.15		x		
17	376.900	972.300	335.64		x		
18	376.720	973.860	335.29		x		
11	378.880	978.170	335.10		x		
12	378.030	979.880	335.50		x		

Fig 4.46. Location of some of the BAT piezometers in the shallow rock (cf. Fig 4.47)

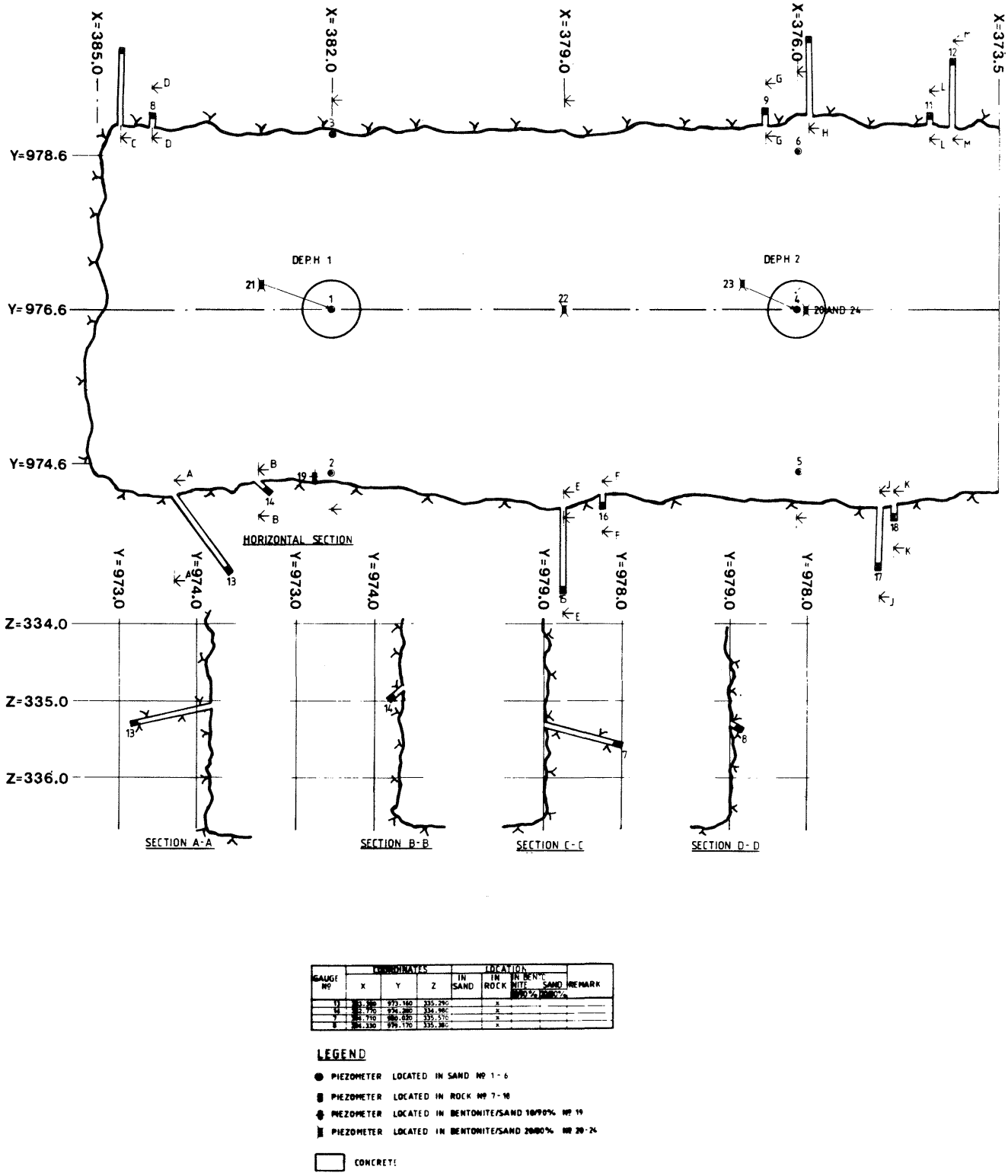

Fig 4.47. Layout of BAT piezometer locations in the shallow boreholes in the rock

4.3.6 Moisture sensors

4.3.6.1 General

Moisture measurement by utilizing the electrical resistivity of the soil is frequently applied in agriculture and various industries. Commercially available sensors are usually large and expensive, however, and not very well suited for the BMT. It was obvious already at an early stage of the planning that the moistening of the 19 cm thick annulus of highly compacted bentonite that surrounds the heaters cannot be reasonably well identified by having less than three to four radially distributed moisture sensors at each monitored level. This implied that the volume of the sensors had to be less than a couple of cubic centimeters, an additional requirement being that the sensors need to sustain mechanical pressure of up to 10 MPa and temperatures of as much as 90°C. These rather special demands made it necessary to develop a new sensor and this was made at the Division of Soil Mechanics, University of Luleå (LuH). Prototypes were tested in 1980, and in 1981-82 560 sensors were installed in the clay materials on the BMT site. The new equipment was a product of a team work in which Dr Arvid Jacobsson, Mr Thomas Forsberg, and Mr Ole Kvamsdal were the main members (19).

4.3.6.2 Gauges

The sensor consists of a cylindrical brass electrode and a central pin electrode, between which the same clay material is applied as the sensor is inserted in (Fig 4.48). For use in the highly compacted bentonite in the heater holes, small cylinders of compacted bentonite with central holes were prepared in advance and applied in the electrode gap before inserting the sensor in its prebored hole in the bentonite block. The sensors in the bentonite/sand

backfill were filled with backfill material, which was compacted to approximately the same density as that of the backfill into which they were pushed.

The brass electrodes were gold-coated (3 micrometers) in order to prevent corrosion. The cables, which consisted of an outer plastic shielding surrounding the coaxial cables, were tightly connected to the sensor body by a polyurethan jacket, confined by a heat-shrinkable tubing. This arrangement was chosen so as to prevent water from entering the cables.

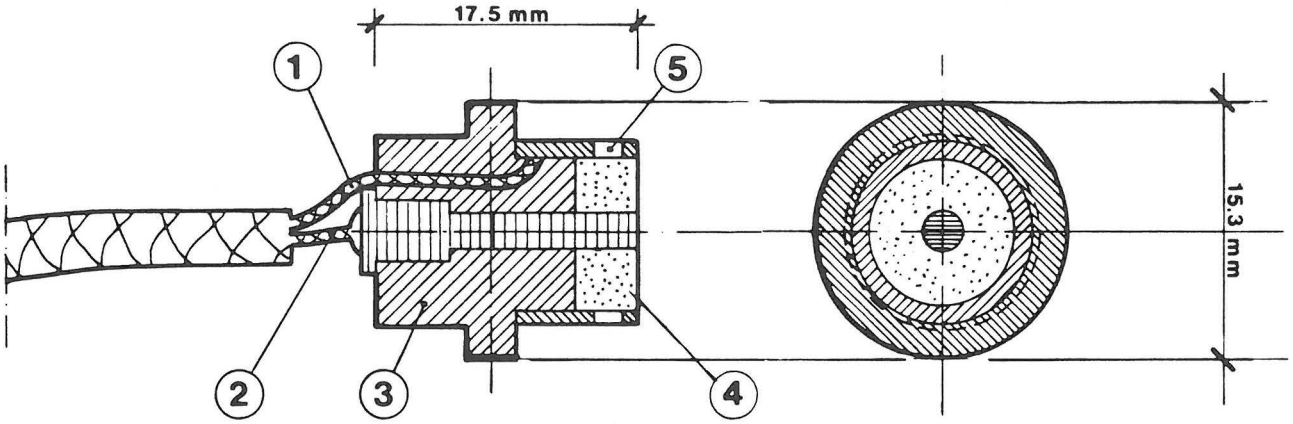

LEGEND:

1. WIRE TO OUTER ELECTRODE OF GOLD-PLATED BRASS
2. WIRE TO CENTRAL ELECTRODE OF BRASS PIN WITH GOLD-PLATED END
3. PLEXIGLASS INSULATOR
4. COMPACTED SOIL (BENTONITE OR BENTONITE/SAND MIXTURE)
5. HOLE FOR ENTRANCE OF MOISTURE

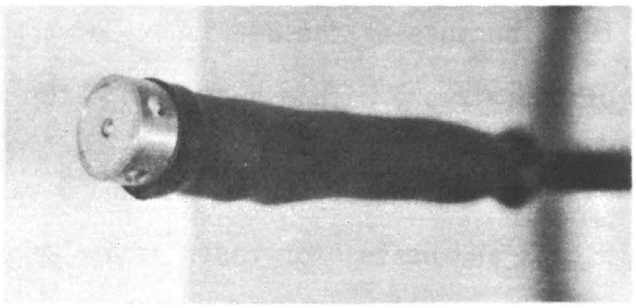

Fig 4.48. The LuH moisture sensor

4.3.6.3 Function, Calibration

At the measuring, an AC voltage with a frequency of 200 Hz passed through the circuit consisting of the sensor and its content of clay material. The current through the circuit, which is a measure of the soil resistivity or rather its capacitance, is a complex function of the water content, the water chemistry, and the temperature.

The calibration involved several laboratory test series which were run with Stripa water and with the sensors embedded by clay material under completely confined conditions so that the dry density (ratio of mineral mass to the total volume of a soil element) remained constant. Under such circumstances, the water content can be fairly accurately estimated from the recorded voltages. In practice, however, water uptake in the clay is associated with a drop in dry density, and this was expected to lead to a transient change in the sensor signal at high degrees of water saturation. Heating was assumed to yield an overestimation of the water content, particularly at a low degree of saturation. The accuracy of the interpreted water content values was accordingly low and it was concluded that the recordings should therefore be used merely as a check of whether any change in water content had taken place in a certain period of time. The least reliable information of such changes was received from the moisture sensors in the bentonite/sand mixtures because of the difficulty of achieving the same bulk density of the mixture within and outside the sensors.

In connection with reloading of heater hole no 3 with a second set of bentonite blocks and heater for tests at higher temperatures, 4 special gauges were installed in a radial array at mid-height of

the heater to record the relative humidity. These gauges* were commercial Vaisala RH sensors type HMP 19 UT, which record the humidity as a function of capacitance changes of a polymer film.

4.3.6.4 Positions

The degree of uniformity of the water uptake and redistribution in the highly compacted bentonite was one of the main items of the BMT, and a maximum number of gauges was therefore required. For practical reasons, mainly the difficulty of finding space for the rather big bundles of cables without affecting the physical interaction of rock and bentonite, the instrumentation had to be confined to five levels over the heater length in one plane only, i.e. in the cross sections perpendicular to the tunnel axis. Every second level had three sensors in radial arrays, while the others had only two. The arrangement is illustrated in Fig 4.49, which is representative of the cross sections through heater holes no 1 and 2, and which also shows the location of the moisture sensors in the tunnel backfill. Fig 4.50 illustrates the corresponding instrumentation in heater holes no 3-6 and the overlying backfill.

The large number of moisture sensors required systematic handling and application as in the case of the thermal elements. The sensors were inserted in drilled holes in the bentonite blocks with only slightly larger diameter so that a very good fit was achieved. Great care was taken in the cutting of well fitting grooves for the cable bundles in the blocks. In the bentonite/sand backfill the sensors were simply pushed into the fill after punching holes for them.

The coding was analoguous to that of the other gauges which were connected to the data acquisition system. Here the letter coding

---

* Vaisala OY PL 26, 00421 Helsinki 42, Finland

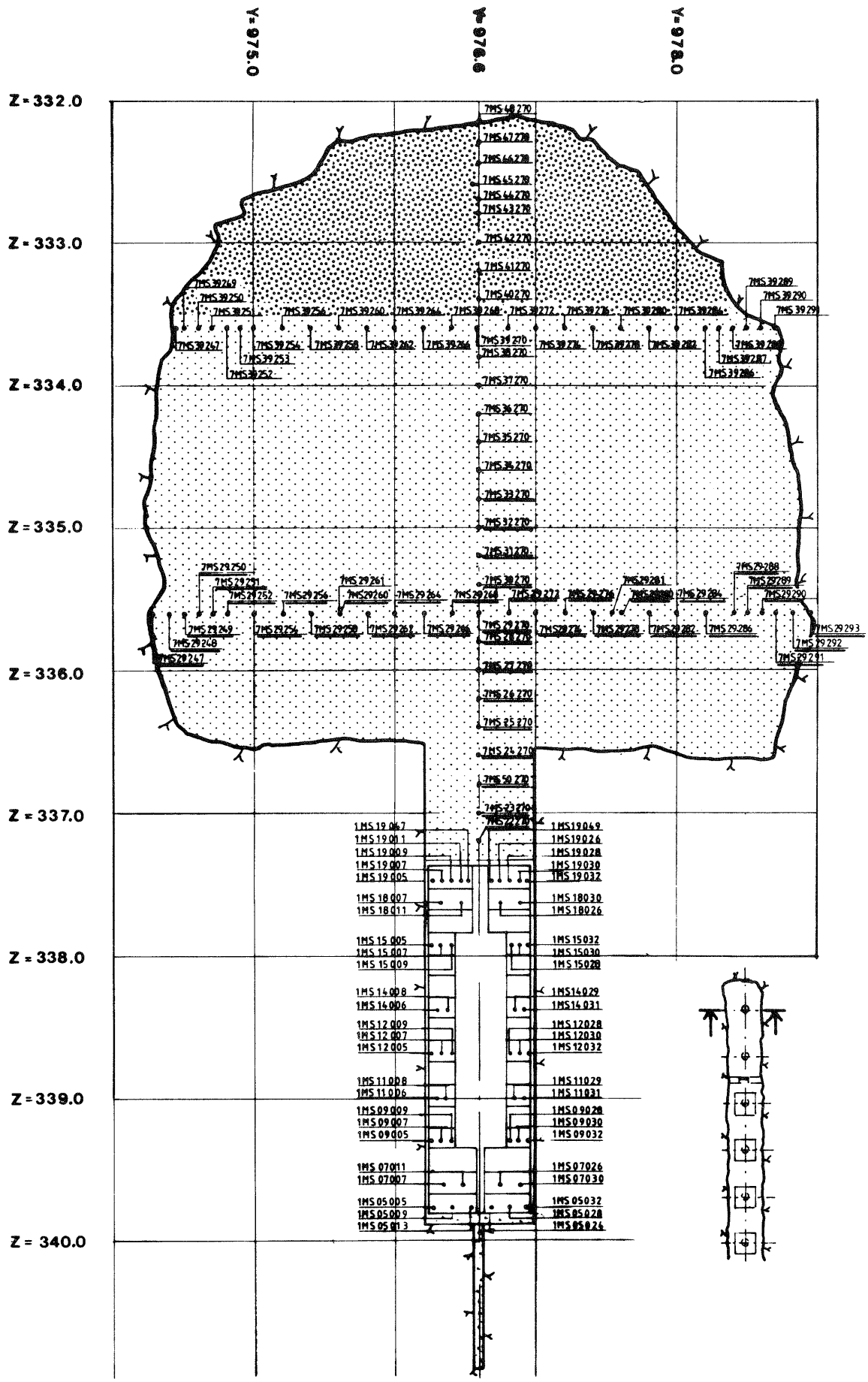

Fig 4.49. Cross section through heater hole no 1, illustrating the positions of the moisture sensors

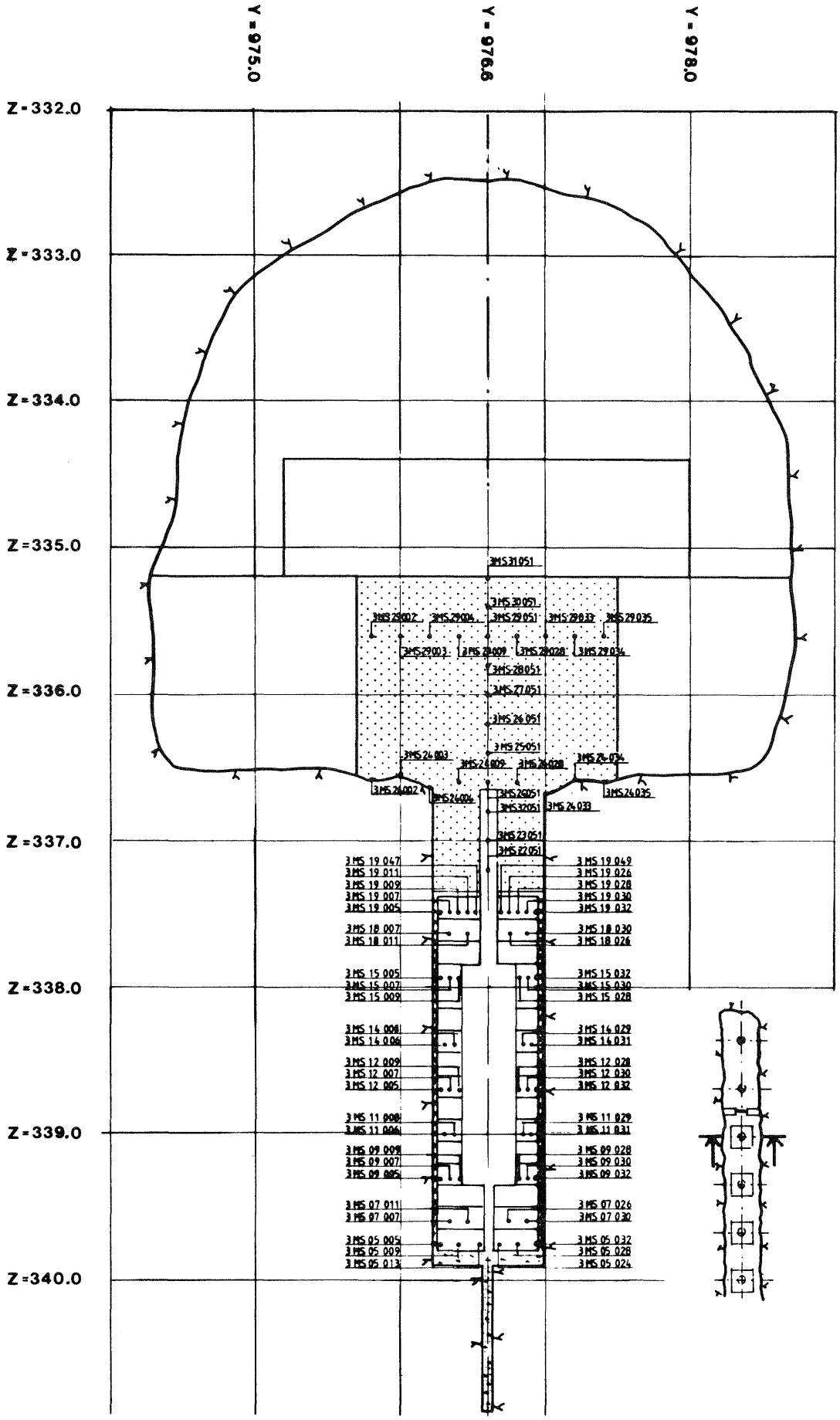

Fig 4.50. Cross section through heater hole no 3, illustrating the positions of the moisture sensors

was MS, while the subsequent two symbols refer to the level (z-coordinate), and the last three represent the lateral position (y-coordinate). Thus, 2 MS 05013 means a moisture sensor at the lowest level in heater hole no 2, the sensor being located close to the symmetry axis of the hole.

4.3.7 Displacement and deformation of buffer materials

4.3.7.1 General

The water uptake in the highly compacted bentonite in the heater holes was expected to be associated with swelling, causing displacement of the interface between the dense bentonite and the overlying backfill. Such displacements were assumed to be developed at least in the three "wet" heater holes (i.e. no 1, 2 and 5) during the test period and several techniques for their determination were discussed but it was concluded that the accuracy of most systems based on mechanical devices or electronic transducers would be too low. It was therefore decided to try to determine the displacements only at the end of the test through a careful direct measurement of the positions of a number of reference objects that moved with the clay.

4.3.7.2 "Coins"

40 coin-sized copper discs were applied on the upper surface of the top layer of the highly compacted bentonite blocks in all the heater holes (Fig 4.51). Since the level of this surface was carefully determined at the preparation of the test, it was assumed that an equally careful measurement of the coin positions after excavation would yield displacement recordings with an accuracy of about ±3mm.

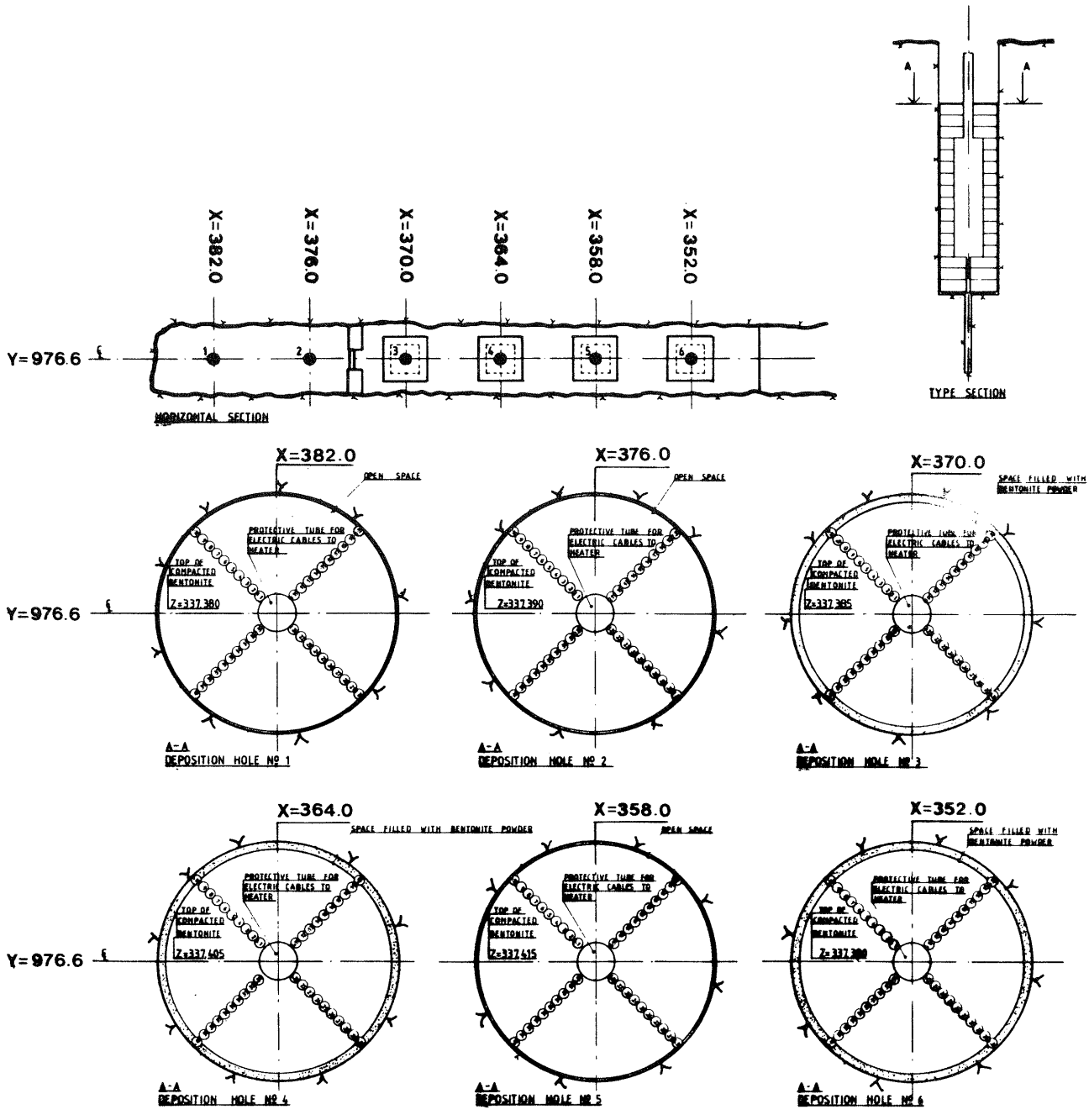

Fig 4.51. "Coins" as reference objects for determination of the expected displacement of the interface between the highly compacted bentonite and the overlying backfill

4.3.7.3 "Tape"

The upward displacement of the interface between the highly compacted bentonite and the overlying backfill was expected to be several centimeters in heater holes no 1 and 2 and to be measurable also in the overlying tunnel backfill. For this purpose, plastic tape was rolled out on two levels, i.e. about 1 and 2 meters above the tunnel floor, in the course of the application of the backfill (Fig 4.52). The z-coordinate was determined at 1 m intervals so that at least a rough estimation could be made of future vertical displacements. The accuracy was estimated at ± 1 cm.

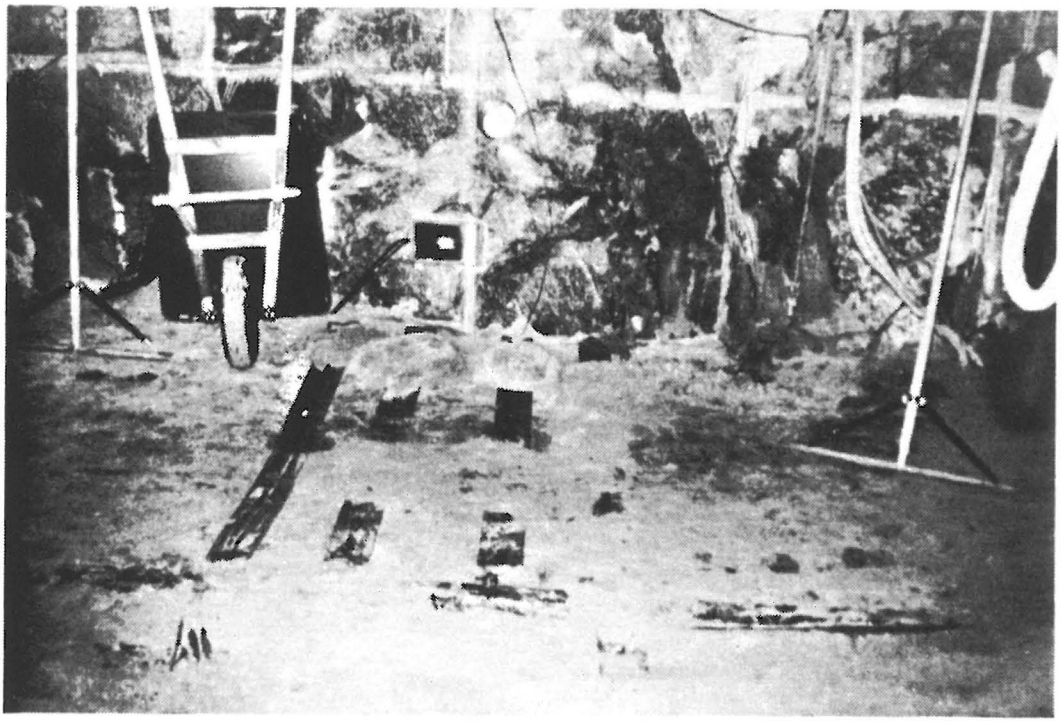

Fig 4.52. Backfilling in the tunnel; notice the tape stripes

4.3.8 Rock Strain

4.3.8.1 General

The swelling of the highly compacted bentonite was assumed to produce shear stresses at the rock/clay interface in the upper part of the heater holes, which could possibly lead to a widening of horizontal or slightly inclined joints in the rock. The development of swelling pressures acting radially on the rock surface in the heater holes were also assumed to affect the aperture of certain joints, i.e. those which are steeply oriented and intersect the holes. An attempt was therefore made to measure possible effects of this sort, which requires precision measuring technique. The "sliding micrometer - ISETH"* (Kovari instrument) was used in the present investigation (20).

4.3.8.2 Principle of measurement

The ISETH micrometer is suitable for determining axial displacements in boreholes. For this purpose a steel casing is grouted in the hole, the casing being subdivided into 0.5 - 1 m long elements separated by measuring marks. These marks consist of cone-shaped seats of stainless steel into which the sphere-shaped marks (heads) of the instrument fit (Fig 4.53). The instrument is simply an installing rod at which end an about 1 m long invar steel measuring rod with two heads is attached. When measurements are made, the instrument is inserted in the hole and twisted so that the measuring rod can enter the respective casing interval. A defined pulling force is then applied so that complete contact is established between the cone and sphere marks, the actual distance between the cast-in marks then being signalled by the transducer in the measuring rod.

---

*Solexperts Ltd, P.O. Box 274, CH-8034 Zürich, Switzerland

The instrument is temperature-compensated and equipped with a thermal element in the front-part so that the temperature of the environment can be determined within $\pm 0.5^{o}C$.

The accuracy of the recorded values is better than 2 micrometers according to the manufacturer. This requires calibration at each time of measurement, i.e. about 5 times per year according to the plans. In practice, the net accuracy can be taken as ±10 micrometers.

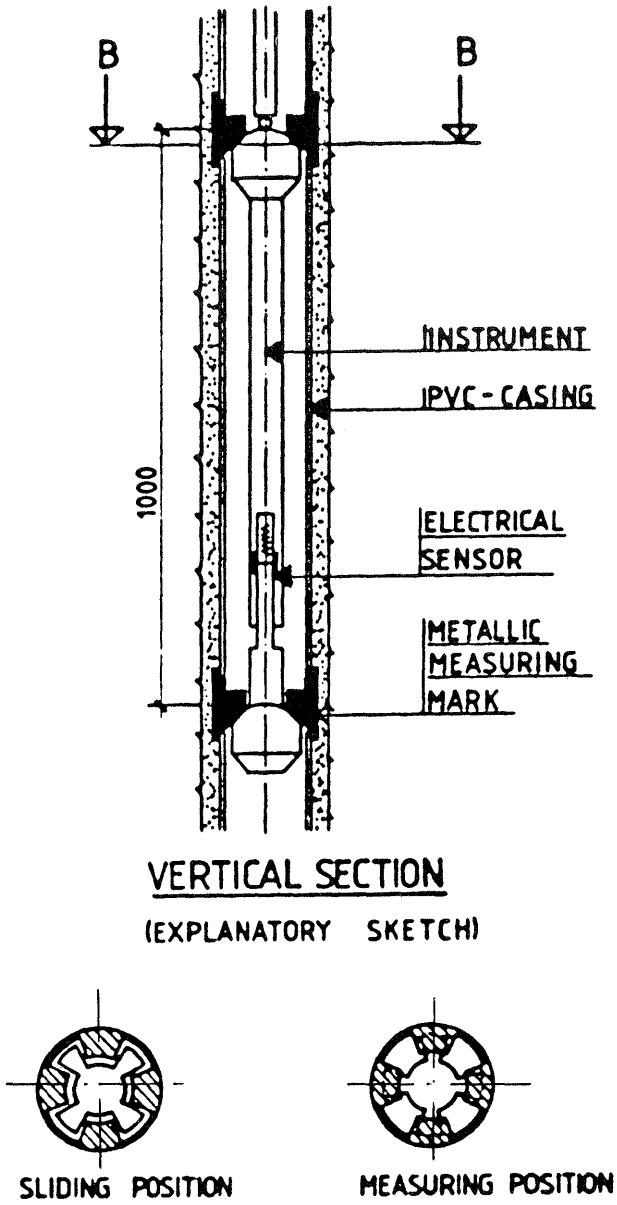

Fig 4.53. Main features of the Kovari equipment

4.3.8.3 Positions

Four vertical Ø 86 mm boreholes were drilled parallel and close to heater hole no 5 (Fig 4.54). The figure shows the 13 measuring sections located so that the possible change of aperture of a well defined, steeply oriented joint could be identified. Also, the expansion of several, less well defined subhorizontal joints and fractures close to the tunnel floor should thereby be identified. Hole no 5 was chosen for this type of measurement because the water uptake and associated swelling effects were expected to be developed earlier in this hole than in holes no 3, 4 and 6. The tie-rods for the lid anchoring were only slightly prestressed (less than 10 kN) in this hole in order to allow for rock joint expansion.

4.3.9 Additional

In the early planning of the BMT it was considered to be of value to prepare for possible tracer diffusion experiments. For this purpose four long filters were applied in heater hole no 5 at the rock/bentonite interface and in contact with the heater (Fig 4.55). The filters consisted of 3 mm copper pipes richly perforated by applying laser technique, and surrounded by finely porous sintered brass filter segments which prevent smectite particles from the clay to enter the pipes. The pipes extended to the upper surface of the concrete slab and offered a possibility of percolating solutions or gas in the system.

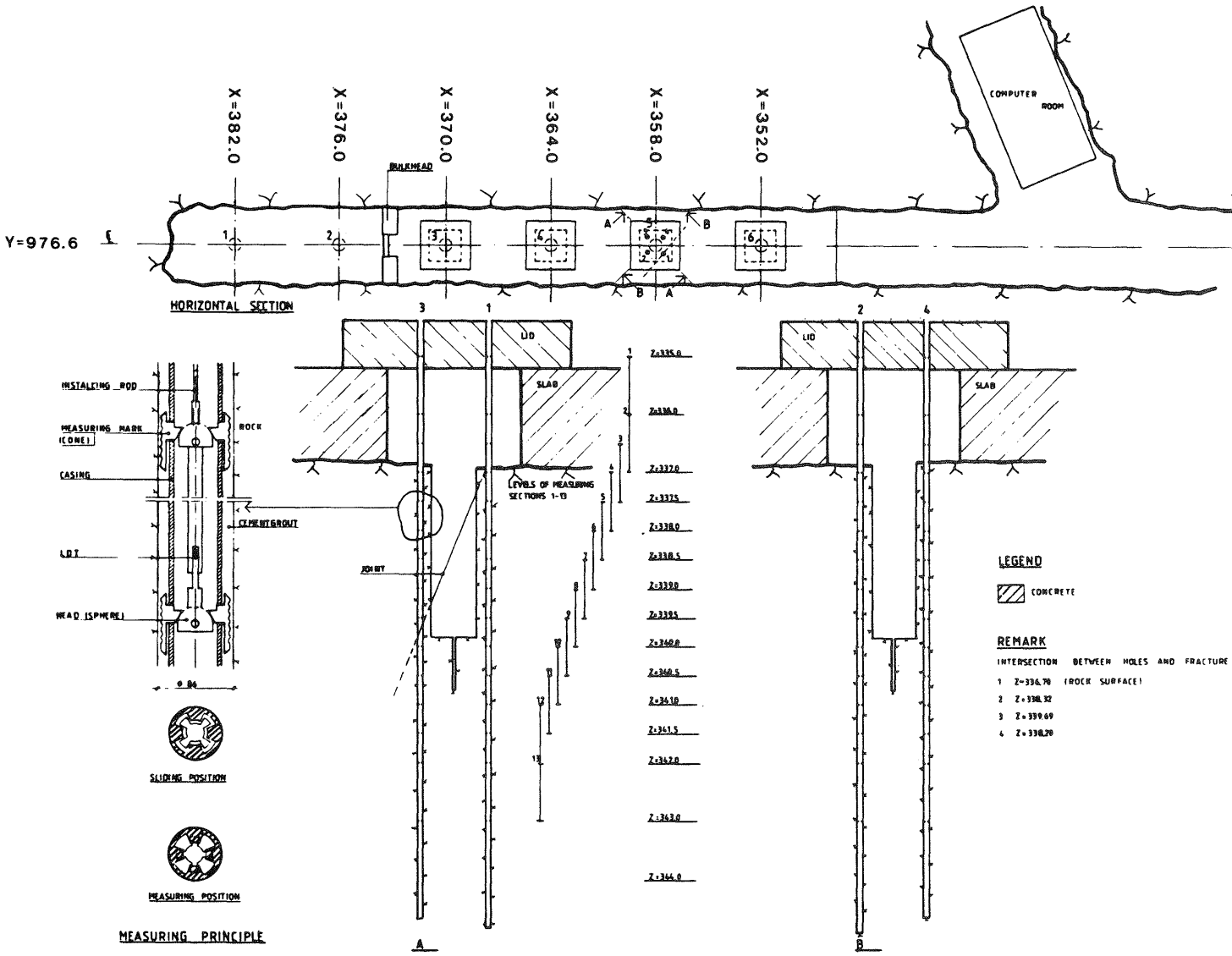

Fig 4.54. Arrangements for measuring of changes in the aperture of rock joints in heater hole no 5

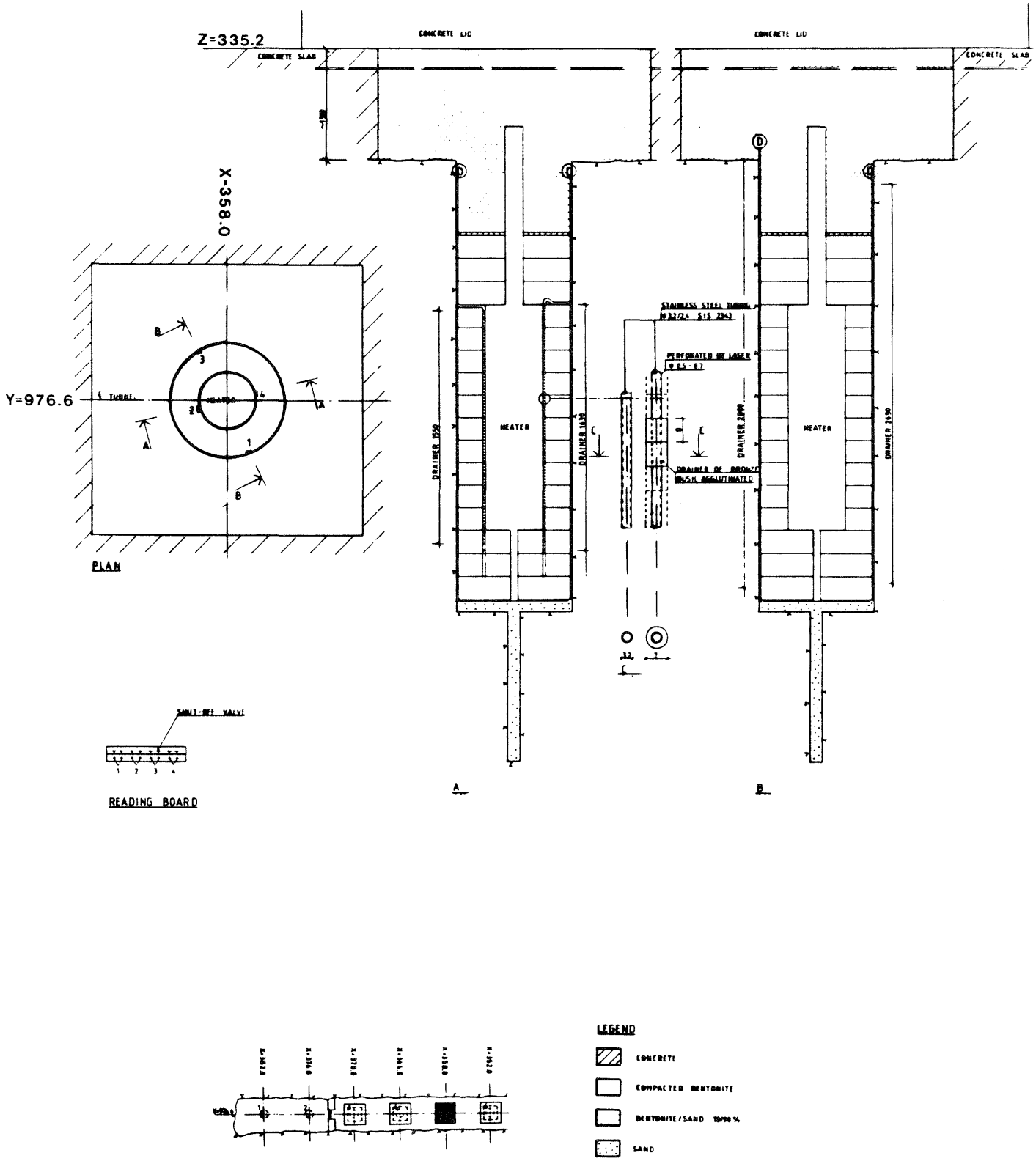

Fig 4.55. Filter arrangement in heater hole no 5

4.4 Data Acquisition and Data Processing Systems*

4.4.1 Introduction

Data logging and processing of measured data from the Buffer Mass Test were handled by use of two separate computer systems. A data acquisition system in Stripa produced raw-data log tapes and copies of these tapes were mailed to the computer center at the University of Luleå for processing of the data. The BMT staff in Stripa had access to the data base in Luleå by use of a graphic terminal and a modem. A general layout of the systems is shown in Fig 4.56.

The data acquisition system in Stripa was designed mainly to provide a system with high reliability. The computer systems in Luleå offer a range of processing facilities, such as large mass storage units, plotting facilities, and programs for processing and monitoring. These facilities were initially used for all the processing and plotting activities but most of this work was successively transferred to Stripa where a suitable multi-color plotter was installed and where Gunnar Ramqvist and Sven-Eric Tegelmark were entirely responsible for the data processing in the main part of the test.

---

* This chapter is a rewritten version of an early description, the author of which was Björn Hagvall, Computer Center, University of Luleå

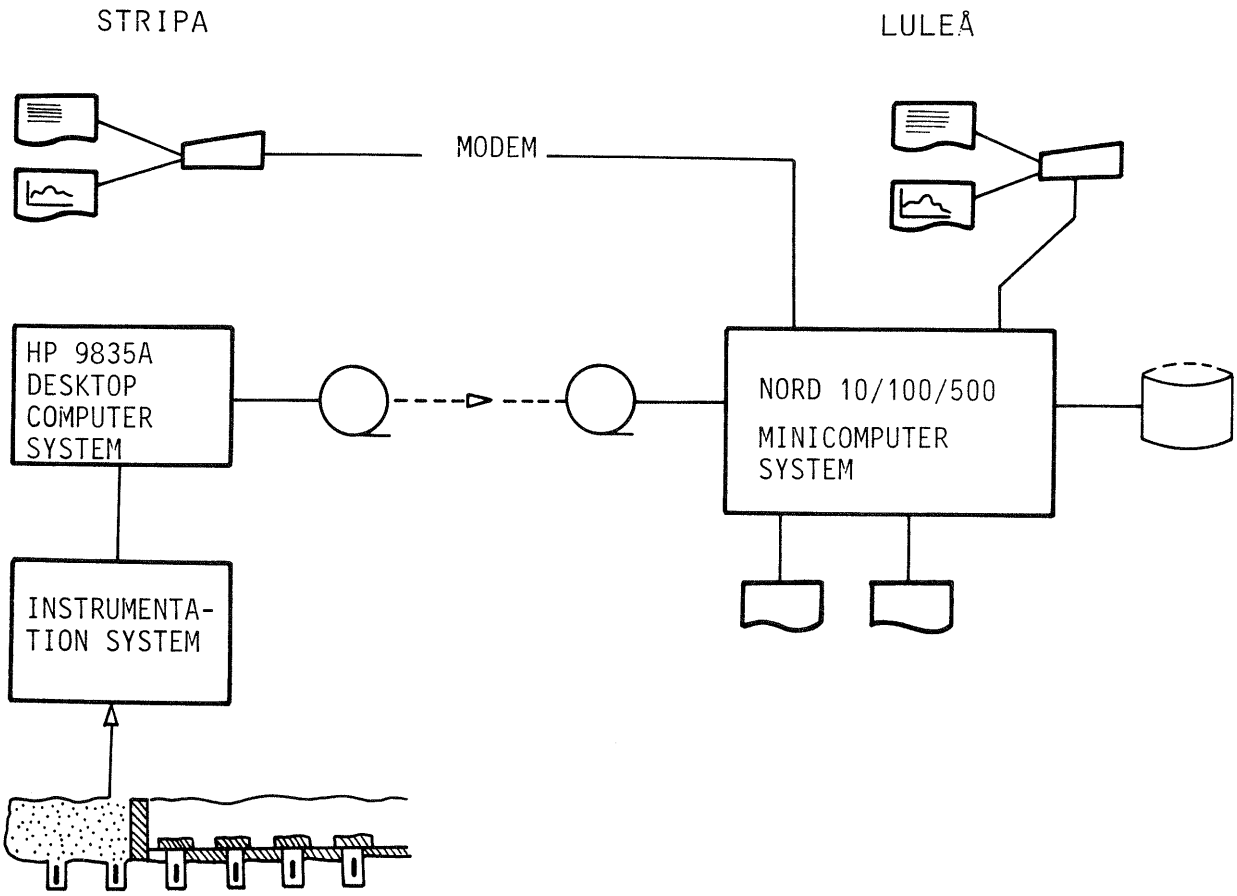

Fig 4.56. BMT computer systems

4.4.2 Data Acquisition System

The data acquisition system consisted of a computer part located in the Stripa mine office building at the ground surface and an instrumentation part located in the underground data acquisition center close to the experimental area at about 340 m depth. The computer system communicated with the instrumentation part by a 1500 meter cable. The electronic gauges were connected to a number of switch-boxes in the experiment area. Shielded and twisted pair cables in turn connected these boxes to the scanner systems in the data acquisition center down in the mine (Fig 4.57).

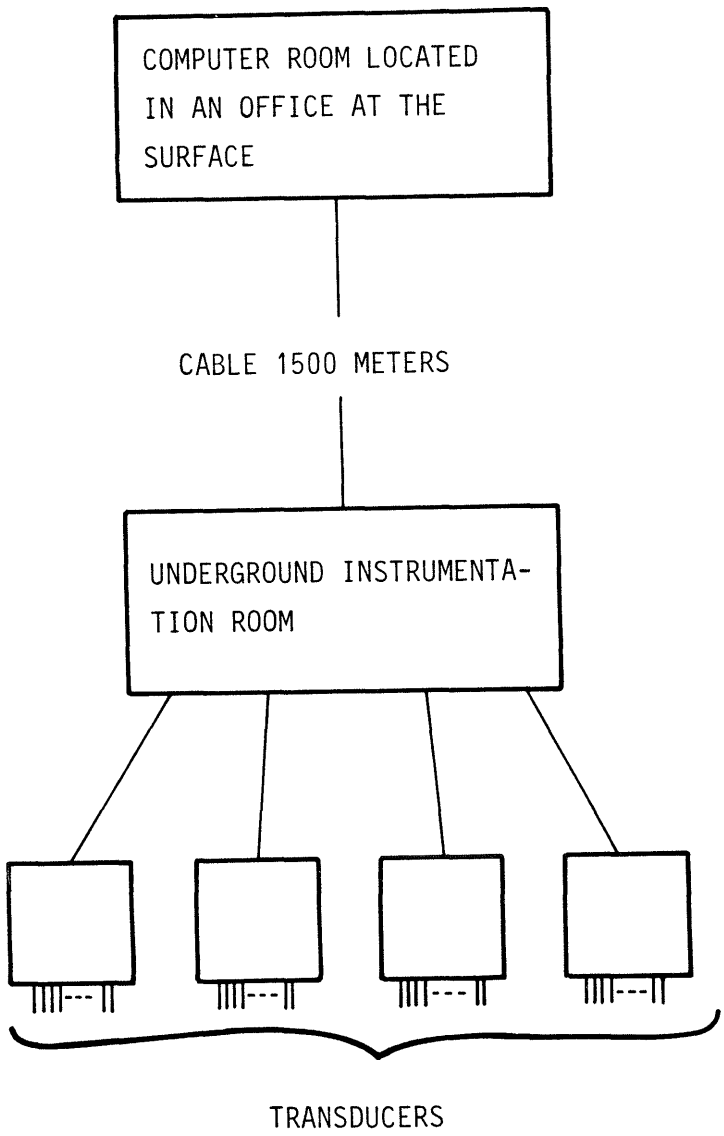

Fig 4.57. The BMT acquisition system

4.4.2.1 Desktop Computer System

A Hewlett-Packard HP-9835A computer provided the basis of the computer system. Two nine-track, 800 bpi magnetic tape stations were used to store experimental data on tape. These data were also stored on a flexible disc unit. The operator could communicate with the system by the keyboard on the desctop computer or by a terminal located in the underground instrumentation room. Printouts were obtained on a matrix printer or on the terminal in the instrumentation room. Certain printouts could also be obtained on the internal 16 character printer of the desctop computer. Commu-

nication between the computer part and the instrumentation part was maintained on GPIB by the long cable. The terminal and Gloetzl equipment used the same cable for asynchronous communication with the computer system. The Gloetzl system is specified for the reason that signals were not continuously available from the recording unit; the scanning involved activation of valves and pumps before the transducer yielded relevant signals.

The desktop computer system is schematically visualized in Fig 4.58.

Specifications:

2 desktop computer systems HP-9835A including:

256 k bytes read/write memory
tape cartridge 217 k bytes
CRT 80 alphanumeric characters x 24 lines
thermal printer, line width 16 characters
real-time clock
GPIB-interface (IEEE-488)
RS232-interfaces

1 flexible disk unit HP-9895A, 2 x 1.2 M bytes

1 matrix printer HP-2631B

2 magnetic tape stations including:

magnetic tape controller/formatter
Dylon model 1015A
magnetic tape transport Kennedy Co
model 9800, 800 bpi, 25 ips,
automatic restart

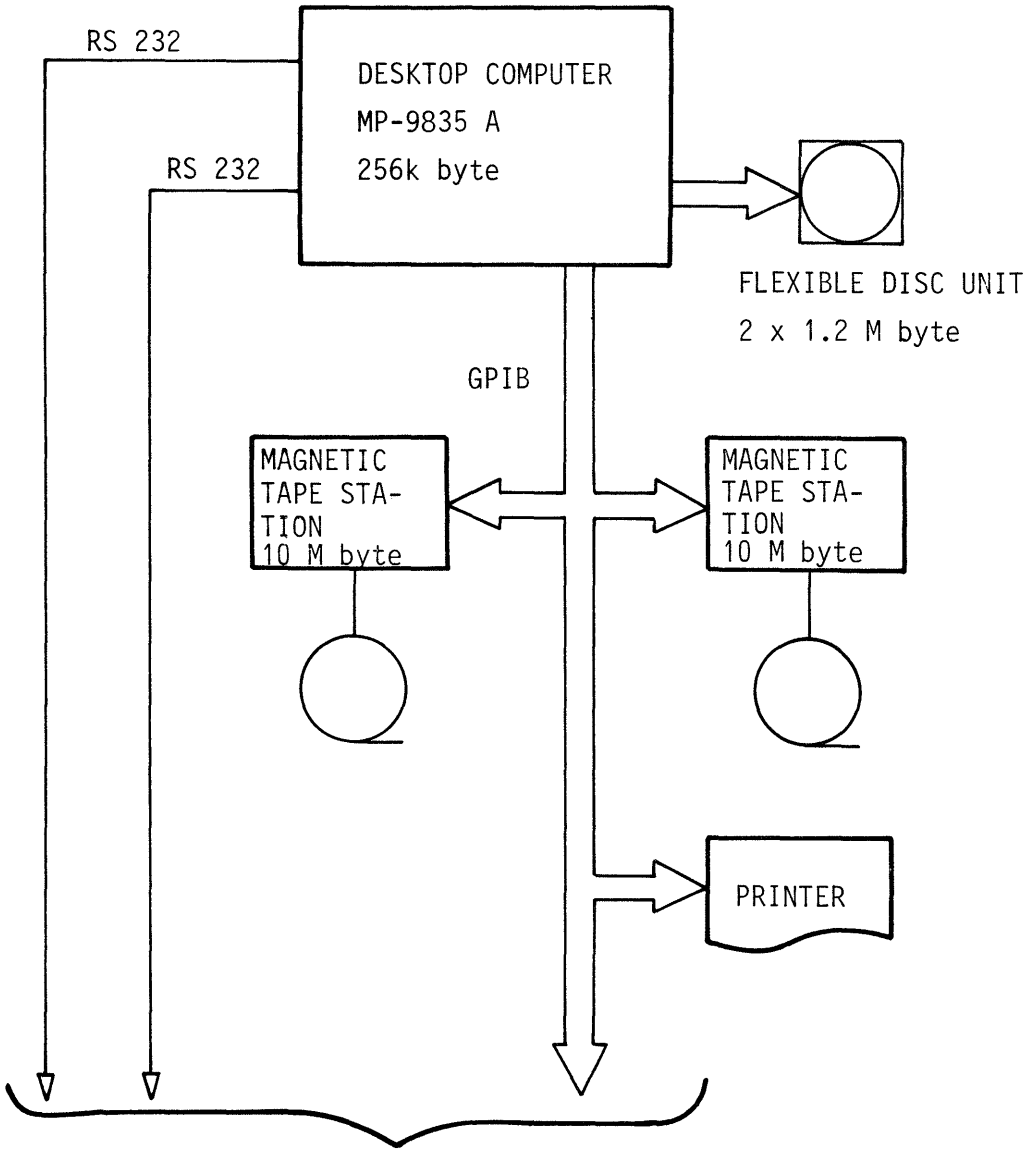

Fig 4.58. Desktop computer system

4.4.2.2 Communication System

The desktop computer system communicated with the instrumentation part in the underground data acquisition center by a shielded, 15 twisted pair cable. The communication link consisted of two asynchronous RS232 lines (4 pairs) and one GPIB line (2 pairs). The two RS-232 lines operated by short haul modems on the cable at 30 characters per second, the GPIB first being converted to a two-pair line by a GPIB extender unit. The extender operated by short haul modems on the cable at 1920 characters per second. The arrangement is schematically vizualised in Fig 4.59.

Scanners and voltmeters communicated by GPIB. The terminal and Gloetzl equipment used the two RS-232 lines.

Specifications:

2 GPIB extenders HP-37201A

2 short haul modems HP-37230A

4 short haul modems Westermo Teleindustri AB type KM-1

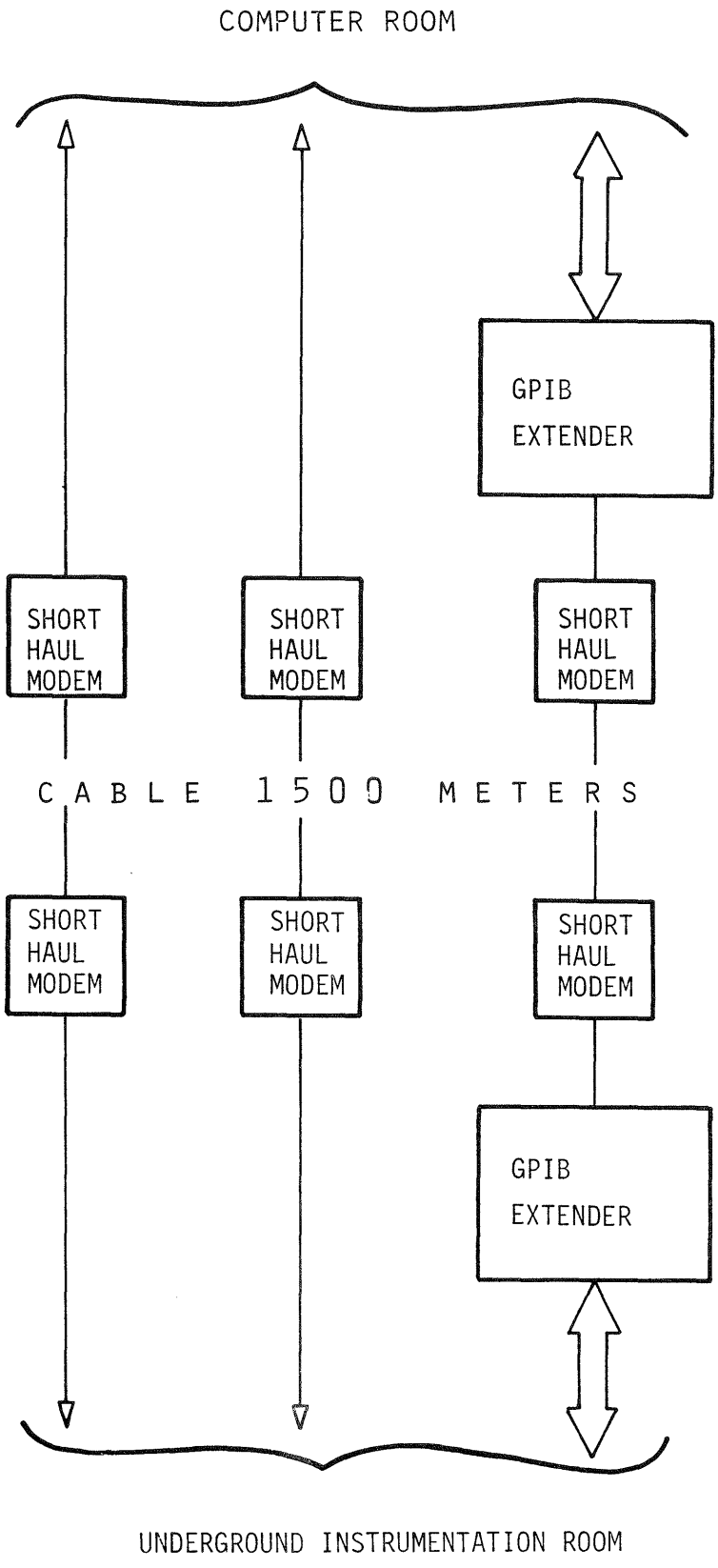

Fig 4.59. Communication system

4.4.2.3 Instrumentation System

The scanner system and the main part of the electronics of the Gloetzl equipment were located in the underground acquisition center where a terminal for communication with the computer was also placed. The terminal and the Gloetzl equipment communicated by RS-232 lines. The scanner equipment used GPIB communication. Schematically, the arrangement was that shown in Fig 4.60.

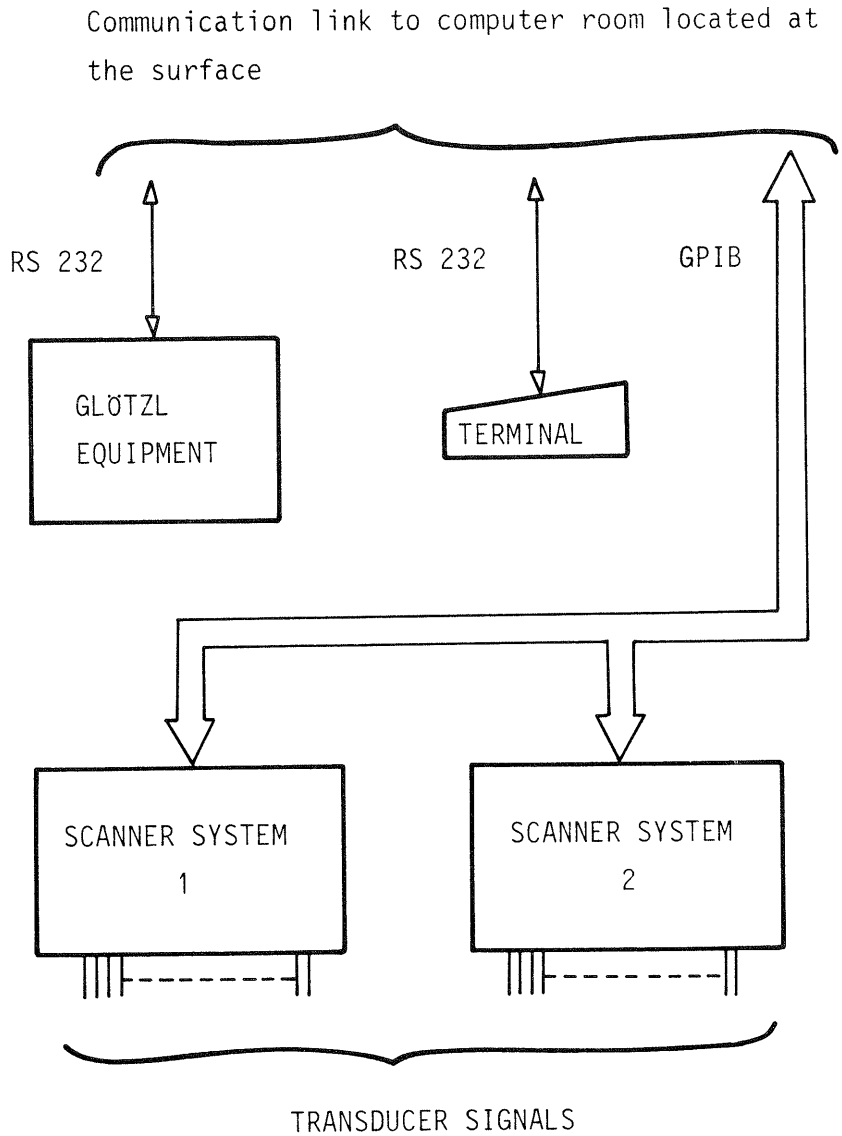

Fig 4.60. Instrumentation system in the underground data acquisition center termed "instrumentation room" in the block diagram

The scanner system consisted of two symmetrical parts, each containing a digital voltmeter. The transducers were connected to the two parallel system parts in such a way that each of them covered the entire experimental area, i.e. so that neighboring transducers were scanned by different systems. By this arrangement sufficient information was still expected even if one of the systems broke down.

The arrangement is schematically visualized in Fig 4.61. The transducer signals were transferred from the experimental area to the underground acquisition center on 20 pairs shielded cables.

Specifications:

2 systems including:

1 digital voltmeter HP-3456A

2 scanner/control units HP-3497A
100 analog channels/unit

5 scanner/extender chassi units HP-3498A
200 analog channels/unit

GPIB

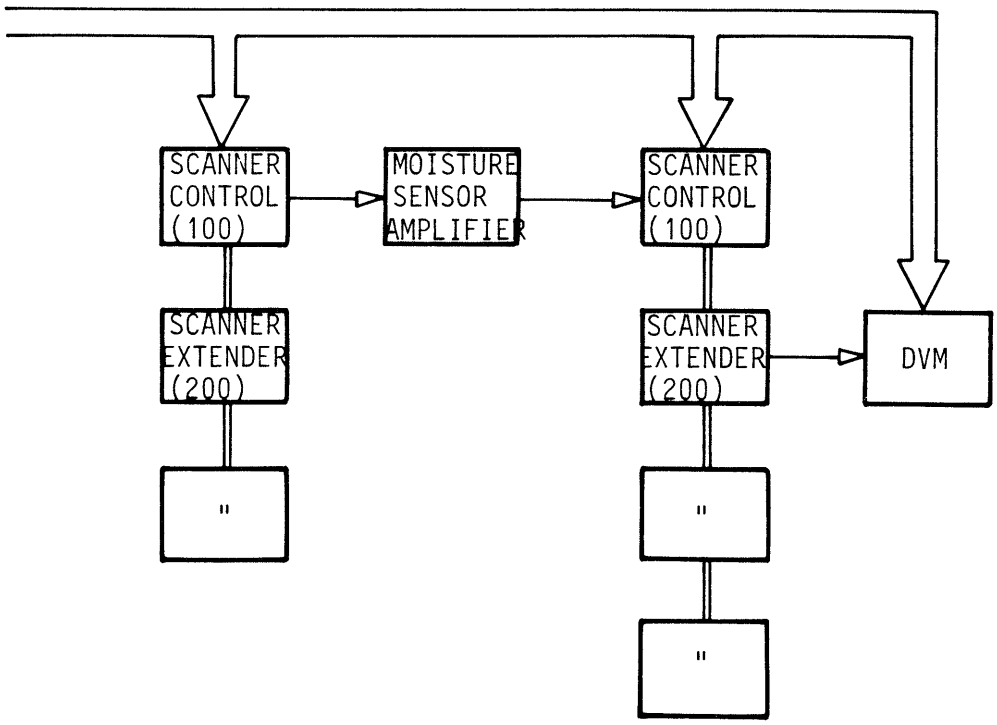

Fig 4.61. One of the twin scanner systems

4.4.3 Software

The software system was designed to activate scanning as well as to measure and store transducer signal values. It also provided a lot of service functions like printing of transducer signals, printing of data previously stored on floppy disks, and reporting of transducers that had activated their alarms. The system also continuously checked the status of voltmeters, scanners, printers etc and reported failing devices. The software was written for the presently used Hewlett Packard 9835A desktop computer (cf Fig 4.62).

The data acquisition software consisted of the following programs:

TERMIN - terminal input program
AUTOST - autostart program
MSRPGM - measurement program

service programs for initializing
tape cartridges and floppy disks

The terminal input program (TERMIN) was used for activation of the scanning operation. Transducer parameters, alarm limits, measuring intervals etc were keyed in this program, all information given to the program being filed on tape cartridges. This file was termed the 'description file'. Compact versions of the description file provided input data to the recording programs AUTOST and MSRPGM.

The autostart program (AUTOST) was automatically activated when the main power to the desktop computer was turned on. This program read the compact version of the file on the tape cartridge. The program also checked all parts of the computer system, the scanners and the voltmeters and wrote a system status report. Finally it ordered the computer to load and run the measurement program MSRPGM.

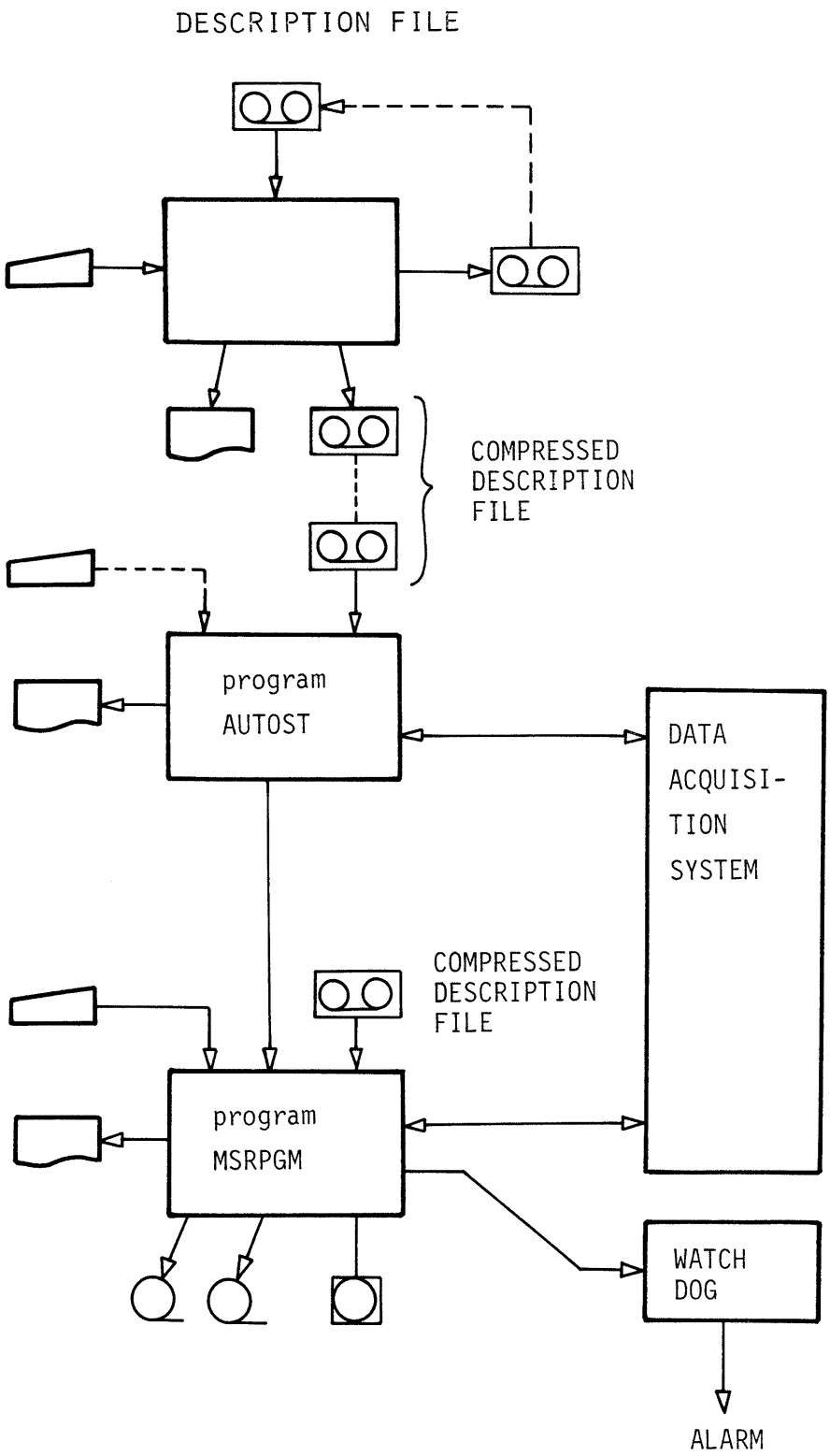

Fig 4.62. Data acquisition software system

The desktop computer system also included a watch dog. Thus, if the measurement system exceeded preset alarm limits, or if the computer failed, this watch dog equipment started up the main alarm system.

4.4.4 Data processing

Transducer signal values from the data acquisition system were ASCII encoded and logged on magnetic tapes as the experiment proceeded. The time between loggings changed from 2 hours during the first months of the experiment period to 24 hours during the last part of the experiment, additional changes being introduced in the course of the test. Raw data tapes were stored in an on-site tape library, copies of the tapes being mailed to Luleå every second week.

When magnetic tapes were received at the computer center in Luleå, they were read and introduced in the mass storage system. These data could then be delivered via the Nord computers at this center. By use of a modem the staff in Stripa also had access to this information.

Processing of data were mainly conducted through the interactive program MUMS, which is a general program for processing and monitoring of large amounts of data. It consists of a series of interactive individual, or sets of commands. This makes the program well suited both for large regulary processings and for unplanned exploratory study of measurement data.

The program has commands for calculating mean-, minimum- and maximum values for a given time increment and time period. Arithmetic expressions can be used to rescale data and in case of missing data there are different strategies to substitute these values. It

also has commands for printing and plotting and a number of plotting layouts were initially produced and tested through the Luleå computer center. However, the access to a very efficient HP-connected plotter in Stripa and to the excellent programming aid of Harald Abelin, made it more feasible and economical to run the plotting work in Stripa.

4.5 Heaters

4.5.1 Design and construction

4.5.1.1 Criteria

The following criteria and specifications were found to be relevant to the design and construction of the heaters:

1 The test period may last for at least 4 years, possibly 10 years. Malfunctioning heaters cannot be repaired without ruining the test

2 Dimensions of the heaters are about 1500 mm in length and 380 mm in diameter excluding protective tubings for connecting cables and basal support, which must not produce much heat

3 The heaters must contain three completely independent heating components

4 Maximum electric power of the heaters is set at 3000 W

5 Maximum heater surface temperature is 100°C, distributed as evenly as possible

6 Maximum swelling pressure in the bentonite will be 10.0 MPa

7 Corrosion is not of great concern but the heater material must be selected so that possible corrosion effects do not significantly affect the clay

8 The connecting cables must be protected and heat resistant

9 Power source is 200/380 V 50 Hz

10 The heaters must be earthed

The available power supply of the mine and the test area, and the earthing system are shown in Figs 4.63 and 4.64. Also given was the specification that the heaters must be detachable parallel to

the excavation of the bentonite clay at the termination of each heater test. Otherwise it would not be practical to take well defined samples in the deep 19 cm wide space between the rock and the heater in the planned, comprehensive sampling operation. Furthermore, it was required to equip the lower end of the heaters with a strong support consisting of a rod and a perforated basal plate that must not produce much heat. These arrangements were necessary in order to carry the heavy bentonite column and make the heater and bentonite blocks stick together as one unit at the emplacement in the heater holes. While the major part of the bentonite blocks may well be applied one by one in the deposition holes of an actual repository, the instrumentation of the bentonite in the present test required that the heater/bentonite unit was built up outside the heater holes into which it was subsequently submerged.

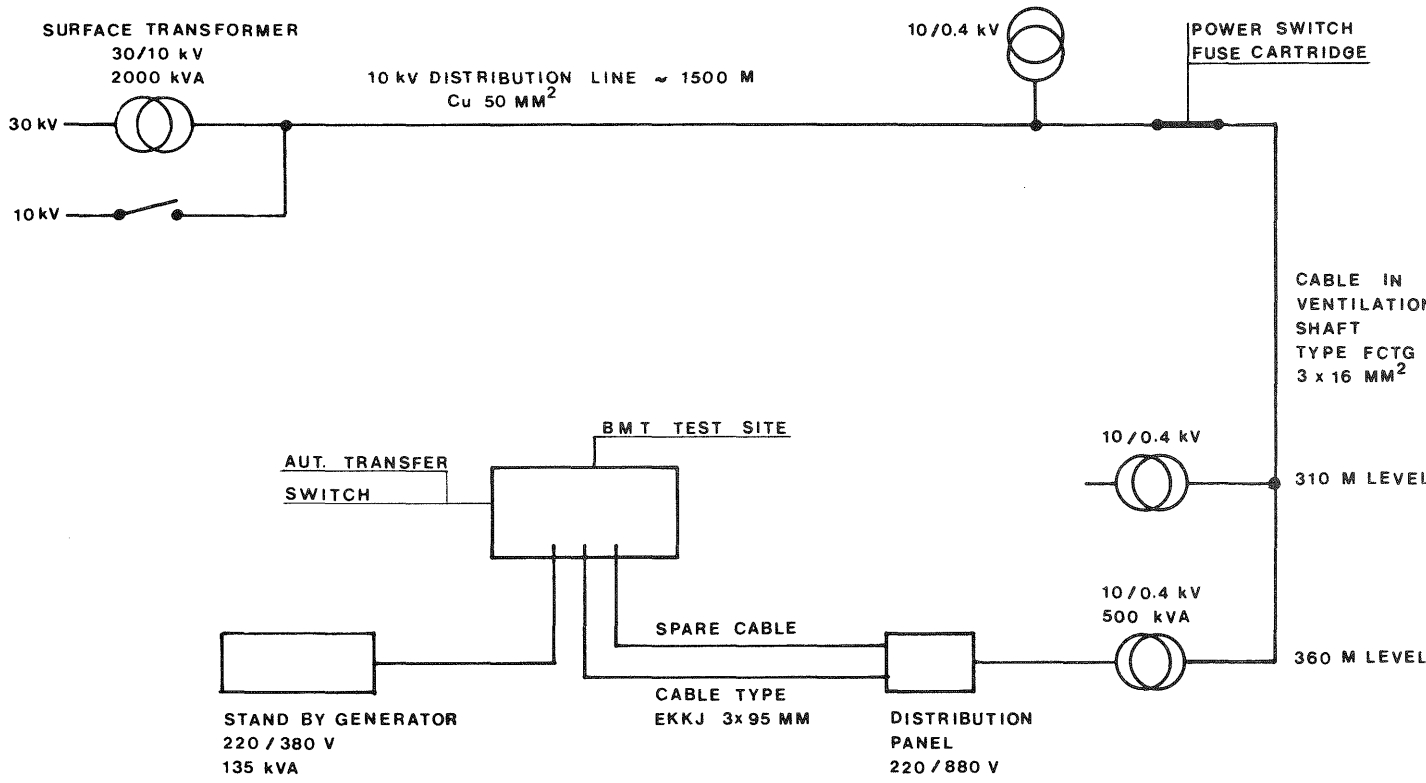

Fig 4.63. Power svpply of the mine and the test area

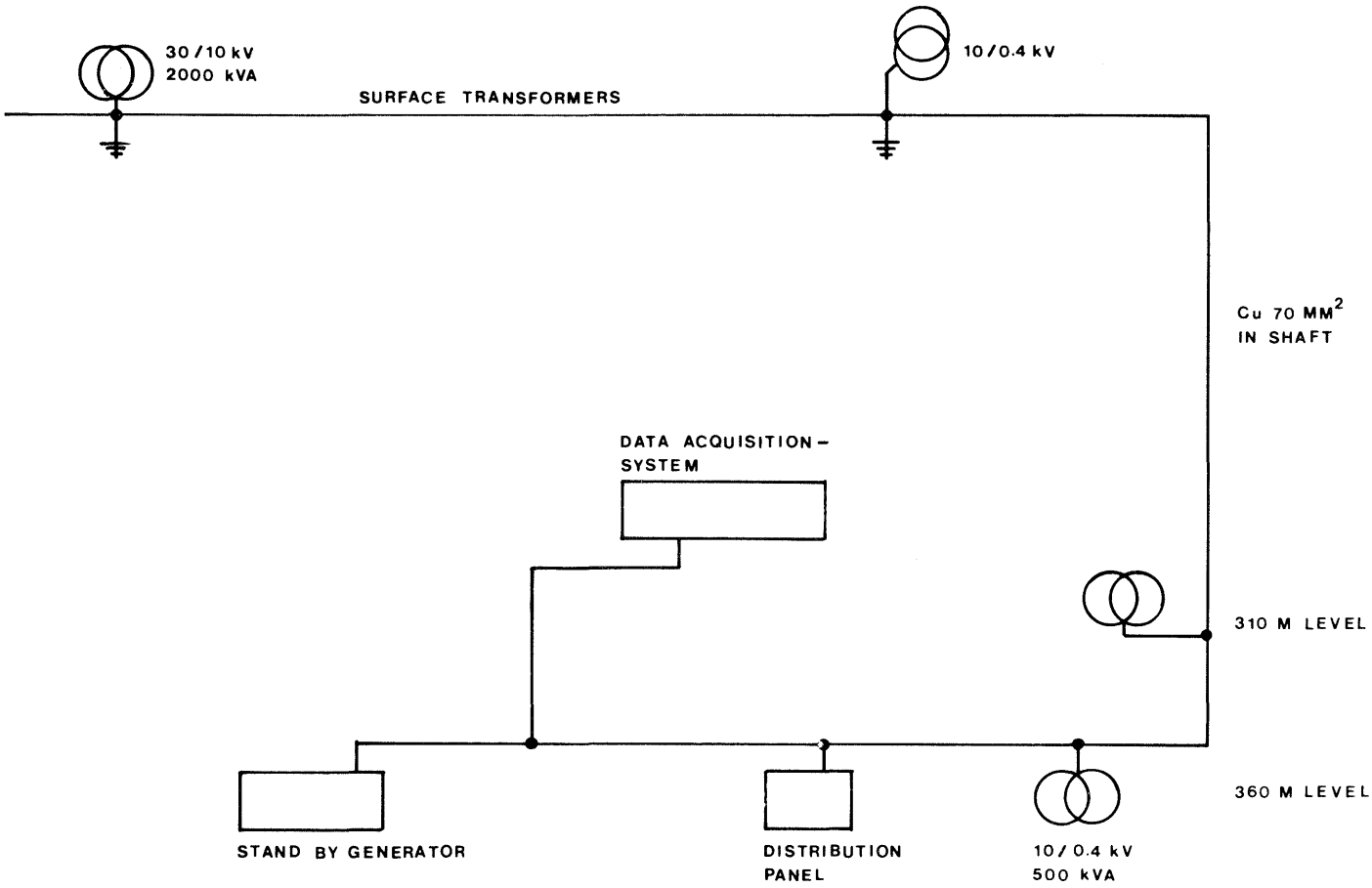

Fig 4.64. Earthing system of the mine

As to the operation of the heaters and their power supply, the following aspects had to be considered:

* It is important for the interpretation of the test results that the control system maintains the applied power as constant as possible during the entire test period. Power recording must be available and alarm yielded in the case of breakdown or substantial deviation from the intended value

* The system must be designed so that the heaters can be powered with 600 W with the possibility of either increasing or decreasing this value. Maximum power should be 3000 W

* Each heater must be supplied with three independent heating circuits all in operation with 200 W in the standard state with the heater running at 600 W. If one element fails, the control system shall automatically compensate for this by utilizing the remaining two elements. Maximum accepted deviation from any chosen power should be ±10W

* Auxiliary power must be available within 10-15 seconds if the main power source of the mine should fail.

4.5.1.2 Design principles

ASEA-ATOM designed and constructed the heaters which consisted of a central solid casing in which 3 symmetrically arranged hairpin-like elements were located. The elements were fixed in place with brackets and cast in an aluminum alloy in order to yield uniform heat flow. In the upper part of the casing, which protruded from the heater unit, the elements were insulated with rock-wool. The casing was surrounded by a central tube of stainless steel which was subdivided into 5 parts in the axial direction. This tube was confined by two thick aluminum segments separated by wedges of the same material. These segments and wedges were subdivided into 5 parts in the same manner as the stainless steel tube. All the components of the respective, detachable segment were held together by six bolts of stainless steel and the whole set of segments had end plates of the same metal. The steel quality used for the heater elements was Incaloy 800, while SIS 2343 was used for all other steel components. The alloy casting for the elements was

aluminum SIS 4261. The segments and wedges were made of string cast aluminum SIS 4244. All aluminum components were electrolytically treated after completion in order to resist corrosion.

The protective tubings for the heat-resisting cables to heaters no 1 and 2 were made of plastic. Steel was used for the other heaters.

The earthing system consisted of stainless steel earthing wires with a diameter of 16 mm attached to the basal plates.

The design of the casing with heater elements is illustrated in Fig 4.65, and of the complete heater unit in Fig 4.66.

4.5.2 Power supply

The only expected BMT-heater problem was actually short term power cuts. The Stripa Mine is supplied with power from the national network by means of a 30 kV cable. In the event of lengthy power cuts in this supply, a 10 KV reserve supply can be switched on manually. Cuts of this type are, however, very rare - hardly more than 1-2 times a year. A further reserve supply arranged for various projects exists in the form of a diesel driven power station at the 350 m level in the vicinity of the BMT-area. This reserve supply is equipped with an automatic system which continously checks the power supply to the heaters as well as the computers. If the voltage drops below a given figure, the diesel engines are automatically started and power is available within 15 seconds. This reserve supply can operate for 3-4 days without refill.

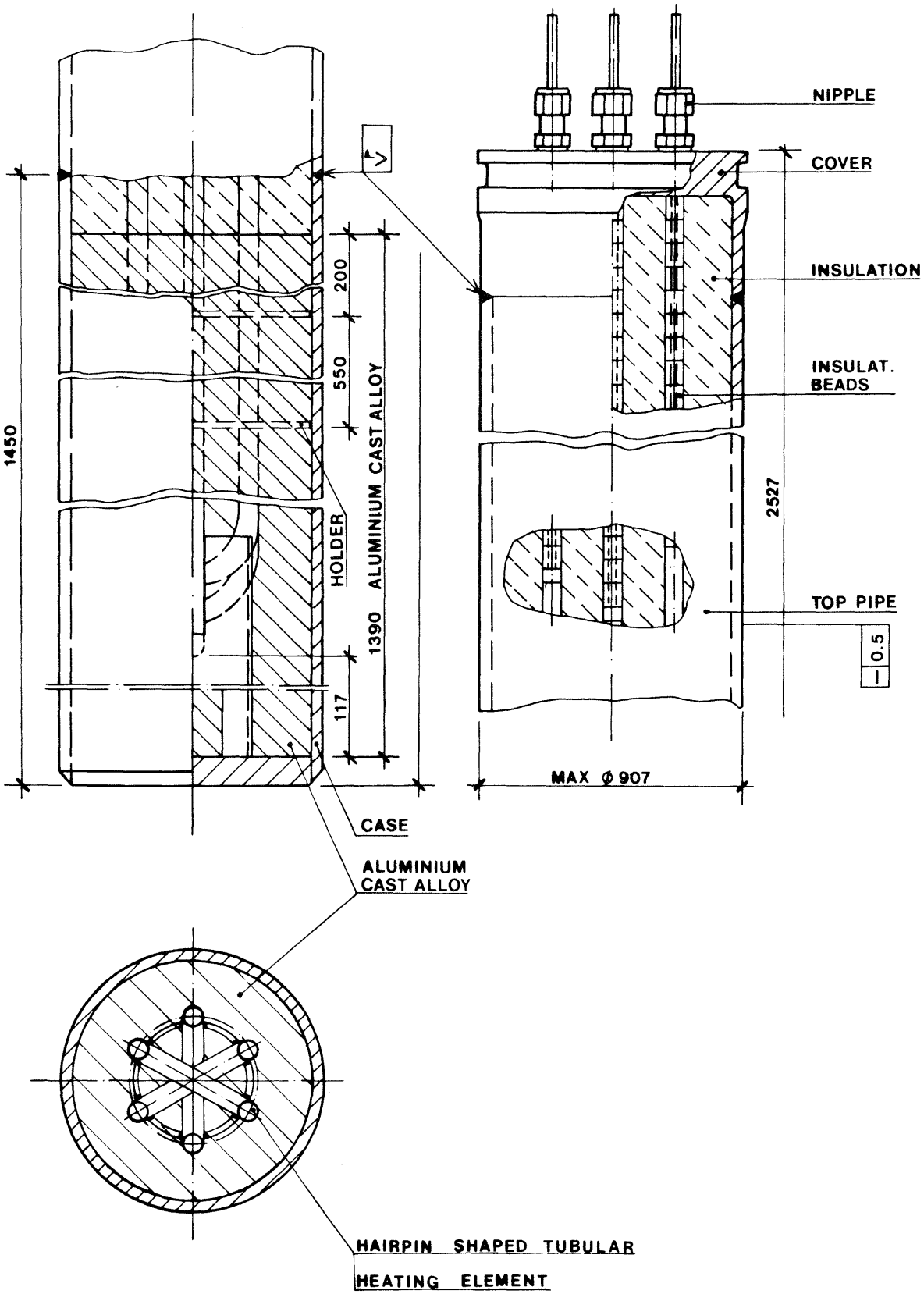

Fig 4.65. Heater casing with heating element

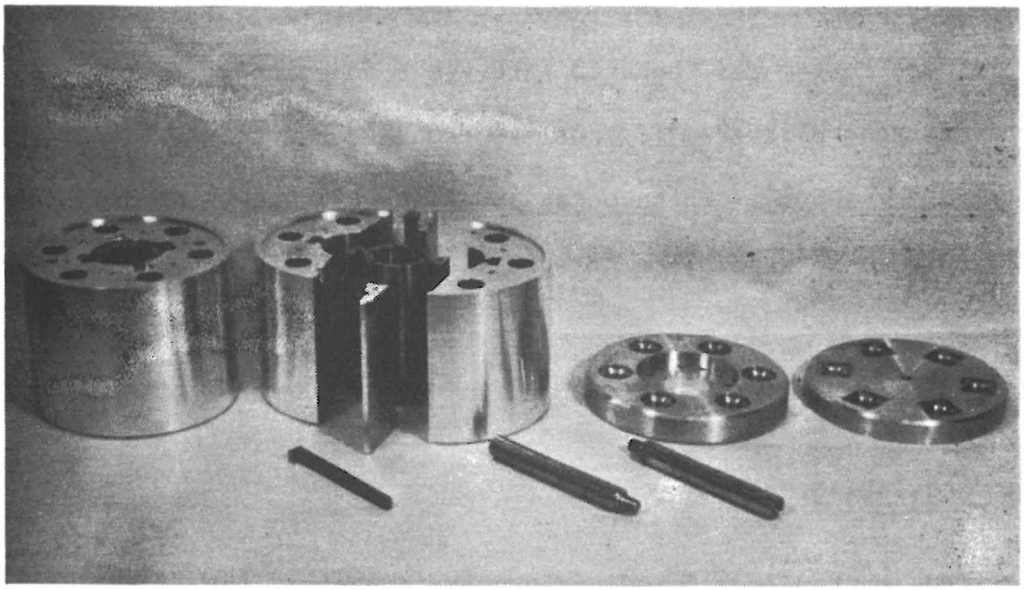

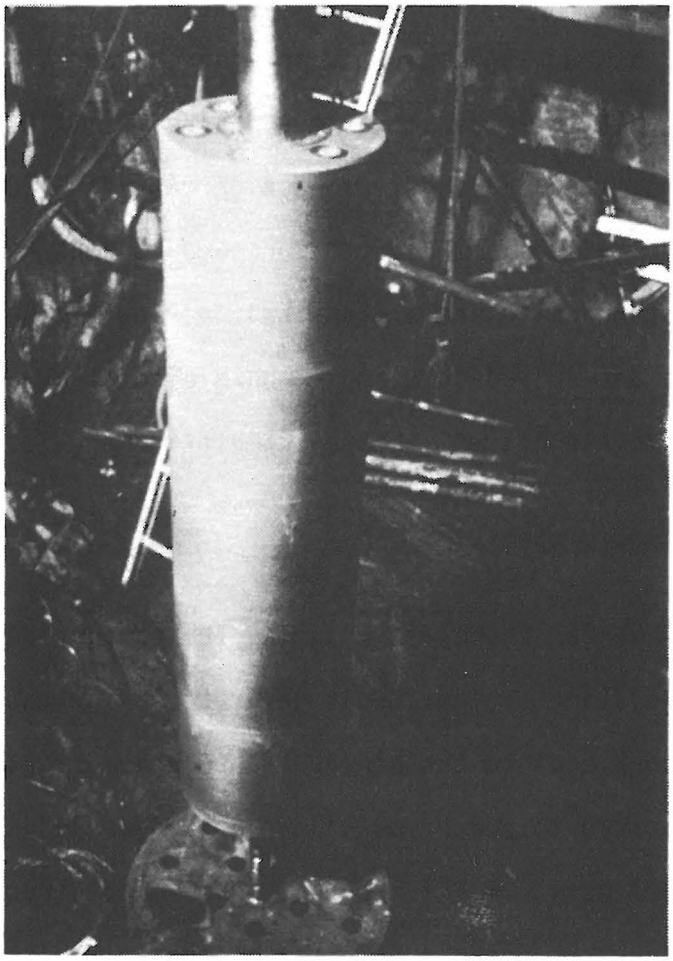

Fig 4.66. Heater details and assembled heater

When the ordinary power supply is reconnected, it is automatically switched on while the diesel driven supply is still in operation. This change was found to take place so quickly ($\simeq$ 30-40 ms) that the control system for heaters remained operative. Normal cuts in power supply, which occur about 5-7 times a year did therefore only cause negligible interruption in heating.

4.5.3 Power control system

4.5.3.1 Regulating system

The system consisted of three main parts: the transducer, the electronic control unit, and the thyristor commutating switch (Fig 4.67). The transducer was connected to the cables supplying power to the heater and converted power to current (4 - 20 mA). The control unit could be set at the desired amplification, integration time, etc and it generated a current (4 - 20 mA) that fed the thyristor switch. The switch turned on the AC mains to the heater at a certain phase angle every half period of the AC voltage. The current determined this angle which also dictated the power that was fed to the heater, thereby completing the loop.

4.5.3.2 Measurement system

For each heater there was a second transducer identical to that of the regulating system and it generated a current (4 - 20 mA) that was proportional to the power. The transducer was very sensitive - it responded to power variations in a few milliseconds (settling time = 300 ms). If this current is sampled directly, the recorded value is very unstable for reasons that are discussed later. It was therefore necessary to use the mean value of the current over several minutes to obtain a stable signal. A microcomputer with

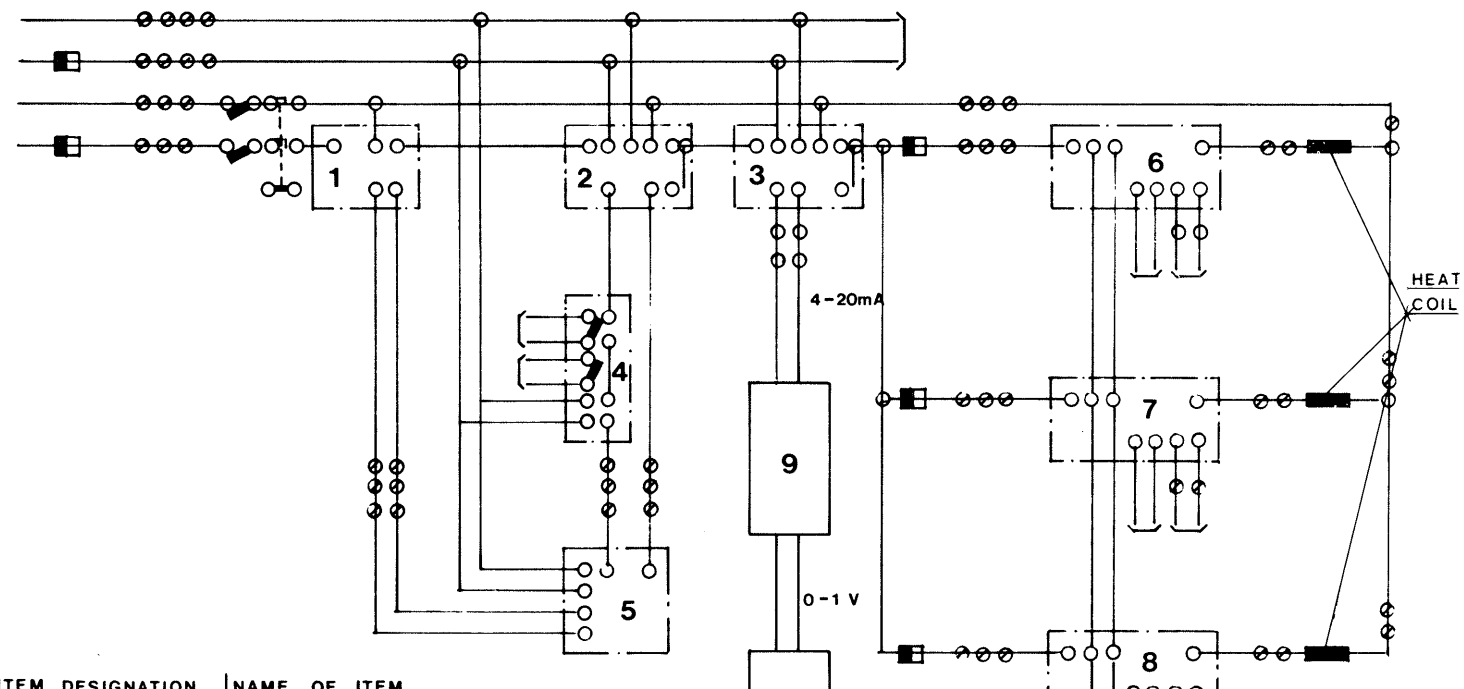

ITEM DESIGNATION	NAME OF ITEM
1	THYRISTOR REGULATOR
2 - 3	WATT TRANSDUCER
4	HI-LO LEVEL TRANSDUCER
5	REGULATOR
6	CURRENT TRANSDUCER
7	" -
8	" -
9	MEAN VALUE PROCESSOR
10	MAIN COMPUTER SYSTEM

Fig 4.67. Block diagram of the control system

an A/D converter was used to calculate the mean value and feed the result to the main computer that collected data from all test points in this experiment. The main computer was unable to make the mean value calculations simultaneously to recording the data.

4.5.3.3 System components

Each of the six electric heaters used in this experiment contained three resistors that governed the heating. Each resistor was supplied with power from a separate power cable, so that if one resistor or cable broke down there would still be two left. The resistors were designed to discharge 1000 W of power each but the actual power supply for one heater during this test was usually only 600 W. This means that one resistor alone could supply the required power to the heater. Normally the three resistors operated parallel and discharged 200 W each.

As mentioned above, the transducer measured the electric power and discharged a current that was proportional to the power. The procedure was the following:

The voltage and current were transformed to a suitable level by two separate transformers. These also provided galvanic isolation between input and output of the transducer. The momentary values of the current and the voltage were then multiplied using the "pulse width/pulse amplitude" method, which means that the width of each pulse is proportional to the voltage and the amplitude proportional to the current. The pulses were then low-pass filtered the result being a signal that was proportional to the momentary product of the current and the voltage. The pulse frequency determined the highest permitted frequency of the input. As the pulse frequency is about 5 kHz, input frequencies of up to 500 Hz were measured with retained accuracy.

The input in this case was not a true sinus voltage as the thyristor switch considerably distorted the sinusoide. When sampling this distorted voltage the result was very unstable and varied with time. However, as there was no synchronization between the pulse frequency (5 kHz) and AC frequency (50 Hz), the mean value was correct. Experiments showed that an integration time of 5 to 10 minutes gave a stable signal within 0.2 %.

The control unit was a general purpose differential amplifier with adjustable characteristics. The reference value as well as the gain and integration time were adjustable by knobs which were manipulated at the installation until the power of the heater became correct. As the power was supervised during the test period by the measurement system, there was no need to adjust the control unit as long as the power remained correct. Any inaccuracy in the control unit was immediately monitored.

The thyristor switch turned on the AC voltage 100 times a second. The exact moment to turn on the voltage was controlled by the current fed to the control input of the switch.

The mean value processor was a specially built unit which contained a one-chip microprocessor. The unit processed the signals from all 6 transducers and discharged 6 analogue voltages that were to be sampled by the HP data acquisition system which collected all measurement data during the experiment.

The signal from each transducer was firstly transformed from current to voltage. This voltage was low-pass filtered in a simple RC link with a time constant of 0.1 seconds. All six signals were then multiplexed and fed to an A/D-converter. The digital values were added during a period of time that was chosen by a switch to one of 14 values from 0.125 seconds to 8.5 minutes. The sums were

stored for each signal in a cyclic way so the last 8 sums were available in the memory. The mean value of each signal was computed from the eight sums and fed to a D/A-converter. After demultiplexing and buffering, the six computed values were discharged to the HP. The precision of the A/D and D/A conversions were 12 bits.

4.5.3.4 Installation

Fig 4.68 illustrates the arrangement of the components of the control and data acquisition systems, while Fig 4.69 shows the three cabinets for the power control system. Two of the cabinets contained thyristors and the alarm panel, while the third contained the control units for the heating effect. The measuring equipment which was connected directly to the computer is shown in Fig 4.70.

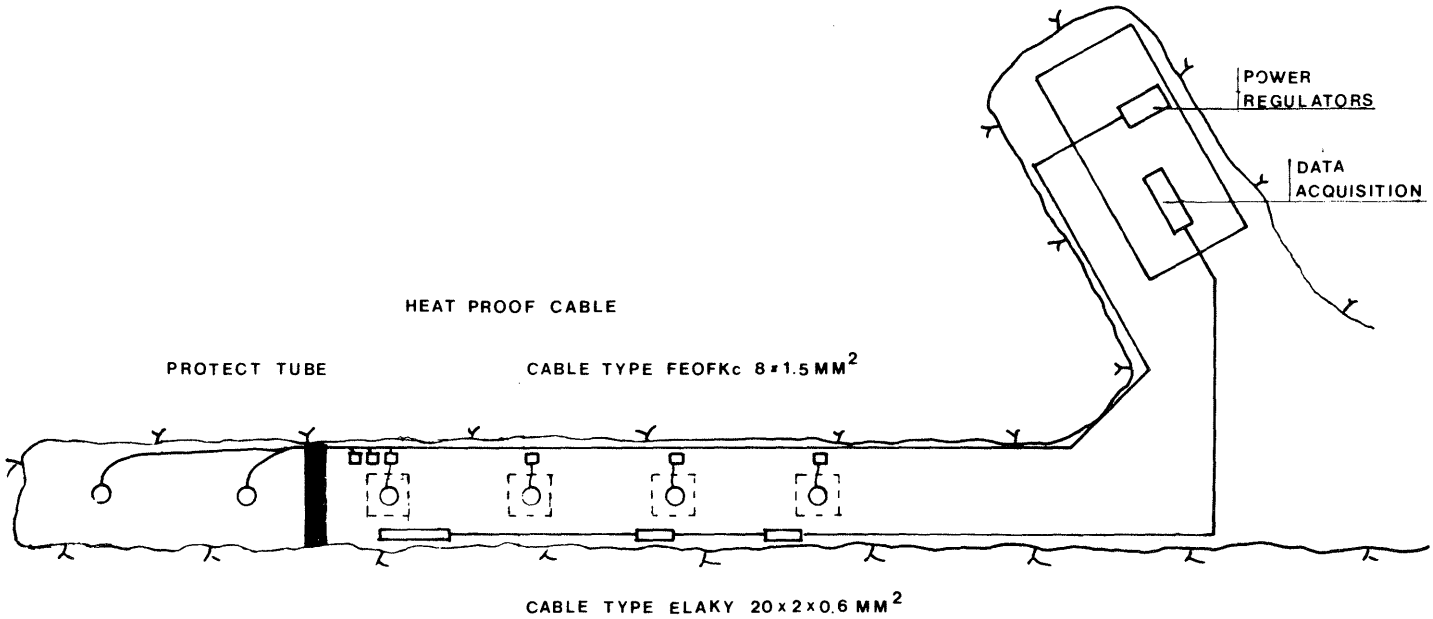

Fig 4.68. Relationships between the components of the control system

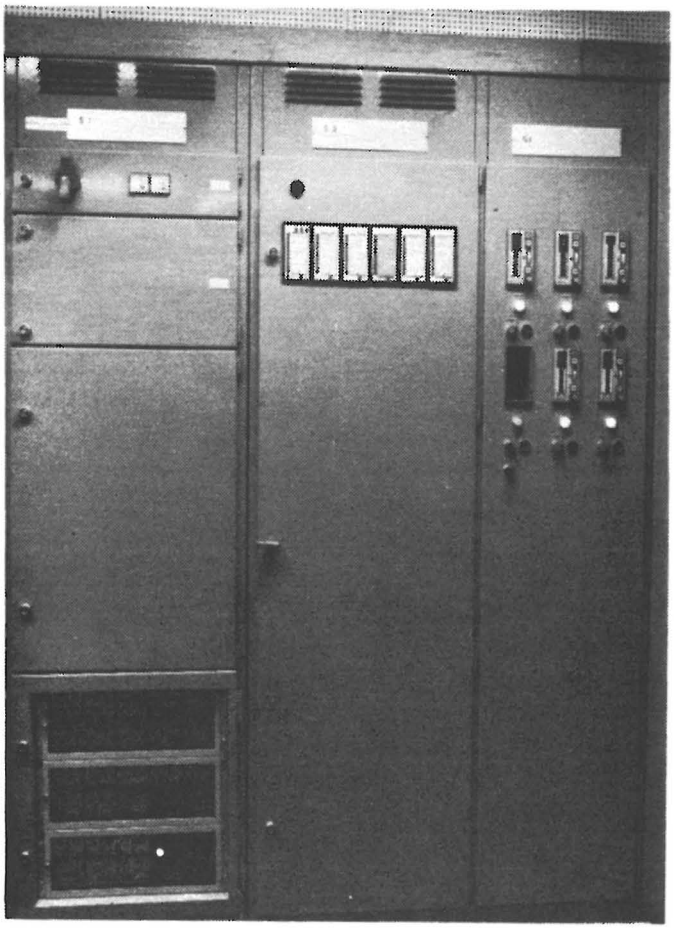

Fig 4.69. Cabinets for the power control system

Fig 4.70. Cabinets for the measuring equipment

4.5.4 Laboratory function tests

4.5.4.1 General

The fact that the entire BMT largely depended on the function of the heaters called for comprehensive laboratory investigations.

The following tests were carried out in the laboratories of ASEA-ATOM:

* Testing of the heat flow of the casing in air
* Testing of the heat flow of the entire heater unit in air
* Assembly, trial operation for 14 days and dismantling. These tests were carried out in a sand-filled test rig equipped with thermocouples and with the same geometry as the heater holes in Stripa.

4.5.4.2 Test of casing in air

Following assembly, the distribution of temperature in the casing was tested with 1, 2 and 3 elements in operation and with a total effect in all cases of 600 W. The temperature was measured when a stable situation had been reached for each combination, using a contact thermometer at 18 levels with 8 points at each level. The room temperature was measured simultaneously. The casing temperature became 110^{o}-130^{o} at a room temperature of 22^{o}C. In the upper part of the casing, where the elements were insulated with rock-wool, the temperature decreased rapidly from about 110^{o}C near the cast-in part to about 30^{o}C at the top. Exactly the same heat flow pattern appeared whether one, two or three of the elements were in operation.

4.5.4.3 Test of heater in air

An assembled heater was tested in the same manner as the casing. The radial distribution of heat was found to be very uniform as

shown in Fig 4.71. The temperature distribution along the upper part which protruded from the casing, and along the rod between the base of the heater and the basal plate, varied from about 70°C close to the encased part of the heater, to about 25°C at both the top and bottom of the assembled heater.

4.5.4.4 Test of heater in simulated heater hole

One of the heaters was installed in a test rig consisting of a steel pipe with the same dimensions as a heater hole. The pipe, which was insulated with rock-wool, was filled with water saturated olivine sand to simulate the thermal and mechanical properties of the bentonite in Stripa. The instruments consisted of 39 thermocouples placed at 5 levels, the positions of which are shown in Fig 4.72. The primary purpose of the test was to check the reliability of the equipment over a longer period and to make sure that the units could be dismantled in the intended manner. A stable situation of the temperature distribution was attained after 10 days and it was then found that thermocouples 11 and 12 at the base of the heater 19 and 20 at the center, and 27 and 28 at the top all showed almost identical temperatures.

Dismantling of the heater unit showed that the construction functioned as planned. Several stages are illustrated in Figs 4.73 and 4.74.

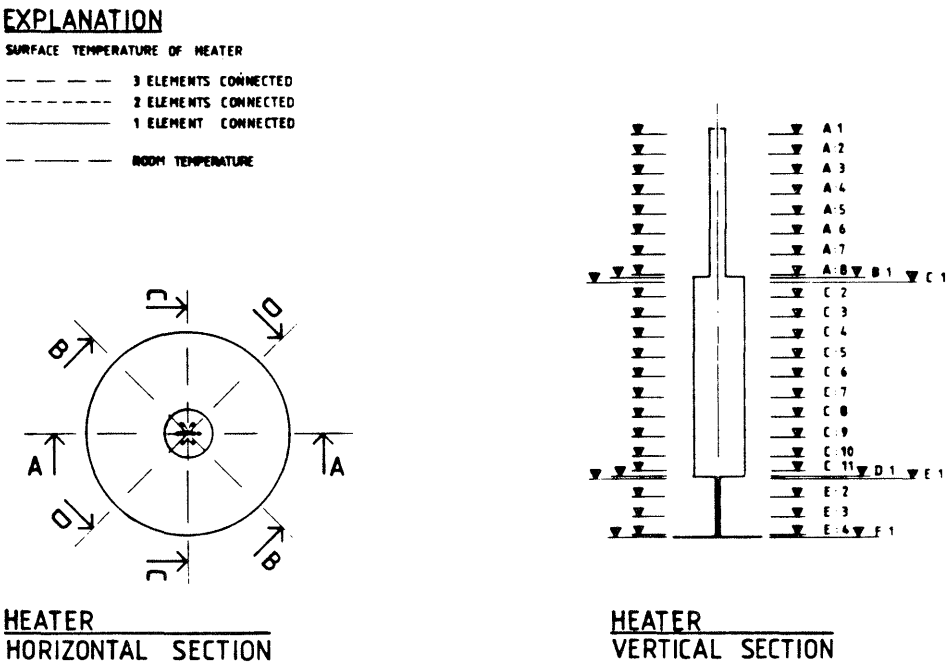

HEATER
HORIZONTAL SECTION

HEATER
VERTICAL SECTION

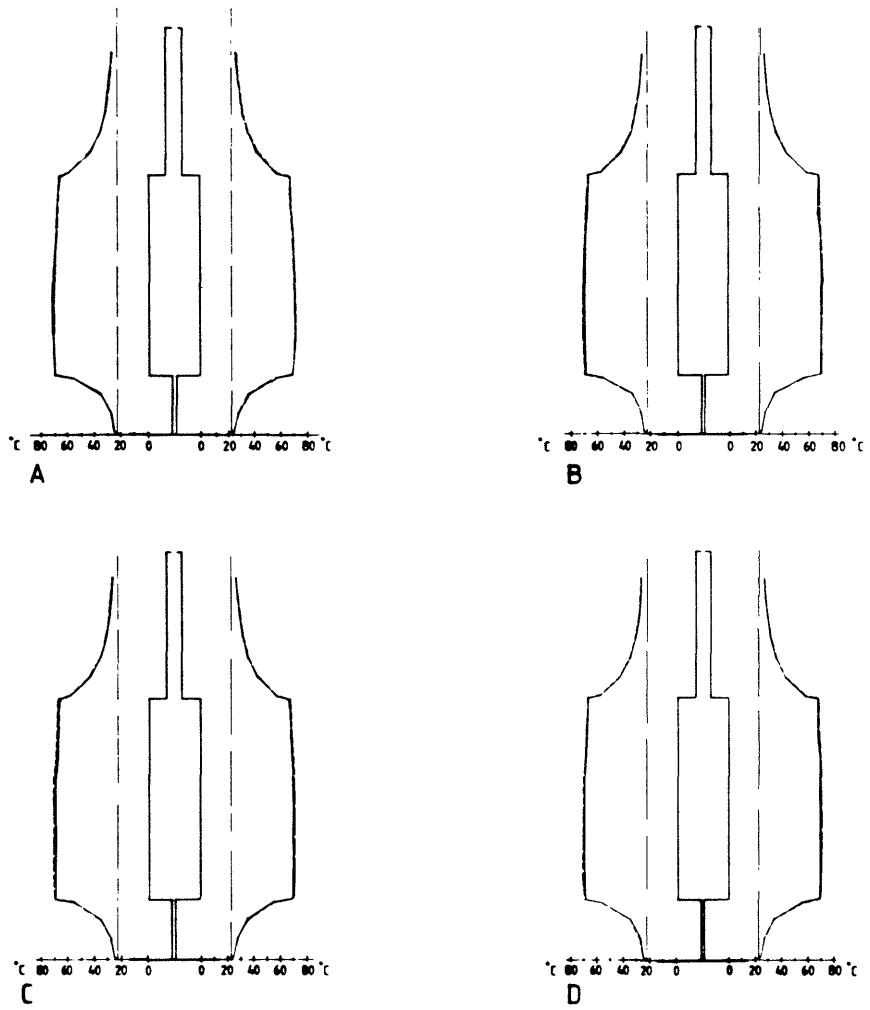

Fig 4.71. Laboratory test of heater in air. Vertical sections

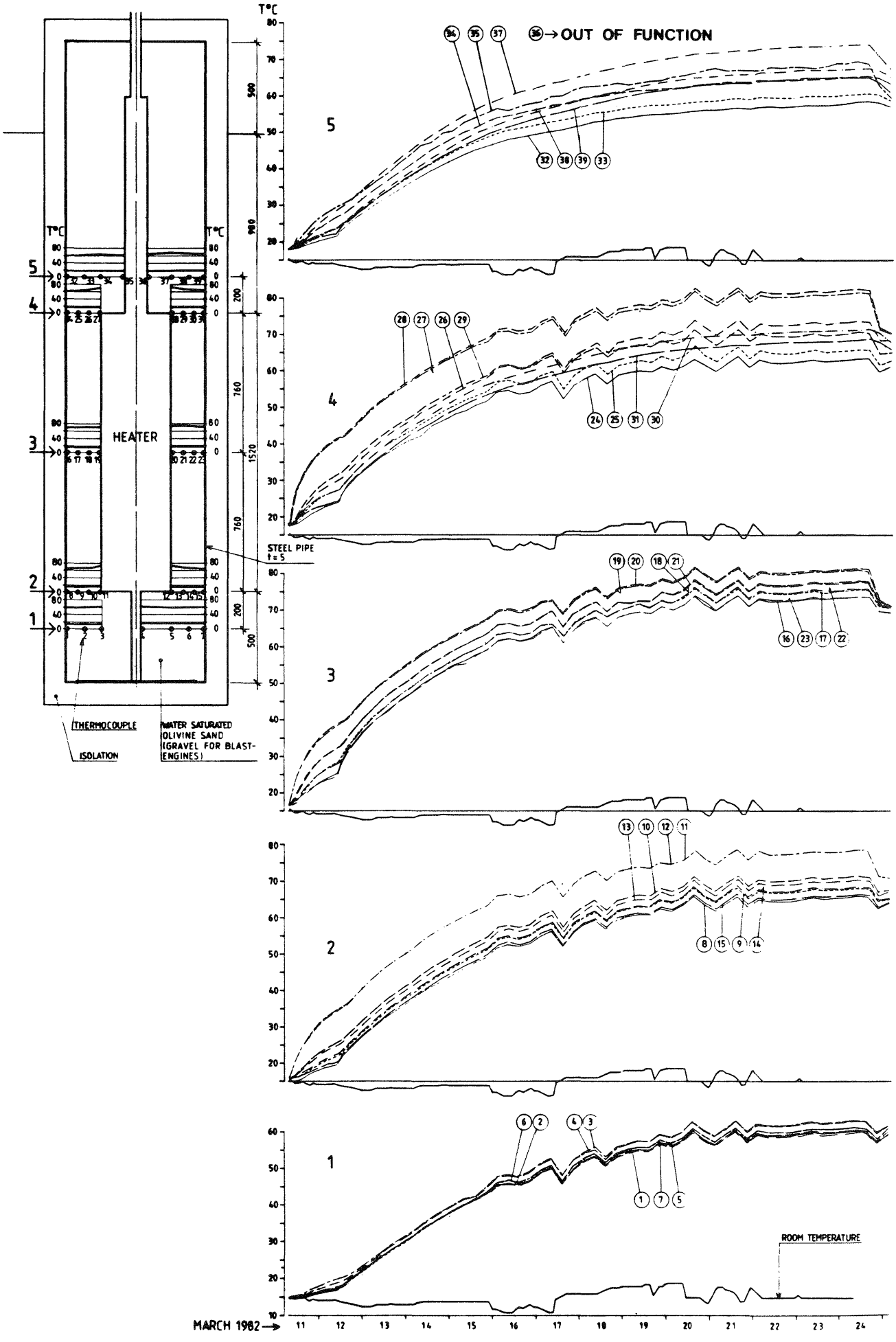

Fig 4.72. Temperature distribution in test rig

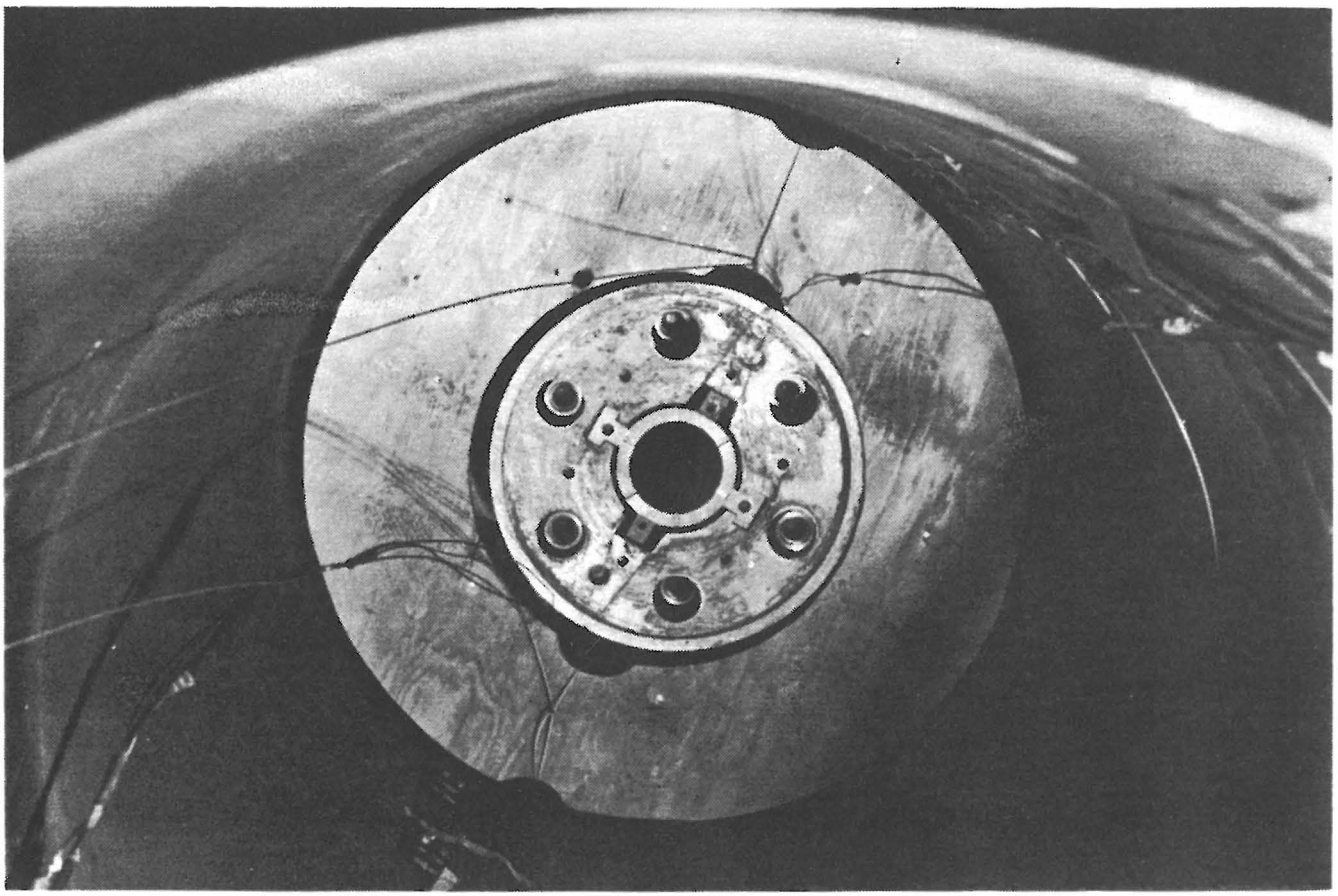

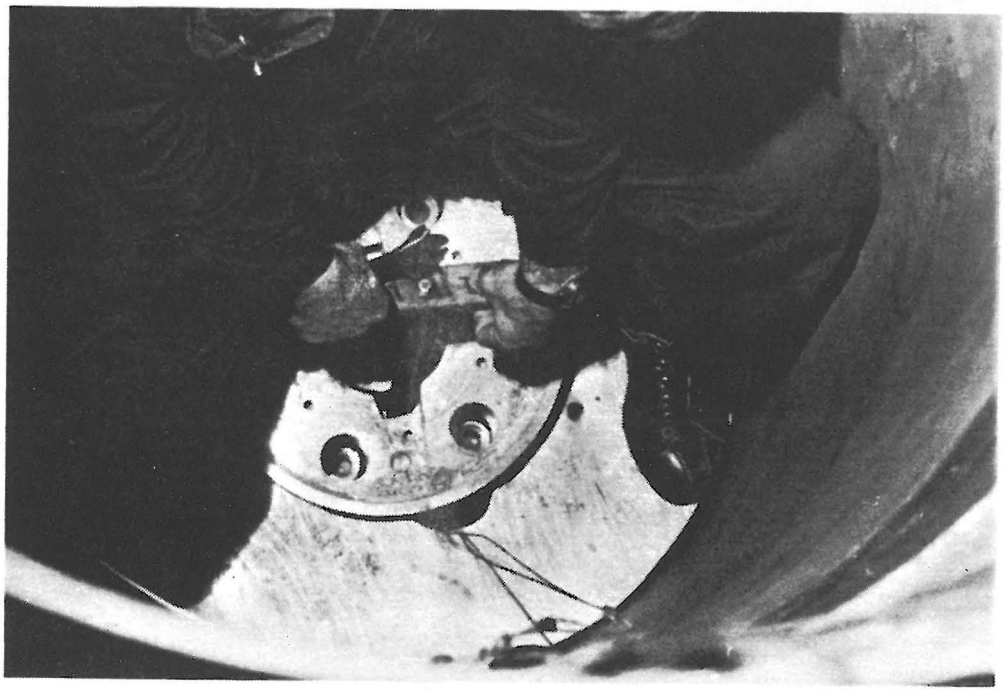

Fig 4.73. Dismantling of heater in test rig

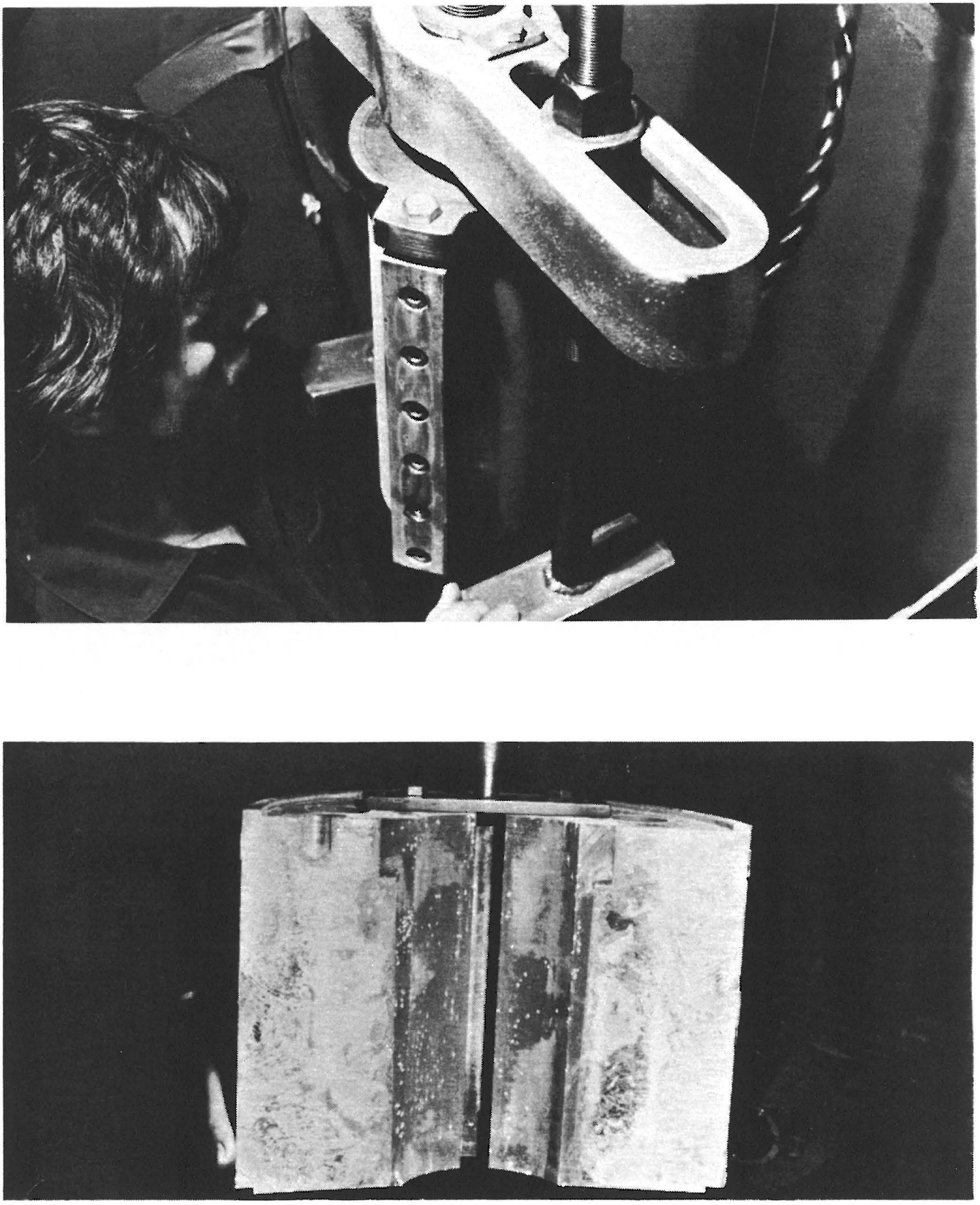

Fig 4.74. Heater parts with lifting equipment

4.5.5 Operating experience, accuracy

4.5.5.1 Heaters

The six heaters were put in operation on the following dates: no 1 in October 5, 1981; no 2 in October 7, 1981; no 3 and no 4 in January 20, 1982; and no 5 and no 6 in March 24, 1982. The first experience as to the possibility of dismantling the heaters was gained in late 1982 when hole no 4 was excavated. It is concluded that the 600 W heaters have operated quite satisfactorily and according to the plans, both with respect to installation, operation, and dismantling. In a late phase of the BMT, two heaters were run at 1200-1800 W and apart from one element breakdown they behaved according to the expectations also at this elevated power.

4.5.5.2 Control system

The control system, once properly adjusted, has worked very well and reliably. The accuracy was estimated as follows for the various components.

Errors and accuracy

Errors in the control system will affect the constancy of the power supply, both on a short and long term basis. Power variations of ordinary magnitude in time periods shorter than 10 to 20 minutes were not significant to the test results as long as the mean value was recorded. Long term variations over weeks or months were monitored by the measuring system and could be compensated for manually when necessary.

An attempt to estimate the maximum errors in the measurements was based on the data sheets for the various components.

Power loss

The transducers recorded the power of the heaters and the electric cables. The power in the cables has been calculated by ASEA-ATOM, the maximum error in calculated power loss being 1 W.

Transducer errors

The data sheets for the transducer show that the accuracy was about 0.5 %. It has been verified by experiments that the transducer is not significantly affected by power voltage distortion. The maximum error of the transducer was then 0.5 % x 1000 W = 5 W.

Mean value computation error

The mean value processor was designed to produce an error of less than 0.1 % of FSR which means 0.1 % x 1000 W = 1 W. This has been verified at the time of installation.

Total error

It is concluded that the heating power was measured with an absolute error of less than 5 + 1 + 1 = 7 W. The actual heater power is given in Table 4:10.

Table 4:10. Power loss and nominal power of the heaters

Heater no	Power loss, W	Nominal power, W
1	24.9	600
2	22.3	600
3	18.6	618.6
4	16.9	616.9
5	14.9	614.9
6	12.9	612.9

The power loss through cable resistance etc, was compensated for in the case of heaters no 3, 4, 5 and 6, while this was not the case for heaters no 1 and 2. Thus, the net power was 600 ±7 W for heaters no 3-6 and about 575 ±7 W for heater no 1 and 577 ±7 W for heater no 2.

5 ACKNOWLEDGEMENTS

The planning and conducting of the field work as well as the preparation of drawings and instructions, has been made by AB Jacobson & Widmark, Luleå, under the direction of the senior author. Continuous contact and cooperation has been maintained with the SKBF/KBS through their representatives L.R. Nilsson, A. Bergström, H. Carlsson, H. Åhagen and Å. Nässil, and with the Division of Soil Mechanics, University of Luleå.

The field work, which involved a number of difficult activities, could not have been conducted successfully without the invaluable assistance of the late mine engineer Per-Axel Halèn as well as all other Stripa Mine employees. The authors express their sincere gratitude to all of them and to Sven-Eric Tegelmark who very skillfully assisted in most field activities and who was responsible for much of the advanced computer plotting.

Special thanks are due to the members of the Technical Subgroup no 2, particularly to its chairman Paul Gnirk, for valuable suggestions and positive criticism.

6 REFERENCES

1 "Bentonite-based Buffer Substances for Isolating Radioactive Waste Products at Great Depths in Rock". Pusch, R., Jacobsson, A., and Bergström, A., 1980. Underground Disposal of Radioactive Wastes, Vol. I., IAEA-SM-243/22, Vienna.

2 "Geology and Fracture System at Stripa". Swedish-American Cooperative Program on Radioactive Waste Storage in Mined Caverns in Crystalline Rock. Olkiewics, A., Gale, J.E., Thorpe, R., and Paulsson, B., 1979. LBL-8907, SAC-21, UC-70.

3 "A Pilot Heater Test in the Stripa Granite". Swedish-American Cooperative Program on Radioactive Waste Storage in Mined Caverns in Crystalline Rock. Carlsson, H., 1978. LBL-7086, SAC-06, UC-70.

4 "Petrological Changes and Damage in the Stripa Quartz Monzonite in Response to Heater Tests". Swedish-American Cooperative Program on Radioactive Waste Storage in Mined Caverns in Crystalline Rock. Flexser, S., Wollenberg, H., and Wedge, D.E., 1982. LBL-14929, SAC-41, UC-70.

5 "Borehole Sealing with Highly Compacted Na Bentonite". SKBF/KBS Teknisk Rapport 81-09. Pusch, R., 1981.

6 "Geochemistry and Isotope Hydrology of Groundwaters in the Stripa Granite; Results and Preliminary Interpretation". Swedish-American Cooperative Program on Radioactive Waste Storage in Mined Caverns in Crystalline Rock. Fritz, P., Barker, J.F., and Gale, J.E., 1979. LBL-8285, SAC-12, UC-70.

7 "The Macropermeability Experiment". Geological Disposal of Radioactive Waste, In Situ Experiments in Granite. Gale, J.E., Witherspoon, P.A., Wilson, C.R., and Roleau, A., 1982. Proc of the OECD/NEA Workshop, Stockholm, October 25-27, 1982.

8 "Geohydrological Data from the Macropermeability Experiment at Stripa, Sweden". Swedish-American Cooperative Program on Radioactive Waste Storage in Mined Caverns in Crystalline Rock. Wilson, C.R., Long, J.S., Galbraith, R.M., Karasaki, K., Endo, H.K., DuBois, A.O., McPherson, M.J., and Ramqvist, G., 1981. LBL-12520, SAC-37, UC-70.

9 "Sorption av långlivade radionuklider i lera och berg". Del 2. Allard, B., Kipatsi, H., and Torstenfelt, B., 1978. KBS Teknisk Rapport No 98.

10 "Permeability of Highly Compacted Bentonite". Pusch, R., 1980. SKBF/KBS Teknisk Rapport 80:16.

11 "Swelling Pressure of Highly Compacted Bentonite". Pusch, R., 1980. SKBF/KBS Teknisk Rapport 80-13.

12 "Water Uptake, Migration and Swelling Characteristics of Unsaturated and Saturated, Highly Compacted Bentonite". Pusch, R., 1980. SKBF/KBS Teknisk Rapport 80:11.

13 "Ion Diffusion through Highly Compacted Bentonite". Eriksen, T., Jacobsson, OA., and Pusch, R., 1981. SKBS/KBS Teknisk Rapport 81-06.

14 "Heat Conductivity of Bentonite Buffer Materials". Knutsson, S., 1982. SKBF/KBS Teknisk Rapport 83-

15 "Transport of Oxidants and Radionuclides through a Clay Barrier". Neretnieks, I., 1978. KBS Teknisk Rapport no 79.

16 "Ice Nucleation and the Substrate-Ice Interface". Anderson, D.M., 1967. Nature, Vol 216, Nov 11.

17 "Versuche über die Sohldruckverteilung unter starren Gründungskörpern auf kohesionslosem Sand". Leussink, H., Blinde, A., and Abel, P-G., 1966. Heft 22, Inst für Bodenmechanik und Felsenmechanik der Techn Hochschule Fridericiana in Karlsruhe.

18 "Evaluation of the Gloetzl Stress Gauge for Use in Concrete Structures". Grainger, B.N. 1978. Central Electricity Research Laboratories, Report RD/L/N 51/78, Job no VH 126.

19 "Fuktmätning i Bentonit". Kodaxis, G., 1982. Thesis No 1982:076 E, Div of Soil Mechanics. University of Luleå.

20 "Field Instrumentation in Tunneling as a Practical Design Aid". Kovari, K., Amstrad, Ch., 1979. Proc 4th Int Congress for Rock Mechanics, Montreux 1979. Balkema Publishers, Rotterdam, Vol 2.